

STRUCTURAL BEHAVIOUR OF PLASTERED STRAW BALE ASSEMBLIES UNDER CONCENTRIC AND ECCENTRIC LOADING

by

Stephen Peter Vardy

A thesis submitted to the Department of Civil Engineering
in conformity with the requirements for
the degree of Doctor of Philosophy

Queen's University
Kingston, Ontario, Canada

(May, 2009)

Copyright © Stephen Peter Vardy, 2009

*The problems that exist in the world today cannot be solved by the level of thinking
that created them*

Albert Einstein

*This is the moment when we must come together to save this planet. Let us resolve
that we will not leave our children a world where the oceans rise and famine spreads
and terrible storms devastate our lands*

Barack Obama

*The solutions of tomorrow are not stashed behind the walls of bureaucracy or
political halls. They are in the minds of engineers, designers, innovators,
researchers, environmentalists, geographers and other spirited individuals*

Stuart Barea

Abstract

The use of plastered straw bale walls in residential construction is growing as builders and owners seek environmentally friendly alternatives to typical timber construction practices. Straw has excellent insulation properties and is an agricultural bi-product which is annually renewable, and is often considered a waste product of grain production.

This thesis presents new models for predicting the compressive strength of plastered straw bale assemblies subjected to concentric and eccentric load. A constitutive model for lime-cement plaster is adapted from a stress-strain model for concrete, available in the literature. Twenty-two cylinder tests on plasters typically used for straw bale construction were used to verify the constitutive model.

The models for plastered straw bale assemblies were verified by testing plastered straw bale assemblies under concentric and eccentric compressive loads. An innovative steel frame test jig was designed to facilitate fabrication and testing of the specimens. Using this jig, 18 specimens of height 0.33 m, 0.99 m, 1.05 m or 2.31 m were subjected to concentric or eccentric compressive load until failure. The experimental strengths of the assemblies ranged from 23 kN/m to 61 kN/m, depending on the eccentricity of the load, the plaster strength, and the plaster thickness. Results indicated that the specimen height did not significantly influence the strengths of the specimens.

The models predicted the ultimate strength of the assemblies to be, on average, 6% less than the experimentally determined strengths, with a standard

deviation of 13%. The models were also used to predict the theoretical ultimate strengths for a number of plastered straw bale wall assemblies described in the literature. The fabrication techniques for these specimens were more representative of conventional straw bale construction techniques, and it was found that the experimental results were 30% of the theoretical strengths for assemblies with plaster strength less than 10 MPa and 6% of the theoretical strengths for assemblies with plaster strength greater than 10 MPa. Thus, to account for construction imperfections and potential alternative failure mechanisms, a reduction factor of no more than 0.3 for plaster less than 10 MPa is suggested in order to predict the strength of plastered straw bale walls constructed using conventional construction techniques.

The results presented herein provide support for the use of plastered straw bale walls in residential construction and indicate the applicability of models based on the compressive behaviour of lime-cement plaster for modelling the behaviour of plastered straw bale walls under eccentric and concentric compression.

Acknowledgements

I will remember my time at Queen's University as an extremely positive experience, both academically, and socially. I am forever grateful for the unwavering support of the faculty and staff and the endless encouragement from family and friends. My time at Queen's University has also been highlighted by the formation of friendships and relationships which will undoubtedly last a lifetime. While there are many people who have positively influenced my experience at Queen's over the past nine years, I'd like to recognize some who have contributed significantly to my happiness and success.

I would first like to thank my supervisor, whose open-mindedness and environmental conscience made this research program possible. Sincere thanks go to Dr. Colin MacDougall who provided me with invaluable guidance, support and advice which have not only contributed to the completion of this research, but which provided an enjoyable and successful environment for my introduction to research and education. I have thoroughly enjoyed my academic experiences at Queen's University, and for this I am truly grateful.

I would also like to thank Dr. Luke Bisby, whose encouragement and advice as both a mentor and a friend have influenced me, not only on an academic level, but also on a personal level. His dedication to learning, teaching, and research are nothing short of inspirational.

Many thanks also go to the staff, faculty, graduate students, and undergraduate students who have been essential to the completion of this research

program. Thanks go to Dr. Amir Fam, Dr. Mark Green, Dr. Dave Turcke, Dr. Andy Take, Fiona Froats, Maxine Wilson, Cathy Wagar, Paul Thrasher, Dave Tryon, Lloyd Rhymer, Jamie Escobar, Neil Porter, Mike Rakowski, Bryce Daigle, Lucio Amato, Colin Smith, Tim Tipping, Adam Shaw, and Brendan Taylor.

I would also like to recognize Chris Magwood, a straw bale builder, whose dedication and creativity continue to contribute to the growing acceptance of straw bale construction. Chris and his team provided valuable advice, guidance and energy to the completion of this research program.

I would like to thank: the Natural Sciences and Engineering Research Council and the Canadian Mortgage and Housing Corporation for their financial support.

I would like to thank all of my friends who supported me and encouraged me through my time at Queen's University. Specifically I would like to thank J.C., S.D., J.H., S.S., T.B., S.R., A.T., M.B., M.R., C.S., B.H., J.B., A.W., A.D., A.L., A.B., K.P., M.R., and M.B. I know that these friendships will last a lifetime, and that the last 9 years are only the tip of the iceberg.

My family I would like to thank for always being at my side, and for providing me with unconditional encouragement, support, and inspiration. I wish to thank Phil and Carolyn for their support and advice in all facets of life, and mom and dad for raising me to love education and science, and for teaching me the importance and meaning of happiness.

Finally, I would like to thank my future wife Janet, whose patience and love have overpowered even the greatest challenges I have faced. For this unwavering dedication, patience and love I am truly grateful.

Table of Contents

Abstract	iii
Acknowledgements	v
Table of Contents	vii
List of Figures	xv
List of Tables	xxiii
Notation	xxv
Chapter 1 : Introduction	1
1.1 Background.....	1
1.2 History.....	3
1.3 Advantages	4
1.4 Concerns.....	6
1.5 Construction Practices and Constitutive Materials	8
1.5.1 Construction Practices	8
1.5.2 Description of Straw	11
1.5.3 Plaster	13
1.5.3.1 Introduction	13
1.5.3.2 Earthen Plaster	13
1.5.3.3 Lime-Cement Plaster	14
1.5.3.4 Summary.....	15
1.6 Research Objectives.....	15
1.7 Thesis Outline	17
Chapter 2 : Literature Review	22
2.1 Introduction	22

2.2 Construction Practices	24
2.3 Un-Plastered Straw Bale Properties and Testing	26
2.3.1 Introduction.....	26
2.3.2 Stress-Strain Relationship.....	26
2.3.3 Other Properties	29
2.3.4 Summary	30
2.4 Plaster Structural Properties and Testing	30
2.4.1 Introduction.....	30
2.4.2 Lime-Cement Plaster.....	32
2.4.2.1 Introduction	32
2.4.2.2 Ultimate Compressive Strength	32
2.4.2.3 Stress-Strain Behaviour	38
2.4.2.4 Tensile Strength.....	39
2.4.2.5 Summary.....	40
2.4.3 Earthen Plaster.....	41
2.5 Straw Bale Wall Properties	43
2.5.1 Response to Compressive Loading	43
2.5.1.1 Concentric Compressive Loading.....	43
2.5.1.2 Eccentric Compressive Loading	46
2.5.1.3 Influence of Shear Stress	47
2.5.2 Response to Other Types of Loading	49
2.5.2.1 Introduction	49
2.5.2.2 In-Plane Lateral Loading.....	49
2.5.2.3 Sustained Loading	49
2.5.2.4 Impact Loading	50
2.5.2.5 Response of Un-Plastered Walls.....	51
2.5.3 Standard Test Methods for Compression Testing.....	51
2.6 Summary.....	53
2.6.1 Limitations of Results	53
2.6.2 Relevant Plaster and Straw Properties	53
2.6.3 Relevant Plastered Straw Bale Wall Properties	55
2.6.4 General Deficiencies in the Literature	56

Chapter 3 : Constituent Material Properties	63
3.1 Introduction	63
3.2 Plaster Testing.....	65
3.2.1 Design and Fabrication of Specimens	65
3.2.1.1 Constituent Materials	65
3.2.1.2 Mix Proportioning.....	66
3.2.1.3 Mixing Procedure	66
3.2.1.4 Slump Test and Preparation of Strength Test Specimens	67
3.2.2 Instrumentation.....	68
3.2.3 Test Details	69
3.2.4 Results and Discussion	71
3.2.4.1 Introduction	71
3.2.4.2 Modelling Lime-Cement Plaster Stress-Strain Behaviour	71
3.2.4.3 Quantifying Variability in Plaster Strength	80
3.2.4.4 Effect of Mix Procedure on Plaster Variability.....	82
3.3 Straw Bale Compressive Testing.....	88
3.3.1 Introduction.....	88
3.3.2 Design and Fabrication	88
3.3.3 Instrumentation.....	89
3.3.4 Results and Discussion	90
3.4 Conclusions	91
Chapter 4 : Preliminary Compression Testing of Plastered Bale Assemblies	106
4.1 Introduction	106
4.2 Design and Fabrication.....	107
4.2.1 Materials.....	107
4.2.1.1 Straw Bales.....	107
4.2.1.2 Plaster Design and Mixing	108
4.2.2 Fabrication Procedure	109
4.2.3 Description of Completed Specimens	111
4.3 Instrumentation	113
4.4 Procedure	114

4.5 Results	114
4.5.1 Description of Structural Behaviour.....	114
4.5.2 Plastered Bale Ultimate Strength	116
4.6 Theoretical Concentric Compression Behaviour	116
4.6.1 Theoretical Strength Model	116
4.6.2 Calculation of Theoretical Strength	118
4.7 Discussion.....	121
4.7.1 Experimental to Theoretical Strength	121
4.7.2 Failure Mode Discussion	122
4.8 Experimental and Construction Recommendations	123
4.9 Conclusions	124

Chapter 5 : Concentric Compression Experiments of Plastered Straw Bale

Assemblies	134
5.1 Introduction	134
5.2 Design and Fabrication.....	135
5.2.1 Materials.....	135
5.2.1.1 Straw Bales.....	135
5.2.1.2 Plaster Design and Mixing	136
5.2.2 Fabrication Procedure	137
5.2.2.1 Design of Fabrication and Testing Jig	137
5.2.2.2 Detailed Fabrication Procedure	138
5.3 Experimental Program	139
5.4 Instrumentation	140
5.5 Procedure	142
5.6 Results and Discussion	143
5.6.1 Plaster Strength Results and Discussion	143
5.6.2 Wall Assembly Results and Observations	143
5.6.2.1 Ultimate Load and Vertical Load-Deflection Results	143
5.6.2.2 Lateral Deflection Results	145
5.6.2.3 Failure Modes	146
5.6.3 Wall Assembly Theoretical Behaviour.....	147

5.6.3.1 Ultimate Strength	147
5.6.3.2 Load-Deflection Response	148
5.6.4 Wall Assembly Discussion	149
5.6.4.1 Effect of Specimen Height on Ultimate Strength	149
5.6.4.2 Comparison of Experimental and Theoretical Ultimate Strength.....	150
5.6.4.3 Plastered Bale Assembly Load-Deflection Response	150
5.6.4.4 Lateral Deflection	151
5.7 Conclusions	153

Chapter 6 : Eccentric Compression Experiments of Plastered Straw Bale

Assemblies	172
6.1 Introduction	172
6.2 Design and Fabrication	174
6.2.1 Materials	174
6.2.2 Wall Assembly Fabrication Procedure	174
6.3 Experimental Program	175
6.4 Instrumentation	176
6.5 Procedure	177
6.6 Predictive Model for Straw Bale Assemblies Subjected to Eccentric Load ...	178
6.6.1 Assumptions.....	178
6.6.2 Eccentric Theoretical Model	180
6.6.3 Calculation of Vertical Displacements	183
6.6.4 Calculation of Lateral Displacements	184
6.6.5 Input Parameters	185
6.7 Results and Observations.....	186
6.7.1 Ultimate Load Results	186
6.7.2 Load-Deflection Results	186
6.8 Discussion.....	187
6.8.1 General Behaviour and Failure Mechanisms	187
6.8.2 Eccentric Compression Experiments	189
6.8.2.1 Ultimate Strength	189
6.8.2.2 Vertical Load-Deflection Relationship.....	191

6.8.2.3 Lateral Deflection Behaviour.....	191
6.8.2.4 Failure Mode Discussion.....	193
6.8.3 Concentric Compression Experiments.....	193
6.8.3.1 Ultimate Strength.....	193
6.8.3.2 Vertical Load-Deflection Relationship.....	195
6.8.3.3 Failure Mode Discussion.....	196
6.9 Conclusions.....	197
Chapter 7 : Research Summary and Design Recommendations.....	220
7.1 Introduction.....	220
7.2 Summary and Analysis of Ultimate Strength Data.....	221
7.2.1 Comparison of Ultimate Strength Results.....	221
7.2.2 Comparison of Experimental Results with Theoretical Behaviour.....	222
7.2.3 Explanations for Strengths Lower than Theoretical.....	224
7.3 Parametric Study.....	226
7.4 Design Recommendations.....	228
7.4.1 Introduction.....	228
7.4.2 Design and Construction Recommendations for.....	229
Plastered Straw Bale Walls	
7.4.3 Lime-Cement Plaster Design Considerations.....	233
Chapter 8 : Conclusions.....	241
8.1 Summary.....	241
8.2 Key Findings.....	242
8.2.1 Major Conclusions.....	242
8.2.2 Conclusions from Experiments on Lime-Cement Plaster and.....	242
Un-Plastered Straw Bales	
8.2.3 Conclusions from Experiments on Centrally Compressed.....	243
Plastered Straw Bale Assemblies	
8.2.4 Conclusions from Experiments on Eccentrically Compressed.....	245
Plastered Straw Bale Assemblies	
8.3 Design Recommendations for Straw Bale Construction.....	246

8.4 Recommendations for Future Research.....	247
References	252
Appendix A: Experimental Procedures and Instrumentation.....	261
A.1 Introduction.....	261
A.2 Experimental Procedures and Instrumentation	261
A.2.1 Plaster Mixing Apparatus	261
A.2.2 Plaster Capping Techniques.....	262
A.2.3 Load and Deflection Application and Measurement	263
A.2.4 Data Acquisition	263
Appendix B: Particle Image Velocimetry Details	265
B.1 Introduction.....	265
B.2 Reason for Use.....	265
B.3 Materials and Procedure	267
B.4 Expected Precision.....	269
B.5 Validation.....	269
Appendix C: Experimental Results	275
C.1 Introduction.....	275
Appendix D: On-Edge Assembly Results	282
D.1 Introduction.....	282
D.2 Fabrication.....	282
D.3 Results and Discussion	283

Appendix E: Validation of Behaviour Assumptions	290
E.1 Introduction.....	290
E.2 Failure Mode Assumption.....	291
E.2.1 Introduction	291
E.2.2 Local Buckling.....	291
E.2.3 Global Buckling	294
E.2.4 Analysis.....	295
E.3 Analysis of Straw/Plaster Interface and Shear Distortion.....	296
Appendix F: Analysis of Assembly Plaster Thickness.....	300
F.1 Introduction	300
F.2 Procedure	300
F.3 Results.....	301
Appendix G: LP Measurement Correction.....	309
G.1 Introduction	309
G.2 Procedure for Correction Determination	310
Appendix H: Eccentric Model Coding	314
H.1 Introduction.....	314
H.2 Main Program.....	315
H.3 Sub-Programs	321
Appendix I: Supplemental Lateral Deflection Plots	322
I.1 Introduction	322
I.2 Results	322
I.3 Discussion.....	323
I.3.1 Eccentric 0.33 m Specimens.....	323
I.3.2 Concentric Specimens	324
I.4 Conclusions	325

List of Figures

Chapter 1

Figure 1.1a:	Simplified Typical Wall Details 19 (Un-Plastered, Incomplete Box Beam)
Figure 1.1b:	Simplified Typical Wall Details (Completed Wall) 19
Figure 1.2:	Image of Base Plate 20
Figure 1.3:	Strapping for Pre-Compression 20
Figure 1.4:	Construction of Box Beam 20
Figure 1.5:	Mesh Applied to Straw Bale Wall 21
Figure 1.6:	Bales Laid Flat and on Edge 21

Chapter 2

Figure 2.1:	Stress -Strain Curves for Flat Three-String Wheat Bales 59 (Bou-Ali, 1993)
Figure 2.2:	Stress-Strain Curves for On Edge Three-String Wheat Bales 59 (Bou-Ali, 1993)
Figure 2.3:	Influence of the Ratio of Cementitious Materials Volume (V_{cm}) to 60 Sand Volume (V_s) on Lime-Cement Plaster Ultimate Strength
Figure 2.4:	Influence of the Ratio of Cement Volume (V_c) to Lime Volume (V_l).... 60 on Lime-Cement Plaster Ultimate Strength
Figure 2.5:	Influence of Curing Time on Lime-Cement Plaster Ultimate Strength 61
Figure 2.6:	Stress-Strain Curves For Varying Cement : Lime : Sand 61 Ratios (Kaushik et al., 2007)
Figure 2.7:	Concentric Load on Straw Bale Wall 62
Figure 2.8:	Eccentric Load or Moment on Straw Bale Wall 62
Figure 2.9:	Shear Stress in Straw Bale Wall Causing Slippage 62
Figure 2.10:	Shear Stress in Straw Bale Wall Causing Shear Distortion 62

Chapter 3

Figure 3.1:	Setup of Compression Test of Plaster Cylinder	95
Figure 3.2:	Sample Stress-Strain Curve up to 40% of Ultimate Load	95
Figure 3.3:	Plaster Modulus of Elasticity as a Function of Cylinder Strength for .. Individual Plaster Specimens	96
Figure 3.4:	Concrete Stress-Strain Model (Desayi and Krishnan, 1964)	96
Figure 3.5:	Comparison of Theoretical and Experimental	97
	Stress-Strain Curves I	
Figure 3.6:	Comparison of Theoretical and Experimental	97
	Stress-Strain Curves II	
Figure 3.7:	Comparison of Theoretical and Experimental	98
	Stress-Strain Curves III	
Figure 3.8:	Relationship between Cube (f'_{cube}) and Cylinder (f'_{cyl}) Strength	98
Figure 3.9:	Variability of Specimen Strength (f'_{cube}) within a Batch	99
Figure 3.10:	Variability of Compressive Strength between Batches	99
Figure 3.11:	Influence of Dry Material Mix Proportions on Compressive	100
	Cube Strength	
Figure 3.12:	Influence of Practical Dry Material Mix Proportions on Compressive	100
	Cube Strength	
Figure 3.13:	Relationship between w/cm Ratio and Compressive Strength	101
Figure 3.14:	Relationship between Slump and Compressive Strength	101
Figure 3.15:	Strength Gain with Curing Time Less than 28 Days	102
Figure 3.16:	Straw Bale Fabrication Jig	102
Figure 3.17:	Trimming Straw Bale in Fabrication Jig	103
Figure 3.18:	Straw Bale Compression Test Setup	103
Figure 3.19:	Load-Deflection Curve for Flat Un-Plastered Bale	104
Figure 3.20:	Load-Deflection Curve for On-Edge Un-Plastered Bale	104
Figure 3.21:	Stress-Strain Curve for Flat Un-Plastered Bale	105
Figure 3.22:	Stress-Strain Curve for On-Edge Un-Plastered Bale	105

Chapter 4

Figure 4.1:	Procedure for Preparing Plastered Straw Bale Assemblies	126
Figure 4.2:	Dimensions of Fabricated Plastered Straw Bale Assemblies	127
Figure 4.3:	Trimmed Bale with Edging	127
Figure 4.4:	Plastered Straw Bale with Edging.....	128
Figure 4.5:	Completed Plastered Bale	128
Figure 4.6:	Plastered Straw Bale Compression Test Instrumentation Setup.....	129
Figure 4.7:	Plastered Straw Bale Compression Test Setup and Loading.....	129
	Plate Design	
Figure 4.8:	Photograph of Test Setup for Preliminary Assembly Testing	130
Figure 4.9:	Typical Load-Displacement Response of Plastered Straw Bale Assembly Measured with Six LP's (DISP 1 - DISP 6)	130
Figure 4.10:	Bearing Failure of a Plastered Straw Bale	131
Figure 4.11:	Averaged Pre-Failure Load-Displacement Response for Plastered Straw Bale	131
Figure 4.12:	Schematic of Plastered Straw Bale.....	132
Figure 4.13:	Free-Body Diagram of Loading Plate.....	132
Figure 4.14:	Ratios of Experimental to Theoretical Strengths for Plastered	133
	Straw Bales	

Chapter 5

Figure 5.1:	Steel Testing and Fabrication Jig.....	157
Figure 5.2:	Fabrication of 2.31 m Wall Using Testing and Fabrication Jig.....	157
Figure 5.3:	Plastered Straw Bale Assembly Test Instrumentation Setup	158
Figure 5.4:	Test Setup for 0.99 m Specimens.....	158
Figure 5.5:	Test Setup for 2.31 m Specimens.....	159
Figure 5.6:	Lateral LP Orientation	160
Figure 5.7:	Lateral LP Setup for Three Bale Tests #1 and #2	160
Figure 5.8:	Photograph Used for PIV Analysis.....	161
Figure 5.9:	Load-Deflection Response of 0.99 m Plastered Wall Assembly #1..	162
Figure 5.10:	Load-Deflection Response of 0.99 m Plastered Wall Assembly #2..	162
Figure 5.11:	Load-Deflection Response of 0.99 m Plastered Wall Assembly #3..	163

Figure 5.12: Load-Deflection Response of Plastered Wall	163
Assembly #4 (2.31 m #1)	
Figure 5.13: Load-Deflection Response of Plastered Wall	164
Assembly #5 (2.31 m #2)	
Figure 5.14: Load-Deflection Response of Plastered Wall	164
Assembly #6 (2.31 m #3)	
Figure 5.15: Load-Deflection Curves for 0.99 m Plastered Straw.....	165
Bale Assemblies	
Figure 5.16: Load-Deflection Curves for 2.31 m Plastered Straw.....	165
Bale Assemblies	
Figure 5.17: Modified Load-Deflection Curves for 0.99 m Plastered Straw.....	166
Bale Assemblies	
Figure 5.18: Modified Load-Deflection Curves for 2.31 m Plastered Straw.....	166
Bale Assemblies	
Figure 5.19: Lateral Load-Deflection Response of 0.99 m Plastered Wall	167
Assembly #1	
Figure 5.20: Lateral Load-Deflection Response of 0.99 m Plastered Wall	167
Assembly #2	
Figure 5.21: Lateral Load-Deflection Response of 0.99 m Plastered Wall	168
Assembly #3	
Figure 5.22: Lateral Load-Deflection Response of Plastered Wall	168
Assembly #4 (2.31 m #1)	
Figure 5.23: Lateral Load-Deflection Response of Plastered Wall	169
Assembly #5 (2.31 m #2)	
Figure 5.24: Lateral Load-Deflection Response of Plastered Wall	169
Assembly #6 (2.31 m #3)	
Figure 5.25: Lateral Deflections from PIV of Plastered Wall.....	170
Assembly #6 (2.31 m #3) Entire Wall Height at Ultimate Load	
Figure 5.26: Typical Compression Failure of Plastered Straw Bale.....	170
Wall Assemblies	
Figure 5.27: Progressive Failure of Plastered Straw Bale Wall Assemblies.....	171

Chapter 6

Figure 6.1:	330 mm Specimen Subjected to Eccentric Load	201
Figure 6.2:	Top Plate of Modified Loading Jig Subjected to Eccentric Load.....	201
Figure 6.3:	Concentric Loading of Specimen in Modified Jig	202
Figure 6.4:	Eccentrically Loaded Plastered Straw Bale Assembly Test Setup ...	202
Figure 6.5:	Rotation of Top Plate with Bale Rebound and Eccentric Load	203
Figure 6.6:	Flow-Chart for Eccentric Theoretical Analysis	204
Figure 6.7:	Loading Diagrams for Eccentric Model	205
Figure 6.8:	Stress-Strain Profile for Eccentric Model	206
Figure 6.9:	Curvature Analysis for Eccentric Model	206
Figure 6.10a:	Vertical Load-Deflection Plot for Specimen E11	207
Figure 6.10b:	Failure of Specimen E11	207
Figure 6.11a:	Vertical Load-Deflection Plot for Specimen E12	208
Figure 6.11b:	Failure of Specimen E12	208
Figure 6.12a:	Vertical Load-Deflection Plot for Specimen E13	209
Figure 6.12b:	Failure of Specimen E13	209
Figure 6.13a:	Vertical Load-Deflection Plot for Specimen E31	210
Figure 6.13b:	Failure of Specimen E31	210
Figure 6.13c:	Mid-Height Lateral Load-Deflection Plot for Specimen E31	210
Figure 6.13d:	Full-Height Lateral Deflection at Ultimate Load for Specimen E31...	210
Figure 6.14a:	Vertical Load-Deflection Plot for Specimen E32	211
Figure 6.14b:	Failure of Specimen E32	211
Figure 6.14c:	Mid-Height Lateral Load-Deflection Plot for Specimen E32	211
Figure 6.14d:	Full-Height Lateral Deflection at Ultimate Load for Specimen E32...	211
Figure 6.15a:	Vertical Load-Deflection Plot for Specimen E33	212
Figure 6.15b:	Failure of Specimen E33	212
Figure 6.15c:	Mid-Height Lateral Load-Deflection Plot for Specimen E33	212
Figure 6.15d:	Full-Height Lateral Deflection at Ultimate Load for Specimen E33...	212
Figure 6.16a:	Vertical Load-Deflection Plot for Specimen C11	213
Figure 6.16b:	Failure of Specimen C11	213
Figure 6.17a:	Vertical Load-Deflection Plot for Specimen C12	214
Figure 6.17b:	Failure of Specimen C12	214

Figure 6.18a: Vertical Load-Deflection Plot for Specimen C13.....	215
Figure 6.18b: Failure of Specimen C13	215
Figure 6.19a: Vertical Load-Deflection Plot for Specimen C31.....	216
Figure 6.19b: Failure of Specimen C31	216
Figure 6.20a: Vertical Load-Deflection Plot for Specimen C32.....	217
Figure 6.20b: Failure of Specimen C32	217
Figure 6.21: Load-Deflection for Entire Duration of Experiment C31.....	218
Figure 6.22: Load-Deflection for Entire Duration of Experiment E33.....	218
Figure 6.23: Tensile Failure of Second Plaster Skin	219

Chapter 7

Figure 7.1: Summary of Experimental Ultimate Strengths.....	235
(Multiple Bars Indicate Test Repetition)	
Figure 7.2: Summary of Experimental Results from the Literature	236
(Multiple Bars Indicate Test Repetition)	
Figure 7.3: Summary of Experimental to Theoretical Strength Ratios for.....	237
Results from the Literature (Multiple Bars Indicate Test Repetition)	
Figure 7.4: Relationship Between Plaster Strength and Experimental to	238
Theoretical Strength Ratio	
Figure 7.5: Effect of Eccentricity on Plastered Straw Bale Assembly Strength ..	238
Figure 7.6: Effect of Specimen Height on Plastered Straw Bale.....	239
Assembly Strength	
Figure 7.7: Effect of Plaster Thickness on Plastered Straw Bale.....	239
Assembly Strength	
Figure 7.8: Effect of Plaster Strength on Plastered Straw Bale	240
Assembly Strength	

Appendix B

Figure B.1: Comparison of PIV and LP Data.....	272
Figure B.2: Colour Texturing of Plastered Straw Bale Wall Assembly for PIV	272
Figure B.3: Camera Set-Up for PIV	273
Figure B.4: Control Test #1 – Zero Load	273

Figure B.5: Control Test #2 – Known Displacement.....	274
---	-----

Appendix D

Figure D.1: Procedure for Preparing On-Edge Plastered Straw Bale Assemblies	287
Figure D.2: Typical Load-Displacement Response for On-Edge Plastered Straw Bale	288
Figure D.3: Typical Failure of an On-Edge Plastered Straw Bale	288
Figure D.4: Relationship Between Plaster Strength and Assembly Strength for On-Edge Assemblies	289

Appendix E

Figure E.1: Slippage at Straw/Plaster Interface.....	299
--	-----

Appendix F

Figure F.1: Measurement of Plaster Thickness.....	304
Figure F.2a: E11 Failure Side.....	305
Figure F.2b: E11 Non-Failure Side.....	305
Figure F.3a: E12 Failure Side.....	305
Figure F.3b: E12 Non-Failure Side.....	305
Figure F.4a: E13 Failure Side.....	305
Figure F.4b: E13 Non-Failure Side.....	305
Figure F.5a: E31 Failure Side.....	306
Figure F.5b: E31 Non-Failure Side.....	306
Figure F.6a: E32 Failure Side.....	306
Figure F.6b: E32 Non-Failure Side.....	306
Figure F.7a: E33 Failure Side.....	306
Figure F.7b: E33 Non-Failure Side.....	306
Figure F.8a: C11 Failure Side	307
Figure F.8b: C11 Non-Failure Side	307
Figure F.9a: C12 Failure Side	307
Figure F.9b: C12 Non-Failure Side	307

Figure F.10a: C13 Failure Side	307
Figure F.10b: C13 Non-Failure Side	307
Figure F.11a: C31 Failure Side	308
Figure F.11b: C31 Non-Failure Side	308
Figure F.12a: C32 Failure Side	308
Figure F.12b: C32 Non-Failure Side	308
Figure F.13a: C33 Failure Side	308
Figure F.13b: C33 Non-Failure Side	308

Appendix G

Figure G.1: Diagram of Deformation in HSS Section.....	312
Figure G.2: Aluminum Plates in Testing Jig.....	312
Figure G.3: Correction Amount	313

Appendix I

Figure I.1a: Mid-Height Lateral Load-Deflection Plot for Specimen E11	326
Figure I.1b: Full-Height Lateral Deflection at Ultimate Load for Specimen E11... ..	326
Figure I.2a: Mid-Height Lateral Load-Deflection Plot for Specimen E12	326
Figure I.2b: Full-Height Lateral Deflection at Ultimate Load for Specimen E12... ..	326
Figure I.3a: Mid-Height Lateral Load-Deflection Plot for Specimen E13	327
Figure I.3b: Full-Height Lateral Deflection at Ultimate Load for Specimen E13... ..	327
Figure I.4a: Mid-Height Lateral Load-Deflection Plot for Specimen C11	327
Figure I.4b: Full-Height Lateral Deflection at Ultimate Load for Specimen C11 ..	327
Figure I.5a: Mid-Height Lateral Load-Deflection Plot for Specimen C12	328
Figure I.5b: Full-Height Lateral Deflection at Ultimate Load for Specimen C12 ..	328
Figure I.6a: Mid-Height Lateral Load-Deflection Plot for Specimen C13	328
Figure I.6b: Full-Height Lateral Deflection at Ultimate Load for Specimen C13 ..	328
Figure I.7a: Mid-Height Lateral Load-Deflection Plot for Specimen C31	329
Figure I.7b: Full-Height Lateral Deflection at Ultimate Load for Specimen C31 ..	329
Figure I.8a: Mid-Height Lateral Load-Deflection Plot for Specimen C32	329
Figure I.8b: Full-Height Lateral Deflection at Ultimate Load for Specimen C32 ..	329

List of Tables

Chapter 2

Table 2.1:	Modulus of Elasticity Values for Lime-Cement Plaster	57
Table 2.2:	Modulus of Rupture Values for Lime-Cement Plaster	57
Table 2.3:	Ultimate Strength Values for Plastered Straw Bale Walls under Concentric Load	58

Chapter 3

Table 3.1:	Comparison of Experimental vs. Theoretical Average..... Cube Strengths	94
Table 3.2:	Bale Modulus Values for Un-Plastered Straw Bales.....	94

Chapter 4

Table 4.1:	Test Parameters for Compression Tests of Individual..... Plastered Straw Bales	125
Table 4.2:	Experimental and Theoretical Plastered Straw Bale Strengths.....	125

Chapter 5

Table 5.1:	Comparison of Plastered Straw Bale Wall Assembly Theoretical Strength to Experimental Strength	156
------------	---	-----

Chapter 6

Table 6.1:	Description of Experimental Parameters and Theoretical Strengths	200
Table 6.2:	Comparison of Experimental and Theoretical Strengths	200

Appendix A

Table A.1:	Load and Deflection Application and Measurement Apparatus.....	264
------------	--	-----

Appendix C

Table C.1:	Plaster Compression Test Results.....	277
Table C.2:	Assembly Testing Results.....	281

Appendix D

Table D.1: Results for On-Edge Plastered Straw Bale Assemblies 286

Appendix E

Table E.1: Theoretical Strength Analyses 298

Appendix F

Table F.1: Summary of Plaster Thicknesses 303

Notation

A_A	area of aluminum
A_{straw}	area of straw
$Corr$	correction for LP measurement for concentric experiments
$Corr_{EccFail}$	correction for failure side LP for eccentric experiments
$Corr_{EccNonFail}$	correction for non-failure side LP for eccentric experiments
CV	coefficient of variation (standard deviation divided by mean)
E	Modulus of Elasticity
E_A	Modulus of Elasticity of aluminum
E_c	Modulus of Elasticity of concrete
E_{cube}	Modulus of Elasticity of plaster cube specimen
E_{cyl}	Modulus of Elasticity of plaster cylinder specimen
E_{straw}	straw bale modulus
e	eccentricity of compressive load application
e_1	eccentricity of plaster skin number 1
e_2	eccentricity of plaster skin number 2
f'_c	cylinder strength of concrete
f'_{cube}	cube strength of plaster (generic)
f'_{cube28}	cube strength of plaster at 28 days

f_{cyl}	cylinder strength of plaster
f_1	non-failure side stress at extreme fibre of plastered straw bale assembly subjected to eccentric load
f_2	failure side stress at extreme fibre of plastered straw bale assembly subjected to eccentric load
f_c	stress in concrete at given strain ϵ
F_{Ult}	force in plastered bale assembly at ultimate failure
h	height of plastered bale assembly
h'	height of straw required to provide the necessary lateral support to prevent local buckling
I	moment of inertia
k	effective length factor for compression members
k'	constant for Collins and Mitchell (1997) concrete stress-strain relationship
L	length of plaster skin for plastered straw bale wall assemblies
L_A	length of aluminum column for deflection calculation
n	constant for Collins and Mitchell (1997) concrete stress-strain relationship
P	applied load
P_1	load resistance of plaster skin number 1

P_2	load resistance of plaster skin number 2
P_A	load applied to aluminum
P_{cr}	critical axial load for buckling failure
S_B	bond strength for straw/plaster bond
S_p	patch size for Particle Image Velocimetry (PIV) analysis
t	time
t_d	design thickness of plaster for plastered straw bale assembly
t_p	thickness of plaster for plastered straw bale assembly
V_c	volume of cement in plaster mix
V_{cm}	volume of cementitious materials (cement and lime) in plaster mix
V_l	volume of lime in plaster mix
V_s	volume of sand (not including moisture) in plaster mix
W	width of plastered straw bale wall assembly, typically including the straw width and two times the plaster width
w/cm	water/cementitious materials ratio: mass of water divided by the mass of cementitious materials (cement and lime)
W_s	width of straw bale

Δ_A	deflection in aluminum
ε	strain
ε_1	non-failure side strain at extreme fibre of plastered straw bale assembly subjected to eccentric load
ε_2	failure side strain at extreme fibre of plastered straw bale assembly subjected to eccentric load
ε_{cube}	strain in plaster cube at ultimate stress
ε_{cyl}	strain in plaster cylinder at ultimate stress
ε_o	strain in concrete at ultimate stress
ρ_{pixel}	conservative estimate of precision error expected using PIV
σ	stress
φ	curvature of eccentrically loaded plastered straw bale assembly

Chapter 1: Introduction

1.1 Background

With concern growing in regards to global warming and the depletion of the Earth's resources, a new focus on environmental sustainability has arisen throughout the world. This concern can be quantified by considering humanity's ecological footprint: defined as "the area of productive land and water ecosystems required to produce the resources that the population consumes and assimilate the wastes that the population produces, wherever on Earth the land and water is located" (Wackernagel and Rees, 1996). According to the 2004 Living Planet Report (World Wildlife Fund, 2004) the 2001 total global ecological footprint was 13.5 billion hectares (and growing), while the actual global capacity was only 11.5 billion hectares. When looking specifically at the construction industry in Canada, Sangster (2006) states that the 12.5 million residential units and 430,000 commercial and institutional buildings account for "33% of total energy use, 50% of natural resource consumption, ... 30% of Canadian greenhouse gas emissions and ... 25% of the

nation's landfill waste." (Sangster 2006) In addition, modern construction materials such as steel, timber, and concrete have greater embodied energy than many alternative options. Embodied energy is defined as the amount of energy which is required to produce a particular service or product

Currently, the construction industry is heavily focused on the use of concrete, steel, timber and stone. It is clear however that this current global trend is not sustainable. Concrete with its massive greenhouse gas emissions, huge embodied energy, and extensive use of natural resources; timber with the danger of deforestation and loss of rainforests; and steel and stone with their consumption of natural resources; all have huge environmental implications associated with their use (Wilson, 1993). Thus, in order to reach a level where society is building in a sustainable manner, it is imperative that more environmentally friendly alternatives to these materials be found and used whenever possible.

As society begins to realize the need for change, a new focus will arise within the construction industry. This focus will center on creating structures that require fewer non-renewable resources, both for their construction and their maintenance. As a result, there is, and will continue to be, a strong desire for more renewable, durable, and low embodied energy construction materials, and for structures which require significantly less energy to heat and cool. One re-emerging construction practice which has shown great promise in meeting this new focus is *straw bale construction*.

1.2 History

The use of straw bales as a construction material is not a new concept. Straw has been used in various forms for construction purposes for thousands of years (Magwood and Mack, 2000). In North America, the earliest documented straw bale structures date back to the 1800's, with the oldest known surviving straw bale house built in 1903 in Alliance, Nebraska (U.S. DOE, 1995). Although this structure was abandoned in the 1950's, the building still stands today, resisting the strong winds and large temperature fluctuations prevalent in the Nebraska region (King, 2006).

These early structures utilized straw as a construction material out of necessity, as the settlers of the Nebraskan Sand Hills found their region devoid of adequate lumber or suitable sod, the more common construction materials of the time. This area was however a well established grain-growing region in which there was a plethora of rectangular straw bales produced by horse-driven baling machines, introduced in the 1870's (Magwood and Mack, 2000). Thus, it was only a matter of time before the inhabitants realized the potential of the rectangular bales as a building material. Early straw bale structures consisted of little more than rectangular bales, stacked and plastered to form the walls with a roof structure placed atop the walls (King, 1996).

Through the late 1800's and the early 1900's the Nebraskan Sand Hills region became the home to approximately 70 straw bale buildings, a number of which are still standing today (Lerner et al., 2000). The success of straw as a building material did not last long however. With the construction of railways and highways across the

1.0 Introduction

globe came the ability to transport timber and other building materials to construction sites and the use of straw as a construction material diminished. The construction industry shifted, and the more popular and well-known materials of today (wood, steel, stone, concrete) became the materials of choice.

The status-quo remained for many years with a strong focus on wood, steel, stone, and concrete within the construction industry. In the 1970's however, things began to change (Lerner et al., 2000). As society started to become aware of the fragility of the environment, more and more people began to look for ways of minimizing their personal impact on the earth. This change in thinking eventually led to the re-discovery of straw bale construction as a viable and environmentally sustainable construction practice. Industry pioneers began building structures and documenting their endeavours. Straw bale construction continued to gain momentum through the 1980's and 1990's, with the beginning of the new millennium seeing this re-emerging technology spreading throughout the world. The straw bale building industry continues to grow today, with over 80 buildings currently listed on the Ontario Straw Bale Building Coalition's (OSBBC's) website (OSBBC, 2004).

1.3 Advantages

There are a number of purported advantages associated with straw bale construction. However, it is the positive environmental impact of straw bale construction that really drives this re-emerging industry. The most notable environmental advantage is the excellent insulation capability of a straw bale wall. There is documented anecdotal evidence of the thermal performance of straw bale

1.0 Introduction

walls. Homeowners around the world agree that the heating and cooling requirements for a straw bale home are much less than required for even a well constructed stud wall home with fiberglass insulation (Magwood et al., 2005). Watts et al. (1995) suggest that the “R-value of the straw bale walls is in the range of super efficient homes.” The R-value of a material describes the ability of the material to resist the flow of heat and thus, a greater R-value is desired. Stone (2003) discusses the thermal performance of straw bale wall systems commenting on the variation in reported R-values in the literature, but concluding that an R-value of R-30 for straw bale walls is acceptable to use in comparison to typical wall designs. This is significant, as a typical stud wall with fiberglass insulation has been found to perform at an R-value of approximately R-11, despite claims that these systems maintain an R-value of R-19 (Stone, 2003).

The environmental benefits associated with straw bale construction extend beyond those associated with the insulative properties of these walls. Considering straw is an agricultural by-product that is often disposed of through incineration, the use of this material in any capacity provides an immediate positive environmental impact to the planet. Straw is annually renewable, has a low embodied energy, and reduces the reliance on lumber, saving valuable forests (U.S. DOE, 1995). Straw is available throughout most of the world and as a result is regularly available locally, and thus can save significant (environmental and financial) transportation costs. It has been stated that “America’s farmers annually harvest enough straw to build about four million, 2,000 square-foot homes each year, nearly four times the houses

currently constructed” (U.S. DOE, 1995), and the quantities will continue to rise as global grain requirements for food and fuel escalate.

1.4 Concerns

There are a number of concerns regarding the use of straw as a construction material. Some of these concerns are valid, while others have been proven moot. One of the most common concerns is regarding fire performance. Loose straw is a very combustible material, but straw which is tightly packed into a bale is much less likely to burn. The density of the straw bales makes it difficult for oxygen to reach and fuel a potential fire, while the plaster coating on the walls provides an insulating barrier keeping exterior flames away from the bales. Evidence of this behaviour has been found in a number of laboratory fire tests. The most significant tests were completed by Intertek Laboratories. These tests showed that a “10 ft x 10 ft [3.05 m x 3.05 m] non-loadbearing wall ... clad on each surface with ... 1” [25.4 mm] of cement/stucco ... successfully met the conditions of acceptance as outlined in ASTM [American Society for Testing Materials] Method E 119-05a Fire Tests of Building Construction and Materials for a fire endurance rating of 2 hours” (Intertek, 2007a) and that a “12 ft x 14 ft [3.66 m x 4.27 m] non-loadbearing wall ... clad on each surface with 1” [25.4 mm] of earthen-plaster ... successfully met the conditions of acceptance as outlined in ASTM Method E 119-05a Fire Tests of Building Construction and Materials for a fire endurance rating of 1-hour” (Intertek, 2007b).

Another major concern is with moisture management within straw bale walls. The potential for rot within the straw and the associated issues are well documented

1.0 Introduction

with anecdotal and research information. There have been limited studies in this regard and King (2006) presents a comprehensive summary of this information. Straube (2006) states that the “primary durability concern for straw bale buildings is wetting by rain, particularly driving rain. However, plumbing leaks, air leakage, ground water, and roof leaks can be problems as well, and must be addressed.” Regarding these concerns, Straube (2006) goes on to state that the “moisture tolerance of houses can be drastically improved through intelligent design of building location, orientation, geometry, HVAC systems, and materials.” Essentially, while moisture is of concern, proper detailing and maintenance of a structure will alleviate these concerns.

Other, less prevalent concerns regarding straw bale construction do exist. It has been reported that some straw bale structures have suffered from insect infestations (King, 2006). Based on evidence from these reports it was discovered that the root cause of the infestations was actually the moisture in the bales. Thus, similar to above, insect problems can be mitigated through appropriate design.

Issues regarding other, larger pests such as mice and rats are non-existent. In contrast to loose straw (and even stud walls), tightly compressed bales, coated in plaster, do not provide an attractive environment for larger pests. There is very little room for such animals to travel in a well-built wall, and the straw itself is unappealing as a food source, given its toughness and lack of nutritional benefit (King, 2006).

The final common concern regarding straw bale construction is in regards to the structural adequacy of this type of construction. This is of major significance for

load-bearing construction, where the plastered straw bale walls act to resist the loading on the structure. From the information presented in Chapter 2 of this thesis it is clear that while there is evidence supporting load-bearing construction, a deficiency in technical data exists in the current knowledge and literature related to the structural performance of plastered straw bale walls and thus, further research is needed.

1.5 Construction Practices and Constitutive Materials

1.5.1 Construction Practices

There are many ways in which straw has been incorporated into a variety of building materials and building techniques over the years. The most common method for using straw in the construction industry is in the form of plastered straw bale walls. There are an abundance of design options available to straw bale builders, but there are a number of specific elements common to all plastered straw bale walls. As shown in Figures 1.1a and 1.1b, the general composition of a plastered straw bale wall includes an inner core of stacked straw bales and two outer plaster skins, which are applied to the interior and exterior surfaces of the wall. The walls may be reinforced using any number of different techniques and materials, and many other details of the wall can vary significantly from one structure to another.

There are two main methods of building straw bale walls. Non-load-bearing construction utilizes the straw solely as an insulation material. The structural capacity of non-load-bearing straw bale walls is provided by other materials such as steel, concrete or timber. The straw is used as an infill to provide insulation for the

1.0 Introduction

structure. This type of construction provides many benefits, but does not allow for the replacement of less environmentally friendly materials such as concrete or timber. Load-bearing construction, or the “Nebraska-style”, utilizes the straw and plaster to provide the structural capacity of the building. The focus of this thesis is on load-bearing straw bale construction, as it is this method for which there is the greatest deficiency in the understanding of the structural behaviour.

A typical load-bearing straw bale wall is shown in Figures 1.1a and 1.1b. With this type of construction, the bales are stacked on a base plate in a “running bond” style. With a running bond, as illustrated in Figure 1.1a, each successive layer is offset a half-bale length from the previous layer. This ensures that bale joints do not occur at the same location in adjoining layers. The design of the base plate on which the bales are laid varies from project to project but typically consists of 2x4’s (38 mm x 89 mm) laid flat with the outer edges in line with the designed location of the outer edge of the plaster skins as can be seen in Figures 1.1a, 1.1b, and 1.2. With the bales stacked on the base plate, a box beam is then placed on the bales and is ratcheted down to compress the wall to a specified height, pre-compressing the bales in the process. There are various methods used to ratchet down the box beam but generally, strapping is run through the base plate (as shown in Figure 1.3) and then through the box beam. This strapping is then mechanically tightened before being fastened in place. The strapping will then get coated over with plaster and sealed into the wall. As with the base plate, the design of the box beam can vary significantly from project to project. A typical box beam is shown in Figures 1.1a, 1.1b, and 1.4, and consists of a 2x4 ladder, constructed with the 2x4s

1.0 Introduction

on-edge, sandwiched between sheets of plywood. As with the base plate, the outer edges of the box beam are designed to fall in line with the designed location of the outer edge of the plaster skins.

With the box beam in place, plaster is then applied to the wall. A typical plaster application will consist of three coats of plaster. The first is intended to create a bond with the straw and to level out any major unevenness of the bales. This coat is worked into the straw to provide the greatest bond possible. The second coat will give the wall its general shape. This coat will bring the level of plaster out from the relatively uneven first coat to approximately the required plaster thickness, leveling the surface of the wall. The final coat is primarily an aesthetic coat, and is very thin, giving the wall its final appearance. Once the plaster has been applied it is left to cure in order to gain strength over time. Some walls contain a reinforcement mesh (steel wire, polypropylene, etc.) between the straw and the plaster. This mesh is placed against the straw, prior to plastering the wall, and is tied through the wall from inside to out as shown in Figure 1.5. The plaster is then applied and pressed through the mesh into the straw forming a mechanical bond between the interior and exterior plaster skins.

It is this general design, shown in Figures 1.1a and 1.1b which must first be understood before one can even begin to consider variations in construction practices. Therefore, the focus of this thesis will be to study the response of this most common, simplified straw bale wall design under compressive loading. The main components of this wall are the straw, plaster, reinforcing mesh, box beam, and base plate. The use of mesh has been shown to be important for some types of

loading, but it creates difficulties in construction, and is omitted from some less conservative designs (King, 2006). Because of this, it was decided to omit the mesh from the walls tested in this thesis in order to be conservative, and to improve the ease of construction. In typical straw bale construction, the box beam and base plate are built of timber, a material that is very well understood. Therefore, for this thesis, the design of the box beam and base plate are not studied. It is the performance of the composite straw-plaster assembly which is the focus of this thesis as it is this aspect of straw bale construction which is not currently well understood.

1.5.2 Description of Straw

Straw is the dried tubular stalk of a plant connecting the roots to the grain head of the plant. Hay, often confused with straw, is the entire plant (excluding the roots). Hay has higher moisture content than straw and is often used as feed for livestock because the grain head of the plant provides nutritional value. Straw is considered to have zero nutritional value and is thus used primarily for animal bedding or simply burned.

There are many different types of straw available. Wheat, barley, oats, rye, rice, and even hemp bales are available throughout the world. The type of straw used for construction purposes generally does not have a great impact on the performance of the structure because it is believed that the straw itself does not typically contribute to the overall plastered straw bale wall strength as will be discussed in greater detail in Chapter 2 (King, 2006).

1.0 Introduction

Straw is produced as a by-product of grain production. The plants are grown in large fields and when the time is right, the grain heads are chopped from the top of the plant leaving the stalk behind. The stalks are then dried, cut, and baled. Straw bales come in a variety of shapes and sizes, from giant round (diameter: 1 – 2 m) and rectangular (1.2 m x 1.2 m x 2.4 m) bales to more manageable two-string or three-string rectangular bales (approx. 0.4 m x 0.5 m x 1.0 m).

The focus of this thesis is on the smallest, most manageable, and widely used bale; the two-string bale. Two-string bales can vary in mass but generally weigh approximately 12 kg, with dimensions of approximately 350 mm in height, 460 mm in width and 890 mm in length (Magwood and Mack, 2000). For construction purposes, bales are used with the longest dimension parallel to the wall. In most construction applications the bales are laid flat with the shortest dimension vertical, but in some cases the bales are stacked on-edge with the shortest dimension perpendicular to the wall (horizontal). Figure 1.6 shows a bale laid flat and a bale on edge. With on-edge construction, the walls are thinner resulting in more interior space for a given building footprint, less bales needed for construction, and less timber used for the base plate and box beam. Because construction with bales laid flat is more common, it is this type of construction which will be the focus of this thesis.

1.5.3 Plaster

1.5.3.1 Introduction

A straw bale wall plaster consists of three main components: aggregate, binder, and water. The aggregate is typically masonry sand or some similar sand. The type of binder used can vary from project to project depending on local conditions and the builder's or owner's preference. The most widely used, and understood plasters are cement-based. These plasters have excellent durability and strength, but the use of cement has a negative environmental impact (Wilson, 1993). More environmentally friendly lime can be added to the cement-based plasters to offset some of the cement; however this comes at a cost of the loss of durability and strength (Pritchett, 2003). For environmental reasons, some builders are experimenting with the use of earthen plasters. For this application, clay, which often comes from a local source, is used as the binder in the plaster.

In addition to the obvious strength requirements, one key property that is desirable for any plaster is the ability to be permeable to vapour. With moisture a key concern in straw bale walls, a vapour-permeable plaster will allow the release of moisture to the atmosphere, should a straw wall become damp. For this reason, the use of plasters with cement as the only binder is unacceptable, and common practice requires either an earthen plaster, or a lime-cement plaster (Pritchett, 2003).

1.5.3.2 Earthen Plaster

Earthen plasters have been used successfully for centuries, but unfortunately, their use continues to be met with scepticism (Magwood and Mack 2000). Typically,

1.0 Introduction

earthen plasters are mixed on-site using local clay-rich soil, sand, and water. Chopped straw may also be added to the mixture to minimize shrinkage cracking and to improve tensile performance. Because of the variability in local soil conditions, it is very difficult to predict the structural behaviour of an earthen plaster. Because of this, some builders have used bagged clay or bulk clay which has been processed to ensure greater quality control. However, this detracts from the positive environmental impact of using local soil. Furthermore, clay plasters typically have low strength and durability and require continuous maintenance throughout the life of the structure (Magwood and Mack, 2000). Earthen plasters are typically mixed by hand or with the help of a mechanical mixer. The earth or clay, sand, and water are mixed together to form the plaster.

1.5.3.3 Lime-Cement Plaster

Plasters using lime and/or cement as the binder have not been around nearly as long as earthen plasters. However, because of their more consistent properties, they have become significantly more popular. Lime-cement plaster is typically mixed in a mechanical mixer, with the dry materials (bagged hydrated lime, cement, sand) added first, followed by the water. Bagged hydrated lime and cement are readily available and are produced under modern quality control standards. The properties of these materials are very consistent and to some extent well understood. Cement is the key component in concrete, a material which is highly engineered, with structural properties and behaviour which are very well documented. An open question is whether models of concrete behaviour can be applied to lime-cement

plaster. Furthermore, there are questions regarding the impact that the proportions of the key materials (lime, cement, sand, water) may have on the properties of lime-cement plasters.

1.5.3.4 Summary

Plaster plays a major role in determining the structural behaviour of a plastered straw bale wall, as will be discussed in Chapter 2. The lack of standard construction practices has led to the use of plasters which vary significantly in composition from site to site. In order to gain greater confidence in the structural adequacy of plastered straw bale walls, it is imperative that building professionals understand the impact that these variations will have on the performance of the walls.

1.6 Research Objectives

This thesis aims to address the aforementioned issues by providing discussions of current literature and results of a series of new experiments on straw bale walls and straw bale wall plasters. The main objective of this thesis is to provide a greater understanding of the structural performance of load-bearing straw bale construction. While designs may vary significantly for this type of construction, this thesis focuses on common designs utilizing bales laid flat with lime-cement plaster. The consistency of the properties of lime-cement plasters relative to earthen plasters provides an added advantage for construction and experimentation of plastered straw bale walls. As noted in Chapter 2, there is a deficiency in the structural knowledge of plastered straw bale walls and thus, any research on the

structural performance of plastered straw bales and straw bale walls is beneficial to the straw bale building community. In addition, it is expected that as the results of this research are published, straw bale construction will gain greater credibility, a very important step for this re-emerging building technique. The specific research goals focus on obtaining a deeper understanding of the mechanics of plastered straw bale walls. These goals are as follows:

1. To develop and experimentally validate an analytical model to predict the structural performance of a plastered straw bale wall subjected to concentric and eccentric compressive loads. This objective will be achieved through Chapters 4 – 6.
2. To use the model to examine the effect of wall height, plaster thickness, and plaster strength on the response of a plastered straw bale wall subjected to concentric and eccentric compressive loading. This objective will be achieved through Chapters 4 – 7.
3. To propose specific design considerations for straw bale construction. This objective will build on objectives one and two, and will be presented in Chapter 7.

In order to develop this model, the following minor objectives will be met within Chapter 3:

- a. To quantify the stress-strain behaviour of lime-cement plasters used in straw bale construction.

- b. To perform a preliminary analysis of the influence of mix proportions and testing methods on the ultimate strength of the plasters, and to quantify the expected variability in the properties of lime-cement plaster.

1.7 Thesis Outline

Chapter 2 provides a review of the literature related to plastered straw bale wall behaviour, and the behaviour of plasters used for the construction of plastered straw bale walls.

Chapter 3 provides details regarding the compressive behaviour of the two key constituent materials of plastered straw bale walls. Results are presented on the compressive behaviour of lime-cement plaster and un-plastered straw bales. A model for the stress-strain behaviour of lime-cement plaster is presented. Portions of this chapter are published in the proceedings of the Engineering Sustainability 2005 Conference (Vardy et al., 2005).

Chapter 4 presents results of the preliminary concentric compressive tests of individual plastered straw bales with varying plaster thickness and strength. Fabrication and testing issues are noted in order to improve on the testing and fabrication methods. A simple model for determination of the ultimate strength of plastered straw bale wall assemblies is presented. Portions of this chapter are published in the Journal of Green Building (Vardy and MacDougall, 2006).

Chapter 5 presents the results of concentric compression tests of plastered straw bale wall assemblies of varying height in order to determine the effect of the

1.0 Introduction

specimen height, and to validate theoretical models for the compressive behaviour of the concentrically loaded plastered straw bale wall assemblies. The experiments utilize an innovative fabrication and testing apparatus, with the goal of producing specimens with consistent dimensions. The results of the experiments are used to validate the model presented in Chapter 4. The stress-strain model for plaster, which was presented in Chapter 3, was used to model the load-deflection behaviour of the plastered straw bale wall assembly specimens. Portions of this chapter are published in the proceedings of the International Conference on Sustainable Construction Materials and Technologies 2007, (Vardy and MacDougall, 2007).

Chapter 6 presents the results of eccentric compression tests of plastered straw bale wall assembly specimens. Specimens of varying height were tested to determine the effect of specimen height on the strength of eccentrically loaded plastered straw bale wall assemblies. The model for the stress-strain behaviour of lime-cement plaster, which was presented in Chapter 3, was expanded to model the behaviour of the eccentrically loaded specimens in order to determine the theoretical ultimate strength and load-deflection behaviour of eccentrically loaded plastered straw bale wall assemblies.

Chapter 7 provides design considerations for straw bale construction professionals. The considerations presented are based on the results presented in previous chapters. Chapter 8 summarizes key findings and design recommendations, and suggests areas for future research.

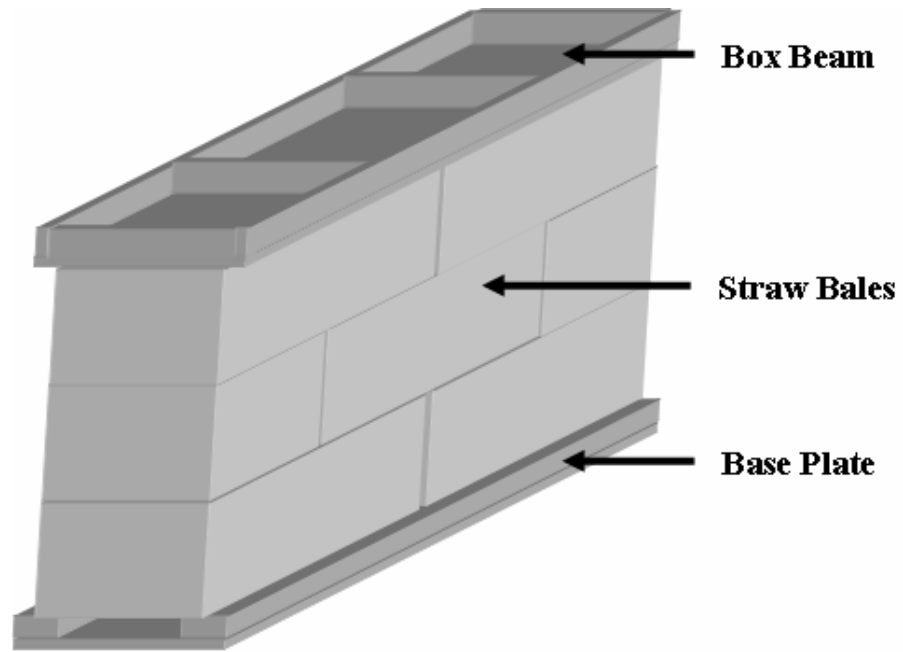


Figure 1.1a: Simplified Typical Wall Details (Un-Plastered, Incomplete Box Beam)

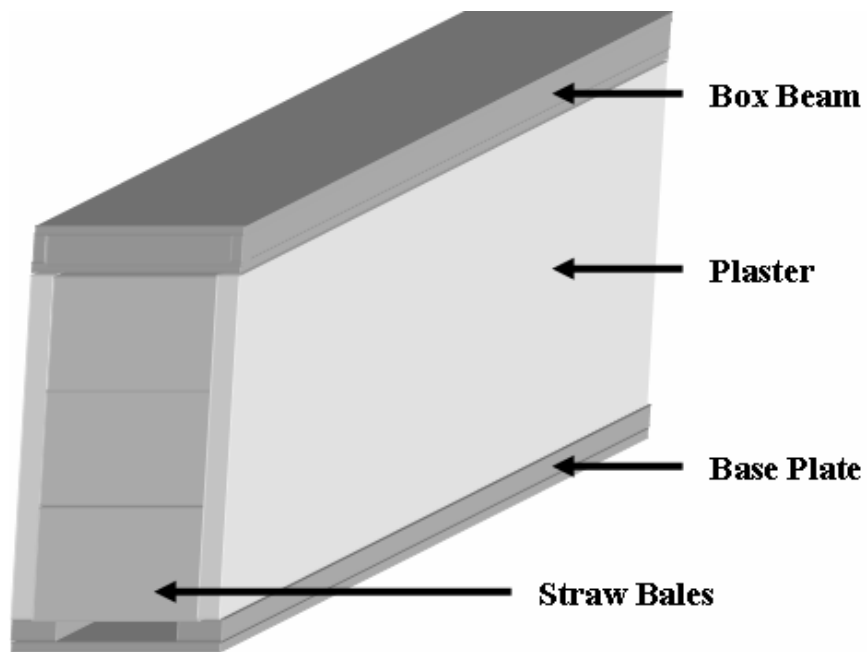


Figure 1.1b: Simplified Typical Wall Details (Completed Wall)

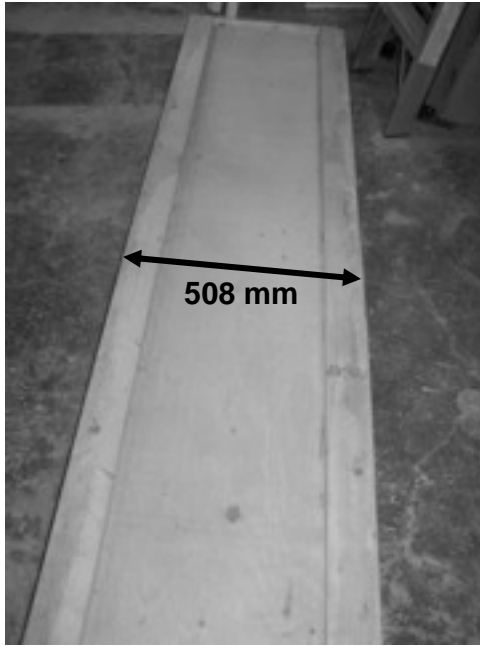


Figure 1.2: Image of Base Plate



Figure 1.3: Strapping for Pre-Compression

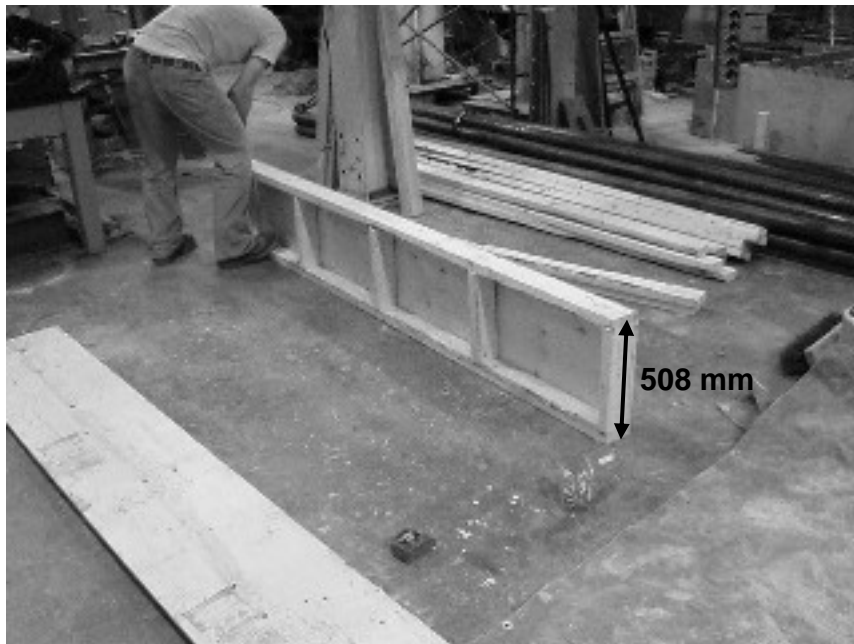


Figure 1.4: Construction of Box Beam



Figure 1.5: Mesh Applied to Straw Bale Wall



Figure 1.6: Bales Laid Flat and on Edge

Chapter 2: Literature Review

2.1 Introduction

With the ever-increasing global desire to live in a more environmentally friendly and sustainable manner, the modern construction industry has begun to utilize alternative materials and construction methods on a more regular basis (Lerner et al., 2000). Many of these alternatives do not make use of new materials or methods, but rather are a modernization of ancient building practices which had been nearly forgotten. The re-birth of straw bale construction, as discussed in the previous chapter, is an excellent example of this modernization of ancient techniques. With this rejuvenation has come the necessity for modern data and research to quantify the structural adequacy of this re-emerging building technique. Where in the past it has been acceptable to build with nothing but limited anecdotal evidence and non-existent structural knowledge, there is now a need for a much greater understanding of the structural performance of straw bale buildings.

2.0 Literature Review

Because of the sporadic nature of the resurgence of straw bale construction, there are currently no standard practices for the construction of straw bale buildings in Canada. The general design of a plastered straw bale wall will follow that described in Chapter 1, but there still exists a great deal of variability in design. Many techniques and designs have been developed in the past, and new ones continue to be developed today. Builders often develop their own personal designs and methods which may even be modified from site-to-site depending on the local conditions and the requirements of the project. Because of this variability, there are many deficiencies and inconsistencies in the currently available literature. In addition, it is currently often required to have a design reviewed by a professional engineer. Because of a lack of codes and design information, engineers may require structural testing on innovative wall designs. This is a time-consuming and expensive endeavour, and the results, though of great significance to the specific project, are difficult to apply to other projects where a different wall design may be used. This is a significant issue, as there is currently very little consistency between wall designs from project to project due largely in part to a lack of building codes for straw bale construction. Of the load-bearing straw bale houses with sufficient detail listed on the OSBBC's website, it was found that both wheat and hemp straw bales have been used. Most of the houses were found to use cement-based plaster, but there were a number that used earthen plaster, and many of the plasters used, though similar in composition, were different in material proportioning (OSBBC, 2004).

2.0 Literature Review

This chapter gives a detailed account of the current knowledge and supportive research data regarding the structural performance of straw bale walls. The design and composition of a typical straw bale wall and the related theoretical mechanics are discussed. The constitutive properties of the two main components of a typical straw bale wall: the plaster, and the straw bales; are presented and a discussion is provided on the significance of these properties. A discussion of all structural testing on straw bale wall assemblies completed to date is presented, with a primary focus on research pertaining to the compressive behaviour of plastered straw bale walls. The deficiencies in the currently available literature are highlighted throughout this chapter. Where applicable, supporting references from the literature are provided, however, it should be noted that because much of the data are not reported in peer-reviewed journals it is difficult to have confidence in the results and conclusions, and it can be very difficult to obtain the reports

2.2 Construction Practices

Numerous reports and books have been published detailing a variety of building techniques and recommended construction details for load-bearing construction. King (1996), King (2006), Lerner et al. (2000), Magwood and Mack (2000), Magwood and Walker (2001), Magwood et al. (2005), and many other similar publications all present suggestions for appropriate construction methods for load-bearing straw bale construction. These suggestions for general “best-practice” techniques are designed to provide guidance to those unfamiliar with current straw bale construction methods, but by no means provide construction standards for the

2.0 Literature Review

industry. While these authors may vary in their opinions on suggested designs, and may even have significant variation within their own suggestions, the generally accepted design follows that described in Chapter 1.

In addition to the aforementioned literature regarding general construction practices, there have also been a number of reports published which provide details on very specific and innovative techniques. Generally, within these reports, the authors are suggesting methods or designs to simplify or improve on current practices. Black and Mannik (1997) suggest a technique of tying the interior and exterior plaster skins through the bales in order to improve performance. Their suggestions are supported by numerical modeling and experimental testing. Similarly, Bolles (1998) suggests that the use of a material such as bamboo, wooden stakes, or steel reinforcing bars oriented vertically on the outside of the bales and tied through the bales will provide supplemental strength and stability to the structure. These techniques are an adaptation of the historical technique of pinning the straw bales through their centers to provide stability and strength, a practice that is now considered unnecessary and outdated (Magwood and Mack, 2000). Mar (1998) designed, constructed, and tested a full-scale straw bale vault in an attempt to prove the effectiveness of an innovative straw bale vaulted roof system. Stephens (2000) provides a brief discussion on the applicability of the use of super-compressed bales for straw bale construction, suggesting that bales that have been highly compressed for shipment overseas would make excellent building materials. While the authors of these reports have shown the potential of their respective techniques, the uniqueness of these techniques makes it such that the data from

these reports have limited value to increasing the in-depth structural knowledge of straw bale construction.

Despite the variety of building techniques and innovative methods of constructing with straw, the general design of a load-bearing straw bale wall has remained relatively unchanged since the early days of straw bale construction. The design given in Figures 1.1a and 1.1b represents the general form of the most common method of constructing load-bearing straw bale walls, and it is this design which is the focus of this thesis.

2.3 Un-Plastered Straw Bale Properties and Testing

2.3.1 Introduction

Considering that straw bales provide the bulk of the volume for a plastered straw bale wall, it seems logical that their properties are important to the structural behaviour of a plastered straw bale wall. There have been a number of experiments conducted to quantify the structural performance of individual straw bales. From these experiments has come a greater understanding of the contribution that the straw makes to the overall structural performance of a plastered straw bale wall.

2.3.2 Stress-Strain Relationship

The stress-strain behaviour of individual straw bales is an important structural characteristic of the bales. Bou-Ali (1993) conducted a series of experiments on three-string wheat bales to determine how they performed under compressive loading. The author observed that the bales tested flat exhibited a strain-hardening

2.0 Literature Review

behaviour, getting stiffer with increasing load, while the bales tested on edge appeared to have a consistent stiffness throughout the experiments. While the author did not provide analysis of the modulus of the bales, this information can be obtained from the raw data which are plotted in Figures 2.1 and 2.2. For the flat bales, the approximate slopes at the beginning and end of the curves were obtained from the data. These slopes (corresponding to the straw bale modulus) were found to be approximately 0.7 MPa at low load and 2.4 MPa at higher load. For the bales on edge, the approximate slope for the entire duration of the data was found to remain constant at approximately 0.67 MPa.

Watts et al. (1995) studied the stress-strain behaviour of wheat, oat, and barley bales noting that “there is considerable variation in the Modulus of Elasticity between bales of the same type and bales of a different type” (Watts et al., 1995). The authors found the straw bale modulus for bales tested flat varied from 0.083 MPa to 0.237 MPa. These values are significantly lower than those found by Bou-Ali (1993). This can be explained by the fact that Bou-Ali (1993) tested the bales to significantly higher stresses than Watts et al. (1995). As will be discussed in Chapter 3, the stresses (and strains) experienced by the bales in a plastered straw bale wall prior to failure are in the range of those described by Watts et al (1995) who only tested the bales to a maximum stress of approximately 0.06 MPa. Regardless of the differences in experimental procedures, both authors agreed on the fact that the straw bale modulus increases with increasing load.

Zhang (2000) conducted experiments on a number of straw bales laid flat and on-edge. The main focus of this work was on qualitative observations of the

2.0 Literature Review

progression of failure in the bales, but the author has presented data suggesting a straw bale modulus for flat bales of approximately 0.31 MPa and for on edge bales of approximately 0.46 MPa. These experiments were conducted up to a stress of approximately 0.2 MPa, a higher stress than Watts et al. (1995), but lower than Bou-Ali (1993). The straw bale modulus value for the flat bale presented by Zhang falls between the values presented by the aforementioned authors, which again supports the statement of increasing straw bale modulus with increasing load for flat bales.

Ashour (2003) conducted numerous experiments on straw bales oriented flat and on edge. Similar to other authors, this author found increasing straw bale modulus with increasing load. It was found that for wheat bales, the straw bale modulus ranged from 0.1 MPa to 0.8 MPa for flat bales and from 0.1 MPa to 0.9 MPa for bales on edge. It was also found that for barley bales, the straw bale modulus ranged from 0.05 MPa to 0.55 MPa for flat bales and from 0.08 MPa to 0.3 MPa for bales on edge. Ashour (2003) also noted that bales with higher density were found to have greater straw bale modulus. The values found by Ashour (2003) are within the same ranges found by other authors and also exhibit highly variable results, similar to what was observed by other authors.

Field et al. (2005) tested un-plastered straw bales oriented flat. These authors found straw bale modulus values between 0.41 MPa and 0.47 MPa for stress up to approximately 0.1 MPa. These values agree with the values found by other authors. The authors found the straw bale modulus to increase with increasing load, similar to the findings presented by other authors.

2.0 Literature Review

In general it was noted that the straw bale modulus values are extremely low and highly variable, ranging from approximately 0.05 MPa to 0.7 MPa at low loads for bales tested flat. For flat bales it was also found that the straw bale modulus increased with increasing load. For on-edge bales, the straw bale modulus was found to remain constant throughout the duration of an experiment with reported values ranging from approximately 0.08 MPa to 0.67 MPa.

2.3.3 Other Properties

Aside from the stress-strain relationship, there are a number of other bale properties which have been studied. While these properties are of much less significance to the current research program than the stress-strain relationship, they are worth noting. Bou-Ali (1993) reported that for flat bales, the bales with a greater density achieved a higher ultimate load. The author also reported that the Poisson's ratio of flat bales was found to be approximately 0.30. Watts et al. (1995) found the Poisson's ratio of flat bales to be approximately 0.37 in the longitudinal direction, and 0.11 in the lateral direction. Zhang (2000) conducted low frequency cyclic loading on individual bales, both flat and on edge. The author concluded that "low frequency cyclic loading has no significant impact on the load resistance property of straw bales" (Zhang, 2000). The author also noted, as other authors have, that the bales rebound very well following release of load. Ashour (2003) conducted many experiments on straw bales finding the Poisson's ratio for flat bales to be in the range of 0.28 – 0.44, and for on edge bales to be in the range of 0.12 – 0.35. These results are in agreement with data found by other authors.

2.3.4 Summary

While the literature does yield some helpful information regarding the structural behaviour of straw bales, the most important conclusion to be drawn from previous testing is that straw bales are extremely variable in their composition and compressive behaviour and thus, great care should be taken in considering the contribution that the straw will make to the performance of a composite plastered straw bale wall assembly.

2.4 Plaster Structural Properties and Testing

2.4.1 Introduction

Plaster plays a significant role in the performance of plastered straw bale walls. The exact role and significance is explained in greater detail in Section 2.5. Given the importance of plaster, it is imperative that the structural behaviour of this material be understood. The general composition of plaster is very similar to concrete, a material whose properties are well documented and understood. Both materials contain binder, aggregate, and water. Unfortunately, it is not known whether the current understanding of concrete can be directly applied to understanding plaster. This is because there are a number of differences between concrete and plaster. The most significant difference is the binder. Concrete uses cement, a very well understood material, as a binder. Plaster for straw bale construction on the other hand uses a combination of cement, lime, and in some cases clay. The use of lime and clay, and the wide range in proportions of plaster

2.0 Literature Review

constituent materials has made it difficult to predict and understand the behaviour of the plasters used for straw bale construction.

To date there have been a number of experiments conducted to better understand the properties of straw bale plasters. However, there has been little effort to comprehend the relationship between the constituent plaster materials and their impact on structural properties. Furthermore, the majority of the experiments conducted specifically on straw bale plaster consist primarily of individual experiments conducted on plasters with little or no information provided regarding the key aspects of the composition of the plaster. These experiments have typically been conducted on plasters used for walls in larger full-scale testing setups simply to correlate the specific plaster strength to the specific wall strength.

As mentioned, little has been done to understand how material proportioning can affect plaster properties. Furthermore, very little has been done to deepen the knowledge beyond simply finding the plaster ultimate strength. Key properties such as the stress-strain behaviour, the tensile capacity, and the interaction between straw and plaster have been scarcely discussed to date. The following sections provide a summary of the currently available knowledge obtained from the literature regarding the structural properties of plasters used for straw bale construction. The data is presented in Figures 2.3 to 2.6 and in Tables 2.1 and 2.2.

2.4.2 Lime-Cement Plaster

2.4.2.1 Introduction

The key difference between a lime-cement plaster and concrete, as mentioned previously, is the binder. Lime, as a binder, has significantly different properties than cement. Hydrated lime, as is used in straw bale construction, will not set under water. It behaves conversely to cement in that in order for a lime-based plaster to cure properly, it must first expel its excess water, and then react with atmospheric CO₂ to harden (Thomson, 2005). For this reason, lime-cement plasters will be kept moist only for a short period of time to allow the cement to begin to cure. Beyond this point it is allowed to cure in a more arid environment to enable the lime to harden. The addition of lime and subtraction of coarse aggregate from the mixture makes the plethora of knowledge regarding standard concrete questionable in relation to the behaviour of a lime-cement plaster. However, there have been some experiments conducted which give insight into the properties of various lime-cement plasters. These experiments are discussed in this section.

2.4.2.2 Ultimate Compressive Strength

To understand the behaviour of a plastered straw bale wall subjected to compressive loading, one must have an understanding of the compressive behaviour of the plaster itself. The bulk of the current research on lime-cement plasters is regarding this important property.

White and Iwanicha (1997) and Nichols and Raap (2000) tested plasters used for full-scale wall experiments. White and Iwanicha (1997) reported average cylinder

2.0 Literature Review

compressive strength to be 1.75 MPa. Nichols and Raap (2000) tested two separate plasters for the first and second coats applied to a plastered straw bale wall. The first coat (or “scratch coat”) had 7 day strength of 24.65 MPa and 13 day strength of 28.53 MPa while the second coat (or “brown coat”) had 7 day strength of 7.316 MPa and 14 day strength of 8.412 MPa. It is clear from these experiments that the ultimate compressive strength expected from a lime-cement plaster can vary significantly from one experiment to another. The reason for this is in the variation in material proportioning between experiments. Unfortunately, neither White and Iwanicha (1997), nor Nichols and Raap (2000) provided details on their mix designs.

To understand the influence that mix proportioning can have on the properties of lime-cement plaster one may begin by looking at concrete and how the mix proportioning can influence its properties. It is well documented that the ultimate compressive strength of concrete can vary significantly depending on the proportions of materials used in the mix (Kosmatka et al., 2002). A similar relationship exists with hydraulic lime mortar. Allen et al. (2003) noted that increasing the binder content of hydraulic lime mortar increases the strength, a similar trend as is observed with concrete. While an understanding of the behaviour of concrete and hydraulic lime mortar may give some insight into the behaviour of lime-cement plaster, the differences between concrete, hydraulic lime mortar, and lime-cement plaster make decisive conclusions impossible. When looking specifically at lime-cement plaster it has been stated that “mortar strength data published in the literature varies tremendously, depending upon ... types of mortar materials used – lime, cement, and sand.” (Boynton and Gutschick, 1964) With this in mind, a

2.0 Literature Review

number of authors have performed compression tests on plasters with varying mix proportions.

Boynton and Gutschick (1964) summarize a number of experiments on lime-cement plasters giving the proportions of dry materials and corresponding compressive strength. In addition, the National Lime Association (NLA) (2002) has produced a fact sheet on the use of hydrated lime in mortar. Within the fact sheet they give specified strengths for four different mixtures. A number of authors have provided ultimate strengths (with mixture proportions) for plasters specifically used in straw bale construction. Grandsaert (1999), Boynton (1999), Lerner and Donahue (2003), and Walker (2004) all provide experimental results on the ultimate compressive strengths of lime-cement plaster. All authors provided proportions of lime, cement, and sand in their mixtures. These results show the significant impact that the mix proportions have on the ultimate strength of lime-cement plaster. Figure 2.3 shows the potential for an increase in strength with an increase in binder volume (represented as the ratio of the volume of cementitious materials (V_{cm}) to the volume of sand (V_s)), while Figure 2.4 indicates the potential for an increase in strength with an increase in the ratio of cement to lime (represented as the ratio of the volume of cement (V_c) to the volume of lime (V_l)). However, as is evident from the R^2 values presented in these figures, it has not been shown that there is a consistent clear relationship for these parameters. As discussed below, there are factors beyond those presented in these figures (such as curing time) which influence the ultimate compressive strength.

2.0 Literature Review

The inclusion of the proportions of lime, cement and sand in the experimental results is a key factor in providing useable data and contributing to a greater understanding of the compressive behaviour of lime-cement plaster. Unfortunately, it is common practice for authors to omit the quantity of water used in their mixes. Generally, an author will provide enough water for their mixture to ensure that it reaches an acceptable level of workability. The National Lime Association (NLA) supports this in suggesting that proper mixing procedure will involve adding the “appropriate amount of water to produce a workable consistency.” (NLA, 2002) Making reference again to the properties of concrete and hydraulic lime mortar, one will find that the quantity of water used in a mixture is extremely important. Kosmatka et al. (2002) state that increasing the water to cementing materials (w/cm) ratio (by mass) of concrete from approximately 0.4 to 0.7 will result in loss of strength of nearly 50%. Similarly, Allen et al. (2003) show that an increase in the water to lime ratio from 1.0 to 1.5 will result in a loss of strength of nearly 65%. Supporting these statements for lime-cement plaster, Boynton and Gutschick (1964) have stated that “regardless of mortar composition, ... compressive strength values increase as the water-cement ratios are decreased.” Unfortunately, Boynton and Gutschick (1964) have not provided any data to support this statement.

None of the previously mentioned lime-cement plaster compressive test results provided the quantity of water used in the mix designs. There have been a few authors who made mention of the quantity of water used in their mixes. Ash and Aschheim (2003) and Kaushik et al. (2007) conducted experiments where at least some data were provided regarding the quantity of water used in their mixes.

2.0 Literature Review

Unfortunately, neither author varied the quantity used in order to study the effect that the w/cm ratio would have on the ultimate strength of the plaster. Differing w/cm ratios between experiments is one factor that may explain the large scatter evident in Figures 2.3 and 2.4.

Further complicating the analysis of the current literature is the issue of curing time. It is well known that concrete gains strength with time. Kosmatka et al. (2002) state that the seven day strength of concrete is approximately 75% of the 28 day strength, while the 56 and 90 day strengths are approximately 10% and 15% greater than the 28 day strength. Similarly, Allen et al. (2003) explain that hydraulic lime mortar continues to gain strength even beyond 375 days. Boynton and Gutschick (1964) make a number of observations regarding strength gain over time with lime-cement mortar. They state that “28-day strengths of mortars, regardless of lime content, average about 60% higher than 7-day strengths”, and that “percentage strength gains between 28 days, 6 months or 1 year are much greater with lime-cement... mortars than with straight cement mortars by about 40% on the average.” A number of authors conducted experiments on plaster which was allowed to cure for varying amounts of time. Nichols and Raap (2001), Ash and Aschheim (2003), Walker (2004), Lerner and Donahue (2003), and Boynton and Gutschick (1964) all provide results for experiments on plasters tested after a variety of curing times. The data is presented in Figure 2.5. As can be seen, the results from these experiments support the fact that lime-cement plasters gain strength with time; however it is difficult to quantify the percentages of strength gain, and the factors that influence those percentages. Additional issues arise from the fact that the type of lime used

2.0 Literature Review

and the type of cement used can significantly influence the rate of strength gain for a lime-cement plaster.

There is still a great deal to be understood regarding the ultimate compressive strength of lime-cement plasters. Nevertheless, the currently available literature has provided a database of results with which to begin to draw conclusions. It has been noted that increasing the w/cm ratio of a lime-cement plaster will lead to a decrease in strength. Unfortunately, there is a lack of data to support this statement. It has also been noted that lime-cement plasters will gain strength with time, but there is insufficient data to quantify this strength gain or to understand the impact that mix proportions have on this time dependent behaviour. There is, however, more data to support the findings that increasing the binder content of a lime cement plaster will increase the strength of the plaster. In addition, it has been found that if the binder content remains constant, an increase in the proportion of lime in the binder will lead to a decrease in strength.

Unfortunately there is still not sufficient data to determine precise relationships between the dry material proportions and the plaster ultimate strength. Figures 2.3 and 2.4 present an attempt to amalgamate the data from the literature to provide relationships between the binder proportions and the ultimate strengths. However, the data is sporadic and the trends are difficult to define. This is largely due to the lack of sufficient details presented by the authors, leading to no consideration being given in these figures to the effect that the w/cm ratios or the curing time may have on the data. Figure 2.5 presents an overview of the influence of curing time on the ultimate strength of lime-cement plaster. This figure shows the

gain in strength with time, but beyond noting this general trend, it is difficult to draw specific conclusions from this data.

Despite the inability to draw specific conclusions, the general trends noted from the literature provide important insight into parameters that influence the compressive strength of lime-cement plaster.

2.4.2.3 Stress-Strain Behaviour

The stress-strain behaviour of straw bale plaster is a significant characteristic for understanding the expected deflection or bending characteristics of plastered straw bale walls. Unfortunately, to date very little information is available regarding this property of lime-cement plaster.

Numerous successful attempts have been made to model the stress-strain behaviour of concrete. Desayi and Krishnan (1964) describe one such model which has proven very accurate in predicting the stress-strain behaviour of concrete. Similarly, a number of models have been created to predict the Modulus of Elasticity of concrete based on the strength and density of the concrete. These models have already been adapted for use in the Canadian concrete design standard, CSA A23.2 (CSA, 2004). Unfortunately, no such attempts have been made to model the stress-strain behaviour, or to predict the Modulus of Elasticity of lime-cement plaster.

Lerner and Donahue (2003) and Kaushik et al. (2007) present Modulus of Elasticity values obtained from experiments on lime-cement plasters. These results are given in Table 2.1. Lerner and Donahue (2003) state that the lime-cement plasters have Modulus of Elasticity “very close to the value[s] predicted by the

2.0 Literature Review

concrete formula” given by the CSA (2004). Further discussion on the relationship between plaster strength and Modulus of Elasticity will be undertaken in this thesis. Kaushik et al. (2007) also discussed the stress-strain curves of lime-cement plasters. The stress-strain figures obtained from Kaushik et al. (2007) are given in Figure 2.6. An attempt will be made in this thesis to capture this behaviour using the model described by Desayi and Krishnan (1964).

The limited data currently available regarding the stress-strain behaviour of lime-cement plaster makes it difficult to make significant conclusions. It is not known if the relationship between ultimate strength and the Modulus of elasticity follows the relationship described by the CSA A23.3 equation. The shape of the stress-strain curve appears similar to that of a concrete stress-strain curve, but with the very limited data available it is impossible to support this theory.

2.4.2.4 Tensile Strength

The tensile strength of a lime-cement plaster may be of importance for some applications however it is outside of the scope of this thesis. Regardless, the following is a summary of current literature regarding the tensile strength of lime-cement plaster.

Kosmatka et al. (2002) discussed the relationship between tensile strength and compressive strength for concrete, while Allen et al. (2003) discuss the impact of hydraulic lime on the relationship between tensile and compressive strength. Boynton and Gutschick (1964) suggest that the tensile strength of a lime-cement plaster is approximately 12% of the compressive strength. Lerner and Donahue

2.0 Literature Review

(2003) conducted experiments to quantify the Modulus of Rupture for a lime-cement plaster. The Modulus of Rupture is an indication of the tensile strength of the plaster. The results found ranged from 1.12 to 1.62 MPa, representing approximately 30 – 60 % of the compressive strength. This data is given in Table 2.2. There appears to be a discrepancy in the literature in the reported relationship between tensile strength and compressive strength of lime-cement plaster. This is an issue which requires further study.

2.4.2.5 Summary

To date, the majority of experimentation on lime-cement plasters has focused on the ultimate compressive strength. However, even this data is greatly deficient in the lack of parametric studies conducted and the general tendency to omit pertinent information in the publication of the results. The variety of materials and test methods used makes it very difficult to compare results from different authors. Variations in water content and curing time may be understood and quantified, but other parameters such as the type of lime, sand, or cement used, the size and type of specimen tested, the rate of testing, and the averaging of data are much more difficult to control, understand, and correct for. Boynton and Gutschick (1964) in summarizing comments from other authors have suggested that reported results may be meaningless unless the authors precisely follow the appropriate ASTM standard test methods. Even then they suggest that differences of up to 200% in reported strengths may arise from variations in the type of lime used, the curing conditions, the size and shape of the specimen, the gradation of the sand used, the

2.0 Literature Review

consistency and precision of the mix, and even the skill and experience of the person conducting the testing. It is because of these concerns that additional, more precise, experimentation on lime-cement plaster is required.

2.4.3 Earthen Plaster

While Portland cement and lime-cement plasters are widely used, many builders have begun to consider earthen plasters as a means of avoiding the negative environmental implications associated with the use of lime, and even more so with the use of cement. The use of earth as a building material is not a new concept, but rather, earth is considered to be the oldest building material on the planet (Lerner et al., 2000). However, the invention of new materials such as cement and steel has led to a massive decline in the use of earth as a building material. As a result, the structural properties, and the parameters that influence these properties are not well understood.

Earthen plaster is composed mainly of clay, sand and water. The clay is obtained from either a manufacturer in the form of bagged clay or bulk quality controlled clay, or from a clay-rich soil which may be locally excavated. Often, chopped straw or other fibrous material is added to the mix in order to increase the tensile strength and minimize the effects of drying shrinkage cracks. According to King (2006), “earth plasters can be formulated with a host of different clays, but it takes experimentation or local experience with the local material to get a high-quality plaster.” The author also states that there “are many, many types and colors of clays with widely ranging properties in terms of shrinkage/expansion and binding

2.0 Literature Review

strength.” It is because of these widely ranging properties that there exists a hesitancy to build with earthen plasters, and a difficulty in studying them.

To date there has been very little research conducted on earthen plaster in order to gain a deeper understanding of the structural behaviour and properties of this material. Furthermore, as with lime-cement plaster, the majority of the literature gives only data on specific plasters, with important details regarding the results and/or the composition of the plaster often being omitted. Generally, the results reported are from a single experiment conducted on a specific plaster used for a particular wall design. Another major issue with earthen plasters (that does not exist with lime-cement plaster) is with the variability of the materials. Specifically, the use of local clay-rich soil (which can vary significantly from site-to-site) in earthen plaster creates significant difficulties with reproducibility and comparability of results. Thus, it is extremely difficult to gain useful information from the data aside from the specific applications discussed for each individual experiment.

Due to the aforementioned issues, earthen plasters will not be studied in this thesis. However, there is still an interest in using earthen plaster and thus there is a potential for further study on the properties of earthen plasters. Below is a summary of a number of insights into the properties of earthen plasters provided by the current literature.

- The composition of the plaster has an influence on the ultimate compressive strength of the plaster. However, the exact relationship is currently undetermined. (Taylor et al., 2006)

- The current literature suggests that earthen plaster gains strength initially to a peak value, but then begins to lose strength with time. However, this is counterintuitive, and thus requires further study. (Lerner and Donahue, 2003)
- The tensile strength increases with increased fiber content. (Lerner and Donahue, 2003)

2.5 Straw Bale Wall Properties

2.5.1 Response to Compressive Loading

2.5.1.1 Concentric Compressive Loading

King (2006), Dick and Britton (2002), and King (1996) provide attempts to describe the theoretical compressive behaviour of plastered straw bale walls. The authors explain that a plastered straw bale wall would theoretically act as a sandwich panel in resisting applied loads. The relatively soft straw core would serve to support the stiffer plaster skins, which will act to resist the applied loading. This behaviour is shown in Figure 2.7. The theoretical behaviour suggests that it is imperative that the wall design allow for the transfer of load from the box beam into the plaster, and then from the plaster into the base plate. This is ensured by designing the box beam and base plate to overhang the width of the straw in order to bear directly onto the plaster. Thus, when the wall is compressed, the straw and plaster compress equally. Appropriate construction practices such as those

2.0 Literature Review

described by Magwood and Mack (2000), Magwood and Walker (2001) and King (2006) will ensure that the load is transferred adequately through the wall.

Carrick and Glassford (1998), Dreger (2002), Faine and Zhang (2000), Faine and Zhang (2002), Fibrehouse Ltd and Scanada Consultants Ltd. (1996), Field et al. (2005), Mar (2003), Walker (2004), Wheeler et al. (2004), and Zhang (2000) reported results of experiments conducted on plastered straw bale walls subjected to concentric compressive load. For most cases, the authors presented the ultimate capacity of the walls. The results vary significantly from one experiment to another as a result of different experimental procedures, wall designs, and plaster properties. Table 2.3 presents a summary of experiments reported with sufficient detail provided to determine the theoretical wall strength. Those without sufficient detail to determine the theoretical wall strength were omitted as it is impossible to compare results. For these experiments, the reported results for the ultimate compressive strengths are compared to the theoretical strength as is shown in Table 2.3. The theoretical strength is calculated by multiplying the plaster strength by the area of plaster upon which the load is being applied. This method of calculation of the theoretical strength is representative of the accepted behaviour of plastered straw bale walls.

It can be seen from Table 2.3 that the data currently available in the literature indicate that plastered straw bale walls do not achieve the ultimate strengths predicted by the theoretical calculations. There are many potential reasons why this may be the case, ranging from construction imperfections to the possibility that the accepted theoretical behaviour is incorrect.

2.0 Literature Review

When a plastered straw bale wall subjected to a concentric compressive load acts as a composite column, the relatively stiff plaster takes the bulk of the load, and the much softer straw will resist very little of the load itself but will serve as lateral bracing for the thin plaster skins. The previous theoretical calculations assumed adequate lateral bracing such that the wall failures were not governed by local buckling. However, King (1996) explains that “if there is a load on the plaster skin ... the straw ... must be capable of bracing the skin ‘column’ in either direction with at least 5% of that same force, which depends on the bond between the straw and plaster”. If adequate lateral support is not provided by the straw, local buckling of the plaster skins may result in premature failure. Grandsaert (1999) noted local buckling as a potential failure mechanism for a number of full-scale plastered straw bale walls tested in concentric compression. However, the author noted a number of issues which arose during construction leading to significant imperfections in the plaster skins. It is unclear if the imperfections lead to the local buckling failure. In order to determine if such a failure mode is significant for a plastered straw bale wall, the lateral bond between the straw and the plaster must be analyzed. To date there are very few experiments published studying the interaction between the straw and the plaster. Boynton (1999) tested the bond strength (S_B) between a cement plaster and rice-straw bales. The author noted that the greatest tensile stress achieved was 8.96 kPa, but that “the tension bond specimens were compromised before testing”. Similar experiments were conducted by Smith and MacDougall (2008) with the authors observing significant variability in the results. Smith and MacDougall observed bond strengths between 2.0 kPa and 85 kPa for varying bale types, bale

2.0 Literature Review

orientations, and plaster types. Given the noted variability with the aforementioned data, it is clear that additional research is required to study the interaction between the straw and plaster in plastered straw bale walls; however, this is outside the scope of this thesis.

Another consideration for plastered straw bale walls subjected to concentric compressive load is the potential for failure as a result of global buckling. King (2006) notes that global buckling is a “rare mode of failure”, and that it occurs “typically when the wall is well-built but eccentrically applied load induces bending”. Grandsaert (1999) noted global buckling as a potential mode of failure for a number of plastered straw bale walls tested eccentrically in compression. Walker (2004) also noted global buckling of un-plastered straw bale walls loaded in concentric compression. However, Walker (2004) did not observe this for a plastered wall.

It is clear that the concentric compressive behaviour of plastered straw bale walls has not been clearly verified. Suggestions of the theoretical strength and potential failure modes exist, but have yet to be validated.

2.5.1.2 Eccentric Compressive Loading

If a compressive load is applied eccentrically it will result in an applied moment on the wall. In this situation, the straw will act to tie the two plaster skins together, allowing them to work as a stressed skin panel to resist the applied load as shown in Figure 2.8. This is similar behaviour to when an out-of-plane lateral load or a bending moment is applied to a wall.

2.0 Literature Review

Grandsaert (1999) conducted experiments on eccentrically loaded walls; however the author noted significant issues with construction which appear to have influenced the results. There have also been a number of experiments conducted to determine the out-of-plane bending behaviour of a plastered straw bale wall. Arkin and Donahue (2001) applied an out-of-plane pressure to a straw bale wall and noted that the wall “panel behaved as a true sandwich panel with fully composite action” between the plaster and the straw. The authors also noted that “virtually all deflection [was] due to shear deformation of the straw bale” and that “the calculated and measured performance of the panel depends on the assumption that the straw bale’s shear modulus” is 345 kPa.

Other out-of-plane bending experiments have been conducted by Black and Mannik (1997), Boynton (1999), Carrick and Glassford (1998), Donahue (2003), and Fibrehouse Ltd and Scanada Consultants Ltd. (1996). The authors found results which varied significantly from one experiment to another as a result of non-standardized testing methods and highly variable wall designs. While the authors provided little discussion on the specific mechanics of plastered straw bale walls loaded with out-of-plane load, they have all shown in general that plastered straw walls are adequate at resisting this form of loading.

2.5.1.3 Influence of Shear Stress

The behaviour of plastered straw bale walls subjected to out-of-plane lateral load differs from those subjected to eccentric compressive load in that out-of-plane lateral loading will induce shear stress within the walls. Some authors have studied

2.0 Literature Review

the potential for slippage at the straw/plaster interface as a result of shear stress in the wall. Figure 2.9 shows how shear stress along the straw/plaster interface can lead to slippage along the interface. Stepnuk (2002) studied the shear stress along the straw/plaster interface. The author found shear flow values ranging from 5.04 kN/m to 18.53 kN/m. The author also found that the use of a mesh between the straw and plaster had insignificant influence on the results. Boynton (1999) conducted bending experiments and found applied shear flow values between 7.3 kN/m and 14.7 kN/m. The author noted that “no deformation between the stucco skin and straw interface was observed.” Riley et al. (1998) determined the shear strength of the bond between plaster and straw to be highly variable depending on the type of bale and the method of application of the plaster. The author found average values of 2.25 kPa for two-string bales with hand applied plaster, 3.02 kPa for three-string bales with hand applied plaster and 1.92 kPa for two-string and three-string bales with spray-on plaster.

Shear stress can also lead to the possibility of shear distortion within the straw. While the relatively stiff plaster is unlikely to distort from shear stress, the soft straw has potential to show significant shear distortion as noted in the results of out-of-plane lateral loading experiments. Figure 2.10 shows the behaviour of a plastered straw bale wall if shear distortion is found to occur. Boynton (1999) subjected individual plastered bales to out-of-plane bending to determine the load-deflection response. While no specific comment was made on the mechanics of the testing regime, the figures presented by the author suggest that they observed shear distortion during testing.

2.5.2 Response to Other Types of Loading

2.5.2.1 Introduction

There have been numerous experiments conducted to determine the response of plastered straw bale walls to various other loading regimes. While these results are not of direct importance to this thesis, the existence of this data in the literature is worth noting.

2.5.2.2 In-Plane Lateral Loading

An in-plane lateral load is a load which is applied horizontally, parallel to the length of the wall. Ash and Aschheim (2003), Carrick and Glassford (1998), Nichols and Raap (2000), Riley et al. (1998), and White and Iwanicha (1997) have all studied plastered straw bale walls under in-plane lateral loads. Generally, all authors commented that with proper detailing a plastered straw bale wall performs adequately when subjected to in-plane lateral loading. However, as with the literature on compression testing, there is a lack of consistency in experimental procedures and a tendency to omit important details such as the plaster properties and wall dimensions from the published reports. As a result, it is difficult to draw conclusions to relate the experimental results with theoretical behaviour, or to determine what factors may affect the performance of plastered straw bale walls subjected to in-plane loading.

2.5.2.3 Sustained Loading

Smith (2003), Carrick and Glassford (1998), and Walker (2004) conducted experiments to study the effect of sustained loading on straw bale walls. Smith

2.0 Literature Review

(2003) and Walker (2004) concluded that un-plastered walls exhibited significant creep. Smith (2003) observed large deformations within the first 1-2 weeks and continued settlement for another 5-8 weeks. After approximately 10 weeks Smith (2003) observed that the wall deflections stabilized and the creep phenomenon subsided. The significance of these results is minimal however, as it is uncommon for a wall to be left un-plastered to withstand loads for significant periods of time. Of more importance is the observation by Smith (2003) that the lime-cement plastered wall was observed to show no noticeable settlement under a sustained load of 5.84 kN/m while an earthen plastered wall showed 38 mm settlement under a sustained load of 1.46 kN/m within the first few weeks as the plaster was still curing. Carrick and Glassford (1998) have suggested that a one-story wall subjected to typical loading conditions may undergo up to 3 mm of long-term deflection. These results give insight into the long-term behaviour of plastered straw bale walls, but further experimentation is necessary to fully comprehend the effect of creep on these walls.

2.5.2.4 Impact Loading

Bilello and Carter (1999) studied the ability of a plastered straw bale wall to resist impact loading from wind-borne debris. The main application of this research was to ensure that debris impacting the structure in wind storms will not penetrate the walls or cause irreparable damage. The authors found encouraging results noting that none of the debris completely penetrated the walls.

2.5.2.5 Response of Un-Plastered Walls

There have been numerous experiments conducted on un-plastered straw bale walls. Bou-Ali (1993), Arbour (2000), Blum (2002), Walker (2004), Donahue (2003), and Smith (2003) conducted experiments on un-plastered straw bale walls under various types of loading. These results shed light on the post-failure potential of straw bale walls. Should a wall be damaged to such an extent that the plaster will be rendered useless in resisting the applied loading, these authors have shown that the walls can continue to withstand loads, albeit with significant deformations. The ability to withstand large deformations and remain standing is a desirable characteristic for buildings constructed in seismic regions.

2.5.3 Standard Test Methods for Compression Testing

Despite the fact that there have already been a number of experiments conducted on plastered straw bale walls, it is difficult to draw any significant conclusions from the existing data. The testing methods presented by previous authors vary so significantly from one author to another that comparison between authors is difficult and the current data appears inconsistent. In many cases, the authors were not equipped with the appropriate apparatus required to conduct the experiments and were forced to improvise. As a consequence, many of the results presented, while providing support for individual scenarios, fail to contribute to a greater understanding of the structural behaviour of plastered straw bale walls, and the parameters which may affect this behaviour.

2.0 Literature Review

There are currently no standards for testing plastered straw bale walls, which is a contributing factor to the variability in testing methods presented in the literature. There are, however, standards which apply to the testing of wall panels. An example is ASTM Standard E-72 the “Standard Test Methods of Conducting Strength Tests of Panels for Building Construction” (ASTM, 2002b), which applies to the testing of walls under a variety of loading conditions. This standard covers essentially all types of tests conducted in the literature. The method describes every aspect of the testing including the following key points:

- Number and size of specimens to be tested.
- Rate and method of application of load.
- Method and required accuracy for recording deformation.
- Method for analyzing and reporting data.

In addition to the variety of methods described in the literature for plastered straw bale wall testing, the methods reported for testing of the plaster itself also vary significantly from author to another. Again, often the authors were not equipped with the appropriate apparatus for conducting experiments, and thus were forced to improvise to conduct their tests. Given the simplicity of plaster testing relative to the testing of an entire plastered straw bale wall, there is much less variability in testing methods compared to the wall tests. However, there still exists significant variability in the test methods used in the literature making it difficult to utilize results beyond the specific application reported by each author.

There are also a number of standards which pertain to the specifications of the constituent materials of the plasters used for straw bale construction. Similar to the testing methods, these standards are generally not mentioned in the literature making it difficult at times to understand exactly what materials were used for specimen fabrication.

2.6 Summary

2.6.1 Limitations of Results

There have been numerous experiments conducted on straw bales, lime-cement plasters, earthen plasters, and plastered straw bale wall assemblies. However, because of a lack of standardized testing, the value of these results has been limited. This has in turn limited the ability to reach decisive conclusions about the structural behaviour of plastered straw bale walls and the constituent materials used to construct them. Despite these issues and others outlined previously, the current literature has shown the potential of straw bale construction and has provided insight into the probable mechanics and failure mechanisms of plastered straw bale walls.

2.6.2 Relevant Plaster and Straw Properties

The literature has provided the following information regarding the structural properties of straw bales:

2.0 Literature Review

- Flat straw bales exhibit strain-hardening behaviour with Modulus of Elasticity ranging from approximately 0.05 MPa to 0.7 MPa at low loads and rising to nearly 2.5 MPa at higher loads.
- On edge straw bales exhibit nearly linear stress-strain behaviour with Modulus of Elasticity values varying significantly between experiments from approximately 0.08 MPa to 0.67 MPa.
- The Poisson's ratio for flat bales has been found to be approximately 0.30 in the longitudinal direction and 0.11 in the lateral direction.
- Bales with a higher density tend to have higher Modulus of Elasticity and reach higher ultimate loads.
- The mechanical properties for straw bales were found to be highly variable.

The literature is deficient regarding the following important structural properties of straw bales:

- The potential for shear distortion in a straw bale.
- The characteristics of the bond between the straw and the plaster.

The literature has provided the following information regarding the structural properties of plasters used for straw bale construction:

- Both earthen and lime cement plasters gain strength with time.
- Increasing the binder content will increase the strength of the plaster.

2.0 Literature Review

- Increasing the ratio of cement to lime will increase the strength of the plaster.
- Decreasing the water-cementitious materials ratio will increase the strength of the plaster.

The literature is deficient regarding the following important structural properties of plasters used for straw bale construction:

- The exact influence of varying the mix proportions (including the water) on the strength of the plaster is not fully understood.
- The stress-strain behaviour of plaster is not fully understood.
- There are numerous other parameters (such as tensile strength) which are outside the scope of this thesis, but must be studied further.

2.6.3 Relevant Plastered Straw Bale Wall Properties

The literature has provided the following information regarding the structural properties of plastered straw bale wall assemblies:

- Plastered straw bale walls appear to have adequate compressive strength, and have shown adequate strength under a variety of other loading conditions.
- The straw plays an important role in laterally supporting the plaster skins under compressive load and in tying the two skins together for bending resistance.

2.0 Literature Review

- There are a number of possible failure mechanisms for a plastered straw bale wall including compressive failure of the plaster, local buckling of the plaster skins, and global buckling.

The literature is deficient regarding the following important structural properties of plastered straw bale wall assemblies:

- The effect of eccentric loading on the compressive response of plastered straw bale walls has not been studied.
- No attempts have been made to predict the load-deflection response of a plastered straw bale wall.
- No attempts have been made to predict the conditions that initiate the various potential failure modes.

2.6.4 General Deficiencies in the Literature

Given the aforementioned deficiencies in the literature it stands to reason that there is much room for new research into the compressive response of plastered straw bale walls and the plasters used for these walls. Furthermore, it is important that any new research be conducted and presented in a manner which gives it credibility and reproducibility. The results must also be presented such that they are accessible and understandable for all parties involved in the straw bale construction industry (including, but not limited to; builders, homeowners, building code officials, architects, and engineers). This is the goal of this thesis.

2.0 Literature Review

Table 2.1: Modulus of Elasticity Values for Lime-Cement Plaster

Proportions (By Volume)				Type of Test	Curing Time (d)	Modulus of Elasticity (MPa)
<i>Cement</i>	<i>Lime</i>	<i>Sand</i>	<i>Water</i>			
1	1	6	Unknown	Cylinder	57	6320 ^a
1	1	6	Unknown	Cylinder	57	9481 ^a
1	0	6	0.7-0.8	Cube	28	545 ^b
1	0	3	0.7-0.8	Cube	28	3750 ^b
1	5	4.5	0.7-0.8	Cube	28	3300 ^b

^a Lerner and Donahue, 2003

^b Kaushik et al., 2007

Table 2.2: Modulus of Rupture Values for Lime-Cement Plaster

Proportions (By Volume)				Type of Test	Curing Time (d)	Modulus of Rupture (MPa)
<i>Cement</i>	<i>Lime</i>	<i>Sand</i>	<i>Water</i>			
1	1	6	Unknown	Beam	57	1.23 ^a
1	1	6	Unknown	Beam	57	1.62 ^a
1	1	6	Unknown	Beam	57	1.59 ^a
1	1	6	Unknown	Beam	57	1.48 ^a
1	1	6	Unknown	Beam	57	1.12 ^a
1	1	6	Unknown	Beam	57	1.40 ^a

^a Lerner and Donahue, 2003

2.0 Literature Review

Table 2.3: Ultimate Strength Values for Plastered Straw Bale Walls under Concentric Load

<i>Type</i>	Plaster Properties		Ultimate Strength (kN/m)		Exp. / Theo. (%)
	<i>Strength (MPa)</i>	<i>Area (mm²)</i>	<i>Experimental</i>	<i>Theoretical</i>	
Earth	0.64	226,590	35.8	53.1	67.4 ^a
L-C	8.89	232,000	46.1	565	8.2 ^b
L-C	8.89	232,000	47.3	565	8.4 ^b
L-C	8.89	232,000	48.5	565	8.6 ^b
L-C	7.50	232,000	34.1	476	7.2 ^b
L-C	7.50	232,000	59.3	476	12.5 ^b
L-C	7.50	232,000	63.8	476	13.4 ^b
L-C	8.89	232,000	98.7	565	17.5 ^b
L-C	8.89	232,000	98.0	565	17.4 ^b
L-C	8.89	232,000	72.9	565	12.9 ^b
L-C	2.9	79,200	41.5	232	17.9 ^c

^a Faine and Zhang, 2002

^b Grandsaert, 1999

^c Walker, 2004

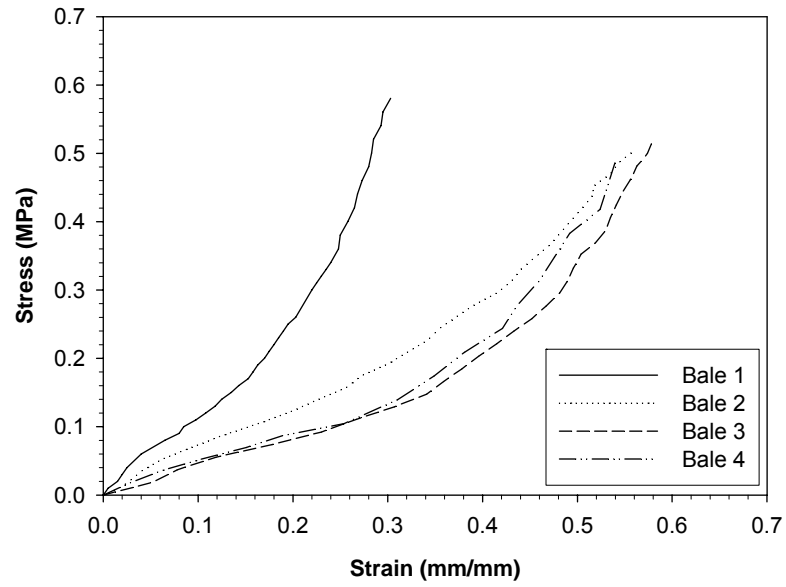


Figure 2.1: Stress -Strain Curves for Flat Three-String Wheat Bales (Bou-Ali, 1993)

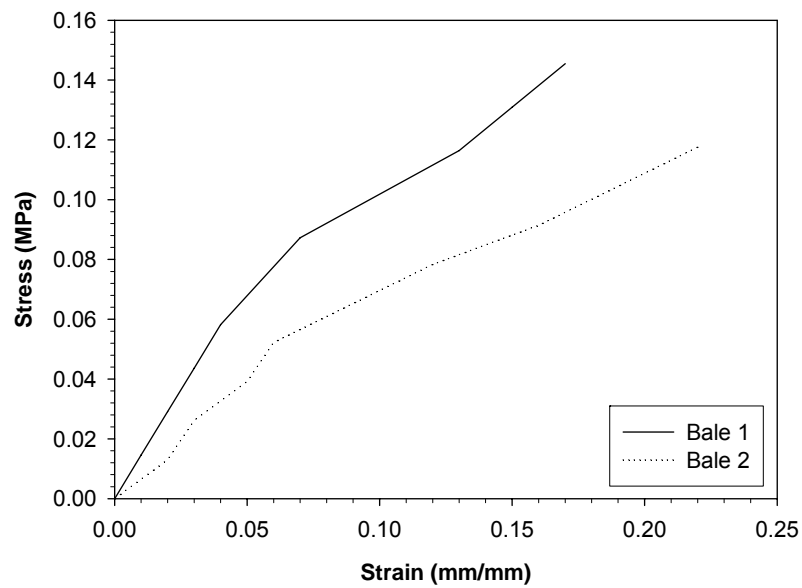


Figure 2.2: Stress-Strain Curves for On Edge Three-String Wheat Bales (Bou-Ali, 1993)

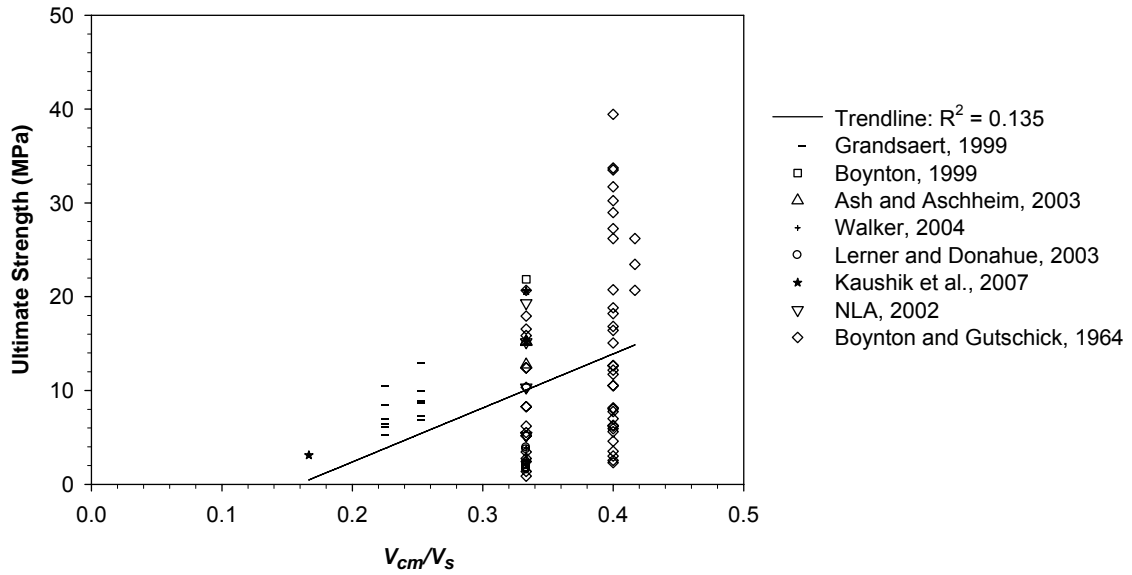


Figure 2.3: Influence of the Ratio of Cementitious Materials Volume (V_{cm}) to Sand Volume (V_s) on Lime-Cement Plaster Ultimate Strength

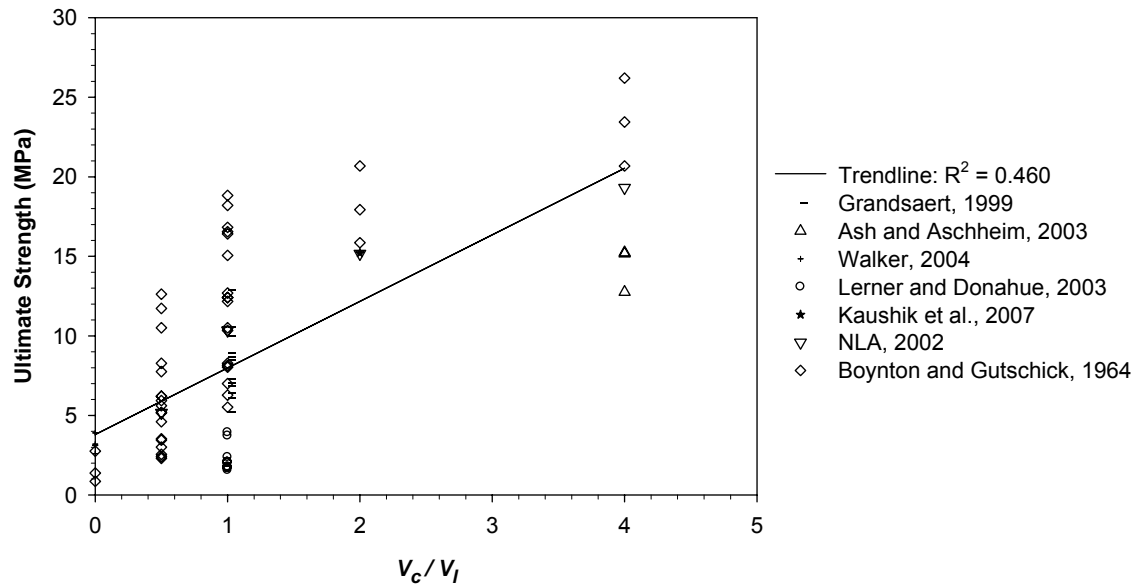


Figure 2.4: Influence of the Ratio of Cement Volume (V_c) to Lime Volume (V_l) on Lime-Cement Plaster Ultimate Strength

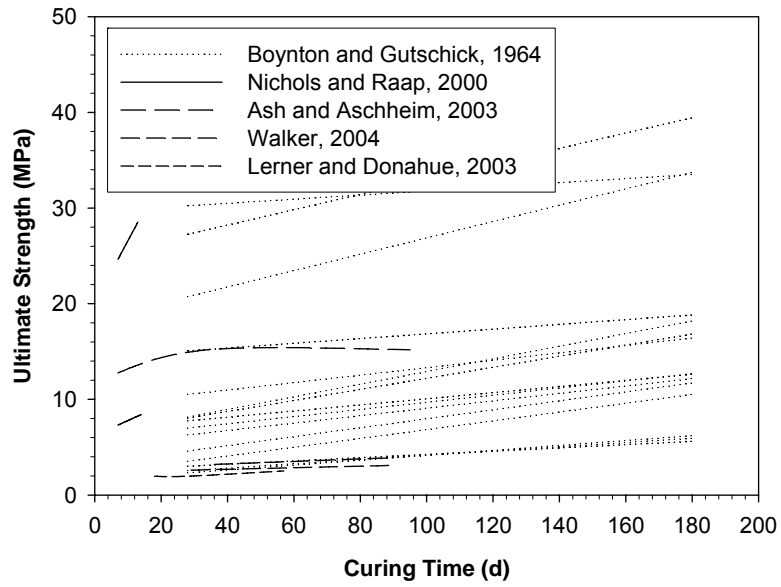


Figure 2.5: Influence of Curing Time on Lime-Cement Plaster Ultimate Strength

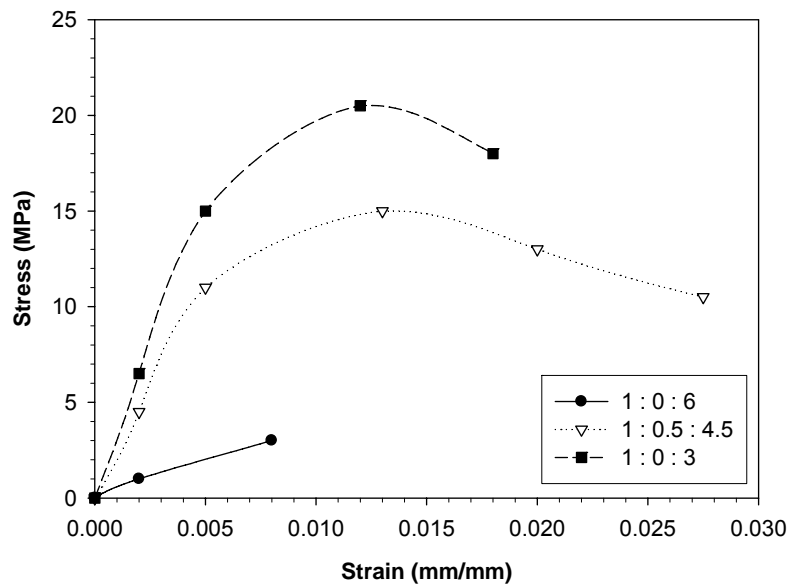


Figure 2.6: Stress-Strain Curves For Varying Cement : Lime : Sand Ratios (Kaushik et al., 2007)

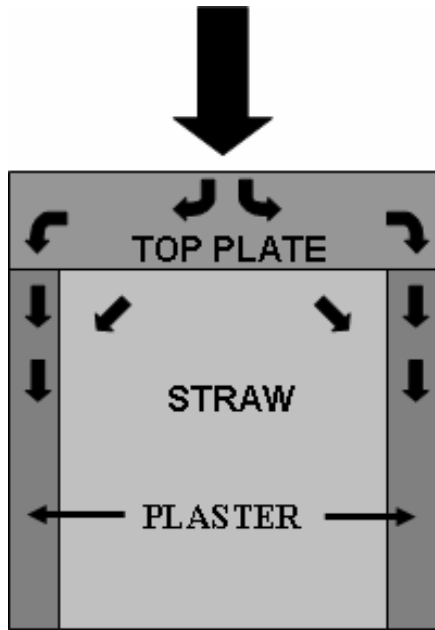


Figure 2.7: Concentric Load on Straw Bale Wall

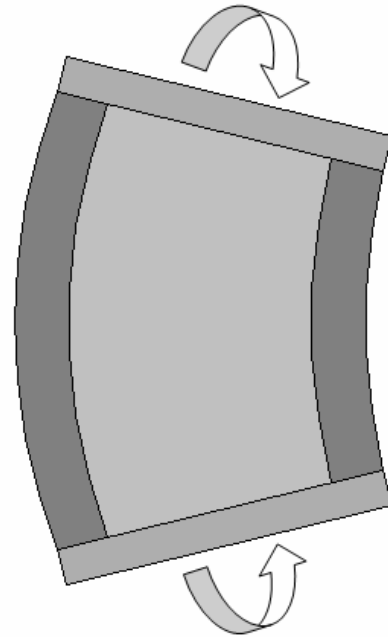


Figure 2.8: Eccentric Load or Moment on Straw Bale Wall

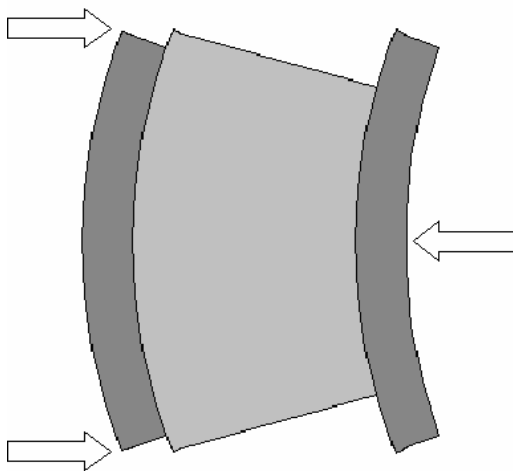


Figure 2.9: Shear Stress in Straw Bale Wall Causing Slippage

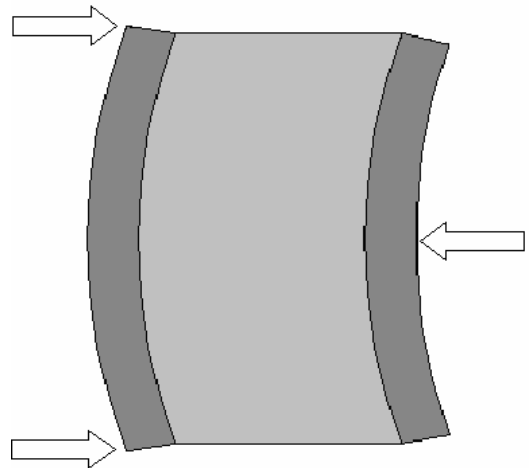


Figure 2.10: Shear Stress in Straw Bale Wall Causing Shear Distortion

Chapter 3: Constituent Material Properties

3.1 Introduction

The first step in attempting to understand the structural behaviour of plastered straw bale walls is to understand the properties of the key materials with which these walls are constructed. The two main constituent materials of plastered straw bale walls are the straw bales themselves, and the plaster.

The main objective of this chapter is to develop and experimentally validate an analytical model for the stress-strain response of lime-cement plaster. The goal of the model is to represent the stress-strain behaviour of the plaster utilizing only the plaster strength as an input parameter. The accuracy of the model will be dependent on the variability in the plaster structural properties as a result of the heterogeneity of the plaster, and as such the inherent variability in the plaster properties (for a plaster of given designed strength) will be studied in this chapter.

3.0 Constituent Material Properties

Additionally, because there are a wide range of mix designs used by straw bale builders there is a need to understand the influence of mix design on the strength of low-strength lime-cement plaster. A complete study of mix design parameters and their influence on plaster properties is outside the scope of this thesis; however a preliminary study is conducted to provide insight into the influence of mix proportions and curing time on the compressive strength of low-strength lime-cement plaster. The primary focus is on plaster with strength less than 10 MPa; however, some data for plaster of greater strength is presented.

Finally a brief discussion regarding the stress-strain response of straw bales is presented.

Wherever possible and appropriate, the methods for testing the constitutive materials followed ASTM methods. However, because of the uniqueness of the materials used, procedures often deviated from the standard methods. The procedures used for testing are described below. Appendix A contains additional specific details on the instrumentation and testing apparatus used.

It is important to note that while the structural properties of mortar and concrete are well documented, the uniqueness of the proportions of lime, cement, sand, and water utilized for plaster used in straw bale construction makes necessary new analysis and experimentation to study the properties of these plasters.

3.2 Plaster Testing

3.2.1 Design and Fabrication of Specimens

3.2.1.1 Constituent Materials

The specimens were fabricated using various proportions of water, sand, cement, and hydrated lime. The water used for the plaster was tap water, provided at room temperature. The reported volumes of water utilized in the mix represent the quantity of tap water added, in addition to the quantity of water contributed from the sand.

The sand was masonry sand which was expected to meet the requirements for ASTM C144 (2004b), the Standard Specification for Aggregate for Masonry Mortar. The quantity of sand utilized in the mix represented the quantity of dry sand added.

The cement met the requirements outlined by ASTM C150 (2007b) and was provided from two separate sources. The first source was standard Type 10 Portland cement. The second source of cement was as a constituent of Mason's Choice High Bond Portland Lime Type N produced by St. Lawrence Cement. This product contains equal portions (by volume) of Type 10 Portland cement and Hydrated Lime.

The lime was hydrated lime which was provided to meet ASTM C207 (2006). There were two sources of lime. The first was as a constituent of Mason's Choice High Bond Portland Lime Type N produced by St. Lawrence Cement. The second source was as Bondcrete® Mason's Lime produced by Graymont Dolime (OH) Inc.

3.0 Constituent Material Properties

3.2.1.2 Mix Proportioning

Typical mix proportioning involved determination of the quantity of High Bond Portland Lime required to provide the appropriate quantity of cement or lime to the mix (whichever was required in the least volume). The additional quantity of Mason's Lime or Portland cement required to achieve the desired cement to lime ratio (V_c/V_l) was then determined. The mass of the sand required to provide the desired cementitious materials to sand ratio (V_{cm}/V_s) was then determined. Note that the mass of sand was considered to be the mass of dry sand. The quantity of water required to achieve the desired water to cementitious materials (w/cm) ratio was determined based on the quantity of cementitious materials in the mix. Note that the quantity of tap water added to the mixture was calculated as the total quantity of water desired minus the quantity of water contributed by the moist sand.

Cement and lime were provided from various sources for the mixes. Experiments were conducted to ensure the consistency of results despite the various sources of lime and cement. The exact source of the lime and cement were shown to be insignificant to the compressive behaviour of the plaster and thus, it is the proportions of the materials, regardless of the source of the lime and cement, which will be discussed herein.

3.2.1.3 Mixing Procedure

For the mixing of the plasters, ASTM C305, the Standard Practice for Mechanical Mixing of Hydraulic Cement Pastes and Mortars of Plastic Consistency (ASTM, 1994) was not followed. Typical straw bale construction practices utilize

3.0 Constituent Material Properties

large drum mixers and thus a larger mixer than that specified in ASTM C305 (1994) was used for specimen preparation. Details on the mixing apparatus are provided in Appendix A. During mixing, sand with known moisture content was added to the mixer first. The lime and cement were then added, and mixed with the sand. Finally, the tap water was added and mixed with the dry materials. The quantity of materials added varied from one experiment to another.

3.2.1.4 Slump Test and Preparation of Strength Test Specimens

After the mixes were prepared, a slump test was typically conducted in accordance with ASTM C 143 (1997). If cubes were required, three cubes were made in accordance with ASTM C 109 (1998). The cube molds used were 50 mm cubes. If cylinders were required, three cylinders of dimensions 100 x 200 mm were made for each set of experiments in accordance with ASTM C 192 (2007a). The specimens were typically kept in a moisture room for seven days before the molds were removed. The specimens were then allowed to cure in the laboratory, outside of the moisture room. In some cases the curing conditions varied from those described above as a result of the specific parameters being studied for the specimens (i.e., when studying varying curing time).

For the compressive experiments conducted on the plaster cylinders it was necessary to provide a cap for the cylinders in order to ensure that the load was applied on a smooth surface. The typical method of capping is with a sulphur compound as described in ASTM C 617 (2003). However, because of the low strength of the plaster, the cylinders were damaged when capped using this capping

3.0 Constituent Material Properties

method. As a result, alternative capping methods were investigated. Appendix A provides a detailed description of these capping methods, and the justification for their use.

In addition to the difficulties found with capping the weak cylinders, it was found that in many cases the cylinders for low strength plasters were damaged upon removal from the formwork.

3.2.2 Instrumentation

For the cube compression experiments the load was recorded manually, directly from the loading machine and only the ultimate load was recorded. For the cylinder compression experiments the load was obtained from a load cell integrated with the loading apparatus and was recorded throughout the duration of the experiments. For these experiments there were a variety of loading apparatus used, based on the availability at the time of testing and on the expected strength of the plaster being tested. It was generally ensured that the machine in use provided accuracy better than +/- 1% of the expected maximum load. Appendix A provides a detailed description of the testing apparatus.

The compressive deformation of the cylinders was obtained using three different methods. Initially a compressometer was used. Eventually an extensometer as shown in Figure 3.1 was used. Finally, for a few experiments, Particle Image Velocimetry (PIV) was used. PIV involved colour texturing the cylinder using splatters of black paint, and taking photographs of the cylinder at 5 second intervals throughout the duration of the experiment. A sample photo is given

3.0 Constituent Material Properties

in Figure 3.1. Further details regarding the compressometer and extensometer are available in Appendix A. Further detail regarding PIV is available in Appendix B. The reason for using three different methods for obtaining the deformation readings comes from the weakness and softness of the plaster. Nevertheless, it was found that the results were similar, regardless of technique used.

3.2.3 Test Details

Plaster cubes and cylinders were fabricated with a wide range of mix proportions and were tested after a variety of curing times. Cylinder experiments were utilized to study the plaster stress-strain behaviour while cube experiments were utilized to study the influence of mix proportioning and curing time on the behaviour of low-strength lime-cement plaster. Analyses of mix design were conducted by varying the parameter being studied while all other parameters remained constant. There is undoubtedly interaction between parameters, but these interactions are outside of the scope of this thesis. Because the plaster study is a preliminary investigation, the number of specimens tested for each analysis varied as the experimental scheme was continuously modified.

Cube compression experiments were conducted to determine the compressive cube strength of some of the plasters. The cubes were tested in accordance with ASTM C109 (1998). The rate of loading was approximately 0.5 mm/min. The load was applied to the cubes until failure. The ultimate load was recorded and the compressive strength was calculated for each cube. The strength of the plaster mix was typically taken as the average strength for three cubes. In

3.0 Constituent Material Properties

some cases four cubes may have been tested if enough plaster was available to fabricate an extra specimen.

Cylinder compression experiments were conducted to determine the compressive cylinder strength, Modulus of Elasticity, and stress-strain profile of some of the plasters. The cylinder compression experiments generally followed the methods described in ASTM C39 (2004a) and ASTM C469 (2002a). There were some deviations from these methods. As described previously, alternative capping techniques were used, and the method of obtaining the deflection data was also modified from the technique described by ASTM C469 (2002a). Due to the low strength of the specimens, the procedure for application of the load deviated from that described in ASTM C469 (2002a). The loading procedure first involved installing the deflection measuring device on the cylinder. Once this was completed, the cylinder was placed in the testing machine. The cylinder was then loaded at a rate of approximately 0.5 mm/min until ultimate failure. The ultimate load was recorded and the corresponding compressive strength was calculated. There was no cycling of the load. The deflection measuring device remained fixed to the cylinder for the entire duration of the experiment in order to capture the entire stress-strain curve. The weakness of the plaster ensured that there were no violent failures which may have damaged the deflection measuring devices. The stress and strain values were calculated from the load and deflection data and the Modulus of Elasticity and stress-strain curves were obtained. The ultimate cylinder strength for the mix was taken as the average of three cylinders for a specific batch. However, in

3.0 Constituent Material Properties

some instances one or more of the cylinders were damaged prior to testing, and thus the results from these specimens were omitted.

3.2.4 Results and Discussion

3.2.4.1 Introduction

Detailed data regarding the exact mix proportions and the specific results obtained from each individual experiment are presented in Appendix C. The following results present the data from various experiments presented to determine specific relationships and properties.

3.2.4.2 Modelling Lime-Cement Plaster Stress-Strain Behaviour

The main objective of the constituent material testing is to model the stress-strain response of low-strength lime-cement plaster. The goal of the modelling is to represent the stress-strain response of a plaster based on the strength of the plaster as determined from cube compression tests. The relationship between strength and Modulus of Elasticity is first analysed. Next a stress-strain model is presented and validated against experimental data.

The Modulus of Elasticity and stress-strain study utilized plaster cylinders. However, there were issues in obtaining satisfactory data from the cylinders due to damage incurred during removal from the formwork and as a result of difficulties with capping the cylinders. As a result, only the cylinders which were undamaged during removal from the formwork and during capping were analyzed. Furthermore, because plaster ultimate strength is typically determined from cube tests a

3.0 Constituent Material Properties

discussion is provided on the influence of experimental specimen size and type. The analyses were conducted utilizing cylinders fabricated with a wide range of mix designs to validate the relationships for a range of practical plaster strengths.

Modulus of Elasticity

Figure 3.2 shows a typical stress-strain curve for a 1.0 MPa plaster up to 40% of the failure stress (ultimate stress). It can be seen that for stress less than 0.1 MPa, or 10% of ultimate load, the strain was too small in magnitude to be accurately measured. This is likely a result of limitations in the device used to record the strain values. Thus, the Modulus of Elasticity was calculated by determining the slope of the experimental stress-strain curve between 10% and 40% of ultimate load.

The Modulus of Elasticity values were found to range from 528 MPa to 20333 MPa with the values generally found to increase with increasing cylinder compressive strength. Figure 3.3 presents the relationship between Modulus of Elasticity (E_{cyl}) and plaster cylinder compressive strength (f'_{cyl}) for individual cylinder specimens. This data indicates a linear relationship between the cylinder strength and the Modulus of Elasticity of the plaster. The relationship is described by the trendline given in the figure with an R^2 value for the trendline of 0.914. The line was forced to pass through the origin. The equation obtained from the trendline is given as Equation 3.1:

$$E_{cyl} = 818f'_{cyl} \quad \mathbf{3.1}$$

Also shown in the figure is the 95% confidence interval for the slope of the trendline.

3.0 Constituent Material Properties

Modelling Plaster Stress-Strain Relationship

Desayi and Krishnan (1964) propose the following model for the stress-strain behaviour of concrete:

$$f_c = \frac{2f'_c \left(\frac{\varepsilon}{\varepsilon_o} \right)}{1 + \left(\frac{\varepsilon}{\varepsilon_o} \right)^2} \quad 3.2$$

$$\varepsilon_o = \frac{2f'_c}{E_c} \quad 3.3$$

where f_c is the stress in concrete at any strain ε , ε_o is the strain in concrete at ultimate stress, E_c is the Modulus of Elasticity of concrete, and f'_c is the specified ultimate compressive strength of the concrete. The Desayi and Krishnan (1964) model is presented in Figure 3.4. If f'_c and E_c are known, while ε_o is unknown, Equation 3.3 can be substituted into Equation 3.2:

$$f_c = \frac{E_c \varepsilon}{1 + \left(\frac{\varepsilon E_c}{2f'_c} \right)^2} \quad 3.4$$

The stress-strain curves for the cylinders used to determine the plaster Modulus of Elasticity were plotted and compared to the theoretical curves obtained using this relationship. In order to determine a theoretical curve for a specimen, f'_c and E_c were determined from the experimental data for each cylinder where $f'_c = f'_{cyl}$ and $E_c = E_{cyl}$. A sample curve is given in Figure 3.5. This figure indicates that while Equation 3.4 captures the initial slope and ultimate stress (corresponding to

3.0 Constituent Material Properties

experimentally determined E_c and f'_c respectively in Equation 3.4), it does not adequately capture the strain at ultimate stress ε_o .

The stress-strain relationship presented by Collins and Mitchell (1997) is another, widely accepted model for the stress-strain behaviour of concrete:

$$f_c = f'_c \left(\frac{n \left(\frac{\varepsilon}{\varepsilon_o} \right)}{n-1 + \left(\frac{\varepsilon}{\varepsilon_o} \right)^{nk'}} \right) \quad 3.5$$

$$n = 0.8 + \frac{f'_c}{17} \quad 3.6$$

$$k' = 0.67 + \frac{f'_c}{62} \quad 3.7$$

This model is appropriate for structural concrete. In order to apply it to low strength plaster, new values of the constants n and k' needed to be derived. This was done using two known boundary conditions for the stress-strain curve. These boundary conditions are:

1. At $\varepsilon = \varepsilon_o$ the stress-strain curve should reach a peak stress of f'_c . As a result, the slope of the curve at this point must be zero.
2. At $\varepsilon = 0$, corresponding to the beginning of the stress-strain curve, the curve is approximately linear with slope equal to E_c .

In order to satisfy both boundary conditions the derivative (slope) of Equation 3.5 was determined. In order to satisfy Boundary Condition #1, the derivative was set equal to zero and the value of ε was set equal to ε_o . The resulting equation was

3.0 Constituent Material Properties

then rearranged and simplified resulting in Equation 3.8. In order to satisfy Boundary Condition #2, the derivative was set equal to E_c , and the value of ε was set equal to zero. The resulting equation was then rearranged and simplified resulting in Equation 3.9.

$$k' = 1 \quad 3.8$$

$$n = \frac{E_c \varepsilon_o}{E_c \varepsilon_o - f'_c} \quad 3.9$$

Equations 3.5, 3.8, and 3.9 were then used to determine the theoretical stress-strain relationships for 22 cylinders of low-strength lime-cement plaster. The values of f'_c , E_c , and ε_o were determined from the experimental data for each cylinder (where $f'_c = f'_{cyl}$, $E_c = E_{cyl}$, and $\varepsilon_o = \varepsilon_{cyl}$). These values were then inputted into Equation 3.9 to determine the value of n . This value, along with f'_c , ε_o , and k' were then input into Equation 3.5 resulting in a relationship between stress (f_c) and strain (ε). A sample curve is given in Figure 3.6 with the same experimental data as presented in Figure 3.5. Figure 3.6 indicates the modified model given with Equations 3.5, 3.8, and 3.9 is an excellent fit to the experimental data. In fact, for the 22 experiments to which this modified model was fit, the average R^2 value was found to be 0.965, with a maximum R^2 of 0.996 and a minimum R^2 of 0.856. The minimum R^2 was, in fact, the only R^2 value below 0.900 of the 22 experiments.

Modification of Stress-Strain Model

It is not common practice to determine the Modulus of Elasticity and the failure strain for every specimen when conducting cube or cylinder strength

3.0 Constituent Material Properties

experiments for a plaster. As a result, often f'_c is the only experimentally determined value. Equation 3.1 provides the relationship between E_{cyl} and f'_{cyl} . This relationship can be used to eliminate the need to experimentally determine the plaster Modulus of Elasticity for use in the model.

It is also desirable to find an alternative to experimental determination of the strain in the plaster at ultimate stress. However, a relationship does not exist to provide an estimate of the strain at ultimate stress as it was found that no correlation exists between the strain at ultimate stress and the plaster strength. The strain in the plaster at ultimate stress was found to be highly variable amongst the plaster cylinder experimental results. In order to determine a value to be used for modelling the stress-strain response of the plaster, the value of ϵ_{cyl} will be estimated as the average strain at ultimate stress for all cylinder experiments. This value was found to be 0.00253 with standard deviation of 0.000857 indicating that the true mean strain at ultimate stress (with 95% confidence) will fall between 0.000816 and 0.00424.

Using Equation 3.1 to define E_{cyl} and setting it equal to E_c , and setting ϵ_o equal to 0.00253, Equation 3.5 simplifies to:

$$f_c = f'_c \left(\frac{764.8\epsilon}{0.935 + \left(\frac{\epsilon}{0.00253} \right)^{1.935}} \right) \quad \mathbf{3.10}$$

This equation will give the stress-strain behaviour of lime-cement plaster based on the strength of the plaster. Figure 3.7 presents a comparison between

3.0 Constituent Material Properties

experimental and theoretical stress-strain curves for 9 plaster cylinders. Cylinders used for the comparison represent three batches with plaster strengths ranging from approximately 0.30 MPa to 5.0 MPa. Note that the data is normalized by f'_{cyl} . It can be seen that because the experimental plaster strength is inputted into the model, the experimental data and theoretical curve terminate at a stress equal to the ultimate strength of the plaster. However, the strain at ultimate stress is variable for the experimental specimens, with the theoretical curve representing the average strain at ultimate stress. It can also be seen that the use of Equation 3.1 for the Modulus of Elasticity for the theoretical curve provides a good representation of the initial slope of the experimental curves.

Effect of Specimen Type on Plaster Stress-Strain Behaviour

The validation of the plaster stress-strain model was conducted utilizing plaster cylinder experiments. However, while the compressive strength of concrete is typically determined by cylinder experiments as described in ASTM C39 (2004a), the compressive strength of hydraulic cement mortars is typically determined by cube experiments as described in ASTM C109 (1998). As a result it is desirable to understand the effect of plaster specimen type on the properties of low-strength lime-cement plaster.

Figure 3.8 shows a plot of the ratio of cylinder strength to cube strength (as determined by the average of three specimens of each type) for a number of plaster mixes with a variety of cube compressive strengths. The y-axis represents the

3.0 Constituent Material Properties

average strength of three cylinders divided by the average strength of three cubes (f'_{cyl}/f'_{cube}). The x-axis represents the average strength of the three cubes (f'_{cube}).

Figure 3.8 indicates that the cylinder strength is nearly always less than the cube strength with only three experiments showing cylinder strength comparable to the cube strength. The trendline plotted in Figure 3.8 indicates that as the cube strength is increased, the ratio of cylinder strength to cube strength increases. The equation obtained from the trendline is given as Equation 3.11:

$$\frac{f'_{cyl}}{f'_{cube}} = 0.0221f'_{cube} + 0.719 \quad 3.11$$

Also shown in Figure 3.8 is the 95% confidence interval for the trendline. The R^2 value for the trendline was found to be 0.08, indicating the variability in the data and the lack of confidence in this equation. The variability in the results is most likely a result of the difficulties in preparing and testing the cylinder specimens. As discussed previously, low strength cylinders were damaged during removal from the forms.

Because of the inclusion of damaged cylinders a comparison of the current test results to literature values indicates some differences. For example, for cube strength of 1.0 MPa (a common approximate strength for plasters discussed within this thesis), Equation 3.11 indicates cylinder strength of 0.741 MPa. Relationships presented by Hansen et al. (1962) and Lyse and Johansen (1962) suggest a cylinder strength of approximately 0.86 MPa for cube strength of 1.0 MPa.

3.0 Constituent Material Properties

Fabrication issues aside, the difference between cube and cylinder strengths is a result of confinement of cube specimens in the testing apparatus and of differences in specimen size and shape between the cubes and cylinders. It is assumed that the confinement of cube specimens in the testing apparatus provides a similar biaxial compression condition as for plastered straw bale wall assemblies where the plaster is laterally reinforced and supported by the straw, which penetrates into the plaster in the bond region between the straw and the plaster. As such it is expected that using cube test results for strength determination for the modeling of plastered straw bale assemblies is appropriate.

Furthermore, while the model presented in Equation 3.10 was developed for cylinder specimens it is assumed that the model will yield the appropriate stress-strain behaviour of cube specimens if cube strength, Modulus of Elasticity, and strain at ultimate failure values are used. To determine the cube Modulus of Elasticity and strain at ultimate failure values it is assumed that the relationship between f'_{cube} and E_{cube} will be equivalent to the relationship between f'_{cyl} and E_{cyl} , and that ϵ_{cube} will equal ϵ_{cyl} .

Summary

The previous discussions validated a model which utilizes plaster compressive strength to determine the stress-strain response of the low-strength lime-cement plaster. The model will be extended in the following chapters to model the compressive response of plastered straw bale assemblies based on the compressive cube strength of the plaster applied to the assemblies.

3.0 Constituent Material Properties

3.2.4.3 Quantifying Variability in Plaster Strength

It is important to understand the expected variability between experimental and theoretical stress-strain data when utilizing the model presented above. As a result, additional objectives of the constituent material properties study are to understand the inherent variability in the plaster strength as a result of the heterogeneous nature of the plaster, and to study the influence of mix design on the strength of low-strength lime-cement plaster.

Variation in Strength for Cubes of the Same Batch

Cube tests are utilized for determination of plaster strength for input into the stress-strain model. For a specific plaster batch three cubes are typically fabricated and tested in compression, with the average strength of the cubes providing the strength of the batch. However, the cubes will have individual strengths which vary from one to another, and which will represent variations in the plaster strength throughout the skin of a plastered straw bale assembly. This strength variability is important in understanding the variability in strengths and stress-strain responses of plastered straw bale assemblies.

For 45 plaster batches of varying strengths, three cubes were produced for each batch and the compressive strength of the specimens was determined. The mean strength and standard deviation for each batch were calculated based on the strength results of the three cubes for each batch. Figure 3.9 presents the results with the average strength of the three specimens from a particular batch (f'_{cube}) plotted on the x-axis and the Coefficient of Variation, CV (standard deviation

3.0 Constituent Material Properties

normalized by the average strength) plotted on the y-axis. From Figure 3.9 it can be seen that the average CV is 0.0814 with a maximum average CV found to be 0.3304. This suggests that the standard deviation of three cube tests of a plaster will be approximately 8.1% of the average strength of the cubes but may be upwards of 33% of the average strength of the cubes.

Variation in Strength for Batches of the Same Mix Proportions

If a plastered straw bale wall is fabricated with a plaster of a given design strength, but the in-situ plaster strength is not determined from cube tests during construction, the plaster which is applied to the wall will vary in strength from the design plaster strength. This is because there is variability in the plaster strength obtained from different batches, even when the same proportions of dry materials are used. To quantify the variability between different batches with the same proportions, eleven separate batches of plaster with volumetric proportions of 0.25 : 1.25 : 4.5 of cement, lime, and sand with *w/cm* ratio of 1.08 were prepared. Three cubes were tested after 7 days of curing to determine the compressive strength for each batch. The results presented in Figure 3.10 indicate that there are differences between the compressive cube strengths for each batch, despite each batch containing the same proportions of mix materials. A one-way analysis of variance was conducted at a 95% confidence level to determine the probability that the data from the eleven experiments can be considered to come from the same population. The P-value from this analysis was found to be 9.59×10^{-8} . The results show that the strengths of the eleven batches are significantly different from one another

3.0 Constituent Material Properties

indicating the variability among batches, even when the proportions of materials are believed to be consistent.

The average cube strengths for each of the eleven batches were calculated and considered as individual data points representing the compressive cube strength for each batch (f'_{cube}). The mean and standard deviation of these eleven values of f'_{cube} were then calculated. The mean value is plotted in Figure 3.10 as a solid horizontal line at 0.783 MPa. This indicates that if a batch is mixed with the proportions outlined above, the average compressive strength of three cubes made from that batch (f'_{cube}) will be approximately 0.783 MPa. In order to understand how much range to expect in this value, two lines representing the mean value +/- two standard deviations are also shown in Figure 3.10. These lines represent the boundaries between which it is expected the true population mean will fall (with 95% confidence). It can be seen that there is a range of +/- 0.176 MPa around the mean value of 0.783 MPa. This represents a range of +/- 22.5%. Note that six of the batches were fabricated with 45 mm x 45 mm cubes due to a shortage of appropriately sized cubes. These six batches represent batches numbered 6 – 11 in Figure 3.10. An analysis of variance proved the appropriateness of considering these six batches in the analysis, despite the variation in apparatus.

3.2.4.4 Effect of Mix Procedure on Plaster Variability

The previous discussion quantified the variability in plaster strength as a result of the heterogeneous nature of the plaster. That discussion provided insight into the expected variation between experimental and theoretical strength and

3.0 Constituent Material Properties

stress-strain behaviour of lime-cement plaster. The following discussion provides a preliminary analysis of the effect of variations in mix proportions and curing time on the strength of lime-cement plaster. The objective of this discussion is to provide design guidance for low-strength lime-cement plaster.

Effect of Dry Mix Proportions

To investigate the sensitivity of plaster strength to variations in mix design, 14 plaster mixes were prepared with various proportions of lime, cement and sand. For these experiments the slump was kept constant at approximately 50 mm. This ensured the plasters were all of acceptable workability. Care was taken to ensure consistency of mixing techniques and accuracy of proportioning to minimize possible influence of variations between batches as discussed above. For each batch, at least three cubes were fabricated and then tested in compression.

In Chapter 2 it was noted that lime-cement plaster strength is affected mainly by the quantity of binder relative to the quantity of sand (V_{cm}/V_s) and the proportion of cement in the binder relative to the proportion of lime (V_c/V_l). Thus, experiments were conducted with four different ratios of V_c/V_l . For each ratio, the value of V_{cm}/V_s was varied for a number of experiments. The results are presented in Figure 3.11. It can be seen that, as expected, increasing the value of V_{cm}/V_s will result in an increase in strength. However, beyond a V_{cm}/V_s ratio of approximately 0.80, increases in cementitious materials do not lead to significant increases in strength.

It is also evident from Figure 3.11 that increasing the quantity of cement relative to the quantity of lime (V_c/V_l) in the plaster will yield a stronger plaster. The

3.0 Constituent Material Properties

plasters with V_c/V_l of 1.2 yielded significantly higher strengths than any of the other plasters. In fact, these plasters are significantly stronger than necessary for single storey straw bale construction.

Based on the above observations, the data from Figure 3.11 is re-plotted in Figure 3.12 with the data excluded for V_{cm}/V_s ratio of greater than 0.80 and for V_c/V_l of 1.2. Furthermore, the values plotted on the x-axis were modified to also account for the varying values of V_c/V_l (thus creating only one relationship to study in the Figure). The resulting plot in Figure 3.12 indicates the linear relationship presented in Equation 3.12:

$$f'_{cube28} = -1.119 + 35.075 \left(\frac{V_{cm}}{V_s} \right) \left(\frac{V_c}{V_l} \right) \quad 3.12$$

This relationship gives an estimate of the plaster strength from the proportions of dry materials for a plaster of average workability (slump = 50 mm). This equation has a R^2 value of 0.942 and is valid for V_{cm}/V_s values approximately 0.8 and below, and V_c/V_l values approximately 0.5 and below. Note that if a mix is created with very low ratios of V_{cm}/V_s or V_c/V_l , Equation 3.12 will suggest the mix has negative strength. This suggests that the equation is not valid for extremely low V_c/V_l or V_{cm}/V_s values. Thus it is suggested that Equation 3.12 is only valid for V_c/V_l values between 0.12 and 0.5, and V_{cm}/V_s values between 0.1 and 0.71 representing the range of experimental data used to determine the equation.

Table 3.1 presents a comparison between experimental cube strength results available in the literature and the values obtained from Equation 3.12. Only the

3.0 Constituent Material Properties

reported results with V_{cm}/V_s and V_c/V_l values within the suggested applicable range for Equation 3.12 are presented. As shown in Table 3.1, the theoretical values do not agree completely with the experimental data. One value is off by as much as 33%, which is significantly greater than the expected deviation of no more than 22.5% (the expected deviation from the mean strength for batches designed to be of the same strength). However, the average of the experimental to theoretical strength ratios is 0.99, indicating that, on average, Equation 3.12 is valid.

Effect of W/CM Ratio

In order to study the effect of water content on the compressive strength of lime-cement plaster, experiments were conducted on plasters with various w/cm ratios. The proportions of dry ingredients were kept constant for all of the batches with volumetric proportions of 0.25 : 1.25 : 4.5 of cement, lime, and sand. The dry ingredients for the different batches were rigorously mixed together before being separated to create the batches with varying water content. This ensured consistency of dry mix proportions for each batch. Three cubes were tested in compression for each batch and the average compressive cube strength was calculated. Figure 3.13 compares the cube strength of the plasters found for a number of different w/cm ratios. Also included in Figure 3.13 is a plot of the relationship between w/cm ratio and strength for a typical concrete mix (Kosmatka et al., 2002).

It can be seen that as the water content is increased, the strength of the plaster decreases significantly. Over the range of water contents tested the strength

3.0 Constituent Material Properties

was found to vary between 0.69 MPa and 1.72 MPa. It is important to note that the range of water contents tested represents the range in which the plaster was considered to be “workable”. This indicates that simply basing the water proportioning on workability, a typical practice for straw bale construction, may lead to highly variable plaster strengths. These results also indicate that the relationship between strength and w/cm ratio for these low-strength plasters is very similar to the relationship observed for structural concrete. Similar results have been reported for Hydraulic Lime Mortar (Allen et al. 2003).

Very few of the results reported in the literature make mention of the water content of the plasters tested, as discussed in Chapter 2. This practice has made it difficult to draw meaningful conclusions from the literature. One reason previous authors have omitted the w/cm ratio is that it can be difficult to determine this value as a result of challenges in accounting for the quantity of water contributed to the mix from the sand. This is especially significant for field work where the water content of the sand can vary significantly, even from one batch to another. As a result, even if the proposed plaster design has properties which are very well understood, variations in the w/cm ratio introduced while mixing may have a significant impact on the in-situ plaster strength.

One method of introducing quality control may be through completion of slump tests. A slump test is an easy test to conduct on-site and gives an accurate indication of the workability, and hence the w/cm ratio of a mix. Figure 3.14 shows the relationship between the slump and strength for the same experiments presented in Figure 3.13. This relationship is similar to the relationship between the

3.0 Constituent Material Properties

w/cm ratio and strength given in Figure 3.13. This suggests the possibility of directly relating the slump to the plaster strength. This would provide a simple and practical quality control test that straw-bale builders could perform in the field. The relationship between slump and strength could be established by experimentation prior to construction for any given set of dry proportions. This would help ensure that the plaster being applied on-site will have strength similar to what may be expected based on the initial design.

Effect of Curing Time

A number of experiments were conducted on lime-cement plasters tested at varying curing times. The volumetric proportions of the plasters were: 0.25 : 1.25 : 4.5 of cement, lime, and sand, with w/cm ratio of 1.18. For this analysis, nine cubes were created from a single batch with the aforementioned proportions. The first three cubes were tested after 7 days, the next three after 14 days and the final three after 28 days. The strengths of each of the cubes at each of the curing times were calculated, and the values were normalized by dividing the cube strengths at the various curing times by the average 28 day compressive strength (f'_{cube}/f'_{cube28}).

Figure 3.15 presents a relationship between the curing time and the average compressive cube strength for curing times 28 days and less. Curing time is plotted on the x-axis while the normalized compressive cube strengths are plotted on the y-axis. Also included in Figure 3.15 are data points representing the suggested relationship between 7 and 28 day strengths presented in the literature. A trendline, with $R^2 = 0.991$, was fitted to the data from the current study and from the literature:

$$\frac{f'_{cube}}{f'_{cube28}} = 0.329\sqrt[3]{t} \quad 3.13$$

where t is the curing time in days.

3.3 Straw Bale Compressive Testing

3.3.1 Introduction

Two un-plastered straw bales were subjected to compressive load. One bale was tested in a flat orientation, while the other was tested in an on-edge orientation. While conducting only one experiment for each orientation does not provide a statistically strong sample, the intent of the experiments was to ensure the bales used had approximately similar stress-strain properties to the bales presented in the literature.

There are currently no standards for the compressive testing of un-plastered straw bales. The methods used are similar to those used by Bou-Ali (1993), Watts et al. (1995), Zhang (2000), Ashour (2003), and Field et al. (2005) in which the bales are compressed between two rigid plates.

3.3.2 Design and Fabrication

The straw bales used in the experiments were two-string wheat bales. They were obtained from a local farmer where they had been stored in a barn and were dry when purchased. The bales varied in mass and dimensions but were 12 ± 3 kg with dimensions of 375 ± 10 mm height, 475 ± 10 mm width, and 800 ± 25 mm length. Prior to testing, the bales were stored indoors in a room-temperature

3.0 Constituent Material Properties

environment with a constant humidity. The bales were less than a year old when tested and were dry and tightly bound at that time.

In order to produce specimens with consistent dimensions, the wooden jig shown in Figure 3.16 was designed. The jig was placed over the bales and nuts were tightened to compress the bale to a height of 330 ± 1 mm as shown in Figure 3.16. Once the bale was compressed, the jig was used as a guide to trim the sides of the bale to approximately 405 mm as shown in Figure 3.17. The width of 405 mm was variable as not all straw stalks reach the outer edge of the bale, leaving voids in the straw bale. However, the trimming ensured maximum bale width of 405 mm. This corresponds to the height of the bale for the on-edge bales.

When the bale was removed from the jig prior to testing, the straw was observed to rebound. As a result, the height of the flat bales varied from 330 mm to 350 mm. This corresponds to the width of the on-edge bales. The length was not controlled for either bale, but was found to be 800 ± 25 mm for both bales.

3.3.3 Instrumentation

The experimental setup for the un-plastered straw bale experiments is shown in Figure 3.18. The instrumentation for the bale tests consisted of a 111 kN load cell, two 100 mm linear potentiometers (LPs), and four 25 mm LPs. As shown in Figure 3.18, the load cell was located in the centre at the top of the testing apparatus and all six LPs were located along the edges at the top of the apparatus. The four 25 mm LPs were located at each for the four corners, while the two 100 mm LPs were located at the edges of the bale, midway along the length of the bale as can be

3.0 Constituent Material Properties

seen in Figure 3.18. The load and displacement were measured at a rate of approximately 16 samples per second and were recorded throughout the duration of the experiments. Additional details regarding the instrumentation may be found in Appendix A.

3.3.4 Results and Discussion

Neither bale reached ultimate load. Both bales were observed to rebound nearly 100% following release of the load at 100 mm deflection. The strings binding the bales were not observed to fail under the applied loads for either specimen. Figures 3.19 and 3.20 show the load-deflection response of the flat bale and on-edge bale respectively. These figures show the results from all of the LPs. It can be seen from these figures that the deflections recorded at each load for each of the LPs are approximately in agreement with one-another, indicating that the load was indeed applied concentrically. For Figures 3.21 and 3.22 the data is averaged and converted to present the stress-strain curves for both the flat and on-edge bales.

Flat Bale

Figures 3.19 and 3.21 both indicate a strain hardening response observed for flat bales tested in compression. As discussed in Chapter 2, this is the expected response for an un-plastered flat straw bale tested in compression. At 100 mm the bale carried a load of 25 kN.

From Figure 3.21, the slope of the stress strain curve can be used to determine the bale modulus. As can be seen from the Figure, the slope increases as the load is increased, thus the bale modulus will increase with increasing load.

3.0 Constituent Material Properties

Based on Figure 3.21, the bale modulus was found to range from approximately 0.15 MPa to 0.43 MPa depending on the load. These results are presented in Table 3.2 along with the values presented in the literature. The average bale modulus from all values is 0.364 MPa.

On-Edge Bale

Figures 3.20 and 3.22 show the linear response of the on-edge bale loaded in compression. Figure 3.20 indicates that under a 100 mm deformation the load resistance of an un-plastered bale on edge is approximately 12 kN. This is approximately half of the load resistance under 100 mm deformation for a flat bale.

Figure 3.22 shows the linear nature of the stress-strain response for on-edge bales. The straw modulus determined from the slope in Figure 3.22 was found to be 0.21 MPa. This value is given in Table 3.2, where it is shown to agree with the values reported in the literature.

3.4 Conclusions

The results presented in this Chapter provide validation for a theoretical model for the stress-strain behaviour of lime-cement plaster. In addition, a preliminary analysis of the parameters which influence the plaster stress-strain behaviour was conducted, and the specific influence of the various parameters was quantified. The following is a summary of the findings:

- The modified Collins and Mitchell (1997) stress-strain model was found to be an appropriate fit for the stress-strain response of lime-cement plasters.

3.0 Constituent Material Properties

If the Modulus of Elasticity, compressive strength, and strain at ultimate stress are known for a plaster specimen, Equations 3.5, 3.8, and 3.9 provide a means of modeling the stress-strain behaviour of the specimen, while if only the compressive strength of a plaster specimen is known, Equation 3.10 provides a means of modeling the stress-strain behaviour of the specimen.

- For the plasters tested, the Modulus of Elasticity of the plaster was found to be 818 times the strength of the plaster.
- For cubes made from the same plaster batch, the coefficient of variation for the strength of three cubes was found to be 8.1%.
- For batches made with the same mix proportions, there is a range of +/- 22.5% for 95% confidence in the mean strength of the batch.
- The relative quantities of lime, cement, sand, and water were all found to influence the compressive strength of low-strength lime-cement plaster. Equation 3.12 presents the influence of the dry mix proportions on the plaster strength, while Figure 3.13 presents the influence of the w/cm ratio on the strength of the plaster.
- For lime-cement plasters, the plaster strength was found to increase with increased curing time and the strength of cube specimens were found to be greater than the strength of cylinder specimens.

3.0 Constituent Material Properties

- A single flat bale was found to have increasing stiffness as the load is increased, with bale modulus values ranging from 0.15 to 0.43 MPa for stress values up to about 0.075 MPa.
- A single on-edge bale was found to behave linearly with a constant bale modulus of approximately 0.21 MPa.

3.0 Constituent Material Properties

Table 3.1: Comparison of Experimental vs. Theoretical Average Cube Strengths

Proportions (By Volume)			Compressive Strength (MPa)		
<i>Cement</i>	<i>Lime</i>	<i>Sand</i>	<i>Theoretical, Eq.3.3</i>	<i>Experimental</i>	<i>Exp./Theo.</i>
1	3	12	2.78	3.10 ^a	1.12
1	2	9	4.73	5.17 ^b	1.09
1	2	7.5	5.90	3.96 ^a	0.67
1	2	9	4.73	5.11 ^a	1.08

^a Boynton and Gutschick, 1964

^b NLA, 2002

Table 3.2: Bale Modulus Values for Un-Plastered Straw Bales

Bale Orientation	Bale Modulus (MPa)
Flat	0.15 – 0.43
Flat	0.7 ^a
Flat	0.083 – 0.237 ^b
Flat	0.31 ^c
Flat	0.05 – 0.8 ^d
Flat	0.41 – 0.47 ^e
On Edge	0.21
On Edge	0.67 ^a
On Edge	0.46 ^c
On Edge	0.08 – 0.9 ^d

^a Bou-Ali, 1993

^b Watts et al., 1995

^c Zhang, 2000

^d Ashour, 2003

^e Field et al., 2005

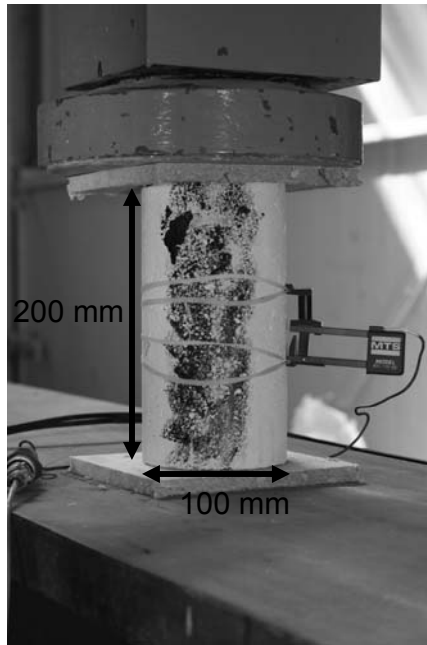


Figure 3.1: Setup of Compression Test of Plaster Cylinder

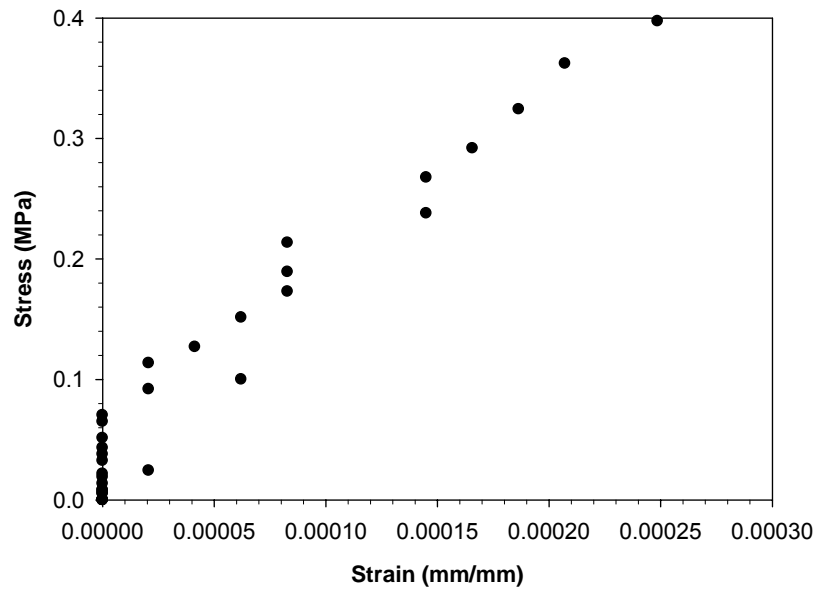


Figure 3.2: Sample Stress-Strain Curve up to 40% of Ultimate Load

3.0 Constituent Material Properties

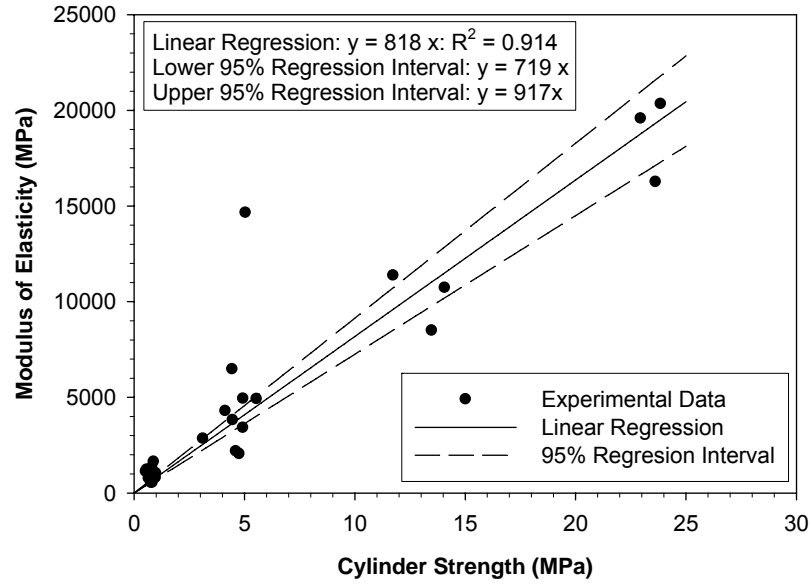


Figure 3.3: Plaster Modulus of Elasticity as a Function of Cylinder Strength for Individual Plaster Specimens

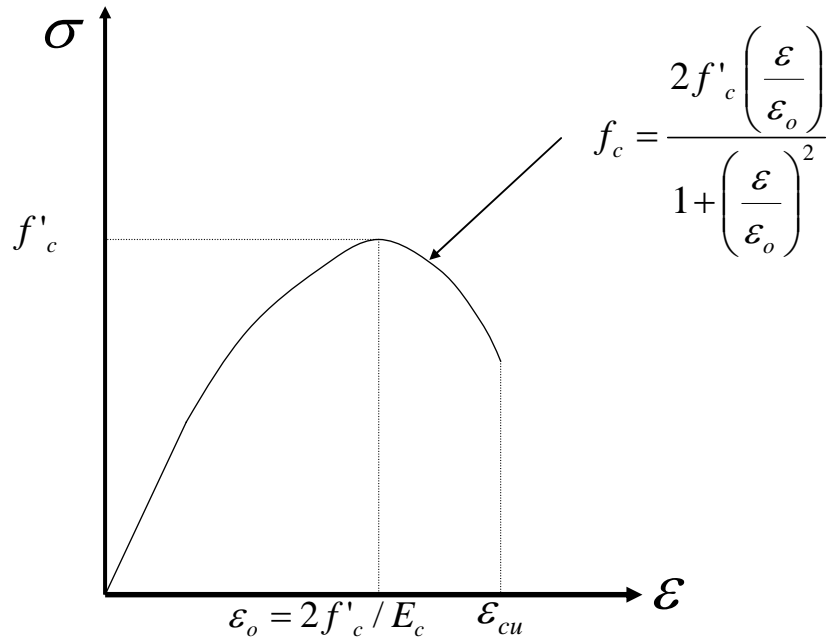


Figure 3.4: Concrete Stress-Strain Model (Desayi and Krishnan, 1964)

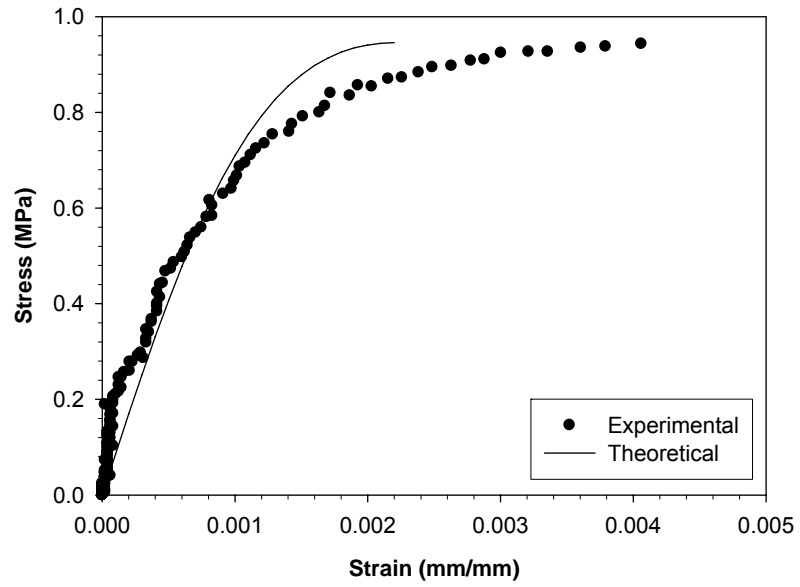


Figure 3.5: Comparison of Theoretical and Experimental Stress-Strain Curves I

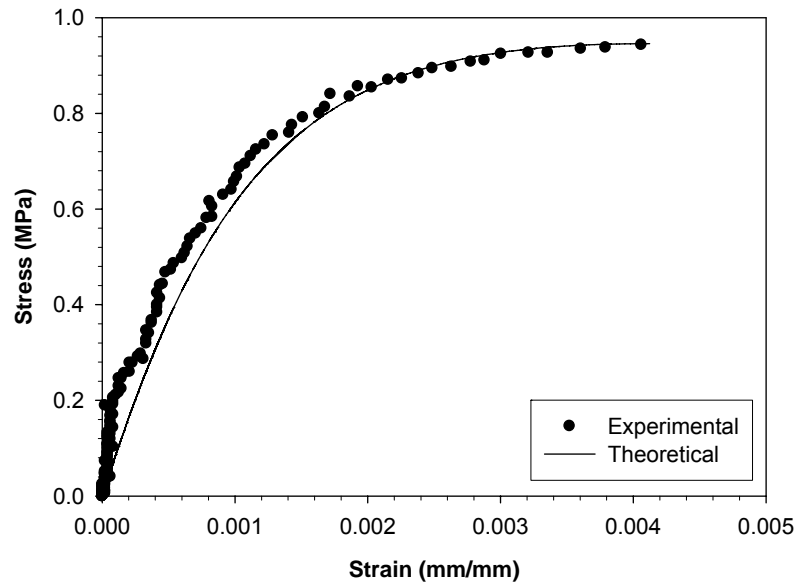


Figure 3.6: Comparison of Theoretical and Experimental Stress-Strain Curves II

3.0 Constituent Material Properties

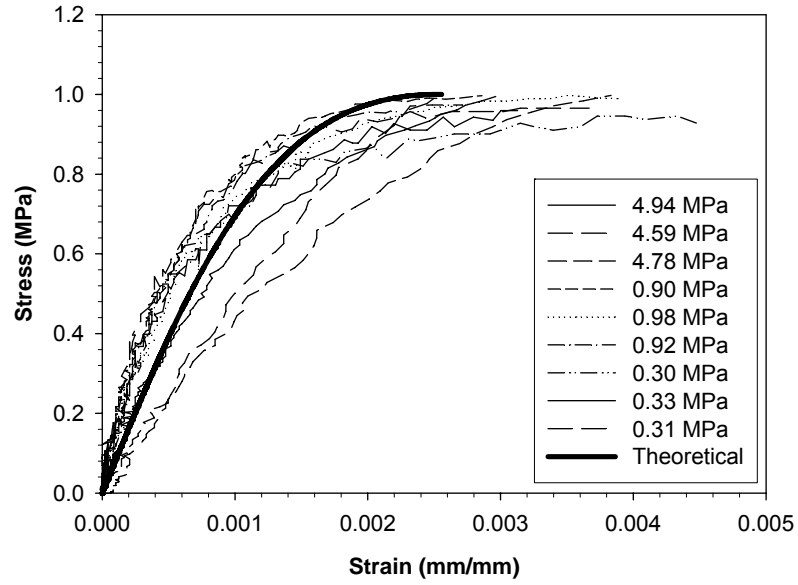


Figure 3.7: Comparison of Theoretical and Experimental Stress-Strain Curves III

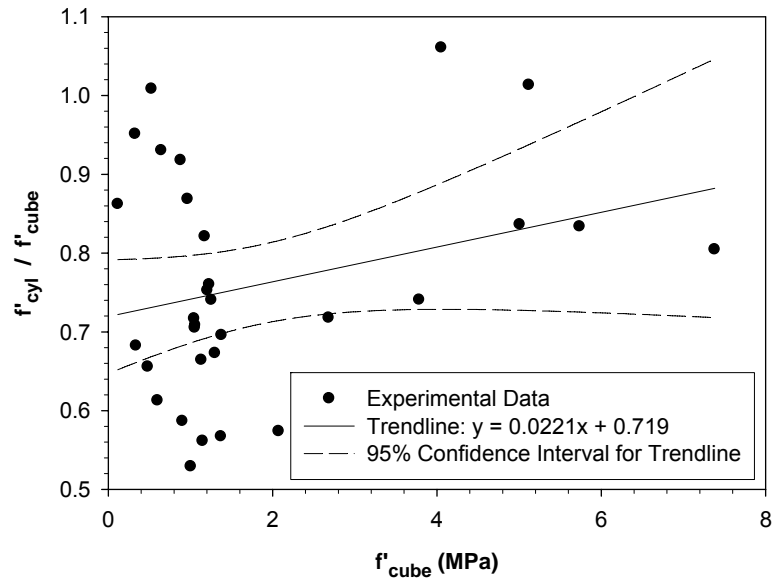


Figure 3.8: Relationship between Cube (f'_{cube}) and Cylinder (f'_{cyl}) Strength

3.0 Constituent Material Properties

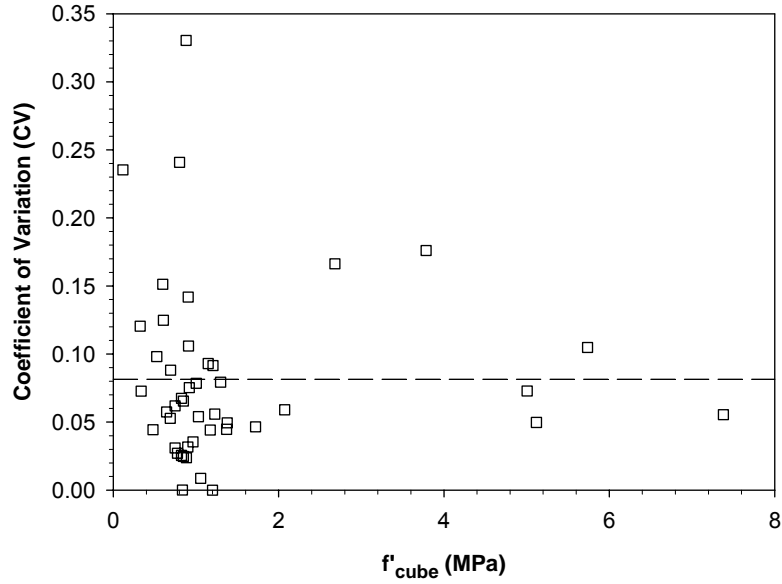


Figure 3.9: Variability of Specimen Strength (f'_{cube}) within a Batch

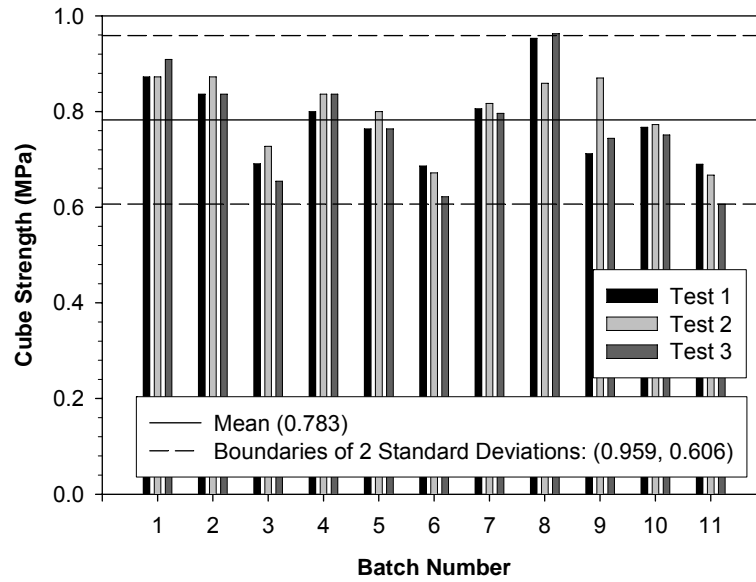


Figure 3.10: Variability of Compressive Strength between Batches

3.0 Constituent Material Properties

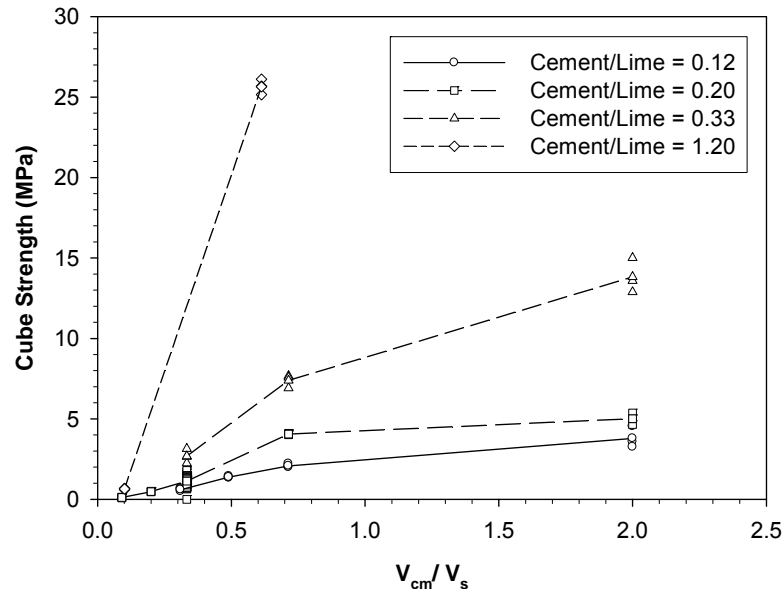


Figure 3.11: Influence of Dry Material Mix Proportions on Compressive Cube Strength

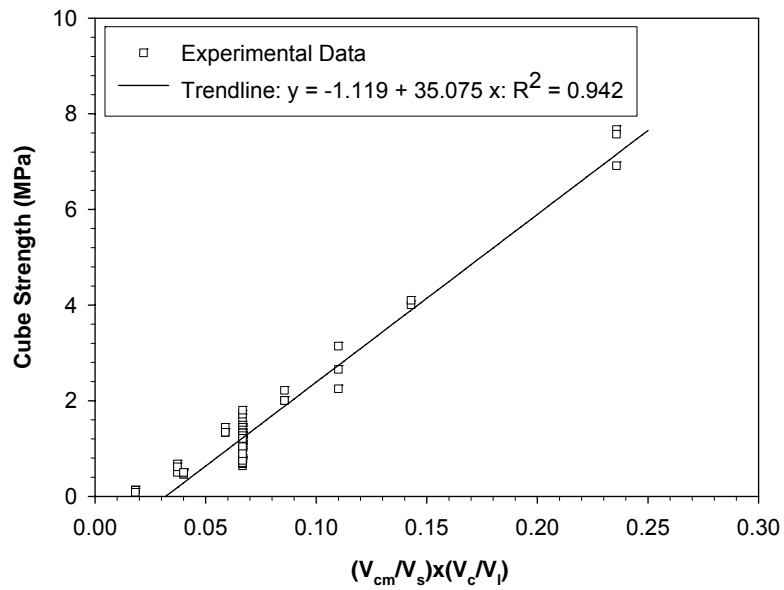


Figure 3.12: Influence of Practical Dry Material Mix Proportions on Compressive Cube Strength

3.0 Constituent Material Properties

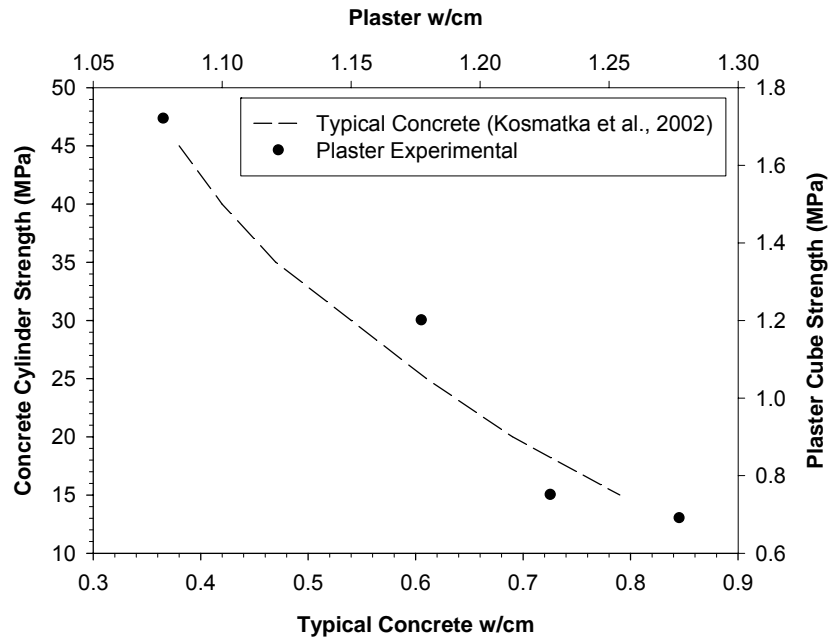


Figure 3.13: Relationship between w/cm Ratio and Compressive Strength

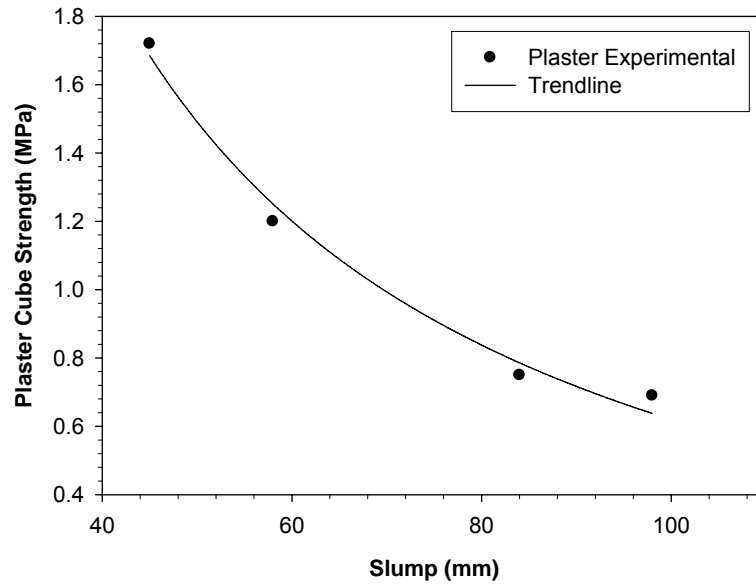


Figure 3.14: Relationship between Slump and Compressive Strength

3.0 Constituent Material Properties

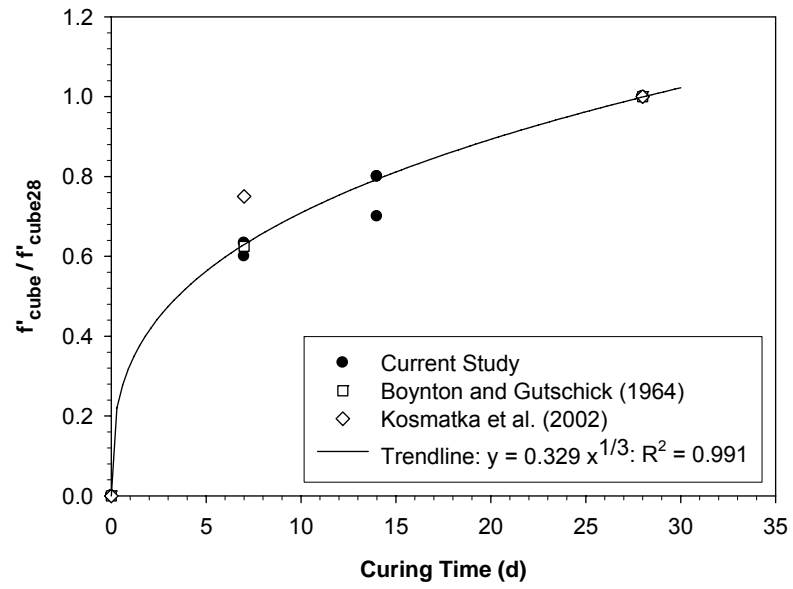


Figure 3.15: Strength Gain with Curing Time Less than 28 Days



Figure 3.16: Straw Bale Fabrication Jig



Figure 3.17: Trimming Straw Bale in Fabrication Jig

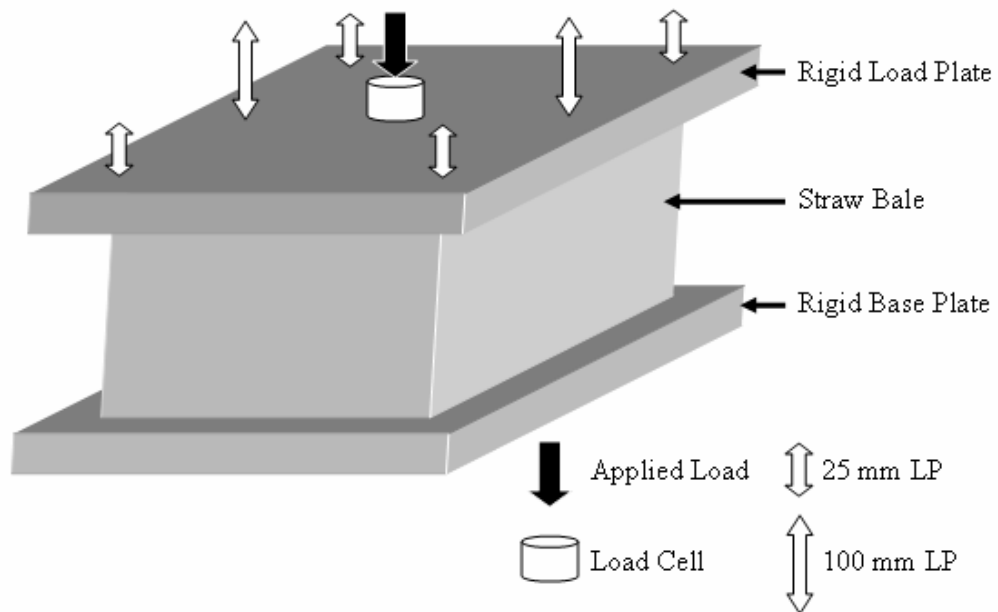


Figure 3.18: Straw Bale Compression Test Setup

3.0 Constituent Material Properties

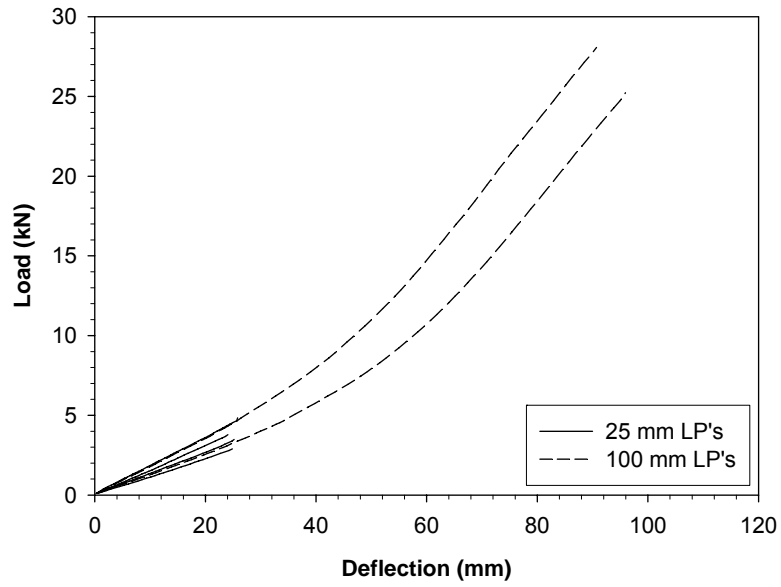


Figure 3.19: Load-Deflection Curve for Flat Un-Plastered Bale

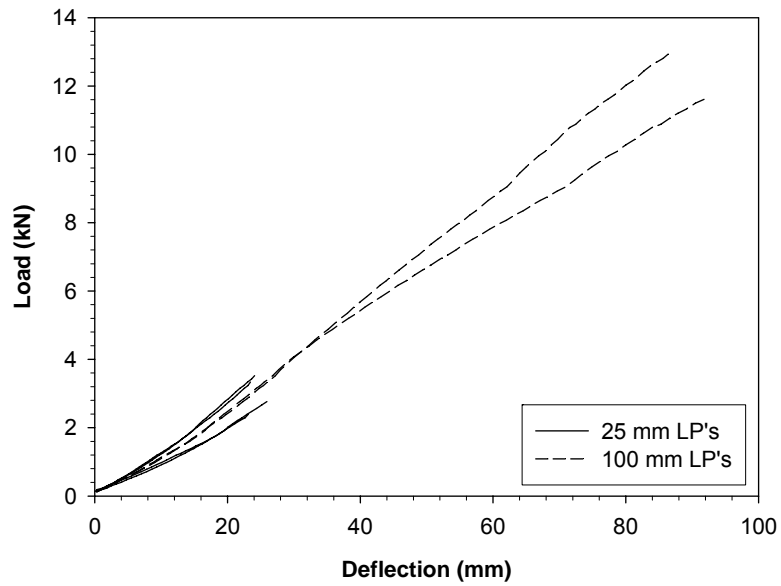


Figure 3.20: Load-Deflection Curve for On-Edge Un-Plastered Bale

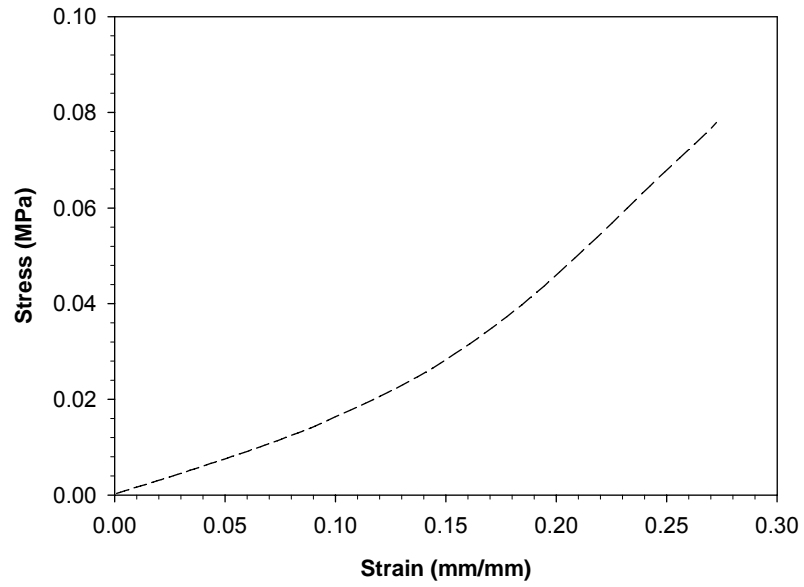


Figure 3.21: Stress-Strain Curve for Flat Un-Plastered Bale

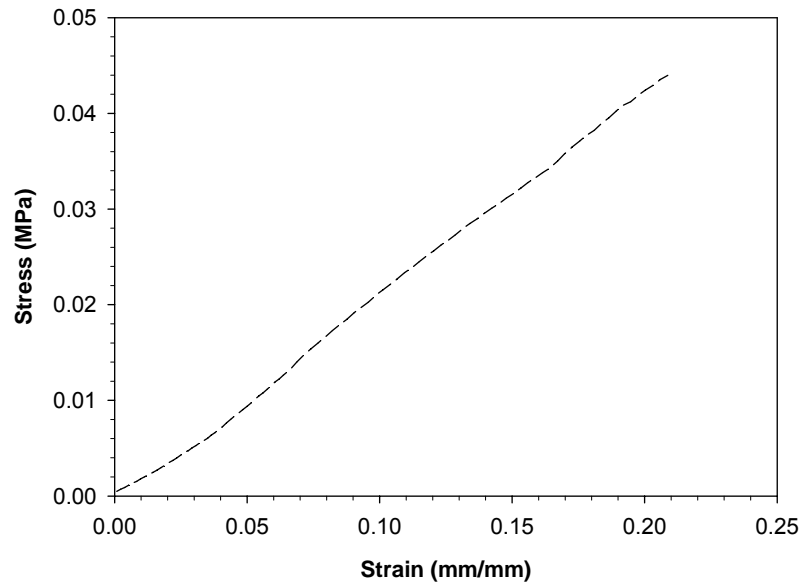


Figure 3.22: Stress-Strain Curve for On-Edge Un-Plastered Bale

Chapter 4: Preliminary Compression Testing of Plastered Bale Assemblies

4.1 Introduction

This Chapter presents the results of testing and analysis of plastered straw bale assemblies subjected to compressive loading. There are currently no standards for testing straw bale assemblies, and as a result there is a lack of consistency in test methods, and a wide range of reported test results. Furthermore, the dimensional inconsistencies of straw bales make it difficult to reproduce results.

A fabrication and testing method is proposed in this Chapter. The specimens simulate straw bale construction but have consistent dimensions that permit repeatable testing.

Thirty plastered straw bale assemblies are fabricated using the method, and are tested in compression to failure. The results of the tests are compared to theoretical predictions assuming the strength of the assemblies is governed by

4.0 Preliminary Compression Testing of Plastered Bale Assemblies

compressive failure of the plaster. The plastered bale specimens were constructed with varying bale orientation, plaster thickness, and plaster strength.

4.2 Design and Fabrication

4.2.1 Materials

4.2.1.1 Straw Bales

The straw bales to be used in the experiments were two-string wheat bales similar to those discussed in Chapter 3. They were obtained from a local farmer and were stored in dry conditions. At the time of fabrication and testing, the bales were less than a year old and, except where specifically noted, they were dry and well bound. The bales had initial dimensions of 375 ± 10 mm height, 475 ± 10 mm width, and 800 ± 25 mm length. The bales were found to have dry bulk densities ranging from 78 to 112 kg/m^3 .

The wide range of dimensions and densities is a function of the imprecision common with baling machines. Even when the same baler is used to produce the bales, the properties of the bales can vary significantly. As a result, the fabrication procedure presented below provides a means of modifying the bales so as to produce specimens with more consistent dimensions. However, the strength and stiffness of the straw are two parameters which are difficult to control. The strength and stiffness of the straw are not an issue as Chapter 3 highlighted the fact that failure of a straw bale will only occur under extreme deformations and that the straw is much softer than lime-cement plaster.

4.0 Preliminary Compression Testing of Plastered Bale Assemblies

4.2.1.2 Plaster Design and Mixing

There is currently no standard for plaster mixtures for straw bale construction. It was determined through discussions with a local straw bale builder that a typical plaster skin is applied in two layers. The first layer is a lime/cement plaster with proportions by volume of 3 : 0.75 : 0.25 of sand, hydrated lime and cement. This layer is typically applied to a thickness of approximately 16 mm. The second layer is a lime plaster with proportions by volume of 3 : 1 of sand and hydrated lime. This layer is typically applied to a thickness of 9 mm. In the current study, a single mix with proportions of 4.5 : 1.25 : 0.25 of sand, lime and cement respectively was applied in one coat to a total thickness of 25 mm. This mix represents a weighted average of the two layers. While a weighted average may not result in a plaster skin of equivalent properties to a skin fabricated in multiple layers, it provides an approximate appropriate mix for use in plastered straw bale wall assemblies. This mix is studied in detail in chapter 3 in order to better understand the variability in the properties of the plaster.

For this mix, the cement was provided as a component of Mason's Choice High Bond Portland Lime Type N, produced by St. Lawrence Cement. This product contains equal portions (by volume) of Type 10 Portland cement and hydrated lime. The remainder of the lime required to provide the desired mix proportions was Bondcrete ® Mason's Lime produced by Graymont Dolime (OH) Inc.

In preparing the plaster, masonry sand was added to the batch mixer (which is described in Appendix A). The appropriate quantities of High Bond Portland Lime and Bondcrete ® Mason's Lime were then added to the mixer and the dry materials

4.0 Preliminary Compression Testing of Plastered Bale Assemblies

were blended together. Finally the desired quantity of water was added to the mix. The quantity of water added was based on the w/cm ratio, where the quantity of tap water required was calculated by determining the total water required based on the w/cm ratio and subtracting the quantity of water already contributed to the mix as moisture in the sand.

The w/cm ratio was varied to provide a range of plaster strengths. The design strengths are 1.43 MPa, 1.12 MPa and 0.80 MPa, representing workable plaster with w/cm ratios of 1.08, 1.18, and 1.28 respectively. These mixes represent plaster with dry, average and wet consistency. Note that while the plaster was designed to achieve strengths as noted above, because of variability amongst batches of the same mix design (as discussed in chapter 3) and because cubes were not fabricated from each batch to confirm the specific batch strength, there is inherent lack of confidence in the exact in-situ plaster strength. However, the plaster applied to the specimens should have strengths which vary about (above and below) the design strengths.

4.2.2 Fabrication Procedure

The fabrication process is illustrated in Figure 4.1. For Steps 1 and 2 the bales were compressed and trimmed using the testing jig shown in Figures 3.16 and 3.17. Note that while trimming of the straw is common building practice, the straw is not typically trimmed to the precision as described for these experimental specimens. Following fabrication it was observed that the maximum bale width was 405 mm. However, due to the inhomogeneous nature of the straw, there were air

4.0 Preliminary Compression Testing of Plastered Bale Assemblies

voids in the straw leading to straw width which ranged from 395 mm to 405 mm. This is shown in Figure 4.2. Note in Figure 4.2 that “ t_d ” refers to the design plaster thickness.

The third step was to attach plastic formwork or “edging” to the sides of the jig, as shown in Figure 4.3 and indicated by Step 3 in Figure 4.1. Note the edging is attached to each side of the jig, although only one side is shown in Figure 4.3. The edging ensured the plaster was applied to a consistent thickness. The thickness of the edging varied between specimens as the desired plaster thickness was varied between specimens. The edging provided formwork to create plaster skins with length of 600 ± 1 mm, height of 330 ± 1 mm and a thickness of 13 ± 1 mm, 25 ± 1 mm, or 38 ± 1 mm. The use of edging deviates from common straw bale construction practice. However, for the purpose of experimentation, the edging was required to ensure that the plaster skins on the sides of each plastered bale had consistent dimensions.

The fourth step, as shown in Figure 4.4 and indicated by Step 4 in Figure 4.1 was the application of the plaster. The plaster was applied to one side of the bales at a time. No reinforcement mesh was applied. The bales were laid so that the surface to be plastered was oriented upwards. The plaster was first worked into the straw by hand, and then was poured into the formwork to a thickness determined by the edging. The outer surface was troweled smooth. A plastered bale with the edging in place is presented in Figure 4.4.

4.0 Preliminary Compression Testing of Plastered Bale Assemblies

Following plastering of the first side of the bales, the specimens were covered with moist burlap and allowed to cure for 12-24 hours. After the initial curing time, the bales were flipped 180 degrees so that the opposite surface to be plastered was oriented upwards. The plastering procedure was repeated for the second plaster skin. The bales were then covered with moist burlap and allowed to cure for an additional 12-24 hours. The bales were then stood on end with the plaster skins oriented vertically, covered with moist burlap, and allowed to cure for three days. This curing scheme was chosen to mimic curing conditions typically found for plastered straw bale construction (Magwood and Mack 2000). The final step in specimen preparation was to remove the formwork as indicated by Step 5 in Figure 4.1. This was done following the full curing period. Figure 4.5 shows a finished flat plastered bale.

It was observed following fabrication that the thickness of the plaster was variable as a result of the plaster being worked into the air voids in the straw bales. As a result, while the minimum thickness was as designed (13 ± 1 mm, 25 ± 1 mm, or 38 ± 1 mm), the plaster in some regions was up to 5 mm thicker than intended, as shown in Figure 4.2. It should be noted that the exact in-situ thickness of the plaster following fabrication was not measured. The values given are based on observations of the width of the straw, and the variability in the edging.

4.2.3 Description of Completed Specimens

The fabrication procedure produced a number of specimens with different design plaster strength and plaster thickness. An overview of the specimens and the

4.0 Preliminary Compression Testing of Plastered Bale Assemblies

design plaster strengths and thicknesses is presented in Table 4.1. Three specimens with the bales laid flat were fabricated simultaneously for a particular combination of design plaster strength and designed plaster thickness. A single plaster batch was used for one side of all three specimens, with a second batch used the following day for the opposite side of all three specimens.

Note that according to the test numbers there are missing configurations. These correspond to specimens fabricated with the bales on-edge. However, these specimens were compromised due to significant fabrication issues as a result of rebounding of the straw bale following fabrication and prior to testing. As a result, these specimens are not discussed in this chapter, but are instead presented in Appendix D. Also note that for tests 19-21, the bales were damaged by flood water during curing, and the straw was wet and mouldy when the bales were tested. As a result, the data from these experiments were omitted from the analysis. Analysis of these results may give insight into the behaviour of water-damaged plastered straw bale walls; however this is outside of the scope of this thesis. Tests 28-30 were a repeat of tests 19-21.

Figures 4.2 and 4.3 provide the dimensions of the fabricated specimens. The length of the straw for the fabricated specimens was 800 ± 25 mm and was not controlled as there was no reasonable method found to control the bale length. Because the bale contributes very little to the overall compressive strength (as discussed further in this chapter), the variability in bale length was not considered to be a significant factor influencing the results. Similarly, the straw width was found to range from 395 to 405 mm. While this variability in straw width will not significantly

4.0 Preliminary Compression Testing of Plastered Bale Assemblies

directly influence the performance of the plastered bale assemblies, the variability in straw width did influence the plaster thickness as discussed previously. Of more significance is the observation of straw rebound following fabrication. When the plastered straw bale assemblies were removed from the fabrication jigs, the straw was observed to rebound upwards as shown in Figure 4.2. As a result, when the assemblies were tested they underwent an initial stage of re-compression of the bales prior to contact being made between the loading apparatus and the plaster skins. Note that the exact height of the rebound was not measured and that the amount of rebound was variable depending on the initial dimensions and density of the bales.

An additional noted fabrication issue was the unevenness of the plaster at the top and bottom surfaces of the plaster skins. The edging was found to be rougher than anticipated, resulting in uneven plaster surfaces upon which the load is applied. The implications of this unevenness will be discussed in the results section.

4.3 Instrumentation

The instrumentation for the individual plastered bale compression experiments is shown in Figure 4.6 and consisted of a load cell, two 100 mm LPs and four 25 mm LPs. The four 25 mm LPs were located at the four corners of the loading plate. The 100 mm LPs were located at the middle of the ends of the bale. The load and deflection were recorded at a rate of approximately 16 samples per second throughout the duration of the experiments. Appendix A provides additional details on the instrumentation and testing apparatus.

4.0 Preliminary Compression Testing of Plastered Bale Assemblies

4.4 Procedure

Figures 4.7 and 4.8 show the loading apparatus which consisted of a steel box-beam, two steel I-sections (W200x19), a 19 mm thick plywood board and a wooden brace. The box beam transferred the load to the steel sections which in turn transferred the load to the plaster skins. The two steel I-sections were situated directly above the plaster skins to ensure the load was transferred directly to the plaster. The plywood was used to ensure even compression of the straw as the plaster skins were compressed. The wood brace was installed in the middle of the loading apparatus in order to prevent upward deflection of the plywood. The loading apparatus was 1.3 m long to ensure the apparatus extended beyond even the longest possible straw bale.

The loading rate was approximately 1 mm/min until the ultimate load was reached. Once an assembly had passed its ultimate load, the loading rate was increased to approximately 2 mm/min. When the four 25 mm LPs had reached their limits, the loading rate was increased to approximately 3 mm/min. The test was stopped when the two 100 mm LPs exceeded their range.

4.5 Results

4.5.1 Description of Structural Behaviour

The axial load versus axial deflection response for a typical plastered bale tested flat is shown in Figure 4.9. The curves labelled DISP 1 through DISP 6 represent the load displacement curves for the plastered bale as measured by the six LPs located at the top of the bale. For this particular figure, the plaster was 25

4.0 Preliminary Compression Testing of Plastered Bale Assemblies

mm thick with design plaster strength of 1.43 MPa. The response of the plastered bale is non-linear up to about 3 mm axial deflection. This represents the region in which the rebounded straw is being re-compressed. Beyond the initial non-linearity the load-displacement response is approximately linear until the maximum load is attained at approximately 36 kN. The deflections obtained by the six LPs at each load level differ by less than 10% prior to reaching the ultimate load. This indicates that the loading applied to the plastered bale was essentially uniform during this portion of the test.

Upon reaching the ultimate load, the plaster was observed to crush as shown in Figure 4.10. This corresponded to a sudden drop in load from about 36 kN to about 15 kN. The post-cracking behaviour was ductile, as the load was taken by the straw bale as the plaster skins deteriorated. There are two peaks observed in the load-deflection plot. These represent the failure of the two sides of the assembly, as the plaster skins did not fail simultaneously. Note that the cracked plastered bale continued to carry about 15 kN, and beyond about 20 mm axial deflection, the load increases gradually.

Figure 4.11 provides a magnification of the area of the typical pre-failure load-deflection behaviour for a plastered straw bale. For this figure the displacement obtained from the six LPs in each experiment was averaged to create a single plot. Figure 4.11 shows the linearity of the load-deflection response from the point following re-compression of the bale to near ultimate. There is some non-linearity noted as the ultimate load is reached.

4.0 Preliminary Compression Testing of Plastered Bale Assemblies

The behaviour of the bales up to the point of first failure is of the greatest importance as it is this initial failure which will result in significant reduction in load carrying capacity and observable damage to the plaster. Thus, for the remainder of this thesis, it is the response of the plastered straw bales up to the point of first load drop (described as the point of ultimate failure), which will be studied. However, it is important to note the significance of the ductile behaviour observed post-failure.

4.5.2 Plastered Bale Ultimate Strength

Table 4.2 presents the experimental ultimate strengths for plastered straw bale specimens with varying plaster strengths and thicknesses. These results are also summarized in Appendix C. Note that the values presented are normalized by dividing the ultimate load by the length of the plaster (600 mm).

4.6 Theoretical Concentric Compression Behaviour

4.6.1 Theoretical Strength Model

Figure 4.12 is a schematic of a simplified plastered straw bale subjected to concentric compressive load. The loading plate is not shown in this figure, but it is assumed that it is perfectly rigid, so that deflections of the straw and plaster are equal. Figure 4.13 is a free-body diagram of the loading plate. If the plastered bale fails when the plaster reaches its cube strength f'_{cube} , with plaster strain at ultimate of ϵ_{cube} , the force in the plastered bale at failure is:

$$F_{Ult} = 2f'_{cube} Lt_p + E_{Straw}\epsilon_{straw}A_{Straw} \quad 4.1$$

4.0 Preliminary Compression Testing of Plastered Bale Assemblies

where F_{Ult} is the force in the plastered bale assembly at ultimate failure, t_p is the thickness of the plaster, L is the plaster length, E_{Straw} is the straw bale modulus, ϵ_{straw} is the strain in the straw, and A_{Straw} is the area of the straw upon which the load is applied.

The thickness of the plaster (t_p) can be taken as the design plaster thickness t_d . Equation 4.1 assumes failure of the specimen when the plaster reaches f'_{cube} . Thus, the strain in the plaster at failure (ϵ_{cube}) can be assumed to be equal to $\epsilon_{cube} = 0.00253$, which was shown in Chapter 3 to be the average strain at ultimate stress for the plaster. If uniform deformation of the plastered straw bale is achieved, the strain in the straw (ϵ_{straw}) will also be approximately 0.00253 at failure. If the bale modulus is taken as the average from all of the values reported in Table 3.1, then for flat bales the bale modulus is 0.364 MPa. Thus, the force in the straw can be found by multiplying together the strain, the modulus, and the area of straw (800 mm x 405 mm), giving a value of 298 N for the contribution from the straw.

In order for Equation 4.1 to be valid, a number of assumptions must be made regarding the behaviour of the plastered straw bale wall assemblies. These are as follows:

- Uniform compression of the plastered bale;
- Failure by crushing of the plaster when plaster reaches f'_c ;
- Strain at failure equal to 0.00253;
- Modulus of straw equal to 0.364 MPa;

4.0 Preliminary Compression Testing of Plastered Bale Assemblies

- Straw provides adequate lateral support to prevent local buckling; and
- Global buckling does not govern failure.

Additionally, assumptions are made that the dimensions of the straw and plaster, and the strength of the plaster were as designed. The validity of these assumptions is discussed in the following sections as well as in following Chapters and in Appendix E.

4.6.2 Calculation of Theoretical Strength

The theoretical strengths determined by Equation 4.1, are presented in Table 4.2. Two values for the theoretical strength are presented for each specimen. The first theoretical strength value is based on Equation 4.1, and assumes that the loading assembly is in direct contact with the plaster and the straw from the beginning of the test. For this calculation the straw and plaster are assumed to deflect equally and thus Equation 4.1 assumes the strain in the straw at failure is equal to the average plaster failure strain. As such, the contribution from the straw for all specimens will be 0.5 kN/m. Considering that the weakest specimen presented in Table 4.2 had strength of 31.6 kN/m, the contribution from the straw based on this calculation will be no greater than about 1.6 %. As such, it is reasonable to neglect the contribution from the straw for this calculation, however, to ensure complete accuracy, the contribution from the straw is included in the theoretical strengths presented in Table 4.2.

The second theoretical strength value takes into account the noted rebound in the straw following fabrication. Because of this rebound, when the assemblies

4.0 Preliminary Compression Testing of Plastered Bale Assemblies

were tested the straw was re-compressed before complete contact was made between the loading apparatus and the plaster skins. The previous theoretical discussion does not account for the load applied to the straw as it is re-compressed. This may lead to errors in the estimation of the theoretical assembly strength.

For this alternative theoretical calculation it is assumed that the assembly will still fail when the plaster reaches its ultimate strength. As a result, the first term in Equation 4.1 remains a valid method of determining the contribution from the plaster. However, the second term in Equation 4.1 requires further consideration as the previous calculation assumed the strain in the straw was equal to the strain in the plaster. However, the strain in the straw will be greater than the strain in the plaster because the straw undergoes the additional deflection (strain) as it is re-compressed at the beginning of the experiment. Thus, when determining the contribution of the straw at ultimate failure of the assembly it is necessary to determine the total deflection of the straw, including the deflection required to re-compress the rebounded straw. As a result, it is required to study the experimental load-deflection response of the assembly. Once the total deflection of the straw is determined, this value can be converted to strain, and be used in place of ϵ_{straw} in the second term of Equation 4.1 to determine the contribution from the straw.

For example, for the specimen presented in Figure 4.11 it can be seen that the total deflection at ultimate failure is 6.8 mm. On the other hand for the 330 mm high plaster skins with assumed strain at failure of 0.00253, the deflection at failure will be 0.835 mm. Thus, the straw deflected 6.0 mm more than the plaster, indicating a 6.0 mm rebound of the straw. This indicates an initial straw height of

4.0 Preliminary Compression Testing of Plastered Bale Assemblies

336 mm. Knowing the initial straw height of 336 mm and the total straw deflection of 6.8 mm, the strain in the straw at ultimate failure can be calculated as 0.0202. Assuming straw bale modulus of 0.364 MPa (as described previously), and straw bale dimensions of 405 mm x 800 mm, the total contribution from the straw for this particular experiment is 2382 N, or 3.97 kN/m (normalized by the length of the plaster). This contribution from the straw is not insignificant, as for this specific case it represents nearly 7% of the total experimental strength.

The contribution from the straw can be added to the contribution from the plaster to determine the total theoretical strength. This procedure is carried out for each specimen and provides the second theoretical strength values calculated and presented for each specimen in Table 4.2. It is important to note that the properties of the straw bales are variable and that this theoretical calculation is only an estimation based on the average contribution from the straw.

It can be seen in Table 4.2 that for some specimens the theoretical strength calculated by accounting for the rebound of the straw is significantly larger than the theoretical strength calculated by ignoring the rebound of the straw. For Test 25, with 13 mm design plaster thickness and design plaster strength of 1.43 MPa, the difference is as much as 20%. This indicates that while the contribution of the straw may be minimal for specimens where rebound does not occur, the rebounding of the straw for the specimens described herein requires that the contribution of the straw be considered for the theoretical strength calculations. This is a significant issue in that in order to account for the contribution of the straw for specimens with straw rebound, it was necessary to study the experimental load deflection curve. This

4.0 Preliminary Compression Testing of Plastered Bale Assemblies

makes it difficult to make estimations of the theoretical strength in advance of testing. It may be possible to estimate the theoretical strength in advance of testing by assuming an average straw rebound. However, the rebound in the straw was found to vary from 1.7 mm to 14.1 mm for the results presented in Table 4.2, thus indicating the difficulty in estimating the amount of rebound in advance. A more practical solution would be to produce specimens which do not rebound, thus allowing for the use of Equation 4.1. Such specimens would be more representative of conditions in a structure where the bales are prevented from rebounding.

4.7 Discussion

4.7.1 Experimental to Theoretical Strength

Figure 4.14 presents the comparison of theoretical values to experimental values for the experiments conducted on plastered straw bales. The comparison can also be seen in Table 4.2, which presents the ratio of experimental strength to theoretical strength for each specimen. The theoretical strength used for this comparison is calculated with consideration given to the additional load required to re-compress the bale at the beginning of the test as discussed above. It can be seen from Figure 4.14 that the average plastered bale achieved strengths of 83% of the predicted value, with the worst performing specimen achieving 61% of the predicted value and the best performing specimen achieving 113% of the predicted value.

The variability noted in the plastered bale strengths may simply be a result of the inherent variability of the plaster. A t-test indicated that at the 99% confidence

4.0 Preliminary Compression Testing of Plastered Bale Assemblies

level, the average experimental to theoretical ratio (83%) is statistically significantly different from the expected average ratio (100%) when considering the variability in experimental plastered bale strengths and the expected variability in plaster strength. It can also be seen from Figure 4.14 that the strength of the specimens does not influence the ratio of experimental to theoretical strength given that there is not a significant increasing or decreasing trend in the ratios with increasing specimen strength from left to right in Figure 4.14.

4.7.2 Failure Mode Discussion

The lower than predicted experimental strengths may be a result of incorrect assumptions regarding the failure mode of the assemblies. It was assumed that compressive failure of the plaster governed the failure of the plastered bales. However, if local or global buckling were to govern the failure of the specimens, they may achieve lower strengths than expected. Appendix E presents an analysis of the theoretical strengths assuming various failure modes. From this analysis it can be seen that with the short height of the individual plastered bales, the failure is not expected to be governed by either local or global buckling. Rather, the assumption that the compressive behaviour of the plaster governs the behaviour of the individual plastered bales appears to be appropriate.

One potential reason for the fact that the theoretical prediction over-estimates the strength of the specimens is the observed failure at the top of the specimens. It is believed that the slight unevenness at the top of the plastered bales, which was

4.0 Preliminary Compression Testing of Plastered Bale Assemblies

noted during fabrication, led to stress concentrations in this region. As a result it appears as if the plaster failed prematurely.

4.8 Experimental and Construction Recommendations

The plastered straw bale assemblies had experimental strengths which were, on average, 17% less than the theoretical strengths based on Equation 4.1. This behaviour was observed for specimens with a wide range of plaster strengths and thicknesses. It is hypothesized that this difference is a result of stress concentrations in the plaster at the plaster/loading plate interface resulting in bearing failure of the plaster in this region. This highlights the importance of this interface in the fabrication and testing of experimental specimens, as well as for the construction of plastered straw bale walls in practice.

In order to fabricate and test experimental specimens which will not fail as a result of bearing failure of the plaster it is important to ensure that stress concentrations at the top of the plaster skins are avoided. In order to achieve this it is important to ensure consistency between the fabrication and testing of the plastered bale assemblies. The bearing failures arose as a result of inconsistencies between the fabrication and testing jig. However, if the same apparatus is used for fabrication and testing, it will be possible to ensure uniform application of the load. Any variation in the plaster height as a result of imperfections in the fabrication jig will be matched in the testing jig. Ensuring consistency between the fabrication and testing apparatus will also serve to better represent field-practice, where the box

4.0 Preliminary Compression Testing of Plastered Bale Assemblies

beam and bottom plate are used as guides for plaster application, and also serve to transfer loads in-to and out-of plastered straw bale walls.

Another important recommendation to avoid bearing failure of plaster at the top (or bottom) of a plastered straw bale wall is in the fabrication procedure. For both experimental specimens and plastered straw bale walls, it is important that care be taken to ensure that at the top and bottom of the plaster skins, the plaster is effectively worked into the straw, and that the plaster is applied to the appropriate thickness. Doing so will ensure that the load is bearing on a section of plaster which is representative of the entire specimen or wall, and which is not compromised as a result of difficulties in plastering in these regions.

4.9 Conclusions

The main objective of this chapter was to fabricate and test plastered straw bale specimens using an innovative fabrication jig and controlled fabrication and testing techniques. The fabrication methods result in dimensionally consistent specimens; however, un-anticipated bearing failure of the specimens resulted in experimental strengths which were, on average, 17% less than expected, based on the compressive strength of the plaster.

4.0 Preliminary Compression Testing of Plastered Bale Assemblies

Table 4.1: Test Parameters for Compression Tests of Individual Plastered Straw Bales

Test Number	Design Plaster Strength (MPa)	Design Thickness (mm)	Bale Orientation	Comments
1,2,3	1.43	25	Flat	
7,8,9	1.12	25	Flat	
13,14,15	0.80	25	Flat	
19,20,21	1.43	38	Flat	Water Damage
25,26,27	1.43	13	Flat	
28,29,30	1.43	38	Flat	Repeat 19,20,21

Table 4.2: Experimental and Theoretical Plastered Straw Bale Strengths

Test #	Plaster Strength (MPa)	Plaster Thickness (mm)	Plastered Bale Strength (kN/m)			
			<i>Experimental</i>	Theoretical (Eq. 4.2)		<i>Exp./Theo. Ratio</i>
				<i>No Rebound</i>	<i>Rebound</i>	
1	1.43	25	59.1	72.0	75.5	0.78
2	1.43	25	57.6	72.0	74.7	0.77
3	1.43	25	61.2	72.0	75.7	0.81
7	1.12	25	51.8	56.5	59.8	0.87
8	1.12	25	41.3	56.5	59.2	0.70
9	1.12	25	57.4	56.5	59.3	0.97
13	0.80	25	49.3	40.5	43.5	1.13
14	0.80	25	48.4	40.5	43.2	1.12
15	0.80	25	31.6	40.5	41.5	0.74
25	1.43	13	34.7	37.7	45.7	0.76
26	1.43	13	38.2	37.7	43.1	0.89
27	1.43	13	33.2	37.7	44.1	0.75
28	1.43	38	82.7	109.2	110.7	0.75
29	1.43	38	68.6	109.2	112.4	0.61
30	1.43	38	91.5	109.2	111.0	0.82

4.0 Preliminary Compression Testing of Plastered Bale Assemblies

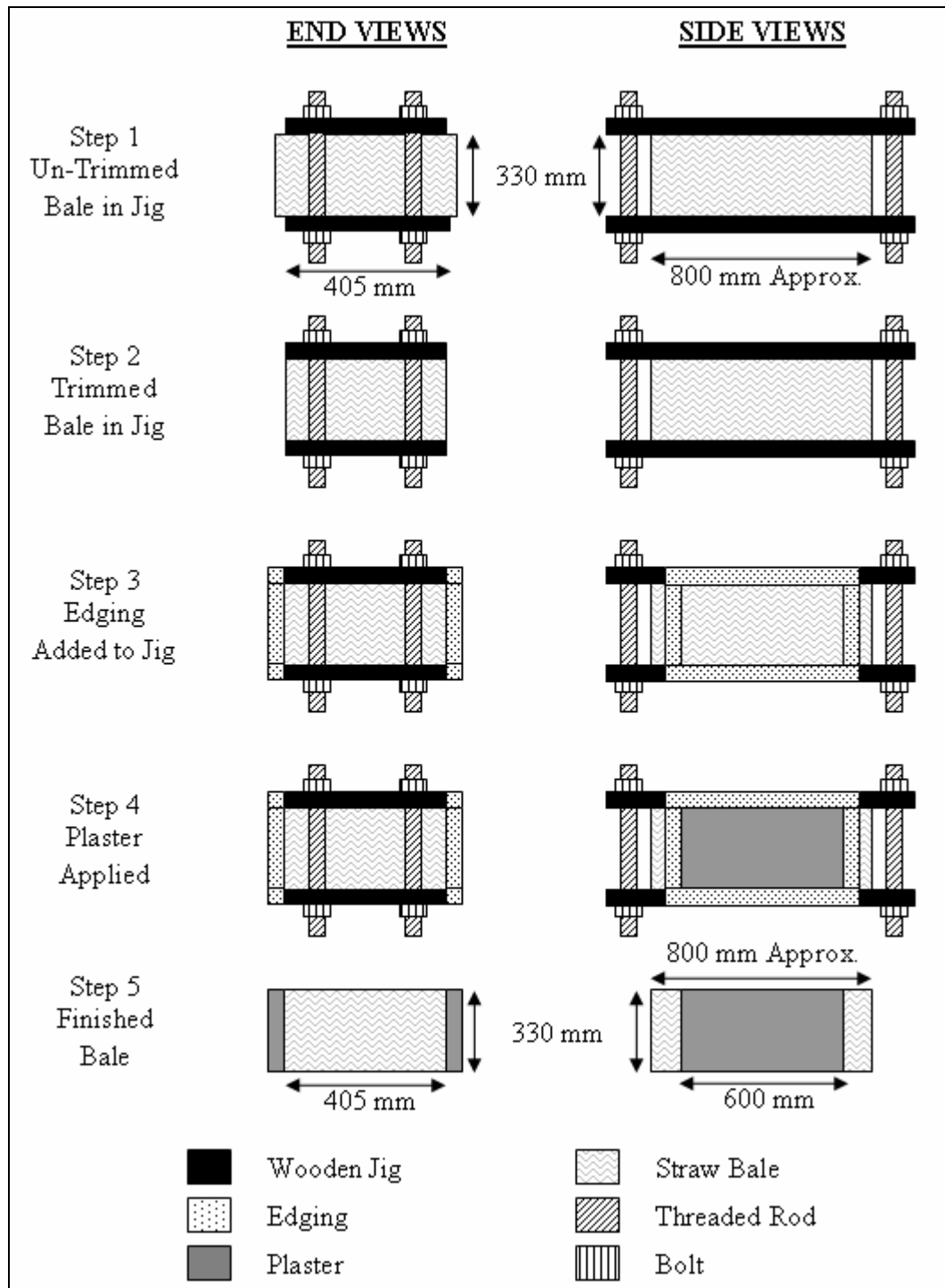


Figure 4.1: Procedure for Preparing Plastered Straw Bale Assemblies

4.0 Preliminary Compression Testing of Plastered Bale Assemblies

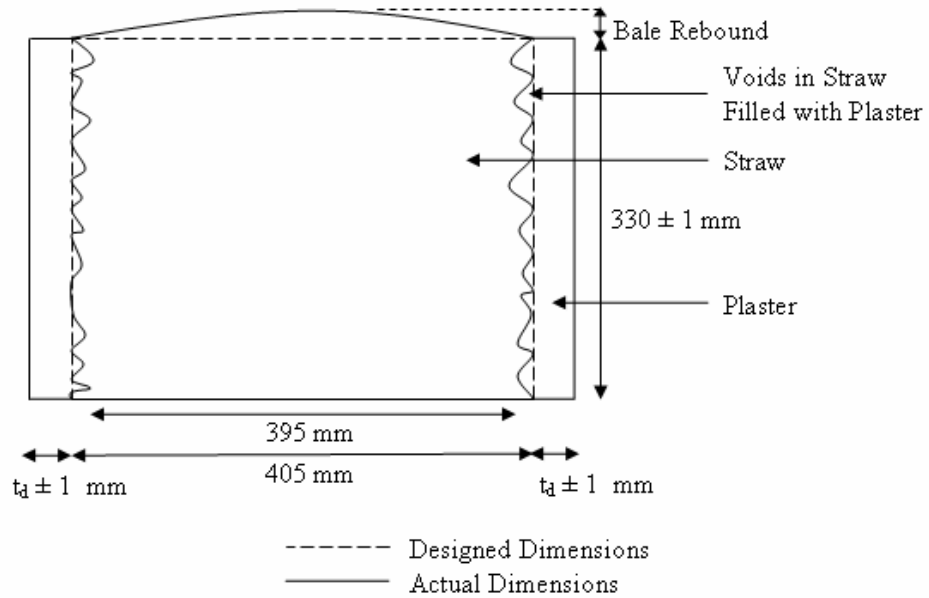


Figure 4.2: Dimensions of Fabricated Plastered Straw Bale Assemblies

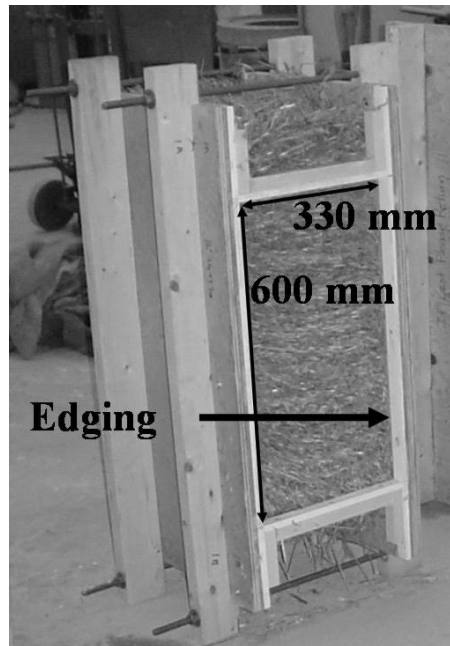


Figure 4.3: Trimmed Bale with Edging

4.0 Preliminary Compression Testing of Plastered Bale Assemblies

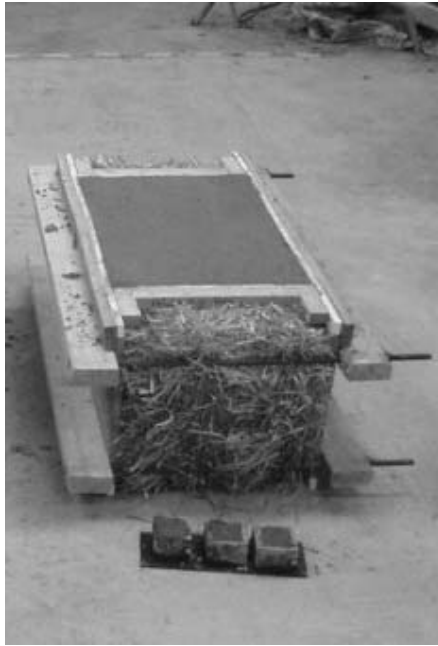


Figure 4.4: Plastered Straw Bale with Edging



Figure 4.5: Completed Plastered Bale

4.0 Preliminary Compression Testing of Plastered Bale Assemblies

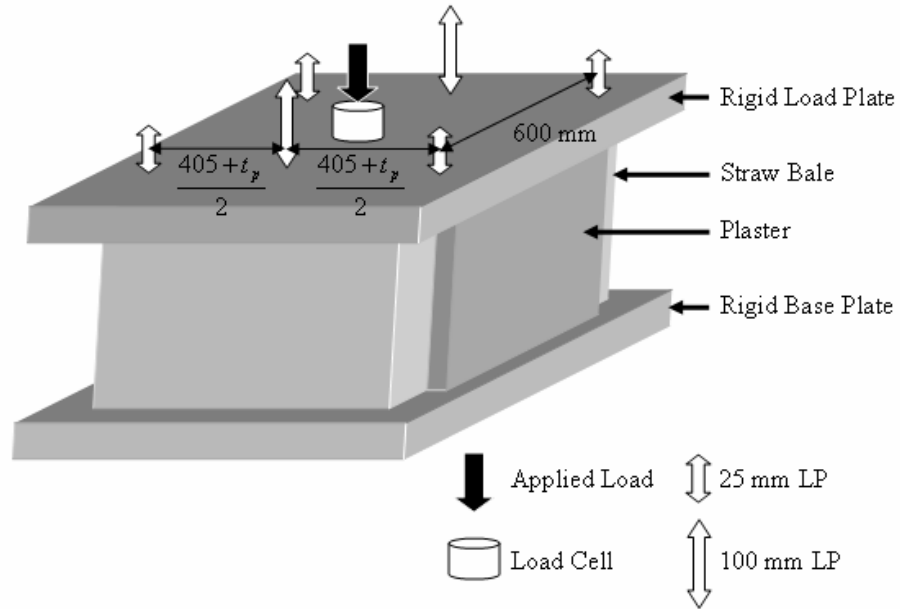


Figure 4.6: Plastered Straw Bale Compression Test Instrumentation Setup

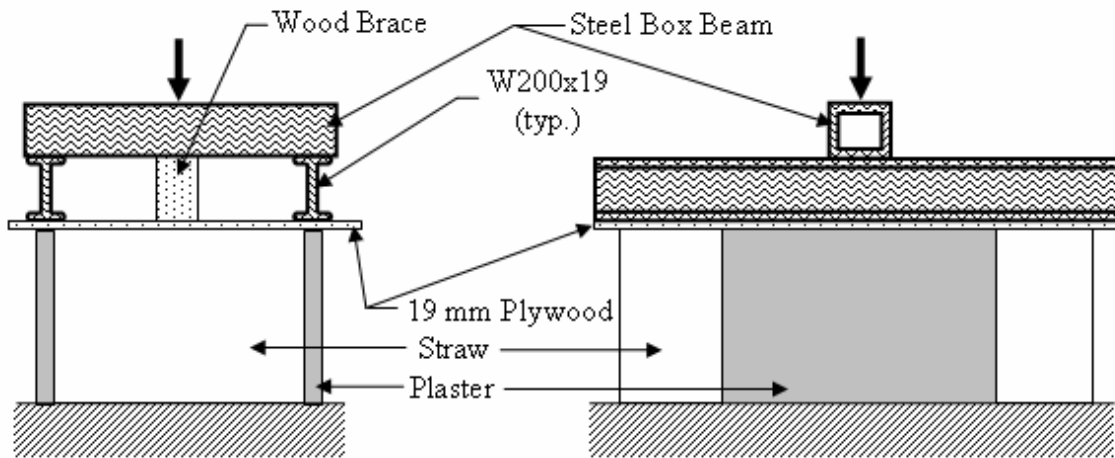


Figure 4.7: Plastered Straw Bale Compression Test Setup and Loading Plate Design

4.0 Preliminary Compression Testing of Plastered Bale Assemblies

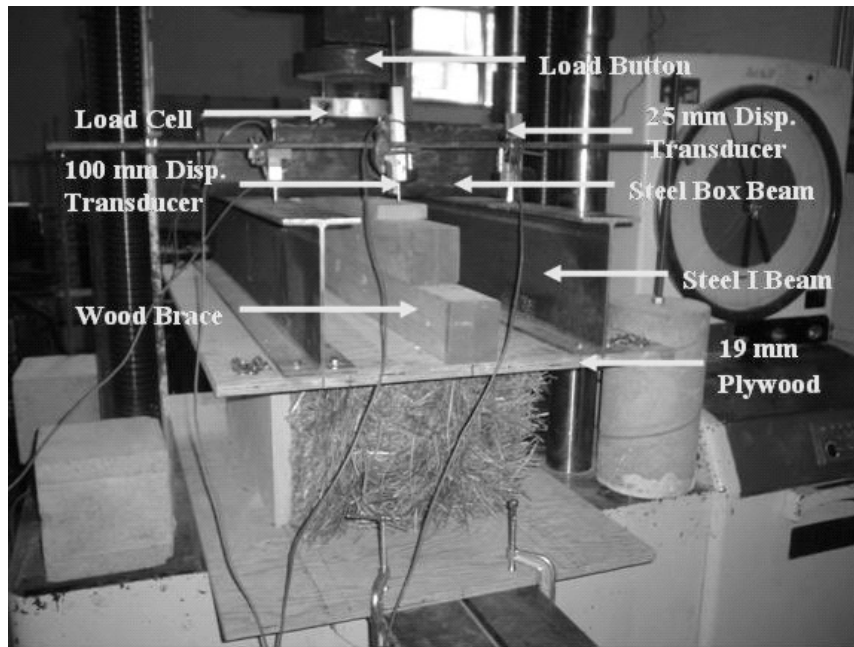


Figure 4.8: Photograph of Test Setup for Preliminary Assembly Testing

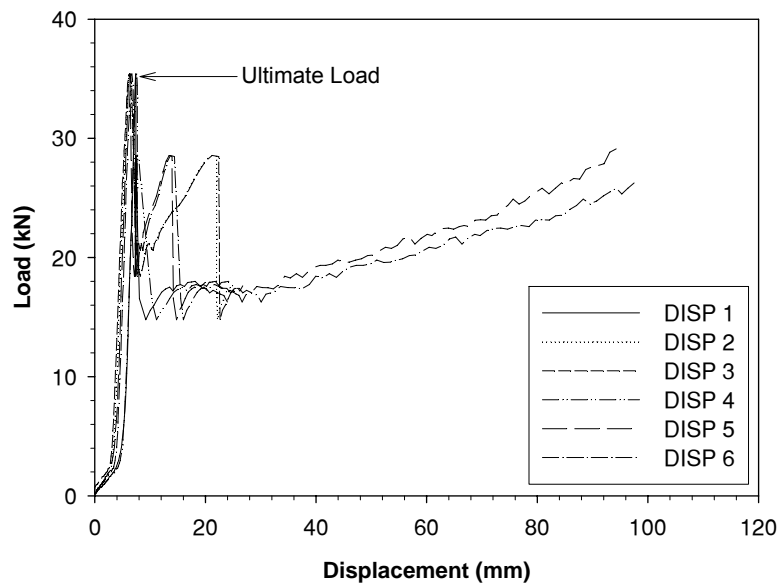


Figure 4.9: Typical Load-Displacement Response of Plastered Straw Bale Assembly Measured with Six LP's (DISP 1 – DISP 6)

4.0 Preliminary Compression Testing of Plastered Bale Assemblies



Figure 4.10: Bearing Failure of a Plastered Straw Bale

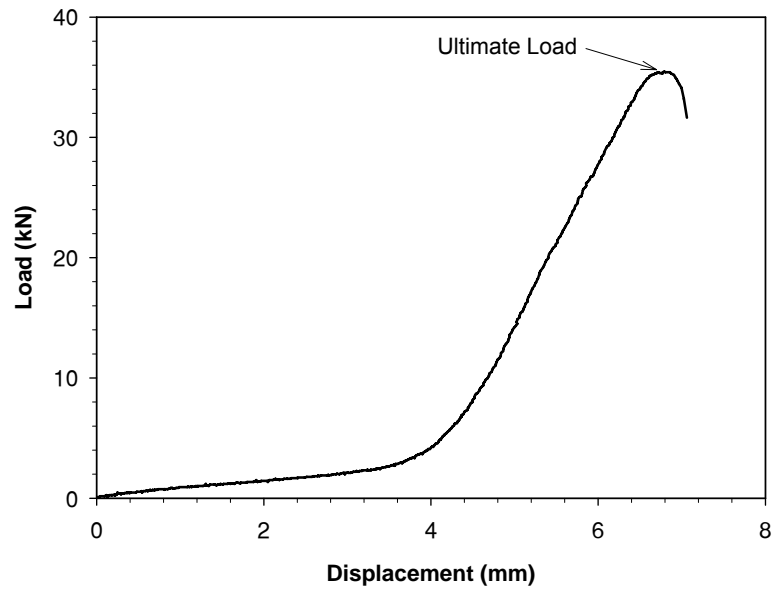


Figure 4.11: Averaged Pre-Failure Load-Displacement Response for Plastered Straw Bale

4.0 Preliminary Compression Testing of Plastered Bale Assemblies

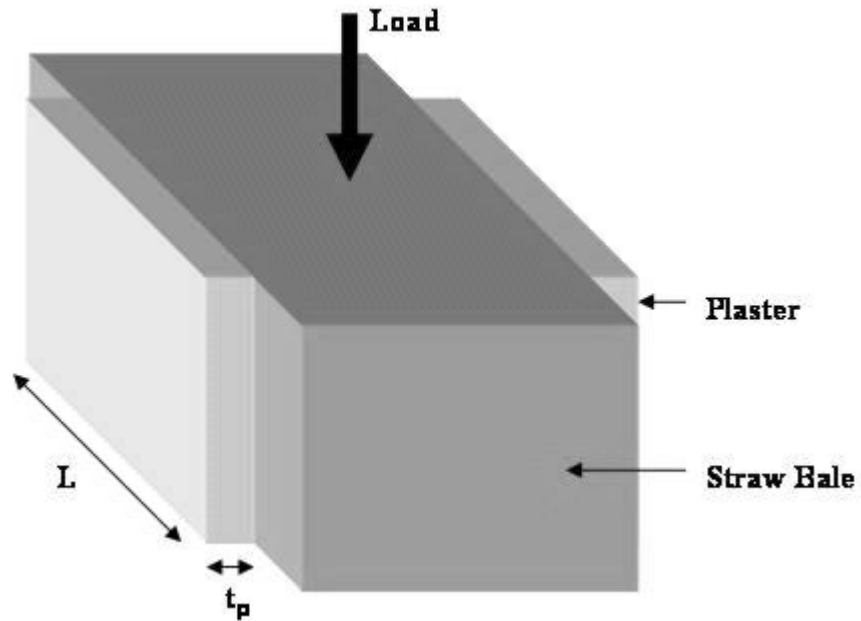


Figure 4.12: Schematic of Plastered Straw Bale

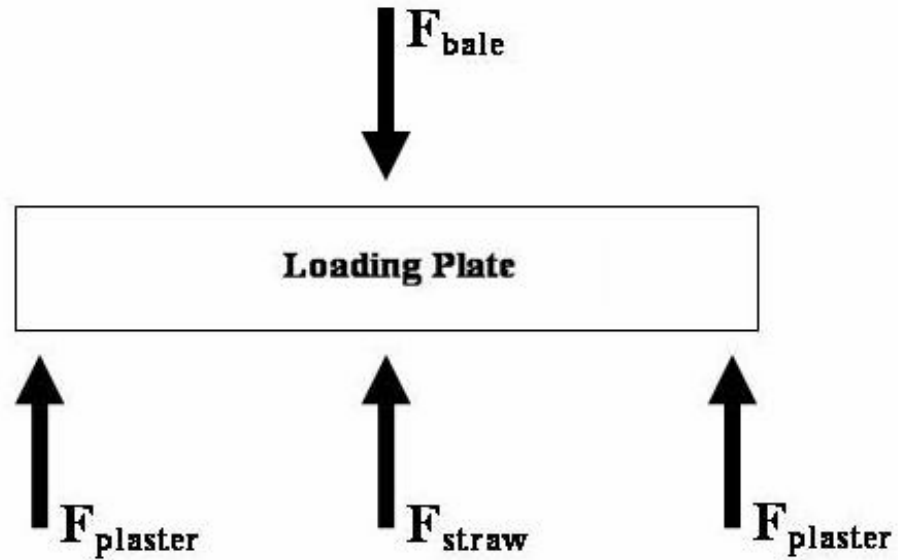


Figure 4.13: Free-Body Diagram of Loading Plate

4.0 Preliminary Compression Testing of Plastered Bale Assemblies

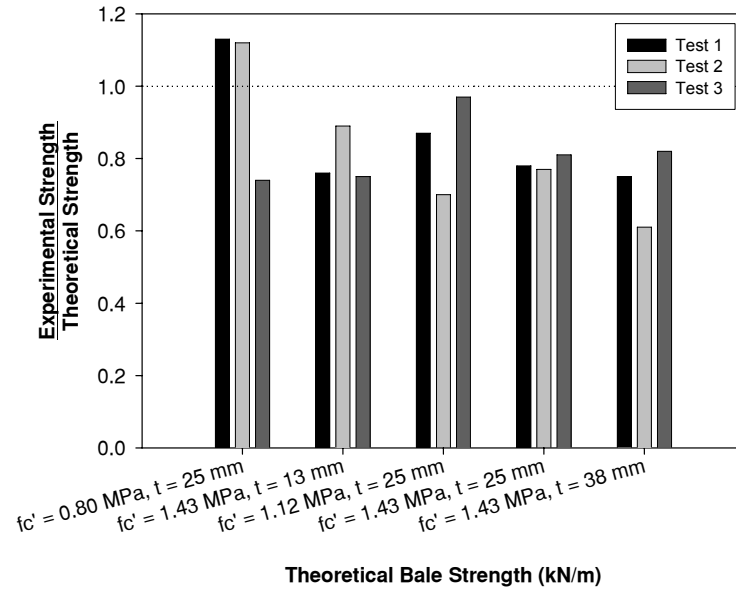


Figure 4.14: Ratios of Experimental to Theoretical Strengths for Plastered Straw Bales

Chapter 5: Concentric Compression Experiments of Plastered Straw Bale Assemblies

5.1 Introduction

Chapter 4 presented an innovative fabrication and testing method for individual plastered straw bales. The results of concentric compression experiments conducted on the specimens fabricated in that Chapter were compared with the theoretical behaviour to determine the effectiveness of the proposed methods. The proposed method was observed to show potential for testing specimens with bales laid flat with a variety of plaster strengths and thicknesses. However, because of a number of noted fabrication issues it was found that the specimens did not achieve strengths anticipated based on the theory. As a result, a number of recommendations were made to improve the fabrication and test methods.

Based on the recommendations presented in Chapter 4, Chapter 5 describes the fabrication and testing of plastered straw bale assembly specimens using one jig

5.0 Concentric Compression Experiments of Plastered Straw Bale Assemblies

for both the fabrication and testing of the specimens. The focus is on specimens constructed with the straw laid flat, and with design plaster thickness of 25 mm. Chapter 4 showed the potential applicability of the proposed method for fabrication and testing of assemblies with a variety of configurations; however, this particular configuration was chosen as it is most reflective of industry practices.

The main objective of this Chapter is to study further the behaviour of straw bale assemblies in concentric compression and to validate theoretical models for the compressive strength and the load-deflection relationship. A secondary objective is to study the applicability of the proposed fabrication and testing methods.

To achieve the objectives, six plastered straw bale specimens were tested in concentric compression and the results were compared to the model. The theory used herein is based on the assumption of compression failure of the specimens. The potential for buckling failure is studied by comparing results for specimens of varying height. Specimens were fabricated with flat bales stacked three and seven bales high to produce specimens of varying height

5.2 Design and Fabrication

5.2.1 Materials

5.2.1.1 Straw Bales

Two-string wheat bales similar to those described in Chapters 3 and 4 were used for all of the experiments. As such, the bales initially had dry bulk densities

5.0 Concentric Compression Experiments of Plastered Straw Bale Assemblies

ranging from 78 to 112 kg/m³ with dimensions of 375 ± 10 mm height, 475 ± 10 mm width, and 800 ± 25 mm length.

5.2.1.2 Plaster Design and Mixing

The plaster used for all six wall experiments was a lime-cement plaster with proportions by volume of 4.5 : 1.25 : 0.25 of sand, lime and cement respectively. The *w/cm* ratio of the plaster was 1.08. Note that this is the same plaster design as was used in Chapter 4; however the curing time was significantly less for the specimens produced in this chapter. For all experiments, the plaster was prepared in the same manner, and with the same materials as the plasters used for the experiments in Chapter 4. The cement was provided as a component of Mason's Choice High Bond Portland Lime Type N, while additional lime was Bondcrete ® Mason's Lime. The sand was masonry sand, and the water was tap water as well as moisture from the sand. The dry components were mixed in a batch mixture prior to the addition of the water. Multiple batches were used for each specimen.

The only notable deviation from the procedure outlined in Chapter 4 was the inclusion of the fabrication of plaster cube specimens for the determination of the plaster compressive strength. Three 45 mm x 45 mm cube specimens were fabricated from one of the batches for each of the plastered bale assemblies, yielding an estimate of the strength of the plaster for the specific specimen.

5.0 Concentric Compression Experiments of Plastered Straw Bale Assemblies

5.2.2 Fabrication Procedure

5.2.2.1 Design of Fabrication and Testing Jig

The fabrication jig is presented in Figure 5.1. This jig consists of a steel base, constructed with 50 mm x 100 mm hollow structural steel (HSS) tubes as shown in Figure 5.1. The base consists of one horizontal steel section to support each of the two plaster skins, with a number of horizontal sections running perpendicular to these two pieces, connecting them together and providing support for the straw. The base is thus shaped like a ladder as can be seen in Figure 5.1. There is also a top piece to the jig, which is the same shape as the bottom piece. The top and bottom pieces are connected by four vertical 50 mm x 50 mm HSS sections. These vertical pieces can be bolted easily to the top and bottom pieces to create a stiff steel frame. Vertical pieces of varying height can be constructed in order to create plastered straw bale walls of varying height. The top and bottom pieces of the jig provide the top and bottom formwork for the plaster, and also provide a top bearing surface for loading the wall, and a bottom base for supporting the wall during testing. As such, there is consistency in the fabricating and testing jig such that any minor deformities in the fabrication jig will not result in misalignment with the testing jig.

The vertical formwork for the plaster is provided by wood strips placed between the top and bottom pieces and laid against the bales as seen in Figure 5.2. These pieces are 25 mm thick to produce plaster skins of that thickness. The entire wall and jig can be moved as a unit, even after plastering, as long as the vertical steel pieces remain connected. In order to test the specimen, all of the vertical pieces (steel pieces and wooden formwork) were removed so that the plastered

5.0 Concentric Compression Experiments of Plastered Straw Bale Assemblies

straw bale wall was supporting the top piece, and any load that was applied to the top piece was thus applied to the specimen. Figure 5.2 is a photograph of a 2.31 m wall being plastered using the jig.

5.2.2.2 Detailed Fabrication Procedure

The fabrication procedure is as follows:

1. The bales were individually trimmed and compressed in the same manner as described in Chapter 4. As a result, the straw width was observed to range from 395 mm to 405 mm.
2. The bales were then placed in the steel frame shown in Figure 5.2. The steel vertical pieces determined the height of the wall and were designed to be 0.99 m high for the three-bale specimens and 2.31 m high for the seven-bale specimens.
3. The bales were compressed in order to fit appropriately into the jig. The vertical steel pieces were then bolted to the steel ladders at the top and bottom of the wall in order to set the height at the desired value.
4. Vertical wood strips were placed against the straw, 600 mm apart, on each side of the wall. These acted as the vertical plaster formwork and were cut to a thickness of 25 mm to provide a guide for the plaster thickness. This procedure produced formwork for plaster skins with length of 600 ± 1 mm, height of 990 ± 1 mm or $2310 \text{ mm} \pm 1$ mm and thickness of 25 ± 1 mm.
5. The plaster was hand applied in three layers, all applied in the span of approximately 4 hours, allowing very little time for curing between layers. The first

5.0 Concentric Compression Experiments of Plastered Straw Bale Assemblies

layer was worked into the straw by hand, the second layer filled the formwork to the approximate plaster thickness, and the third layer was a thin layer which was troweled smooth to create a smooth finished surface of appropriate thickness. The specimens were plastered standing upright, and both sides were plastered at the same time. No reinforcement mesh was applied. Numerous batches were used for each specimen due to limitations with the size of the mixing apparatus. During fabrication of each of the specimens, three cubes were cast from one of the batches used for the specimen. Following fabrication it was observed that while the minimum thickness appeared to be as designed (25 ± 1 mm), the plaster in some regions was up to 5 mm thicker than intended as a result of working the plaster into the voids in the straw. Following testing it was found that the plaster was thinner than designed in some areas.

6. Once plastering was completed, burlap was placed over the wall providing a moist curing environment for approximately three days. The wall then cured for another four days without the burlap cover.
7. The wall sections were tested after seven days, at which time the wall and jig were craned into the loading apparatus, and the vertical steel and wood pieces were removed. The plaster cubes were tested at the same time as the wall specimens.

5.3 Experimental Program

The testing program consisted of compression experiments on six plastered straw bale wall assemblies. To determine the effect that the height of the specimens

5.0 Concentric Compression Experiments of Plastered Straw Bale Assemblies

had on the structural behaviour, three specimens three bales in height were tested, and three specimens seven bales in height were tested. Each specimen had design plaster thickness of 25 mm and design plaster strength of 0.783 MPa.

5.4 Instrumentation

The instrumentation consisted of a load cell, four 100 mm LPs, a number of 25 mm LPs, and the apparatus used for Particle Image Velocimetry (PIV). The four 100 mm LPs were used to measure the vertical displacements and were located at the four corners of the wall at the top of the setup as can be seen in Figure 5.3. For the 0.99 m tests the LPs measured the displacement on the underside of the top steel ladder as can be seen in Figure 5.4, while for the 2.31 m tests the LPs measured the displacement on the top of the steel ladder as can be seen in Figure 5.5.

The techniques used for measuring the lateral displacements varied from wall to wall. Where LPs were used, 25 mm LPs were oriented perpendicular to the wall as shown in Figure 5.6. While this technique did provide data, because of the roughness of the walls it was difficult to have confidence in the results since it was hard to determine if measured displacements were a result of actual wall lateral movement or of the LP moving along the rough surface as the wall was compressed.

For the first 0.99 m wall, lateral displacements were measured with LPs at the top, bottom, and middle of one side of the wall as indicated in Figure 5.7. For the second and third 0.99 m walls, and the first 2.31 m wall, the lateral deflections were measured with LPs at mid-height on both sides of the wall as indicated in Figures 5.4

5.0 Concentric Compression Experiments of Plastered Straw Bale Assemblies

and 5.5. Note that in these figures only one lateral LP is shown in each figure, however, the second lateral LP is located on the opposite face of the wall, at the same vertical location as the one pictured. For the second and third 2.31 m walls, the lateral deflections were measured using LPs at mid-height on both sides of the wall and at the top of the wall on one side of the wall as shown in Figure 5.8.

In addition, for the third 2.31 m wall, the deflections were recorded using PIV as described in Appendix B. The PIV technique involved colour texturing the edges of the plaster skins using splatters of black paint, and having a camera take photographs of the edge of the wall at 20 second intervals throughout the duration of the experiment. The photographs were used to track the lateral and vertical deformations of the plaster skins and the bales throughout the entire experiment. An example of a photograph from the PIV analysis is given in Figure 5.8. PIV allowed the lateral deflections of both plaster skins to be measured simultaneously for the entire height of the wall, and for the full duration of the experiment. The measurements were not expected to be affected by roughness of the plaster surface. Because of the uniqueness of this technique, the results from PIV were compared with measurements using LPs to validate the PIV results. Further PIV validation is presented in Appendix B.

The load was recorded for the three 0.99 m experiments using a load cell integrated with the testing machine. For the three 2.31 m experiments, the load was recorded using a 111 kN capacity load cell located between the hydraulic jack and the steel ladder at the top of the wall. For all experiments, the load was applied as a

5.0 Concentric Compression Experiments of Plastered Straw Bale Assemblies

point load through the centre of the load cell, which was located at the centre of the top steel ladder as shown in Figure 5.3.

The load and deflection were recorded at a rate of approximately 11 samples per second throughout the duration of the experiments. Appendix A provides additional information on the instrumentation and testing apparatus.

5.5 Procedure

The three 0.99 m wall sections were tested in stroke-control at a rate of 1 mm/min until the ultimate load was reached. Beyond this point the loading rate was increased to 3 mm/min. The load was applied concentrically, directly to the top steel ladder, and the wall was supported at the base by the bottom steel ladder, which rested on the base of the loading machine. This test setup can be seen in Figure 5.4. Note that the “ladder” shape of the top and bottom steel pieces allowed the straw to bulge into the gaps during loading, however because the gaps are small, this was expected to have minimal effect on the results.

The three 2.31 m wall sections were tested under a large reaction frame. The frame was fitted with a 111 kN hydraulic jack, which was controlled with a hand pump. The test setup can be seen in Figure 5.5. The rate of loading was variable due to the nature of the hydraulic jack – hand pump system used. It was attempted to load at a slow rate until the ultimate load was reached, and then to increase the rate of loading. Again, the load was applied concentrically, directly to the top of the steel ladder, and the wall was supported at the base by the bottom steel ladder, which rested on the concrete laboratory floor.

5.0 Concentric Compression Experiments of Plastered Straw Bale Assemblies

For all specimens the test was stopped when the LPs measuring vertical deflection exceeded their range.

For each experiment conducted, three 45 mm x 45 mm plaster cubes were tested in compression to determine the approximate plaster strength for the plaster applied to the wall. The cubes were tested at the same time as the wall specimens and were tested in a Reihle universal testing machine at a rate of 1 mm/min. The procedure for testing the cubes was the same as that described in Chapter 3.

5.6 Results and Discussion

5.6.1 Plaster Strength Results and Discussion

The results of the cube tests are presented in Figure 3.10 as batches numbered six through eleven. The results of the compression tests on the six batches discussed in this chapter are presented in Table 5.1 with the corresponding plastered straw bale wall assembly. Detailed results for each individual cube test are presented in Appendix C.

5.6.2 Wall Assembly Results and Observations

5.6.2.1 Ultimate Load and Vertical Load-Deflection Results

Figures 5.9 to 5.14 give the load-deflection responses for each of the plastered straw bale wall assemblies. During testing the HSS sections running along the top and bottom of the plaster skins were observed to deform under load. The result was that the LPs captured the deformations in the HSS sections in addition to

5.0 Concentric Compression Experiments of Plastered Straw Bale Assemblies

the displacements of the wall. Thus, the vertical displacement data was corrected to remove the HSS deformation as described in Appendix G.

The plots presented in Figures 5.9 to 5.14 represent the averaged load-deflection responses for each specimen as determined by averaging the displacements recorded by the four vertical LPs. For each experiment, the data from the four vertical LPs were within 10% of one another prior to reaching the ultimate load. Beyond the ultimate load the data from the four vertical LPs was found to vary significantly as the failure progressed. The ultimate load was determined as the maximum load obtained prior to the first significant drop in load. Table 5.1 presents the experimental strengths (ultimate load) for each of the six specimens. Note that the experimental wall strengths presented in Table 5.1 are normalized by the length of the specimen by dividing the ultimate load by the plaster skin length (0.6 m).

Similar trends in the load-deflection curves can be seen for all six figures. Considering Figure 5.9, it can be seen that the walls behave linearly for the initial portion of the test, exhibiting softening as the ultimate load of approximately 17 kN (for Figure 5.9) is reached. At this point a crack formed on one side of the wall and the load dropped significantly to about 6 kN. The load then rose again to approximately 12 kN, before dropping to about 4 kN when a crack formed on the second side of the wall. The wall then regained some strength to approximately 9 kN and maintained this residual strength for the remainder of the test. This behaviour was noted for all six wall experiments (with varying load values). The ability to resist load post-failure is similar to the response observed for individual plastered straw bales discussed in Chapter 4.

5.0 Concentric Compression Experiments of Plastered Straw Bale Assemblies

Figure 5.15 presents the pre-failure load-deflection curves for the three 0.99 m specimens while Figure 5.16 presents the pre-failure load-deflection curves for the three 2.31 m specimens. For these figures the load-deflection responses for each specimen were normalized by dividing the load by the theoretical ultimate strength for the specimen. The calculation for the theoretical ultimate strength is discussed in Section 5.6.3. It should be noted that for each specimen, the theoretical ultimate strength takes into consideration the estimated plaster strength and thickness for the specific specimen.

Figures 5.15 and 5.16 show that some specimens exhibited a small region of large deformation at the beginning of the experiment. This is an indication of bale rebound. The load-deflection curves were corrected to remove the effect of bale rebound. It was observed that the rebound occurred primarily in the region from 0 to 10% of ultimate. A trendline fit to the experimental data from 10% to 40% of ultimate was extended to the x-axis and used as an estimate of the approximate load-deflection curve for the region from 0 to 10% of ultimate. The entire figure was then shifted to the left in order for the extended trendline to intersect the origin. Using this technique, Figures 5.15 and 5.16 were re-plotted providing the modified normalized experimental plots given in Figures 5.17 and 5.18.

5.6.2.2 Lateral Deflection Results

Figures 5.19 to 5.24 provide plots of mid-height lateral deflection with load for each experiment. The measurements are provided from the start of the test until ultimate failure. Note that where applicable, data is provided for the lateral deflection

5.0 Concentric Compression Experiments of Plastered Straw Bale Assemblies

of both the left and right sides of the wall. Results are not provided for LP measurements at the base of the wall or the top of the wall as the LP measurements confirmed that the bottom of the wall was fixed securely to the base support and that the top of the specimens also did not move laterally.

The lateral deformation plot obtained from PIV is given in Figure 5.25. This plot describes the total magnitude of lateral displacement of both plaster skins for the entire wall height at ultimate failure. This plot confirms the minimal lateral deflections at the top and bottom of the specimen and that the maximum lateral displacement occurs at mid-height of the specimen. It also indicates that the two sides of the wall are deflecting laterally in the same direction, by equal magnitude.

5.6.2.3 Failure Modes

Each assembly failed due to compressive crushing of the plaster along a horizontal plane as indicated in Figure 5.26. The failures were observed to occur at locations which varied from one specimen to another. This is an indication that there is not one specific location of stress concentration common to all specimens. Many of the failures were observed to occur at the boundaries between bales. This is an indication that misalignment of the bales may have resulted in thinner plaster skins in these regions.

There were some failures which were observed to be more prolonged than expected. This can be seen specifically for 0.99 m bale #3, where Figure 5.15 shows that for this specimen the load continued to increase gradually even under significant deformations near ultimate failure. It is believed that this behaviour is a

5.0 Concentric Compression Experiments of Plastered Straw Bale Assemblies

result of the support provided by the straw. For this specimen, the failure region was observed to remain relatively intact, even following the appearance of initial cracks. This can be seen in Figure 5.27. This behaviour is contrary to the typical plaster failure presented in Figure 5.26, for which the plaster was observed to crumble and fall away soon after cracking initiated. The intact failure region was able to continue to sustain load, and even resist increasing loads following the appearance of the first cracks. However, significant deformations were observed prior to failure. Eventually, under increasing load and deformation, the plaster was observed to crumble away from the wall, leading to a sudden drop in load, and the corresponding ultimate failure of the wall.

5.6.3 Wall Assembly Theoretical Behaviour

5.6.3.1 Ultimate Strength

If it is assumed that assembly failure occurs when the plaster reaches its ultimate strength, and that the strain in the plaster and straw at ultimate failure are both equal to the plaster cube ultimate strain, Equation 4.1 may be used to determine the theoretical ultimate strength.

Measurements of the plaster, detailed in Appendix F, indicate that the failure-plane thickness (estimated thickness of plaster in the failure region) is estimated to be 23 mm. Table 5.1 presents the failure-plane thickness, the plaster strength, and the theoretical ultimate wall assembly strength for each specimen. Also presented in Table 5.1 are the ratios of experimental strength divided by theoretical strength for each specimen.

5.0 Concentric Compression Experiments of Plastered Straw Bale Assemblies

5.6.3.2 Load-Deflection Response

The plaster stress-strain model presented in Equation 3.10 was used to predict the pre-failure load-deflection response of the assemblies. The value of f'_c for Equation 3.10 was taken as the measured f'_{cube} for the specific specimen. The load was found by multiplying the stress by the area of plaster ($2x t_p \times 600$) and the deflection was found by multiplying the strain by the specimen height. The theoretical load-deflection response was normalized by the theoretical ultimate strength in order to present a single theoretical curve for a 0.99 m assembly and a single theoretical curve for a 2.31 m assembly. These curves are presented in Figures 5.17 and 5.18 respectively.

It was noted in Section 5.6.2.3 that some specimens appeared to have a progressive failure which deviated from the expected compressive failure. This behaviour may be captured by examining the maximum expected plaster strain at ultimate failure. In Chapter 3 it was stated that the maximum expected plaster strain at failure (for a 95% confidence interval) is 0.00424. It is important to note that this value is determined from cylinder experiments, and that for some experiments the apparatus was observed to confine the cylinder, holding it together as failure was initiated. This behaviour resulted in specimens with high strain at ultimate failure, thus giving the upper 95% confidence value of 0.00424. This is similar to the behaviour noted for the progressive assembly failure.

Using a failure strain value of 0.00424, Equation 3.10 was modified as follows:

5.0 Concentric Compression Experiments of Plastered Straw Bale Assemblies

$$f_c = f'_c \left(\frac{331.4\varepsilon}{0.405 + \left(\frac{\varepsilon}{0.00424} \right)^{1.405}} \right) \quad 5.1$$

Equation 5.1 was used to predict the “Upper Strain Boundary” curve as presented in Figures 5.17 and 5.18.

Also shown in Figures 5.17 and 5.18 are curves labelled “Upper and Lower Theoretical”. The 95% confidence bounds on the plaster strength were 0.606 MPa and 0.959 MPa. The upper bound was substituted in Equation 3.10 while the lower bound was substituted in Equation 5.1 to obtain these curves.

5.6.4 Wall Assembly Discussion

5.6.4.1 Effect of Specimen Height on Ultimate Strength

The data from Table 5.1 indicates that the 0.99 m assemblies had average strength of 32.1 kN/m with a standard deviation of 4.1 kN/m. The average ratio of experimental to theoretical strength was 0.882 with a standard deviation of 0.039. The 2.31 m assemblies had average strength of 36.6 kN/m with a standard deviation of 0.76 kN/m. The ratio of experimental to theoretical strength was 1.105 with a standard deviation of 0.134.

In order to compare the results for the 0.99 m specimens with the 2.31 m specimens, a comparison between the ratios of experimental to theoretical strength was conducted. A t-test indicated that at the 95% confidence level there is not a statistically significant difference between the strength of the 0.99 m assemblies and

5.0 Concentric Compression Experiments of Plastered Straw Bale Assemblies

the 2.31 m assemblies. This suggests that global buckling is not a governing failure mode, as the taller specimens would be expected to have lower strength if buckling were to govern. This is further supported by the fact that it was found that the taller specimens had on average a higher strength than the shorter specimens.

5.6.4.2 Comparison of Experimental and Theoretical Ultimate Strength

Considering the 0.99 m specimens and the 2.31 m specimens together it can be seen that the specimens presented in this study achieved an average ratio of experimental to theoretical strength of 0.994. This indicates the effectiveness of the proposed fabrication and testing methods and confirms that the failure of a straw bale assembly can be predicted on the basis of the plaster cube strength. The standard deviation of the ratio was found to be 0.151, or 15.2% of the average ratio. This is a large variation considering that the standard deviation of the plaster strength was found in Chapter 3 to be only 11.3% of the average strength. However, this greater variability may be a result of the variability in the plaster thickness and the inaccuracy associated with measuring the plaster cube strength for only one of the batches used to fabricate each specimen.

5.6.4.3 Plastered Bale Assembly Load-Deflection Response

The modified load-deflection responses presented in Figures 5.17 and 5.18 present a comparison of the experimental and theoretical load-deflection response for the six tested specimens. The experimental load-deflection curves for all six specimens are observed to fall near the ideal theoretical envelope described by the region between the “Theoretical” line and the “Upper Strain Boundary” line in each

5.0 Concentric Compression Experiments of Plastered Straw Bale Assemblies

figure. However, some results do fall outside of this envelope, such as the 0.99 m wall #2 and the 2.31 m wall #3. At a given load the maximum difference from the theoretical envelope is 50% for loads less than 90% of ultimate.

The broader region bounded by the upper and lower theoretical boundaries defines the theoretical envelope for the load-deflection curves taking into account the plaster strength variability and the potential for larger strains at failure as discussed previously. Encouragingly, it can be seen that aside from a few minor deviations (of no more than approximately 10% of the deflection at a given load), for all six specimens the experimental data falls within this envelope, indicating the appropriateness of the load-deflection models used. The minor deviations occur at small loads and are likely a result of not entirely accounting for re-compression of the straw at the beginning of the experiment.

5.6.4.4 Lateral Deflection

Figures 5.19 to 5.21 indicate that all three 0.99 m specimens exhibited insignificant lateral deflection, with the greatest recorded deflection being only 0.2 mm prior to ultimate failure for Specimen #1. Specimens #2 and #3 both had immeasurable lateral deflection prior to failure.

Figures 5.22 to 5.24 indicate that larger lateral deflections were observed for the 2.31 m specimens. Specifically, Specimens #4 and #6 were observed to have lateral deflections up to 1.6 mm just prior to failure, while Specimen #5 had lateral deflection less than 0.5 mm just prior to failure. For all specimens it can be seen that

5.0 Concentric Compression Experiments of Plastered Straw Bale Assemblies

both sides of the wall are deflecting in the same direction, an indication of bending in the wall. One reason for this may be a slight eccentricity in the load application.

It is important to note in Figures 5.19 to 5.24 that where lateral deflections were measured, the values do not appear to be equal for the left and right sides. This suggests that one of the plaster skins is deflecting more than the other, or that there is error in the measurements. Given that the measured deflections are for the most part less than 1.0 mm, it is possible that there is significant error in the readings as the surface roughness of the plaster skins may be upwards of 1.0 mm.

Figure 5.25 shows the deflected shape of the 2.31 m wall #3 at failure, measured using PIV. It shows that the deflections at both the base and the top of the wall were negligible. Furthermore, as shown in Figure 5.25, it appears both the left and right sides of the wall deflect laterally approximately 1.6 mm. This agrees with the deflection measured using the LP on the left side of the wall as shown in Figure 5.24. However, since Figure 5.25 indicates that the lateral deflections are almost identical for both the left side and right side of the wall, it appears that the mid-height LP measurements for the right side of the wall (given in Figure 5.24) are erroneous. The error in the LP measurements is most likely a result of the uneven plaster surface.

An understanding of the magnitude of the lateral deflections may provide insight into the influence of the deflections on the wall behaviour, and on the potential causes of the deflections. The mid-height deflections were observed to reach a maximum of approximately 1.6 mm prior to failure. This indicates that for a

5.0 Concentric Compression Experiments of Plastered Straw Bale Assemblies

section of the wall located at mid-height, the assumed initially concentric load will be applied at an eccentricity of 1.6 mm. If the plaster skins are assumed to resist load individually this eccentricity may be significant; however, if the wall behaves as a completely composite assembly, as is expected, this deflection will result in an increase in stress in the plaster of approximately 1.6%. This is an insignificant amount considering the inherent variability of the results, leading one to believe that the lateral deflection will not influence the behaviour of the wall. It should be noted however that the experimental results were on average slightly less than the theory would suggest (with average experimental to theoretical strength ratio of 0.994). One reason for this may be the slight increase in stress as a result of the lateral deflections of the wall.

5.7 Conclusions

The ultimate strength discussion indicates that the assemblies up to seven bales high fail by pure compression, with no evidence of local or global buckling, or other alternate failure mechanisms. The measured lateral deflections prior to ultimate failure provide an indication that while compression failure of the plaster may still govern, minor eccentricity in the load application may have led to slightly larger compressive stress in one of the plaster skins, and thus slightly premature failure. However, the results and analysis indicate that the strength of the assemblies can be predicted by the strength of the plaster.

The only deviation from the expected failure mode was the noted excessive vertical deflection for some specimens as failure was reached. This was

5.0 Concentric Compression Experiments of Plastered Straw Bale Assemblies

hypothesized to be due to the straw supporting the failed plaster during failure, enabling the specimen to withstand higher than expected load even after first cracking. It was shown that this behaviour may be accounted for by considering a greater strain at ultimate failure for the theoretical modeling.

The experiments conducted on the six plastered straw bale walls and the plaster used for those walls highlighted a number of important findings related to the concentric compressive performance of plastered straw bale wall assemblies:

- The proposed fabrication and testing methods have resulted in straw bale assembly specimens which are consistent.
- The fabricating and testing issues noted in Chapter 4 were mitigated. However, there was still a small amount of bale rebound noted for the experiments conducted with the new jig making it necessary to adjust the experimental load-deflection plots of the assemblies to account for the initial deflections as the bales were re-compressed. The use of techniques which can measure the load-deflection response of the specimens without being influenced by the straw re-compression appears warranted.
- The plastered bale assemblies discussed herein were observed to achieve average experimental to theoretical strength ratios of 0.994, with the 0.99 m assemblies achieving average ultimate strength of 32.1 kN/m and the 2.31 m assemblies achieving average ultimate strength of 36.6 kN/m.
- At the 95% confidence level there is not a statistically significant difference between the strength of the 0.99 m assemblies and the 2.31 m assemblies.

5.0 Concentric Compression Experiments of Plastered Straw Bale Assemblies

- The results support the statement that the plastered straw bale assemblies fail in pure compression as a result of compression failure of the plaster.
- The stress-strain model presented in Chapter 3 was used to model the load-deflection behaviour of the plastered straw bale walls. The model provides a good representation of the behaviour of the walls up to ultimate failure using only the plaster strength and assembly dimensions as input values.
- The lateral displacement measurements indicate some lateral bending of the wall during loading. These displacements are attributed to slight eccentricity in the loading.

The results presented in this Chapter indicate the effectiveness of the proposed fabrication and testing methods. These findings suggest that when plastered straw bale wall assemblies are subjected to concentric compression they will have predictable behaviour and will fail as a result of compressive failure of the plaster. As such, models based on the compressive behaviour of lime-cement plaster were shown to be appropriate for determination of the ultimate strength and load-deflection behaviour of the walls. The following Chapter provides an analysis of the response of assemblies loaded eccentrically in compression.

5.0 Concentric Compression Experiments of Plastered Straw Bale Assemblies

Table 5.1: Comparison of Plastered Straw Bale Wall Assembly Theoretical Strength to Experimental Strength

Test #	Wall Height (m)	Experimental Strength (kN/m)	Plaster Thickness (mm)	Plaster Strength (MPa)	Theoretical Wall Strength (kN/m)	Exp./Theo. Ratio
1	0.99	28.1	23	0.660	30.3	0.93
2	0.99	31.8	23	0.806	36.9	0.86
3	0.99	36.3	23	0.925	42.3	0.86
4	2.31	35.8	23	0.775	35.5	1.01
5	2.31	36.8	23	0.764	35.0	1.05
6	2.31	37.3	23	0.645	29.7	1.26

5.0 Concentric Compression Experiments of Plastered Straw Bale Assemblies

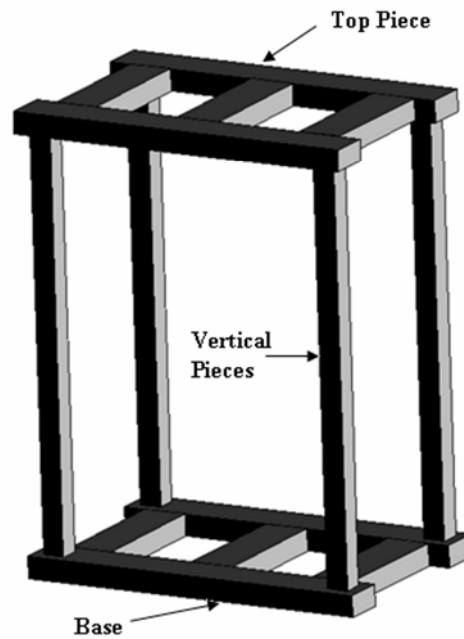


Figure 5.1: Steel Testing and Fabrication Jig



Figure 5.2: Fabrication of 2.31 m Wall Using Testing and Fabrication Jig

5.0 Concentric Compression Experiments of Plastered Straw Bale Assemblies

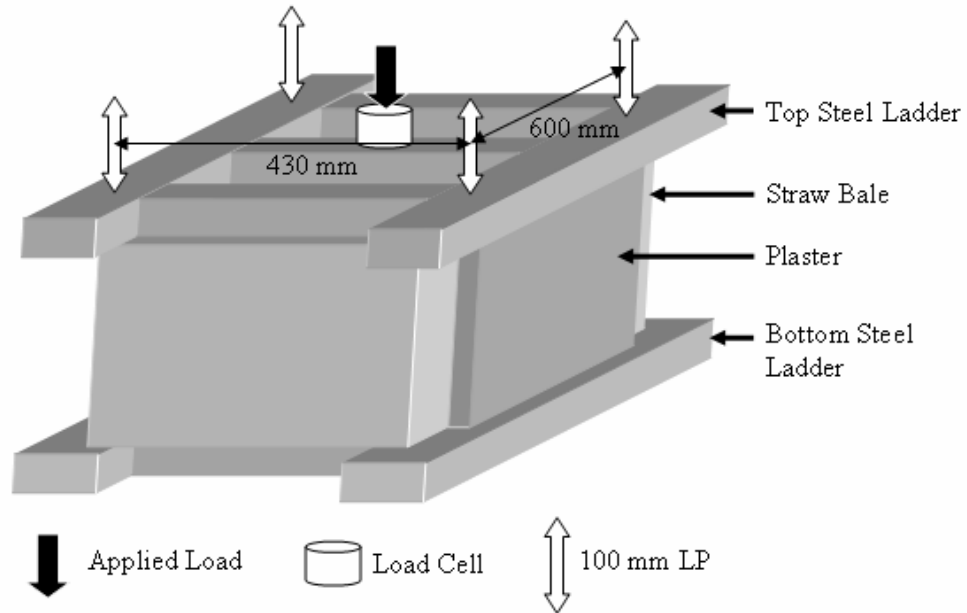


Figure 5.3: Plastered Straw Bale Assembly Test Instrumentation Setup

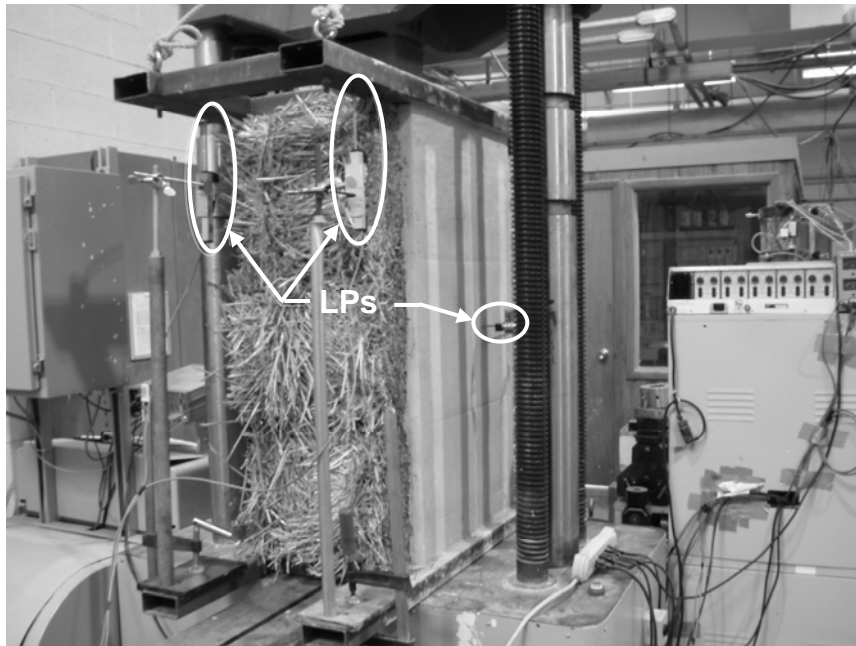


Figure 5.4: Test Setup for 0.99 m Specimens

5.0 Concentric Compression Experiments of Plastered Straw Bale Assemblies



Figure 5.5: Test Setup for 2.31 m Specimens

5.0 Concentric Compression Experiments of Plastered Straw Bale Assemblies

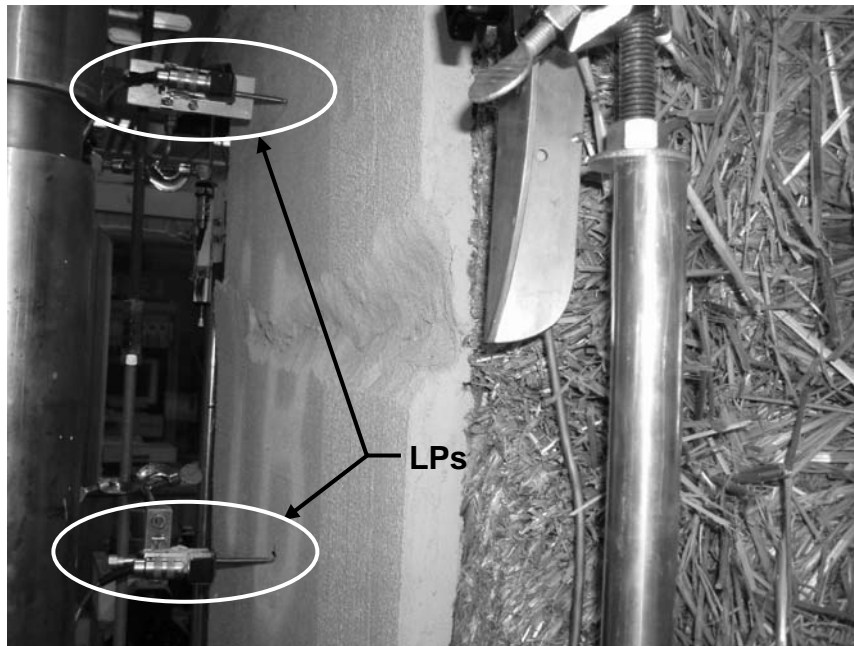


Figure 5.6: Lateral LP Orientation

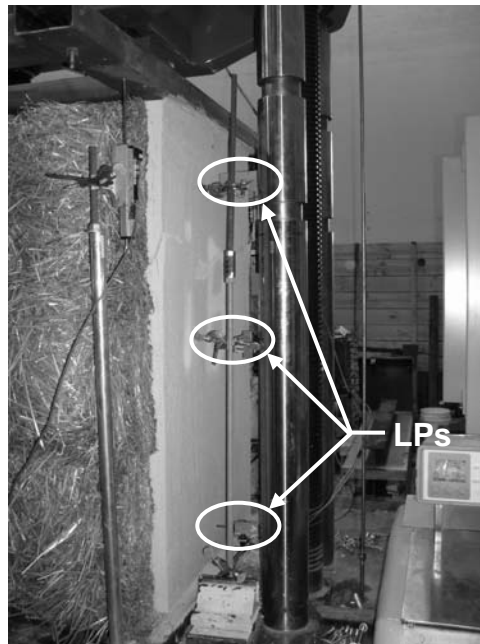


Figure 5.7: Lateral LP Setup for Three Bale Tests #1 and #2

5.0 Concentric Compression Experiments of Plastered Straw Bale Assemblies



Figure 5.8: Photograph Used for PIV Analysis

5.0 Concentric Compression Experiments of Plastered Straw Bale Assemblies

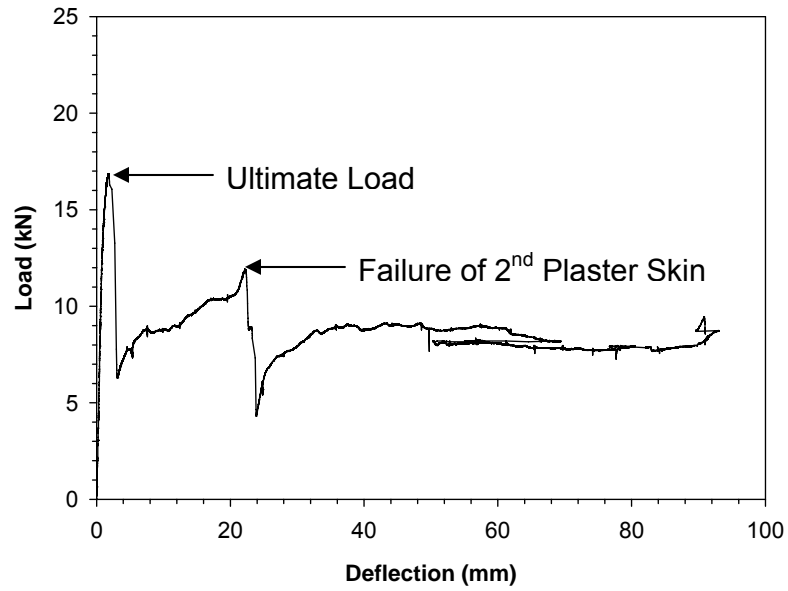


Figure 5.9: Load-Deflection Response of 0.99 m Plastered Wall Assembly #1

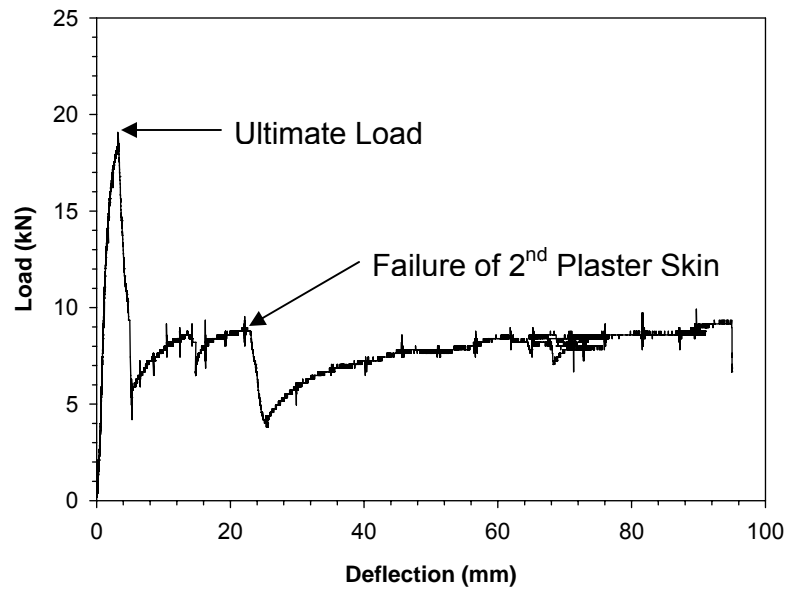


Figure 5.10: Load-Deflection Response of 0.99 m Plastered Wall Assembly #2

5.0 Concentric Compression Experiments of Plastered Straw Bale Assemblies

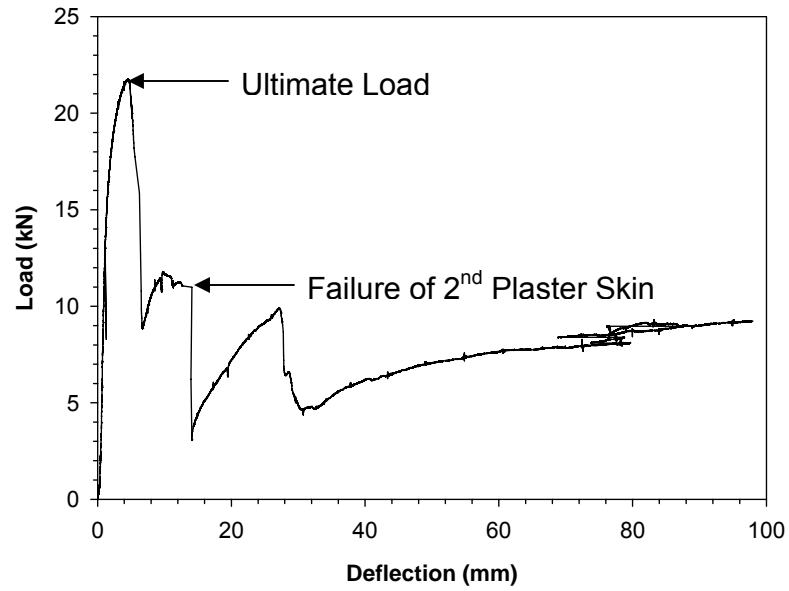


Figure 5.11: Load-Deflection Response of 0.99 m Plastered Wall Assembly #3

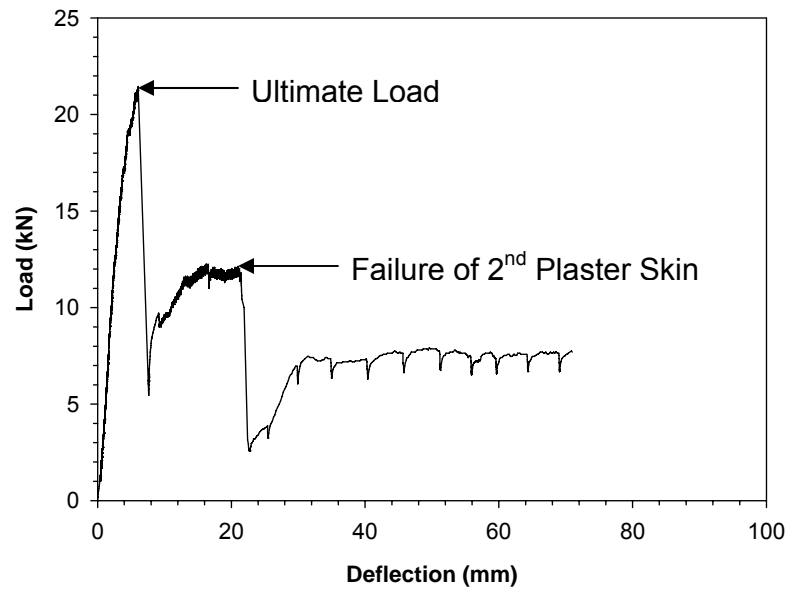


Figure 5.12: Load-Deflection Response of Plastered Wall Assembly #4 (2.31 m #1)

5.0 Concentric Compression Experiments of Plastered Straw Bale Assemblies

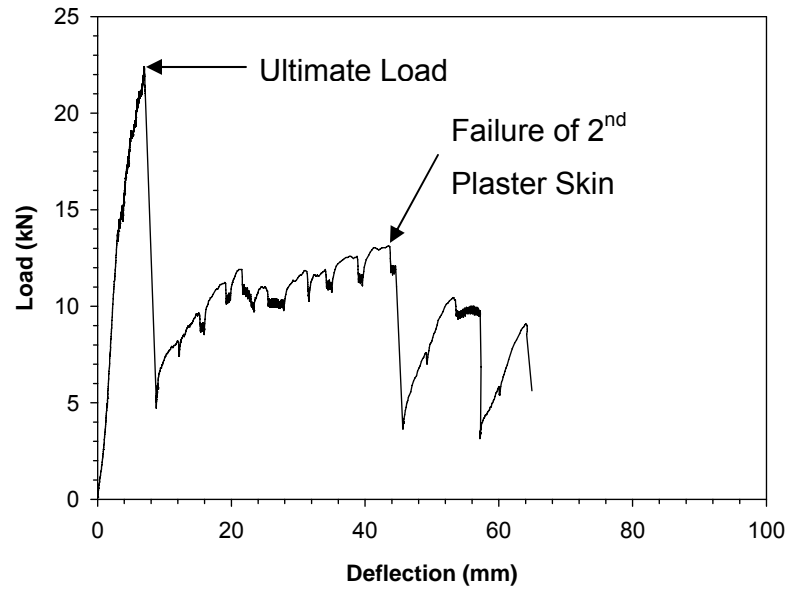


Figure 5.13: Load-Deflection Response of Plastered Wall Assembly #5 (2.31 m #2)

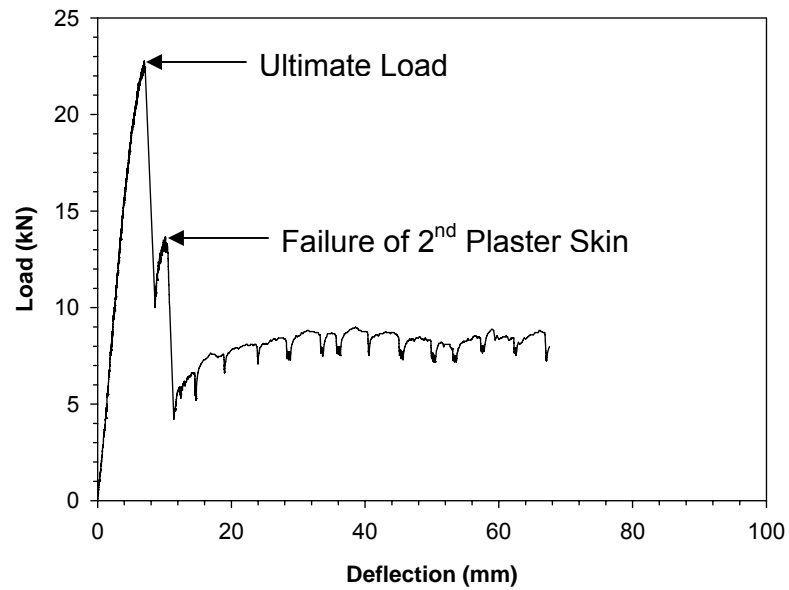


Figure 5.14: Load-Deflection Response of Plastered Wall Assembly #6 (2.31 m #3)

5.0 Concentric Compression Experiments of Plastered Straw Bale Assemblies

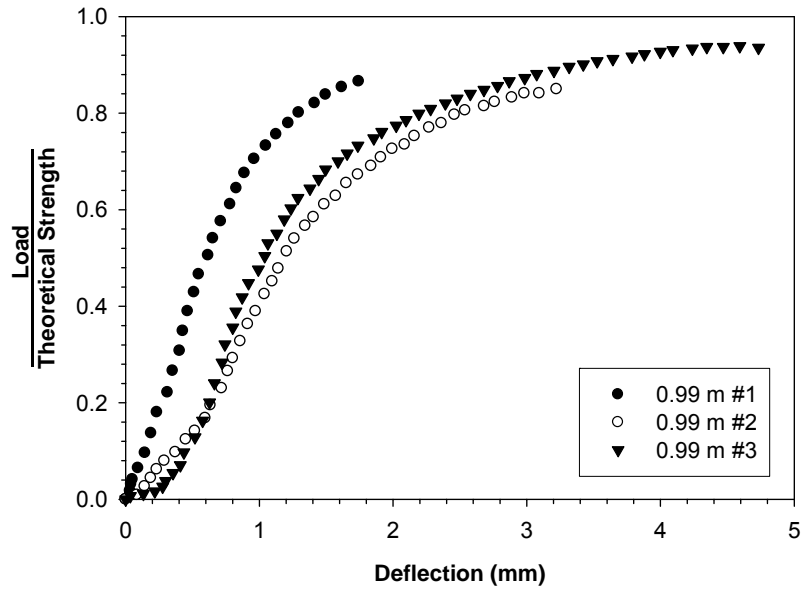


Figure 5.15: Load-Deflection Curves for 0.99 m Plastered Straw Bale Assemblies

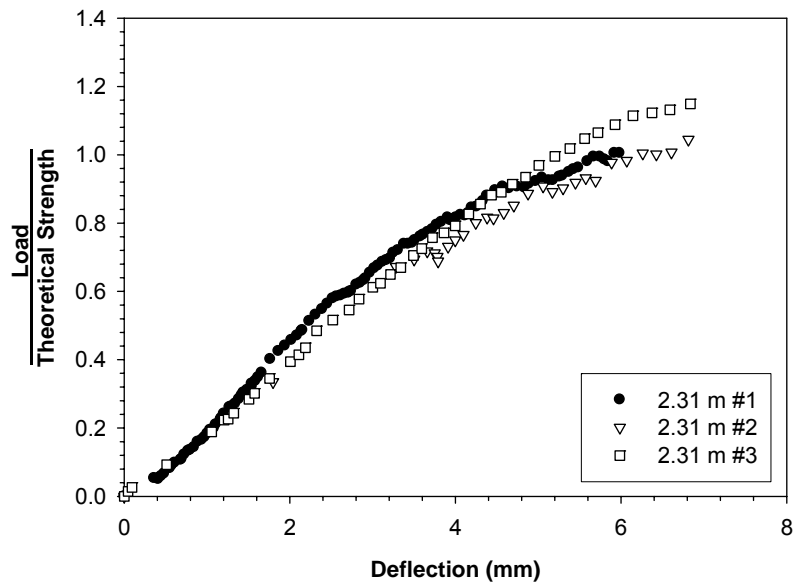


Figure 5.16: Load-Deflection Curves for 2.31 m Plastered Straw Bale Assemblies

5.0 Concentric Compression Experiments of Plastered Straw Bale Assemblies

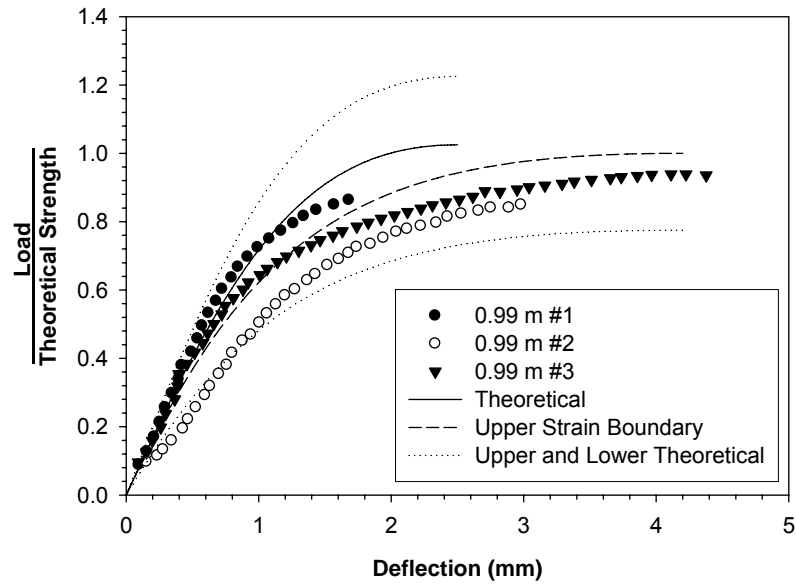


Figure 5.17: Modified Load-Deflection Curves for 0.99 m Plastered Straw Bale Assemblies.

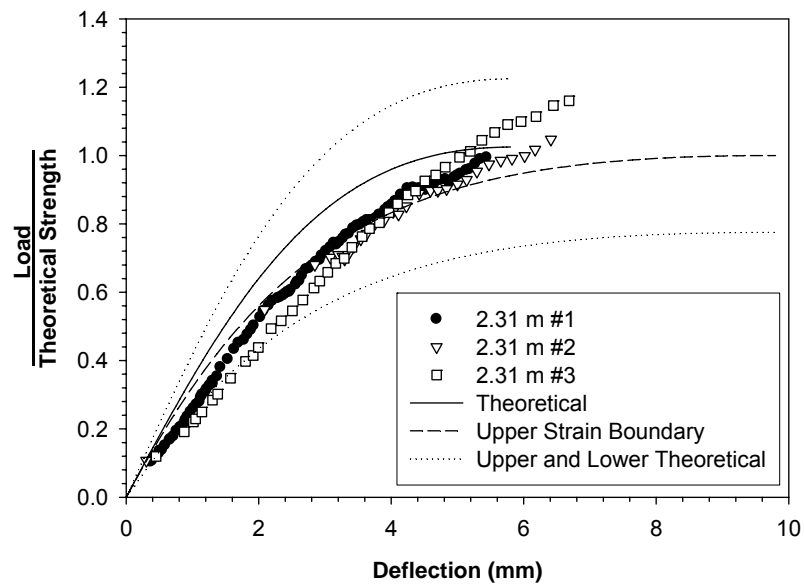


Figure 5.18: Modified Load-Deflection Curves for 2.31 m Plastered Straw Bale Assemblies

5.0 Concentric Compression Experiments of Plastered Straw Bale Assemblies

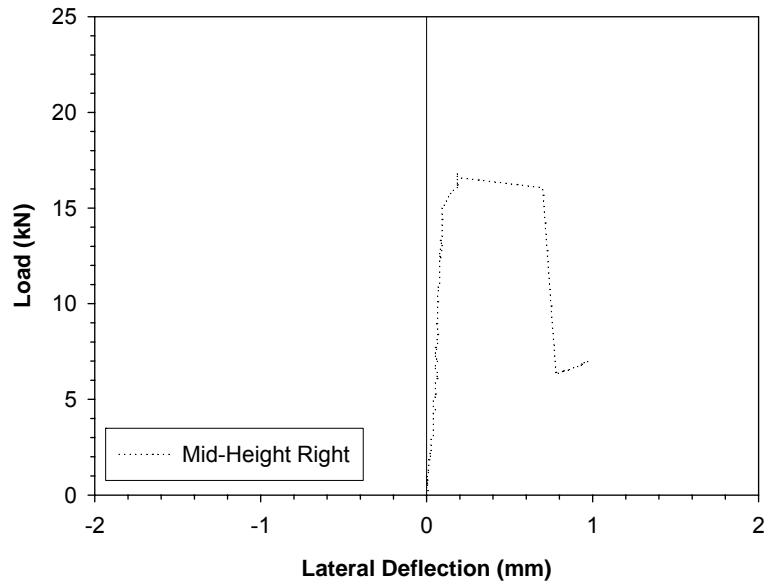


Figure 5.19: Lateral Load-Deflection Response of 0.99 m Plastered Wall Assembly #1

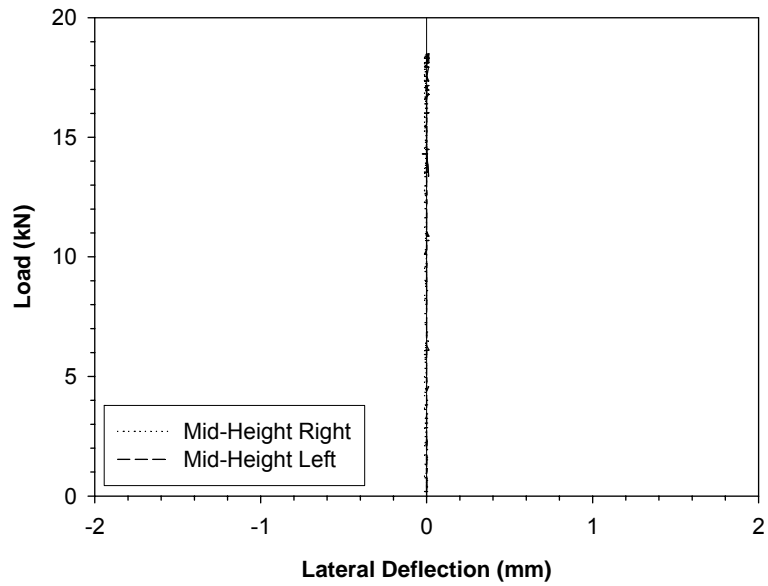


Figure 5.20: Lateral Load-Deflection Response of 0.99 m Plastered Wall Assembly #2

5.0 Concentric Compression Experiments of Plastered Straw Bale Assemblies

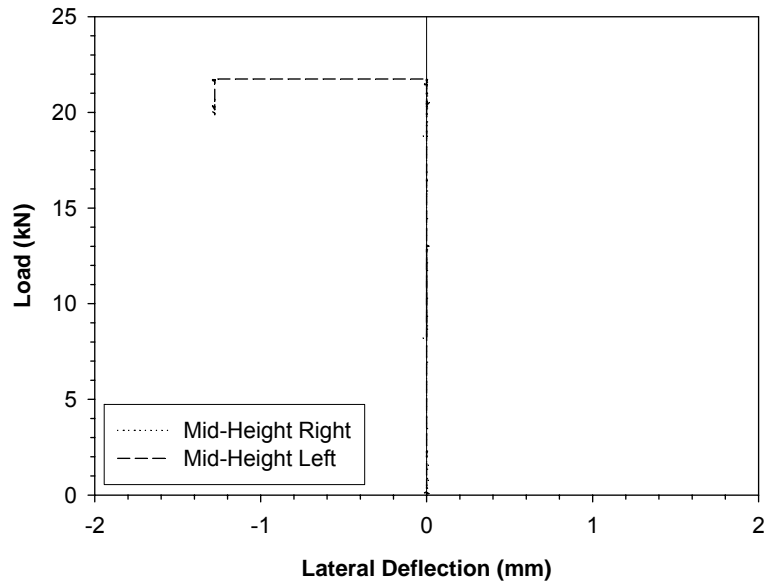


Figure 5.21: Lateral Load-Deflection Response of 0.99 m Plastered Wall Assembly #3

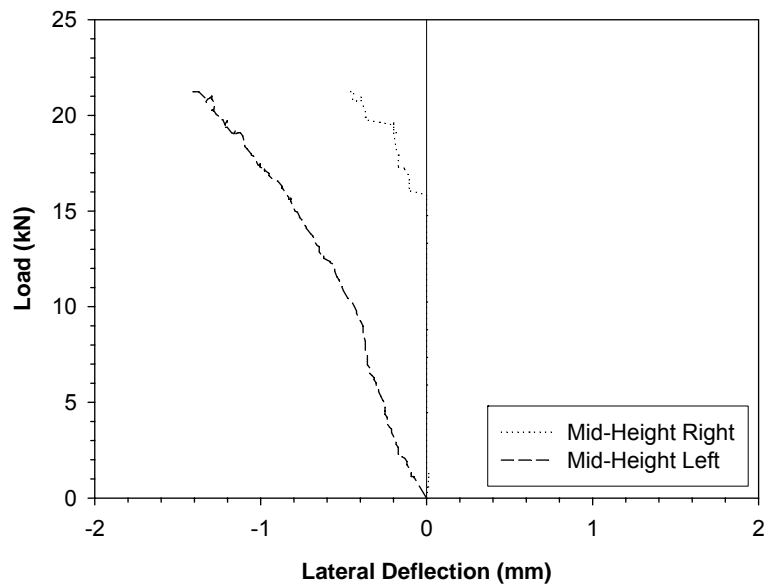


Figure 5.22: Lateral Load-Deflection Response of Plastered Wall Assembly #4 (2.31 m #1)

5.0 Concentric Compression Experiments of Plastered Straw Bale Assemblies

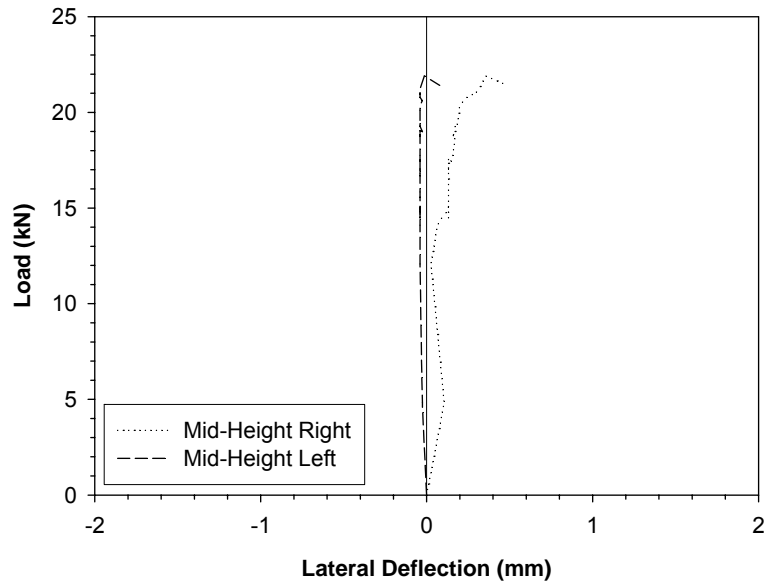


Figure 5.23: Lateral Load-Deflection Response of Plastered Wall Assembly #5 (2.31 m #2)

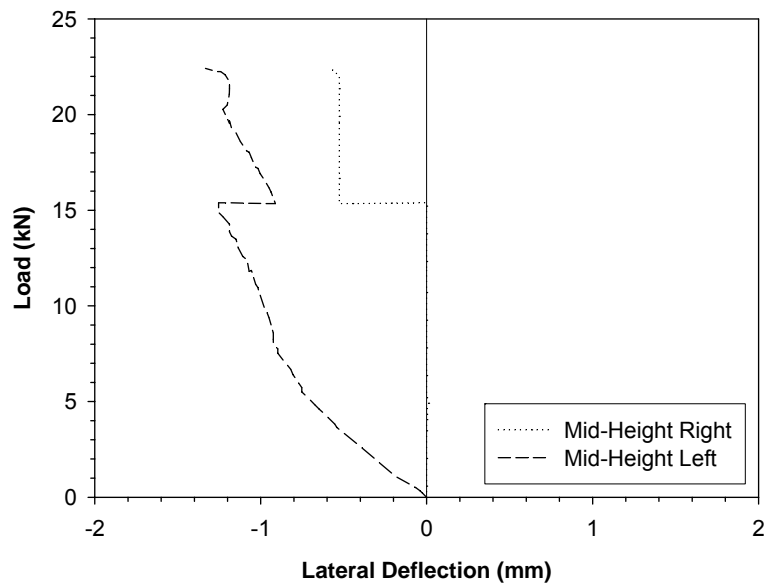


Figure 5.24: Lateral Load-Deflection Response of Plastered Wall Assembly #6 (2.31 m #3)

5.0 Concentric Compression Experiments of Plastered Straw Bale Assemblies

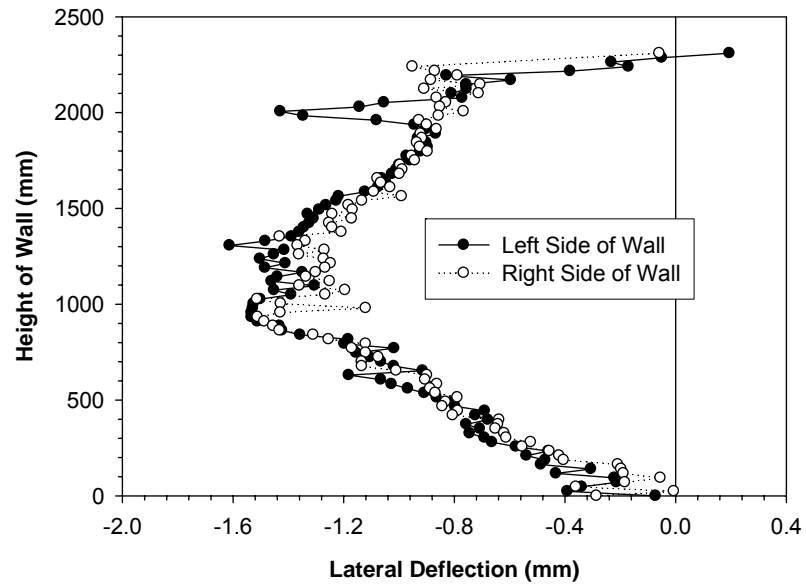


Figure 5.25: Lateral Deflections from PIV of Plastered Wall Assembly #6 (2.31 m #3) Entire Wall Height at Ultimate Load



Figure 5.26: Typical Compression Failure of Plastered Straw Bale Wall Assemblies

5.0 Concentric Compression Experiments of Plastered Straw Bale Assemblies



Figure 5.27: Progressive Failure of Plastered Straw Bale Wall Assemblies

Chapter 6: Eccentric Compression Experiments of Plastered Straw Bale Assemblies

6.1 Introduction

There is a deficiency in the literature regarding the testing and analysis of plastered straw bale wall assemblies. Experimentally, there is a gap regarding the testing of eccentrically loaded specimens, with only a few authors having conducted tests on specimens loaded eccentrically in compression. Furthermore, there is a gap in the literature regarding the theoretical analysis of the behaviour of plastered straw bale wall assemblies. These deficiencies are significant to building professionals as wall designs are currently based primarily on anecdotal evidence, with a lack of a detailed understanding of the theoretical behaviour of the walls.

This Chapter focuses on the behaviour of specimens loaded eccentrically in compression. A secondary focus is on the significance of the end conditions of the specimens.

6.0 Eccentric Compression Experiments of Plastered Straw Bale Assemblies

The specimens presented in this Chapter were fabricated such that they could be considered to have pinned supports at the top and bottom of each specimen. Furthermore, a number of pin-ended specimens were tested in concentric compression to determine the influence of the end conditions on these specimens.

A main focus of this Chapter was on the development of a theoretical model to capture the load and deflection behaviour of eccentrically loaded specimens. The theoretical models which were validated for concentric compression behaviour were extended to produce an analytical model which captured the behaviour of plastered straw bale wall assemblies subjected to eccentric load. The experimental results were compared to theoretical predictions to verify the proposed theoretical model.

The experimental component of this Chapter involved the fabrication and testing of six specimens with the load applied at an eccentricity of 120 mm, the maximum eccentricity possible with the testing apparatus. Six specimens were also tested with the load applied concentrically. Of the six specimens for each set of experiments, three were fabricated with height of 0.33 m while three were fabricated with height of 1.05 m. All specimens were designed to have plaster thickness of 25 mm and length of plaster skin of 600 mm.

6.0 Eccentric Compression Experiments of Plastered Straw Bale Assemblies

6.2 Design and Fabrication

6.2.1 Materials

Two-string wheat bales were used for the experiments presented in this Chapter. These bales were obtained from the same source, and stored in the same manner as those used in the experiments presented in Chapter 5.

The plaster used for the experiments described in this Chapter was prepared using the procedure described in Chapters 4 and 5. The plaster was a lime-cement plaster with proportions by volume of 4.5 : 1.25 : 0.25 of sand, lime and cement respectively, with a *w/cm* ratio of 1.08. Note that a drum mixer was used for the plaster preparation, in contrast to the tests described in Chapters 4 and 5. The dry components were mixed in the drum mixture prior to the addition of the water. One batch was used for each specimen. The cement, lime, sand and water were obtained from the same sources as the specimens described in Chapter 5.

Three 50 mm x 50 mm cube specimens were fabricated for each of the plastered straw bale assembly specimens. The cubes were tested at the same time as the plastered straw bale assemblies.

6.2.2 Wall Assembly Fabrication Procedure

The jig described in Chapter 5 was used for fabrication and testing of the specimens in this Chapter. However, fixed rollers were welded to the bottom and top of the jig in order to facilitate the application of the load through the desired eccentricity, to ensure consistent boundary conditions for each test, and to investigate the effect of pin-ended conditions on straw bale assembly performance.

6.0 Eccentric Compression Experiments of Plastered Straw Bale Assemblies

These modifications can be seen in Figure 6.1 and 6.2. Figure 6.3 provides an example of a specimen with the pins aligned for concentric load testing.

The fabrication procedure for the specimens described herein follows the procedure described in Chapter 5. However, the three-bale specimens presented were designed to be 1050 mm high as opposed to 990 mm. This was done to decrease the pre-compression of the bales for these specimens in an attempt to mitigate the effects of bale rebound following fabrication.

An additional deviation from the procedure presented in Chapter 5 was that only one plaster batch was used for each specimen presented in this Chapter. Cubes fabricated from the plaster were tested at the same time as the wall assembly specimen in order to determine the compressive strength of the plaster.

Despite the steps taken to ensure uniform plaster thickness, there were noted variations as a result of small misalignments of the bales for the 1050 mm specimens and as a result of working the plaster into the straw for both the 330 and 1050 mm specimens. Following testing of each specimen the plaster thickness was measured using the procedure described in Appendix F. Complete plaster thickness results are included in that Appendix.

6.3 Experimental Program

The experimental program consisted of compressive testing of 12 plastered straw bale wall assembly specimens and compressive cube tests for the plasters used for the assemblies. Table 6.1 presents a summary of the parameters examined for the plastered bale assembly experiments conducted in this Chapter.

6.0 Eccentric Compression Experiments of Plastered Straw Bale Assemblies

Note that for the test name, the letter corresponds to eccentric (E) or concentric (C) test, the first number corresponds to the number of bales used for the specimen (1 or 3), and the second number corresponds to the test number for that configuration.

6.4 Instrumentation

Load was applied to each specimen via a Reilhle universal testing machine, and the load was recorded using a load cell integrated with the testing machine. Displacements were measured using two techniques: linear potentiometers (LPs) and Particle Image Velocimetry (PIV). Four 100 mm LPs were mounted to the testing machine as shown in Figure 6.4 to measure the vertical displacements of each specimen. Unfortunately, the top bale of each wall assembly was observed to rebound. As eccentric loads were applied, the top plate was observed to rotate as shown in Figure 6.5, resulting in erroneous readings from the LPs. As a result, PIV was used to track the vertical and lateral wall deflections.

For PIV measurements, cameras were arranged to photograph the face and edge of each specimen. Photographs were taken at 30 second intervals throughout the duration of the experiment. The deflections of the specimens were tracked as pixel displacements in the photographs and were subsequently converted to millimetre displacements utilizing a scale factor. The load at each photograph (30 second intervals) was determined from the load cell, and thus the PIV load-deflection behaviour could be determined. The PIV procedure and apparatus are described in greater detail in Appendix B.

6.0 Eccentric Compression Experiments of Plastered Straw Bale Assemblies

PIV has several limitations. Note that the photographs for the PIV analysis are taken every thirty seconds, and so do not necessarily capture the precise deflection at the ultimate load. Additionally, the precision of PIV is 0.1 mm, as discussed in Appendix B, while for LPs it is 0.01 mm, as discussed in Appendix A. Beyond the ultimate load, the PIV data becomes unreliable as a result of the large deflections and the fracturing of the surface being photographed. A comparison between LP and PIV measurements is provided in Appendix B.

Data acquisition for the load cell and LPs was provided by Measure Foundry® by Data Translation Inc. Data was sampled at a rate of 17 samples per second. Appendix A provides detailed data on the instrumentation and testing apparatus, while appendix B provides further details on the PIV.

6.5 Procedure

All twelve specimens were tested in stroke-control. The load was applied at a rate of 0.5 mm/min prior to achieving ultimate load and 2 mm/min after the ultimate load was achieved. The test was stopped when the LPs exceeded their range. The plaster cubes were tested at a rate of 1 mm/min utilizing the same testing procedure as described in Chapter 3.

6.0 Eccentric Compression Experiments of Plastered Straw Bale Assemblies

6.6 Predictive Model for Straw Bale Assemblies Subjected to Eccentric Load

6.6.1 Assumptions

In order to model a straw bale assembly under eccentric load, a constitutive model of the plaster is necessary. In Chapter 3, the following constitutive plaster model was derived:

$$f_c = f'_c \left(\frac{764.8\varepsilon}{0.935 + \left(\frac{\varepsilon}{0.00253} \right)^{1.935}} \right) \quad 3.10$$

This model will be referred to as the “Theoretical” constitutive model in this Chapter. It assumes that the plaster strain at failure in a straw bale assembly is equal to the average failure strain in the plaster.

In Chapter 5, because of the progressive failure mode observed in certain tests, the following constitutive model was proposed:

$$f_c = f'_c \left(\frac{331.4\varepsilon}{0.405 + \left(\frac{\varepsilon}{0.00424} \right)^{1.405}} \right) \quad 5.1$$

This model will be referred to as the “Upper Strain Boundary” constitutive model in this Chapter. It assumes that the plaster strain at ultimate failure in a straw bale assembly is equal to the maximum expected failure strain based on a 95% confidence interval.

6.0 Eccentric Compression Experiments of Plastered Straw Bale Assemblies

The plastered straw bale assemblies are assumed to act as composite sandwich panels under eccentric load with the following assumptions utilized for the analysis:

- Linear strain distribution across the width of the specimens was assumed. This assumes that there is no slippage at the straw/plaster interface, and that the straw does not undergo shear distortion. This assumption is discussed in Appendix E;
- For the specimens presented in this Chapter it is assumed that globally, plane sections will remain plane.
- Failure is a result of crushing of the plaster when plaster stress reaches f'_{cube} at the extreme compression fibre;
- The straw provides adequate lateral support to prevent local buckling.

For the case of eccentric loading, the strain and corresponding stress distribution are not uniform across all regions of the plaster. Note that the strain profile is linear, with the larger strain on the same side as the eccentricity. As such, under a given strain profile, the corresponding non-linear stress profile must be integrated to determine the applied load and eccentricity. This technique is used to determine the theoretical strength and theoretical load-deflection response of eccentrically loaded plastered straw bale wall assemblies.

6.0 Eccentric Compression Experiments of Plastered Straw Bale Assemblies

6.6.2 Eccentric Theoretical Model

A model to predict the vertical deflection response and lateral deflection response for a straw bale assembly subjected to eccentric loading was derived. Specifics regarding the coding of the model are presented in Appendix H. The model performs a number of analyses to determine the strain profile for a given load and eccentricity. The load is increased incrementally (typically 100 N increments) until the maximum load is reached. For each load increment the lateral and vertical deflections are determined based on the strain profile, and the lateral deflections are added to the eccentricity for the next step to account for increased eccentricity of the load as the specimen deflects laterally (P- δ effect). The main steps in the theoretical analysis are presented in Figure 6.6.

The key input variables in addition to the constitutive models of Equations 3.10 and 5.1; are the specimen height, the eccentricity of the load, the plaster skin length, thickness and strength, the Modulus of Elasticity, and the strain at ultimate stress. These variables are defined in the first step of the model. The second step is to apply the initial load and eccentricity, as shown in the loading diagram in Figure 6.7. The initial load will be the incremental load (typically 100 N), while the initial eccentricity will be as defined by the input parameters. The next steps will determine the strain profile corresponding to the given initial load and eccentricity.

Determination of the appropriate strain profile for the given load and eccentricity is an iterative process. The third step is to assume a particular strain profile. Given the assumed strain profile, such as that presented in Figure 6.7, the fourth step, which is to determine the corresponding stress profile (shown in Figure

6.0 Eccentric Compression Experiments of Plastered Straw Bale Assemblies

6.7), can be completed. Determination of the stress profile is based on the stress-strain profile of the plaster. This is determined by Equation 3.10 or Equation 5.1. Using the known maximum and minimum values on the strain profile (ϵ_1 and ϵ_2), the corresponding maximum and minimum stress values (f_1 and f_2) can be determined. This is illustrated in Figure 6.8.

The fifth step is to determine the load and moment based on the assumed strain profile and corresponding stress profile. The load in each plaster skin can be determined separately by integrating the stress profile for that portion over the area of the plaster skin. The resultant is a load which acts through the centroid of the area under the stress profile for the plaster skin. This is shown in the stress profile in Figure 6.7, with the resultant loads also shown in Figure 6.7. Note that the centroid of the area under the stress profile will not fall in the centre of the plaster skin, thus the resultant loads do not act directly through the centre of the plaster skins.

Once the resultant loads are found for each plaster skin, the total load and corresponding moment and eccentricity can be determined. The total load is calculated as the sum of the loads determined for each plaster skin ($P_1 + P_2$). The moment is calculated as the sum of the moments from each of the plaster skin loads, summed about the centre line for the entire specimen ($P_2 \times e_2 - P_1 \times e_1$). The overall eccentricity can then be found by dividing the moment by the load.

For the sixth step, the load and eccentricity for the assumed strain profile are checked against the initial load and eccentricity. If they are not equal then the assumed strain profile is modified and the process is repeated from step three. Note

6.0 Eccentric Compression Experiments of Plastered Straw Bale Assemblies

that the load is defined as being equal if it is within 1 N, while the correct moment is found when the moment calculated from successive strain profiles fall above and below the true moment. The strains are incremented from zero to the maximum strain (strain at ultimate load) until the appropriate strain profile is found. Note that no less than 2500 increments are used from zero strain to maximum strain.

Once the appropriate strain profile has been found for the initial load and eccentricity, the displacements as a result of that load increment are calculated and stored. The load is then stepped up by the increment value (typically 100 N), and the process is repeated from step three. The procedure of incrementing the load (and eccentricity) and finding the corresponding strain profile is continued until a load is reached where the appropriate strain profile will have maximum strain (ϵ_2) which exceeds the assumed failure strain. Once this has occurred, it is known that the previous load value was the maximum load just prior to ultimate failure, and this value is taken as the theoretical ultimate strength.

It is important to note that the lateral deflection is continually added to the eccentricity for each load increment in order to account for increased eccentricity of the load as the specimen deflects laterally under increasing load. However, because the lateral deflections vary along the height of the specimen, for each load increment the analysis is performed at multiple locations from the base to the top of the specimen. Thus, as the load increases, the eccentricity used in the analysis will be larger at mid-height of the specimen than near the top or bottom. This is because the eccentric loading will cause the specimen to undergo the greatest lateral deflection at mid-height, and zero lateral deflection at the base and top.

6.0 Eccentric Compression Experiments of Plastered Straw Bale Assemblies

6.6.3 Calculation of Vertical Displacements

When the deflections are calculated for a particular load value using the theoretical model, they are calculated assuming loading from zero load up to the particular value. However, this will yield an incorrect value for deflection at that load because the eccentricity is changing throughout the analysis. Thus, at each load value the deflections are only calculated for the loading from the previous load value to the current load value. These incremental deflections are summed to provide total deflections.

The vertical displacements were calculated by determining the average strain in each plaster skin and multiplying it by the height. Note that because analyses were conducted at various points from the base to the top of the specimen, the strain for a particular analysis was actually multiplied by the distance between analysis points. These values were then summed to give the total vertical displacement. This method will result in different vertical displacement values for each plaster skin of a specimen.

Use of the average strain for a plaster skin will provide the theoretical vertical displacement of the centre of the plaster skin. This was done because the PIV measurements for the displacements were taken at the centre of the plaster skins. It should be noted that the deflections at the extreme fibers will be slightly different than the values presented. However, because the plaster skins are thin relative to the overall width of the specimens, the displacements at the extreme fibers are not expected to vary significantly from the displacements at the centers of the plaster skins.

6.0 Eccentric Compression Experiments of Plastered Straw Bale Assemblies

6.6.4 Calculation of Lateral Displacements

The lateral displacements were determined by analysis of the curvature of the specimens. Similar to the vertical displacement analysis, the curvature was calculated for a number of locations from the base to the top of the plaster skins. The curvature is calculated by determining the slope of the strain profile. This is defined as: $(\varepsilon_2 - \varepsilon_1)/W$, where W is the entire width of the specimen. The curvature will be greatest at mid-height of the specimen as a result of the increased eccentricity at this location from lateral deflection. The curvatures calculated at the various analysis points can then be used to determine the true curvature diagram, such as that shown in Figure 6.9. This diagram presents the curvature from the base to the top of the specimen. Once the curvature is known, the deflection can be determined based on Equation 6.1:

$$\varphi = -\frac{d^2v}{dh^2} \quad 6.1$$

where φ is the curvature, v is the deflection and h is the height of the specimen. By performing a double integration of the curvature, the deflection can be determined. Note that because the strain profile is assumed to be linear across the entire width of the specimen, the curvature in the two plaster skins will be equal, and thus the lateral deflections will be equal for the two plaster skins. Also note that to simplify the integration of the curvature, the simplified curvature diagram presented in Figure 6.9 was utilized.

6.0 Eccentric Compression Experiments of Plastered Straw Bale Assemblies

6.6.5 Input Parameters

The key input parameters for the model were noted in section 6.6.2. These input parameters are: eccentricity of the load, specimen height, plaster skin length, plaster thickness, plaster strength, plaster Modulus of Elasticity, and plaster strain at ultimate load.

The eccentricity of the load was 120 mm for all specimens. The specimen height was defined as 0.33 m or 1.05 m. The plaster skin length was defined as 600 mm. The plaster thickness was defined as the minimum failure-plane thickness, while the plaster strength was defined as the average measured cube strength for the specific specimen. The plaster strength and thickness values are presented for each specimen in Table 6.1. The Modulus of Elasticity was taken as E_{cube} , which was determined from the following equation presented in Chapter 3:

$$E_{cyl} = 818f'_{cyl} \quad \mathbf{3.1}$$

where f'_{cyl} is replaced with f'_{cube} to determine E_{cube} . The plaster strain at ultimate was 0.00253 when Equation 3.10 was used, and 0.00424 when Equation 5.1 was used.

It is important to note that many of the input parameters have associated expected variability and thus, while the theoretical model will provide an estimate of the average expected behaviour, experimental results will deviate from the theoretical predictions as a result of variability in such parameters as the plaster strength, and Modulus of Elasticity, and the dimensions of the specimens.

6.0 Eccentric Compression Experiments of Plastered Straw Bale Assemblies

6.7 Results and Observations

6.7.1 Ultimate Load Results

The theoretical strengths for each specimen are presented in Table 6.1 while Table 6.2 presents the experimental strengths and the ratio of the experimental strength divided by the theoretical strength. The theoretical strengths were determined based on the aforementioned model for the eccentric specimens and based on the techniques presented in Chapter 5 for the concentric specimens. The strengths presented in Table 6.2 are obtained by dividing the ultimate loads by the length of the plaster (0.6 m).

6.7.2 Load-Deflection Results

The vertical load-deflection curves for the plastered straw bale wall assemblies are presented in Figures 6.10a – 6.20a. The theoretical vertical load-deflection curves are also presented in Figures 6.10a – 6.20a. The theoretical load-deflection curves were determined based on the aforementioned model for the eccentric specimens and based on the techniques presented in Chapter 5 for the concentric specimens. Note that for the “left” side theoretical curves, which represent the non-failure side, the “Theoretical” curves and the “Upper Strain Boundary” curves are in line with one another. This is because the non-failure side does not achieve strains as high as the failure side, and Equations 5.1 and 3.10 do not differ significantly at low strains.

Figures 6.13c – 6.15c present the mid-height lateral load-deflection curves while Figures 6.13d – 6.15d present the lateral deflection curves for the full height of

6.0 Eccentric Compression Experiments of Plastered Straw Bale Assemblies

the plaster skins at ultimate failure, illustrating the deflected shape of the specimens at ultimate failure. Theoretical lateral deflection curves are presented in Figures 6.13c – 6.15c and 6.13d – 6.15d. Note that lateral deflection curves are only presented for the 1.05 m eccentric specimens as these were the only specimens which were observed to exhibit significant measurable lateral deflection. The lateral deflection curves for the other specimens are provided in Appendix I.

The 0.33 m eccentric specimens are presented in Figures 6.10 – 6.12, the 1.05 m eccentric specimens are presented in Figures 6.13 – 6.15, the 0.33 m concentric specimens are presented in Figures 6.16 – 6.18, and the 1.05 m concentric specimens are presented in Figures 6.19 – 6.20. Note that there are only two figures for the 1.05 m concentric specimens due to failure of the data acquisition apparatus during testing of the third specimen of this configuration.

Each deflection plot (Figures 6.10 – 6.20 (a,c,d)) presents results for the left and right sides of the specimen, corresponding to the two plaster skins of each specimen. The theoretical lateral curves are equal for the right and left sides of the specimens as it is assumed that the straw which ties the two plaster skins together does not compress or expand laterally under bending.

6.8 Discussion

6.8.1 General Behaviour and Failure Mechanisms

All failures were initiated with the compressive failure of one of the plaster skins. Following this initial failure, the behaviour of the eccentric specimens deviated from the behaviour of the concentric specimens. For the concentric specimens, the

6.0 Eccentric Compression Experiments of Plastered Straw Bale Assemblies

failure of the second plaster skin was a compressive failure, and resulted in a second drop in load. This can be seen in Figure 6.21. This is the same behaviour as was noted for the specimens presented in Chapter 5. However, for the eccentric specimens, the initial failure was followed by significant lateral deflection, causing bending of the specimens, and a steep drop in load following ultimate failure. This can be seen in Figure 6.22. This bending put the un-failed plaster skin into tension, eventually resulting in tensile failure of that plaster skin. This tension failure can be seen in Figure 6.23. Note that the tests were stopped much sooner for the eccentrically loaded specimens than the concentrically loaded specimens due to the large post-failure lateral displacement of the eccentrically loaded specimens.

The eccentrically loaded specimens described in this Chapter also differed from those described in Chapter 5 in that the specimens described in this Chapter did not maintain as much strength following ultimate failure. This can be seen in Figure 6.22, which shows the load-deflection plot for the full duration of the experiment. This loss of strength is a result of the large lateral deflections noted for the eccentrically loaded specimens. The pinned ends utilized for the experiments presented in this chapter allowed for rotation of the loading plates as the experiment progressed. This rotation was initiated by failure of the first plaster skin. With one failed plaster skin the eccentrically loaded specimens underwent significant vertical deformation on the failed side, causing rotation of the loading plates, and bending of the specimen.

As the failure of the specimens progressed beyond the tension failure of the second plaster skin, the specimen continued to bend and deform laterally. This

6.0 Eccentric Compression Experiments of Plastered Straw Bale Assemblies

behaviour ensured that the specimen was unable to resist load following the initial ultimate failure. For the 1.05 m specimens, the load resistance of the specimens was nearly non-existent when the tests were stopped. Similar but less dramatic behaviour was also noted for the 0.33 m specimens.

Because the taller specimens were noted to have a more rapid loss of structural integrity, it is expected that if specimens were constructed to a height of 2.4 m (the height of a typical single residential storey), they would see an even more rapid loss in strength as failure progressed. This suggests that further research on the post-failure response of 2.4 m eccentrically loaded specimens may be warranted.

6.8.2 Eccentric Compression Experiments

6.8.2.1 Ultimate Strength

The 0.33 m eccentrically loaded specimens achieved average strength of 31.62 kN/m, while the 1.05 m eccentrically loaded specimens achieved average strength of 24.22 kN/m. This represents a decrease in strength of 23.4% as the specimen height was increased from 0.33 m to 1.05 m. To determine if this decrease in strength is a result of theoretically predicted bending of the taller specimens and differences in the plaster strengths and thicknesses of the specimens, the ratio of experimental strength divided by theoretical strength can be studied. The theoretical strength accounts for the bending of the specimens and differences in the plaster strengths and thicknesses of the specimens, and thus if the 0.33 m specimens and 1.05 m specimens have similar ratios, then the differences in

6.0 Eccentric Compression Experiments of Plastered Straw Bale Assemblies

strength can be considered to be a result of the expected increase in bending with increase in specimen height, in addition to differences in strength and thickness of the plaster between the specimens.

The average ratio of experimental strength divided by theoretical strength for the 0.33 m specimens was found to be 1.07 with standard deviation of 0.06 while the average ratio for the 1.05 m specimens was found to be 0.99 with standard deviation of 0.12. Based on these results, a t-test indicated that there is not a statistically significant difference in the ratios for the two specimen heights ($t=1.060$, $DF= 4.0$, $p=0.349$). This suggests that the differences in strengths between the 0.33 m specimens and the 1.05 m specimens can be attributed to the increased bending for the taller specimens and the differences in plaster strengths and thicknesses of the specimens, as anticipated by the theoretical model. This is an important finding as there was a 23% decrease in strength with increase in height from 0.33 m to 1.05 m. However, it is unclear if this decrease in strength is a result of the increased bending for the taller specimen or differences in strength and thickness of the plaster between specimens. The effect of increasing height on the strength loss of eccentrically loaded specimens is discussed in Chapter 7.

Considering the results for the 0.33 m specimens and the 1.05 m specimens together, the average ratio of experimental strength to theoretical strength for the six eccentric specimens was found to be 1.03 with standard deviation of 0.10. Based on these values, it can be determined with 99% confidence that the true average is between 0.92 and 1.14. This is reasonable considering that the expected ratio is 1.00.

6.0 Eccentric Compression Experiments of Plastered Straw Bale Assemblies

6.8.2.2 Vertical Load-Deflection Relationship

Figures 6.10a – 6.15a present the vertical load-deflection plots for the six eccentrically loaded specimens. The left side (non-failure side) experimental results deviate from the theoretical line by no more than approximately 0.4 mm, and generally are within 0.2 mm for the entire duration of the experiments. This is a good correlation given that the precision of the PIV is +/- 0.1 mm. The right side experimental results are more variable; however, they do still follow the theoretical prediction closely. The experimental data falls between the “theoretical” line and the “upper strain boundary” line, with deviation outside of this envelope typically less than 0.1 mm for loads up to 90% of ultimate. Specimen E12 appears to be an anomaly as it underwent deflections approximately 0.5 mm greater than theoretical for loads greater than 50% of ultimate.

For a number of the specimens the experimental deflection at failure was up to 15% higher than the deflection predicted even by the upper strain boundary line. This most likely is a result of the straw holding the plaster in place even as it begins to fail, yielding increased deflection as the wall continued to withstand load. However, further testing may be required to confirm this hypothesis.

6.8.2.3 Lateral Deflection Behaviour

The lateral deflection behaviour for the 1.05 m eccentrically loaded specimens is presented in Figures 6.13c – 6.15c and in Figures 6.13d – 6.15d. The behaviour for the 0.33 m specimens is presented in Appendix I.

6.0 Eccentric Compression Experiments of Plastered Straw Bale Assemblies

The experimental data follows the same shape as the theoretical curves; however, for specimens E31 and E32 it appears as if the entire specimens shifted laterally during experimentation, and as a result, the data does not directly follow the theoretical curves. This can be seen by looking at the deflection at the bottom and top of the specimens for the full-height figures of these specimens, and by noting that for specimens E31 and E32, the mid-height load-deflection curves appeared to shift by approximately +0.3 mm during the experiment. However, it is important to note that the shapes of the curves for specimens E31 and E32 are similar to the theoretically predicted curves.

Figure 6.15d provides evidence that the theoretical model adequately captures the response of an eccentrically loaded straw bale assembly. It can be seen that the experimental results for specimen E33 only fall outside of the theoretical envelope in a few locations, and that the deviation is no more than 0.2 mm at these locations. This indicates the appropriateness of the theoretical model. However, it should be noted that Figure 6.15c for specimen E33 indicates that the lateral-load deflection response was not entirely as expected for this specimen. The lateral deflections were observed to remain near zero until the load reached nearly 50% of ultimate. This deviates from the theory. However, given the small magnitude of the deflection, the noted precision of the PIV, and the potential sources of error; some deviation from the theoretical behaviour is expected.

6.0 Eccentric Compression Experiments of Plastered Straw Bale Assemblies

6.8.2.4 Failure Mode Discussion

Photographs of the initial failures are presented in Figures 6.10b – 6.15b. These photographs show the mode of ultimate failure of the specimens. From observations during testing it was noted that all specimens failed as a result of crushing of the plaster, indicating that the stress in the plaster had exceeded the strength of the plaster. The typical failure involved an initial crack in the plaster, such as that shown in Figures 6.10b, 6.12b, and 6.15b. The plaster was observed to remain in place following this initial crack, thus enabling the specimen to continue to resist some load under increasing deformation. This was noted previously as it was observed that most specimens reached higher vertical strain than expected. Eventually, under increasing load and deformation the failed portion of the plaster crumbled away from the specimen as shown in Figures 6.11b, 6.13b, and 6.14b.

6.8.3 Concentric Compression Experiments

6.8.3.1 Ultimate Strength

The 0.33 m concentrically loaded specimens achieved an average strength of 51.65 kN/m, while the 1.05 m eccentrically loaded specimens achieved an average strength of 40.23 kN/m. Because the specimens were loaded concentrically, the specimen height was not expected to influence the strength of the specimens. To determine if the strength difference between the 1.05 m specimens and the 0.33 m specimens was a result of the differences in specimen height, the ratio of experimental to theoretical strength can be studied.

6.0 Eccentric Compression Experiments of Plastered Straw Bale Assemblies

The average ratio of experimental to theoretical strength for the 0.33 m specimens was 1.18 with standard deviation of 0.12 while the average ratio for the 1.05 m specimens was 1.14 with standard deviation of 0.09. Based on these results, a t-test indicated that there is not a statistically significant difference in the ratios for the two specimen heights ($t=0.473$, $DF= 4.0$, $p=0.661$).

Because the theoretical model does not consider the height of the specimens for the concentric compression analysis, the lack of a significant difference in the ratios of the 0.33 m and 1.05 m specimens indicates that, as expected, the height did not influence the strength of the specimens. Rather, the differences in strengths between the 0.33 m specimens and the 1.05 m specimens can be attributed to differences in the plaster strengths and thicknesses, which are accounted for in the model.

Considering the results for both the 0.33 m specimens and the 1.05 m specimens it can be seen from Table 6.2 that for all six specimens the experimental strengths exceed the predicted theoretical strengths. The average ratio of experimental strength to theoretical strength was found to be 1.16 with standard deviation of 0.09. Based on these values it can be determined with 99% confidence that the true average ratio will fall between 1.06 and 1.26. Given that this range is greater than the expected average ratio of 1.0, it appears as if the theoretical method underestimated the strength of the specimens, or the experimental method provided stronger than expected specimens. This discrepancy may be a result of the noted variability in the model parameters; however, it is expected that such variability will lead to results which still deviate around an average experimental to theoretical ratio

6.0 Eccentric Compression Experiments of Plastered Straw Bale Assemblies

of 1.0. Furthermore, considering that the average ratio of experimental to theoretical strength for the eccentric specimens was much closer to 1.0, it is surprising that for the concentric specimens the theoretical predictions deviated from the experimental results so significantly.

To further analyze these results a t-test comparing the results from the experiments presented in Chapter 5 with the experiments discussed in this Chapter can be conducted to show that at the 95% confidence level, the results from the two sets of experiments are statistically significantly different. This is because the experimental to theoretical ratio for the Chapter 5 results were closer to the expected value of 1.0. This is significant considering that the methods of determining the plaster strength and thickness were expected to be more accurate for the results presented in this chapter, and thus the experimental to theoretical ratios should be closer to 1.0 for the specimens described in this chapter than for those presented in Chapter 5. A hypothesis regarding the reason for the unexpected results is presented in the failure mode discussion.

6.8.3.2 Vertical Load-Deflection Relationship

The vertical load-deflection responses for the concentric compressive tests are presented in Figures 6.16a – 6.20a. It can be seen that every specimen except C12 was stronger and stiffer than expected, with higher ultimate load and steeper load-deflection response. While specimen C12 was stronger than expected, it was observed to have unexpected large deflection at the beginning of the test. Because PIV tracks only the plaster displacements, this large initial deflection was not the

6.0 Eccentric Compression Experiments of Plastered Straw Bale Assemblies

result of straw re-compressing, as occurred in previous experiments. As such, there is no logical explanation for this behaviour aside from the known imperfections associated with constructing with inhomogeneous materials such as plaster and straw.

6.8.3.3 Failure Mode Discussion

Considering the photographs presented in Figures 6.16b – 6.20b, which show the specimen immediately following ultimate failure, it can be seen that for every specimen the plaster remained attached to the straw, even once it had cracked. This may explain the unexpected behaviour.

One hypothesis for the higher than expected strengths is that when the plaster reached its maximum stress in the failure region, a small portion of the plaster in the thinnest region may have crumbled away from the wall. As the plaster crumbled away from the wall in the thin region, the thicker plaster sections above and below this section may have come to bear upon one-another leading to an increase in plaster thickness in this region, and thus an increase in specimen strength.

With the pinned end conditions, as the failure progressed in this manner, the rotation of the loading plates would have facilitated the shifting of the plaster into the failure region. Eventually, even the additional plaster which had been pushed into the failure region would be insufficient to resist the load and the plaster would fall away from the specimen, resulting in a drop in load, and the ultimate failure of the specimen.

6.0 Eccentric Compression Experiments of Plastered Straw Bale Assemblies

Given that the plaster was typically observed to remain in place more for these concentrically loaded specimens than for other specimens, it appears this may be a feasible hypothesis. However, further testing is required to confirm this.

6.9 Conclusions

Eccentric and concentric compression experiments were conducted on 0.33 m and 1.05 m tall plastered straw bale wall assemblies. The results were analyzed and were compared to theoretical models and the following key findings were observed:

- The 0.33 m eccentrically loaded specimens achieved average strength of 31.62 kN/m, while the 1.05 m eccentrically loaded specimens achieved average strength of 24.22 kN/m. The difference is attributed to the effect of the bending of the taller specimens under eccentric load, and differences in strength and thickness of the specimens.
- The 0.33 m concentrically loaded specimens achieved average strength of 51.65 kN/m, while the 1.05 m eccentrically loaded specimens achieved average strength of 40.23 kN/m. The difference is attributed primarily to differences in the plaster strengths and thicknesses of the specimens, as it was found that the results for the two different heights were not statistically significantly different relative to the theoretical strengths.
- For plastered straw bale wall assemblies which are constructed 1 to 3 bales high, with pinned ends, bales stacked flat, and 25 mm thick low-

6.0 Eccentric Compression Experiments of Plastered Straw Bale Assemblies

strength plaster skins, the results and observations support the assumption that the assemblies fail as a result of compression failure of the plaster.

- The concentrically loaded specimens did not behave as predicted by the theoretical model with experimental results on average 16% higher than the theory suggested. It is believed that unexpected failure mechanisms lead to the deviation from the theory.
- The eccentrically loaded specimens behaved as predicted by the model with experimental strengths ranging from 11% below the theoretical strength to 13% above the theoretical strength. Any deviations were primarily a result of the variability associated with inhomogeneous materials such as plaster and straw.
- The stress-strain models presented in earlier Chapters can be used to model the pre-failure load-deflection behaviour (lateral and vertical) of the eccentrically loaded plastered straw bale walls using the plaster thickness and strength as input parameters. This model also provided an accurate means of determining the theoretical strength of the specimens.

The results presented in this Chapter provide support for the effectiveness of the testing and fabrication techniques utilized for the eccentrically loaded specimens. The eccentrically loaded specimens were found to have load-deflection behaviour (lateral and vertical) which could be predicted by theoretical models based on the stress-strain behaviour of the lime-cement plaster used in fabrication of the specimens. Failure of the specimens was observed to occur as a result of

6.0 Eccentric Compression Experiments of Plastered Straw Bale Assemblies

compressive failure of the plaster, and was predicted based on the theoretical models.

The results for the concentrically loaded specimens presented in this chapter indicated that buckling was not a governing failure mechanism, and that the specimens failed due to the compressive failure of the plaster, as expected. However, the theoretical model under-predicted the experimental strengths by 16% on average. It is believed that this is a result of unanticipated failure mechanisms. As such, there is a need to study further these types of specimens in order to confirm this hypothesis. Because the theoretical model was conservative for the concentrically loaded specimens, it is still appropriate for use in design.

6.0 Eccentric Compression Experiments of Plastered Straw Bale Assemblies

Table 6.1: Description of Experimental Parameters and Theoretical Strengths

Test Name	Wall Height (m)	Eccentricity (mm)	Plaster Strength (MPa)	Plaster Thickness (mm)	Theoretical Wall Strength (kN/m)
E11	0.33	120	0.82	28	29.8
E12	0.33	120	0.85	27	29.0
E13	0.33	120	0.69	34	29.8
E31	1.05	120	0.61	26	20.2
E32	1.05	120	0.82	26	27.2
E33	1.05	120	0.78	27	27.2
C11	0.33	0.0	0.80	23	37.3
C12	0.33	0.0	1.03	23	47.0
C13	0.33	0.0	0.91	24	44.0
C31	1.05	0.0	0.84	18	29.8
C32	1.05	0.0	0.85	21	34.9
C33	1.05	0.0	0.89	22	39.3

Table 6.2: Comparison of Experimental and Theoretical Strengths

Test Name	Wall Height (m)	Eccentricity (mm)	Experimental Strength (kN/m)	Theoretical Strength (kN/m)	Exp./Theo. Ratio
E11	0.33	120	32.3	29.8	1.08
E12	0.33	120	29.0	29.0	1.00
E13	0.33	120	33.6	29.8	1.13
E31	1.05	120	22.6	20.2	1.12
E32	1.05	120	24.2	27.2	0.89
E33	1.05	120	25.9	27.2	0.95
C11	0.33	0.0	40.0	37.9	1.06
C12	0.33	0.0	61.3	47.6	1.29
C13	0.33	0.0	53.7	44.7	1.20
C31	1.05	0.0	36.6	30.4	1.20
C32	1.05	0.0	42.3	35.6	1.19
C33	1.05	0.0	41.7	40.0	1.04

6.0 Eccentric Compression Experiments of Plastered Straw Bale Assemblies

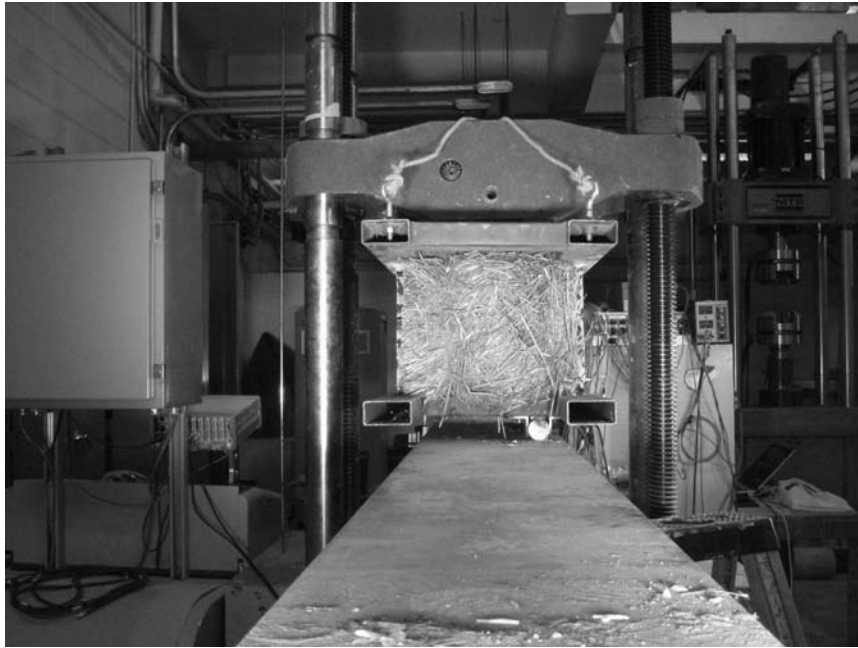


Figure 6.1: 330 mm Specimen Subjected to Eccentric Load

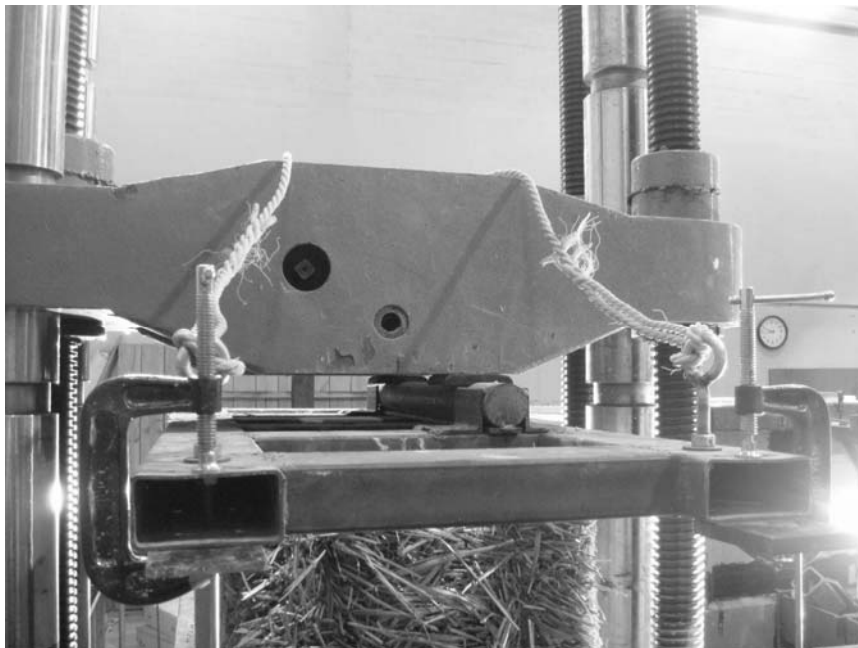


Figure 6.2: Top Plate of Modified Loading Jig Subjected to Eccentric Load

6.0 Eccentric Compression Experiments of Plastered Straw Bale Assemblies

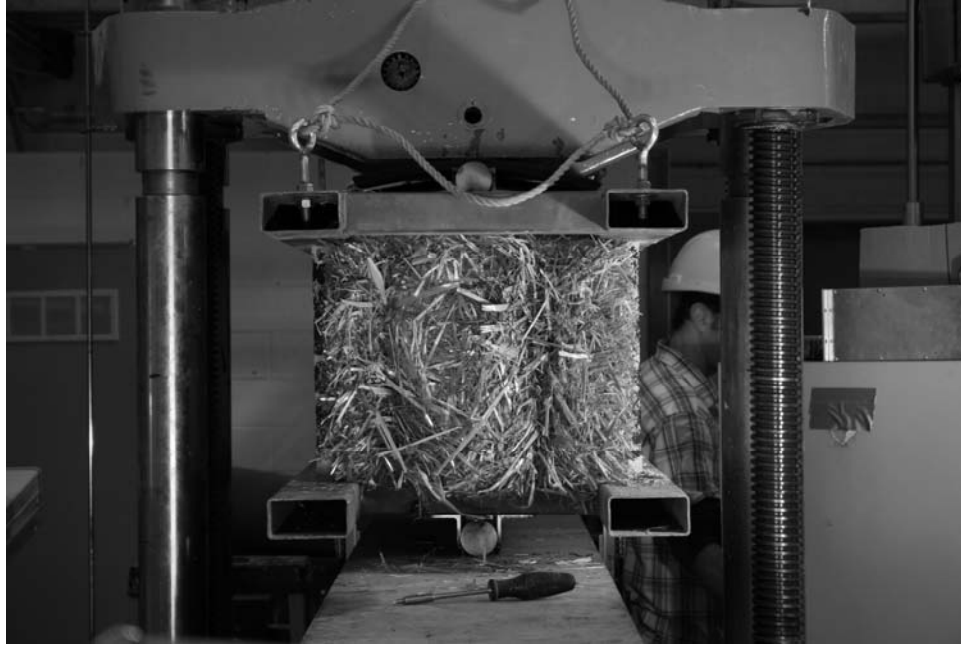


Figure 6.3: Concentric Loading of Specimen in Modified Jig

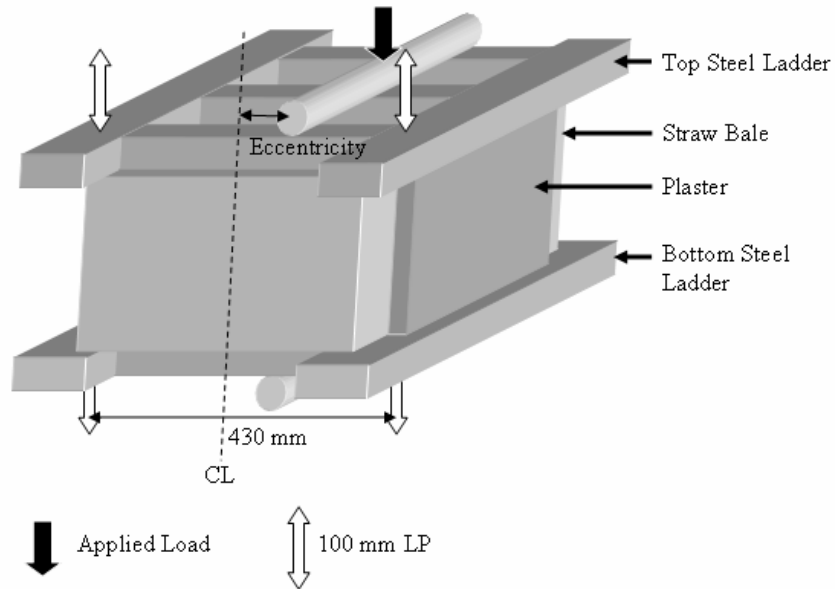


Figure 6.4: Eccentrically Loaded Plastered Straw Bale Assembly Test Setup

6.0 Eccentric Compression Experiments of Plastered Straw Bale Assemblies

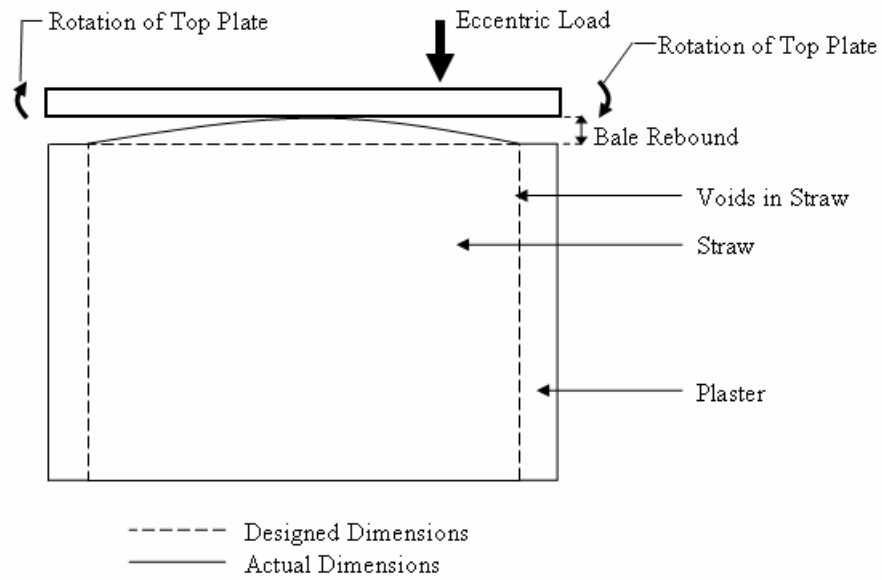


Figure 6.5: Rotation of Top Plate with Bale Rebound and Eccentric Load

6.0 Eccentric Compression Experiments of Plastered Straw Bale Assemblies

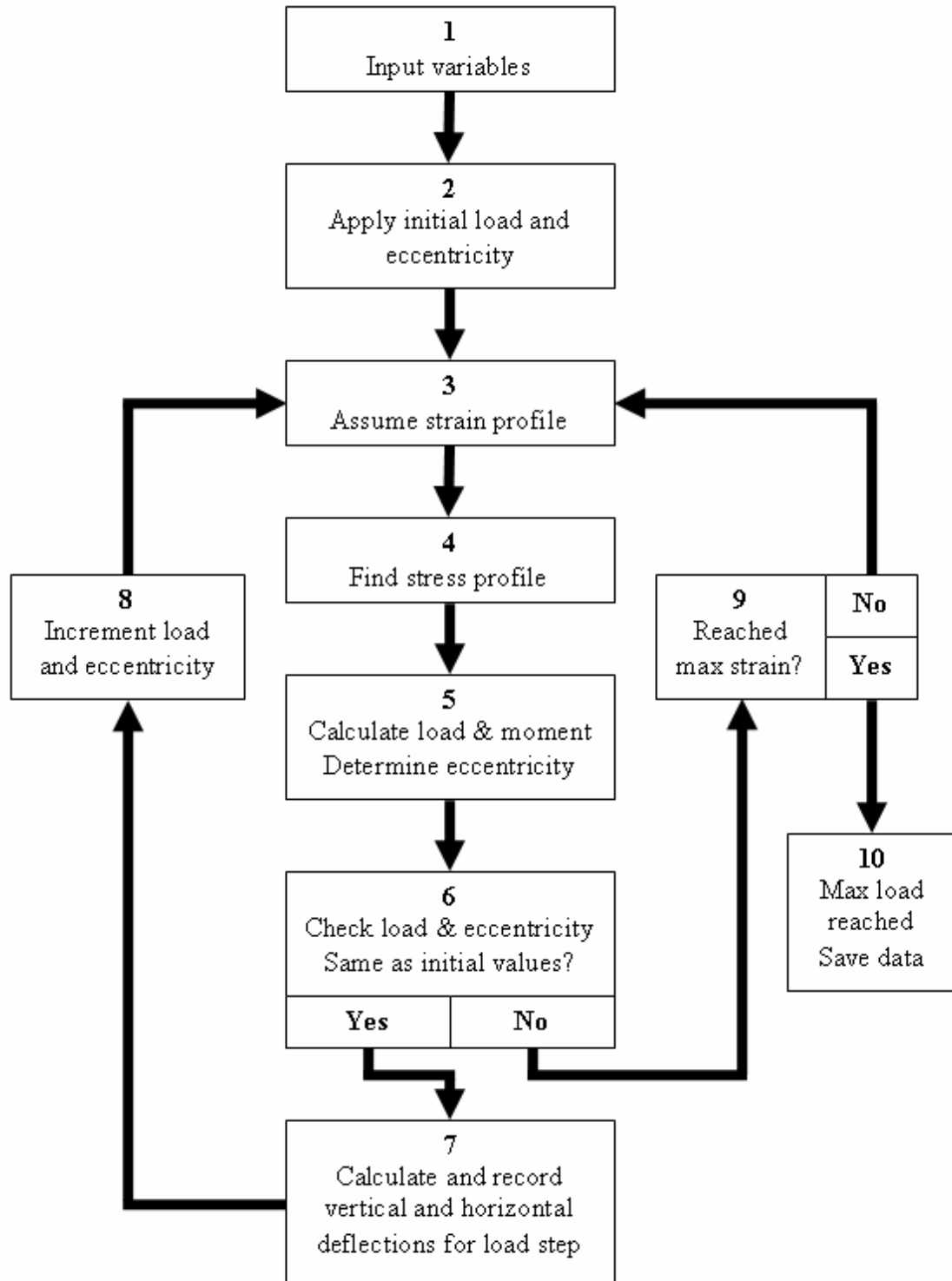


Figure 6.6: Flow-Chart for Eccentric Theoretical Analysis

6.0 Eccentric Compression Experiments of Plastered Straw Bale Assemblies

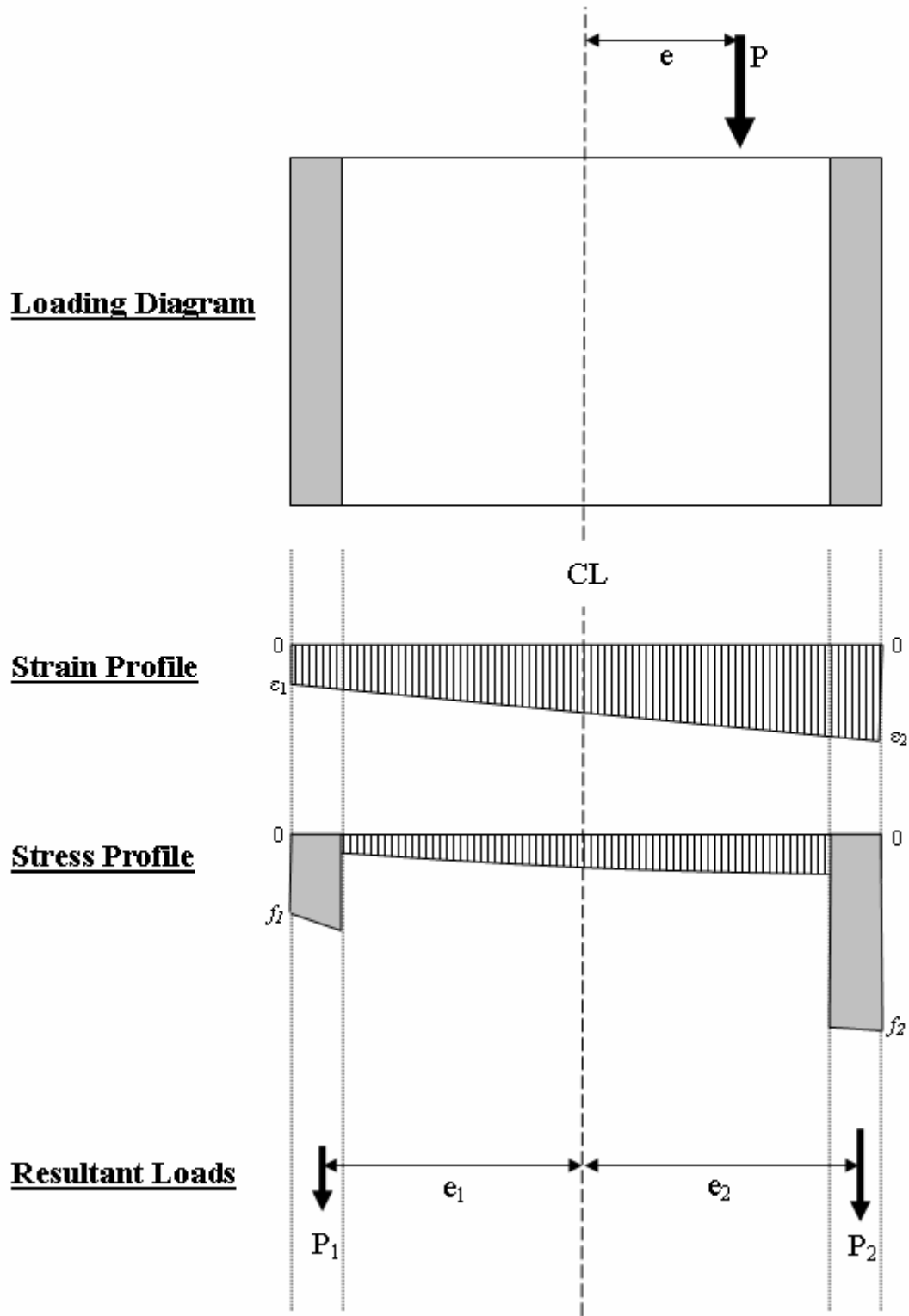


Figure 6.7: Loading Diagrams for Eccentric Model

6.0 Eccentric Compression Experiments of Plastered Straw Bale Assemblies

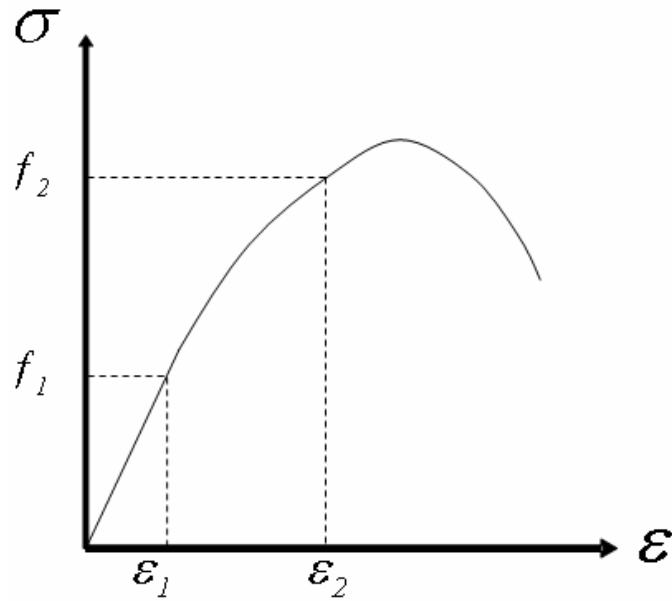


Figure 6.8: Stress-Strain Profile for Eccentric Model

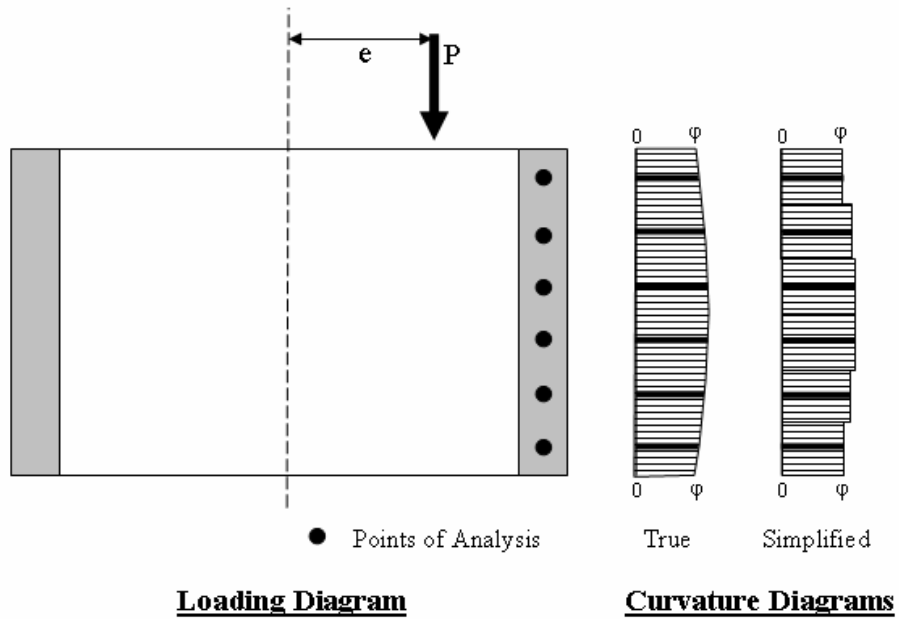


Figure 6.9: Curvature Analysis for Eccentric Model

6.0 Eccentric Compression Experiments of Plastered Straw Bale Assemblies

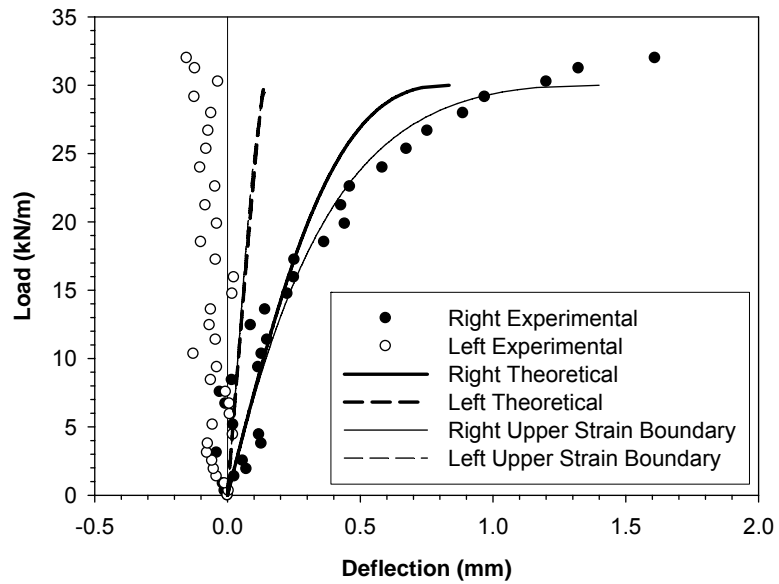


Figure 6.10a: Vertical Load-Deflection Plot for Specimen E11



Figure 6.10b: Failure of Specimen E11

6.0 Eccentric Compression Experiments of Plastered Straw Bale Assemblies

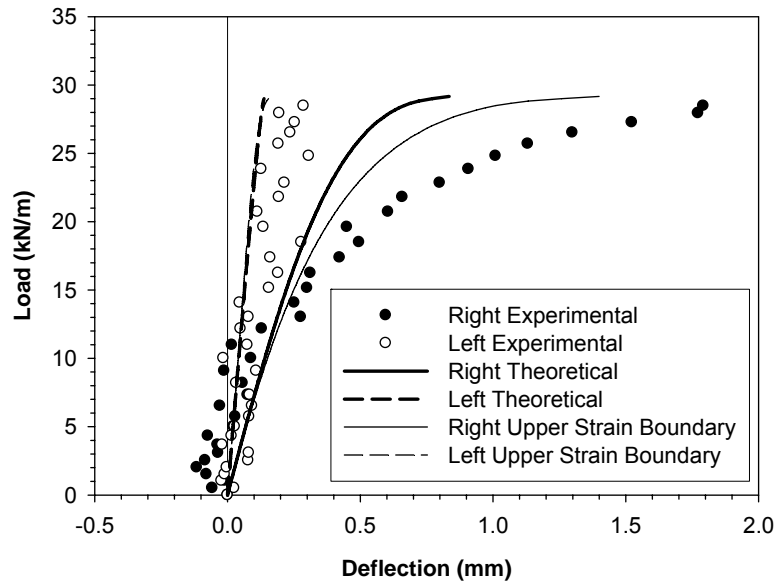


Figure 6.11a: Vertical Load-Deflection Plot for Specimen E12



Figure 6.11b: Failure of Specimen E12

6.0 Eccentric Compression Experiments of Plastered Straw Bale Assemblies

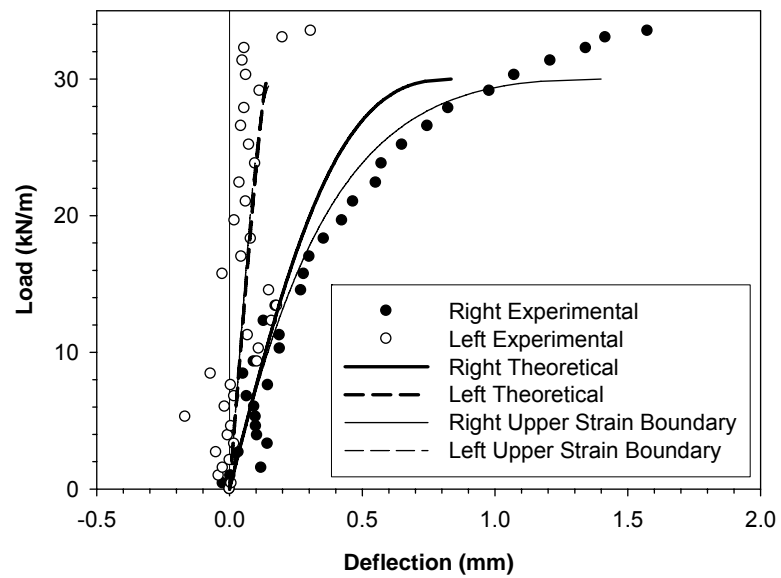


Figure 6.12a: Vertical Load-Deflection Plot for Specimen E13



Figure 6.12b: Failure of Specimen E13

6.0 Eccentric Compression Experiments of Plastered Straw Bale Assemblies

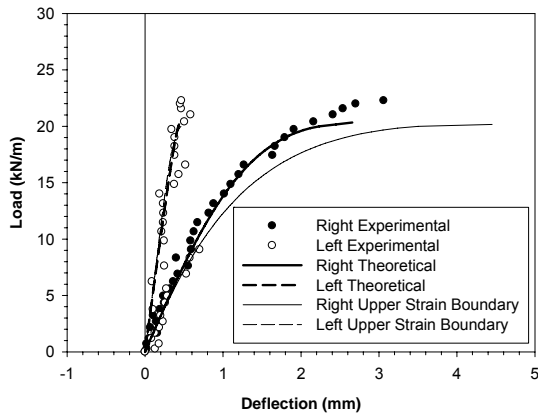


Figure 6.13a: Vertical Load-Deflection Plot for Specimen E31



Figure 6.13b: Failure of Specimen E31

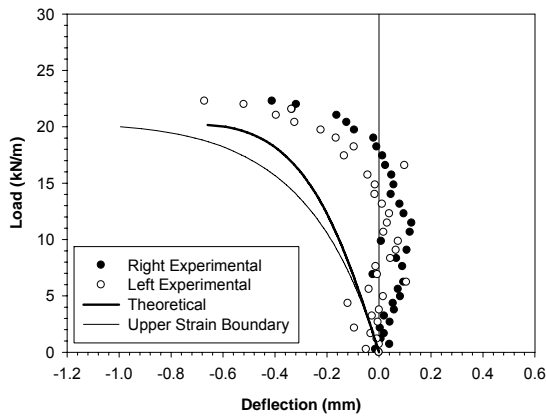


Figure 6.13c: Mid-Height Lateral Load-Deflection Plot for Specimen E31

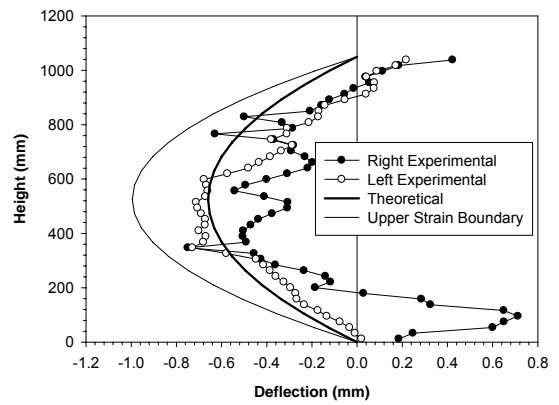


Figure 6.13d: Full-Height Lateral Deflection at Ultimate Load for Specimen E31

6.0 Eccentric Compression Experiments of Plastered Straw Bale Assemblies

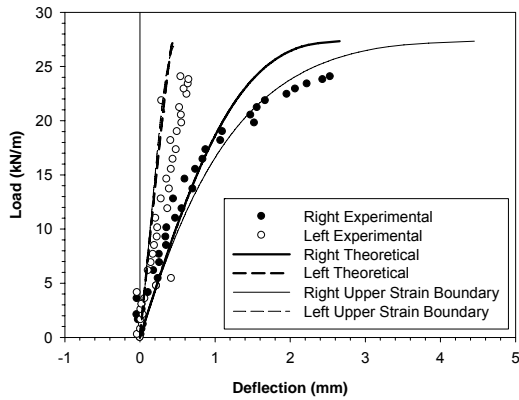


Figure 6.14a: Vertical Load-Deflection Plot for Specimen E32

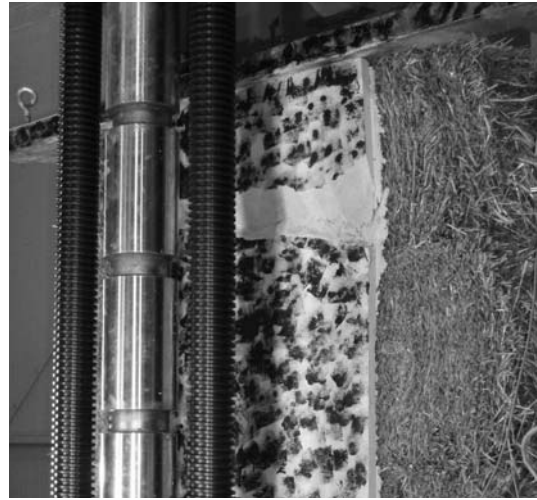


Figure 6.14b: Failure of Specimen E32

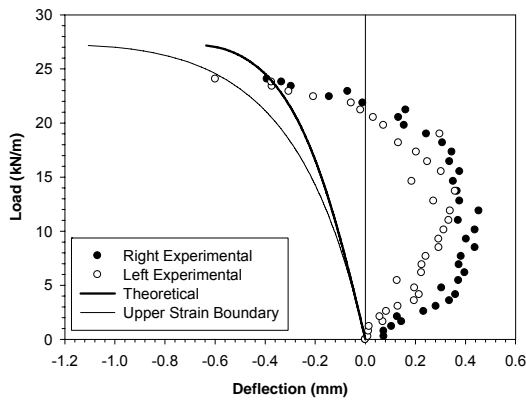


Figure 6.14c: Mid-Height Lateral Load-Deflection Plot for Specimen E32

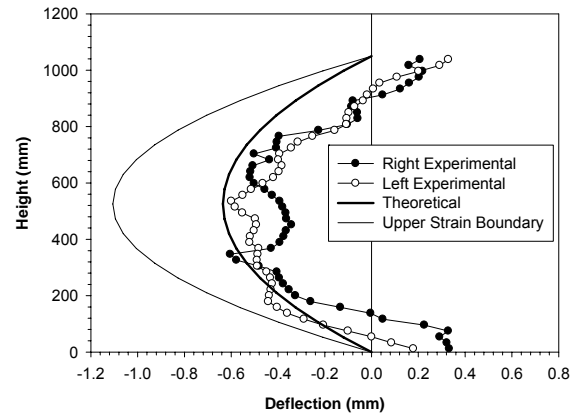


Figure 6.14d: Full-Height Lateral Deflection at Ultimate Load for Specimen E32

6.0 Eccentric Compression Experiments of Plastered Straw Bale Assemblies

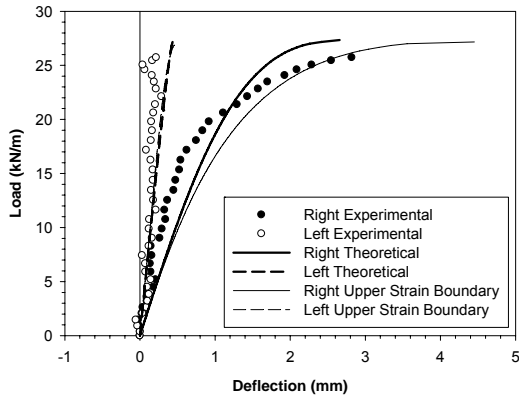


Figure 6.15a: Vertical Load-Deflection Plot for Specimen E33



Figure 6.15b: Failure of Specimen E33

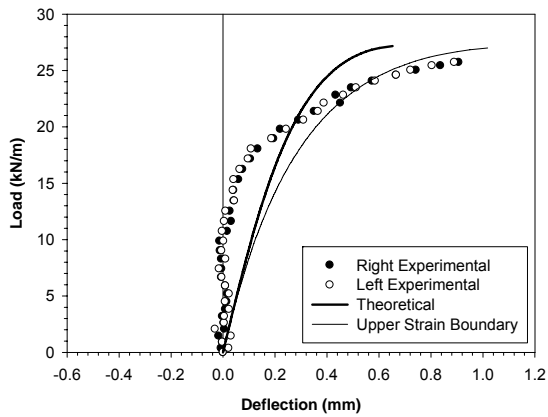


Figure 6.15c: Mid-Height Lateral Load-Deflection Plot for Specimen E33

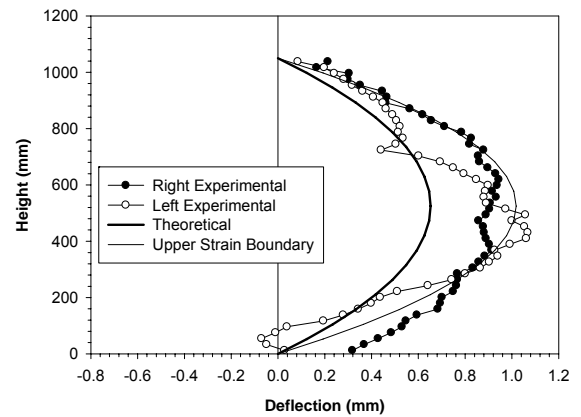


Figure 6.15d: Full-Height Lateral Deflection at Ultimate Load for Specimen E33

6.0 Eccentric Compression Experiments of Plastered Straw Bale Assemblies

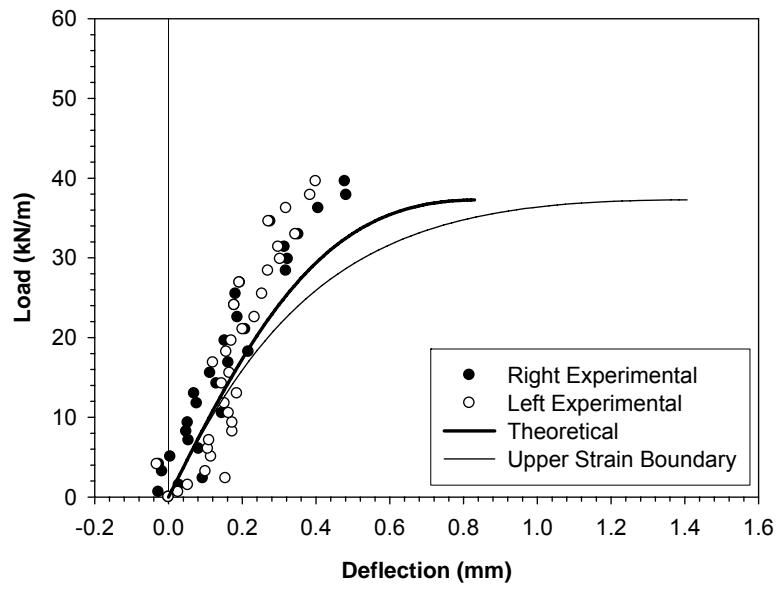


Figure 6.16a: Vertical Load-Deflection Plot for Specimen C11



Figure 6.16b: Failure of Specimen C11

6.0 Eccentric Compression Experiments of Plastered Straw Bale Assemblies

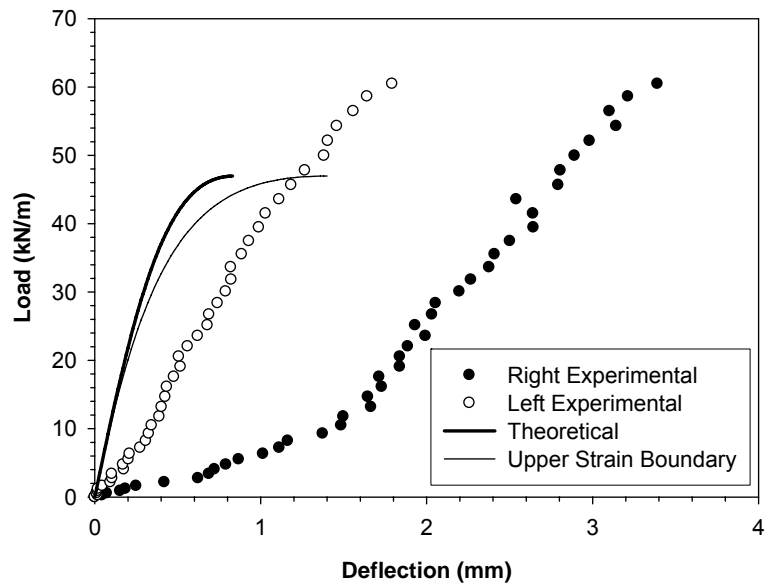


Figure 6.17a: Vertical Load-Deflection Plot for Specimen C12



Figure 6.17b: Failure of Specimen C12

6.0 Eccentric Compression Experiments of Plastered Straw Bale Assemblies

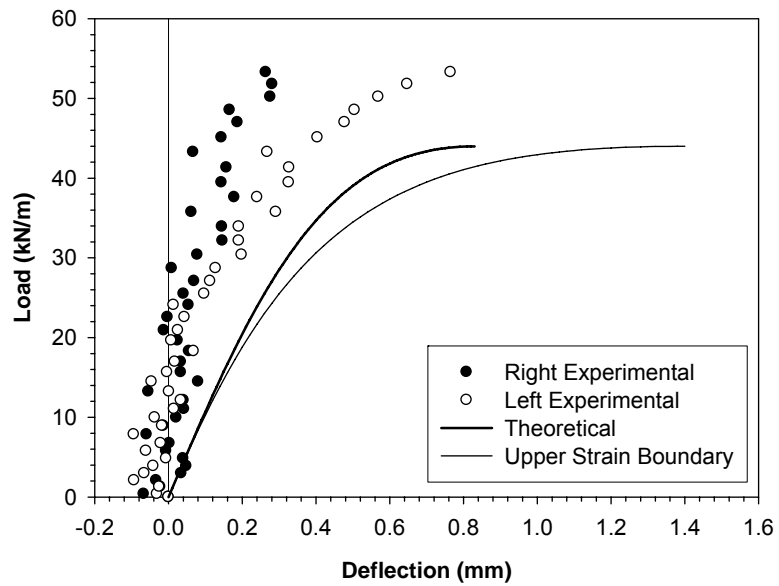


Figure 6.18a: Vertical Load-Deflection Plot for Specimen C13



Figure 6.18b: Failure of Specimen C13

6.0 Eccentric Compression Experiments of Plastered Straw Bale Assemblies

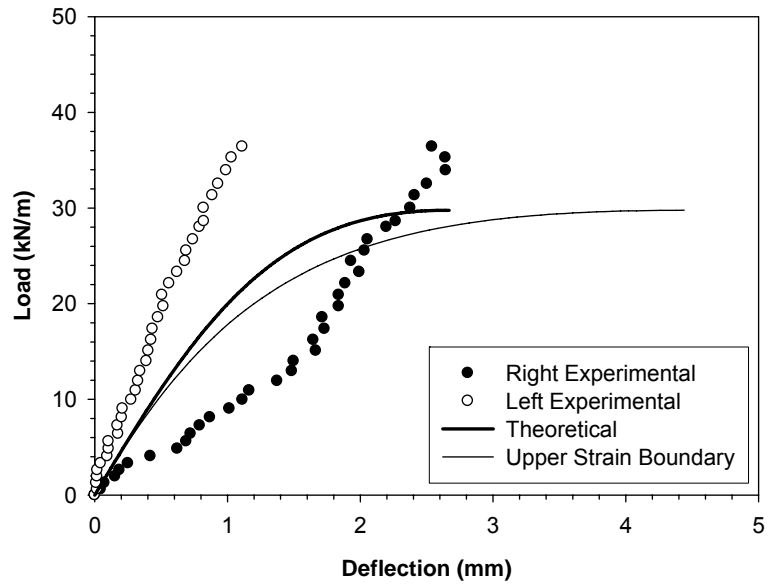


Figure 6.19a: Vertical Load-Deflection Plot for Specimen C31



Figure 6.19b: Failure of Specimen C31

6.0 Eccentric Compression Experiments of Plastered Straw Bale Assemblies

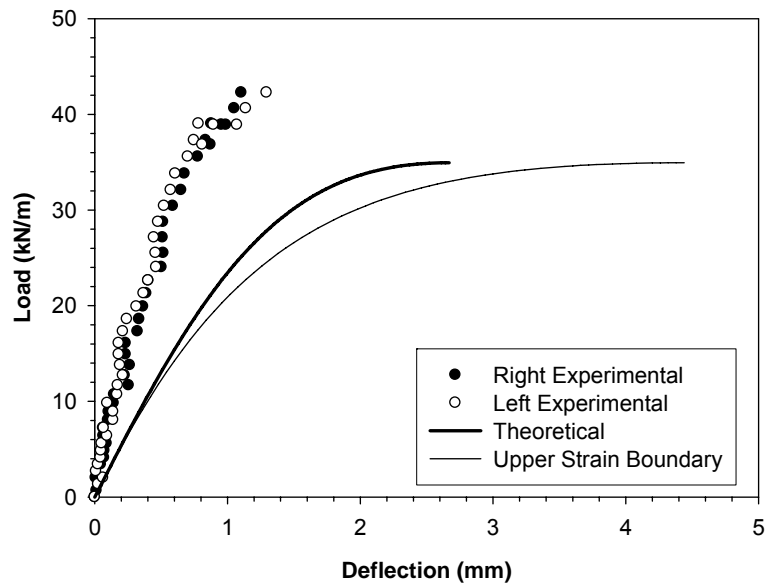


Figure 6.20a: Vertical Load-Deflection Plot for Specimen C32



Figure 6.20b: Failure of Specimen C32

6.0 Eccentric Compression Experiments of Plastered Straw Bale Assemblies

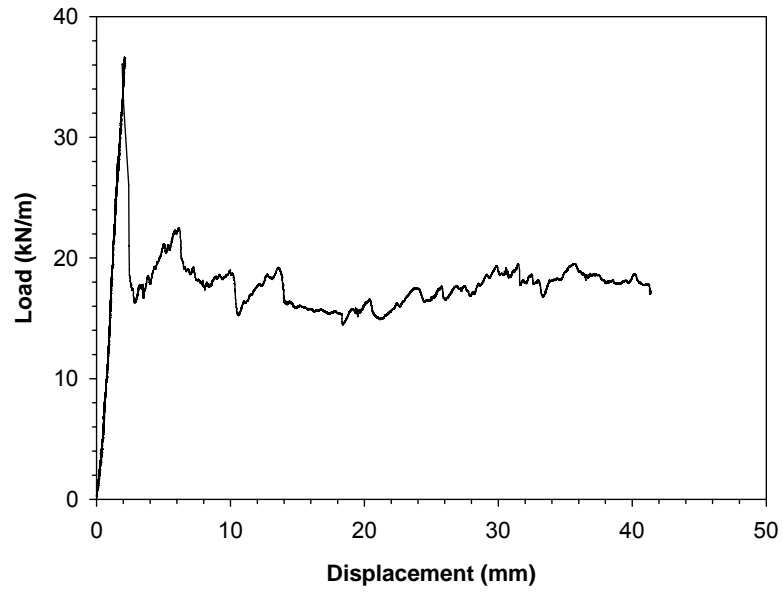


Figure 6.21: Load-Deflection for Entire Duration of Experiment C31

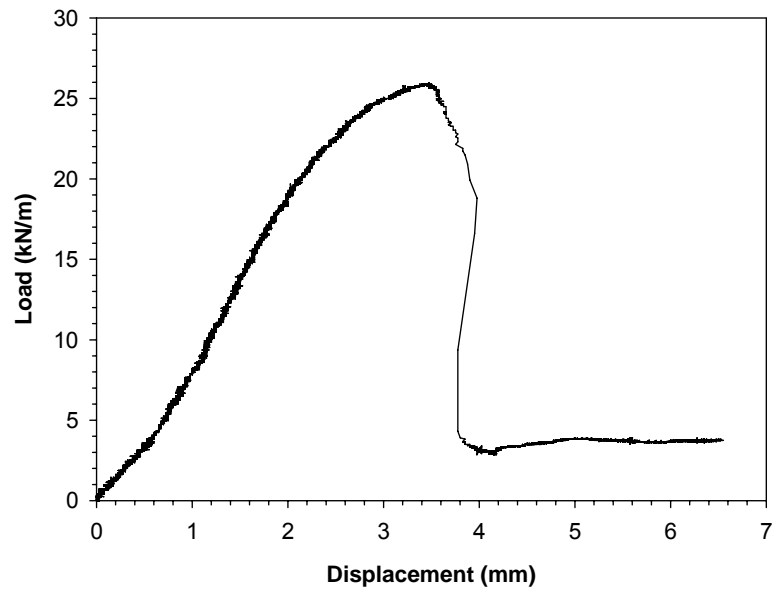


Figure 6.22: Load-Deflection for Entire Duration of Experiment E33

6.0 Eccentric Compression Experiments of Plastered Straw Bale Assemblies



Figure 6.23: Tensile Failure of Second Plaster Skin

Chapter 7: Research Summary and Design Recommendations

7.1 Introduction

An important objective of the testing and analysis of plastered straw bale wall assemblies and plasters reported in this thesis is to provide recommendations on the design and construction of plastered straw bale walls. Furthermore there is a need to synthesize the results of straw bale wall experiments which are presented in the literature and in this thesis in order to provide experimentally supported observations and suggestions regarding the compressive load response of plastered straw bale wall assemblies.

This Chapter is presented in three main sections. The first section provides a comparison of the results presented in this thesis with results provided in the literature for plastered straw bale wall assemblies subjected to compressive load. The second section provides a parametric study of the influence of key design

7.0 Design Recommendations for Straw Bale Construction

parameters on the strength of plastered straw bale wall assemblies. The parametric study is conducted utilizing the analytical model for eccentrically loaded plastered straw bale assemblies. Finally, based on the first two sections, and the results and discussion provided in previous chapters, the third section provides specific recommendations regarding the design and construction of plastered straw bale walls and lime-cement plasters.

7.2 Summary and Analysis of Ultimate Strength Data

7.2.1 Comparison of Ultimate Strength Results

Figure 7.1 provides a summary of all of the results presented in this thesis. Also shown is the range of typical wall strengths for residential construction using conventional 2 x 6 [38mm x 140 mm] timber stud-wall construction (Riley and Palleroni, 2001). Note that where multiple bars are shown for the same experiment, the experiment was conducted more than once. The only experiments with strengths falling below the range for typical stud-wall construction were the on-edge specimens presented in Appendix D. It is important to note that for these specimens the plaster was significantly thinner than designed and that the practice of constructing with bales on-edge is not representative of typical construction practice.

Figure 7.2 presents a summary of the strengths of plastered straw bale walls presented in the literature in relation to the range of typical wall strengths for residential timber construction (Riley and Palleroni, 2001). For all but three experiments the strengths were greater than the lower typical strength for residential timber construction. The three weakest experiments represented experiments

7.0 Design Recommendations for Straw Bale Construction

utilizing weak earthen plaster, and for the two weakest experiments presented by MacDougall et al. (2008) the specimens were fabricated with bales on-edge, which is not representative of typical straw bale construction practice.

Figures 7.1 and 7.2 indicate that the results from this thesis fall within a range of strengths comparable to those seen in the literature. In addition, the strength values obtained in the current study exceed or fall within the range of strengths for typical residential timber construction.

7.2.2 Comparison of Experimental Results with Theoretical Behaviour

This thesis provides analysis of carefully fabricated plastered straw bale wall assemblies. Specimens were fabricated with consistent dimensions, and the compressive properties of the plaster used in fabrication were explicitly quantified. As a result, the specimens tested in the current study (specimens presented in Chapters 5 and 6) achieved overall average ratio of experimental to theoretical strength of 1.06 with standard deviation of 0.13. This indicates the applicability of the presented theoretical models for prediction of the ultimate compressive strength of plastered straw bale wall assemblies. Similarly, models based on the compressive properties of lime-cement plaster were shown to provide an estimation of the pre-ultimate load-deflection behaviour of plastered straw bale wall assemblies.

Conversely, field practice for straw bale construction does not necessarily follow the careful fabrication practices utilized for the specimens presented in this thesis. For example, MacDougall et al. (2008) observed that, for plastered straw bale walls fabricated using standard field construction techniques, the plaster

7.0 Design Recommendations for Straw Bale Construction

thickness, which was designed to be 25 mm, was found to vary between 8 mm and 106 mm. As a result, the authors commented that “the plaster [was] not being used effectively, as cracking and failure will tend to initiate where the thickness is smallest.”

Figure 7.3 presents the ratio of experimental strength to theoretical strength for specimens presented in the literature. Only those experiments for which the authors provided the plaster strength and thickness are presented in this figure. Note that the theoretical strengths are calculated based on Equation 4.1, where the thickness of plaster is typically the nominal thickness, or average thickness, as presented in the literature. For the experiments presented by Grandsaert (1999), the eccentric model presented in Chapter 6 was utilized to determine the theoretical strength, as these experiments were conducted with the load applied at an eccentricity equal to 1/6 of the entire thickness of the specimens. In addition, because MacDougall et al. (2008) presented measurements of the plaster thickness for each specimen, for the experiments presented by these authors the results are presented twice: once utilizing the design plaster thickness of 25 mm for the theoretical calculation, and a second time utilizing the minimum measured plaster thickness for each individual specimen.

By considering tests numbered 1 – 4 in Figure 7.3 it can be seen that when the design plaster thickness is utilized in calculation of the theoretical strength, the experimental results do not achieve strengths as predicted. The average ratio of experimental to theoretical strength for these specimens is 0.251. Additionally, it is important to note that some specimens achieved experimental to theoretical strength

7.0 Design Recommendations for Straw Bale Construction

ratios as low as 0.04. Test number 5 in Figure 7.3 indicates that even when the minimum measured plaster thickness is used in calculation of the theoretical strength, the average ratio of experimental to theoretical strength is still only 0.411, with minimum ratio of 0.08.

Note that comparisons of the experimental to theoretical load-deflection responses of the results from the literature were not possible as a result of a lack of load-deflection data from the literature.

7.2.3 Explanations for Strengths Lower than Theoretical

It is expected that the specimens presented in the literature will achieve strengths less than predicted by the theoretical models because of inconsistencies in the plaster thickness and strength, as well as in the dimensions and alignment of the straw bales. There are however a number of additional factors which may contribute to the lower than predicted strengths.

Firstly, the loading techniques may differ from one author to another resulting in specimens which do not behave as theoretically predicted. For example, while the theoretical models assume compressive load applied primarily to the plaster via rigid top plates and base plates, the design of some top plates and base plates which are only as wide as the straw, and which do not extend to the outer surface of the plaster, will result in the load being applied primarily to the straw. This technique will induce shear stress at the straw/plaster interface as the load is transferred from the straw to the plaster. This technique was noted for the specimen presented by

7.0 Design Recommendations for Straw Bale Construction

Walker (2005) and may be a contributing factor to this specimen achieving lower than theoretical strength.

A second factor which may contribute to the lower than theoretically predicted strengths presented in the literature is the potential for buckling as a governing failure mode. It was shown in Appendix E that buckling was not expected to govern the failures of the specimens presented in this Thesis. However, it is possible that the specimens presented in the literature may be governed by buckling failure. Grandsaert (1999) and MacDougall et al. (2008) noted that local buckling may govern for specimens with stronger and stiffer plaster. For these specimens, it is expected that as the load increases to the point where local buckling governs, the straw will no longer have the capacity to laterally support the plaster skins, and the plaster will buckle away from the straw.

If buckling becomes a contributing factor for plastered straw bale assemblies it is expected that specimens fabricated with stronger and stiffer plaster will achieve lower ratios of experimental to theoretical strength. Figure 7.4 presents the influence of plaster strength on the experimental to theoretical strength ratio of plastered straw bale wall assemblies presented in the literature. Note that the design thickness of 25 mm is utilized for the MacDougall et al. (2008) specimens in order to remain consistent for comparison with results presented by other authors. It can be seen that the ratio of experimental to theoretical strength decreases with increasing plaster strength. For plaster strengths less than 10 MPa, the average ratio is 0.310, while for plaster strengths greater than 10 MPa, the average ratio is 0.063. This

7.0 Design Recommendations for Straw Bale Construction

suggests that buckling may be occurring for specimens fabricated with stronger plaster.

While there are a number of noted factors which contribute to the lower than theoretical strengths reported in the literature for plastered straw bale assemblies subjected to compressive load, a number of key design and construction recommendations may be utilized to limit the influence of these factors.

7.3 Parametric Study

A parametric study using the eccentric compression analytical model can yield important information on the influence of a number of key parameters on the strength of plastered straw bale wall assemblies. The parameters studied were: eccentricity; wall height; plaster thickness; and plaster strength. The results of the parametric study provide guidance regarding the impact of changes in wall design on the strength of plastered straw bale walls. Furthermore, the parametric study yields insight into the significance of the noted variability in plaster strength and thickness for experimental specimens. It is important to note the possibility of alternate failure mechanisms and other factors which may exist for wall designs which differ from those with which the model was verified in this thesis.

The parametric study assumed a plastered straw bale wall assembly which is 2.4 m in height and 1.0 m in length, which has plaster strength of 1.0 MPa and thickness of 25 mm, which has straw width of 405 mm, and which has a the load applied at an eccentricity of 120 mm. The parameters were varied within the model

7.0 Design Recommendations for Straw Bale Construction

and the impact on the ultimate strength of the plastered straw bale assemblies was noted.

Figure 7.5 presents the influence of increasing eccentricity on the relative strength of plastered straw bale wall assemblies. An increase in the eccentricity from 0 mm to 120 mm resulted in a 37% loss in strength. Furthermore, at a maximum eccentricity of 180 mm the strength was reduced by 46%. Beyond this eccentricity, the specimen was expected to undergo tension failure if it is assumed that the plaster has zero tensile strength. Figure 7.5 also indicates that for the eccentricities studied, regardless of the eccentricity, the theoretical strengths were all greater than the typical construction limits.

Figure 7.6 presents the influence of changes in specimen height on the relative strength of plastered straw bale wall assemblies. An increase in height from 2.4 m to 4.8 m (representing an increase in height from one storey to two storeys for typical residential construction) resulted in only a 2.4% loss in strength. For all heights analyzed, the theoretical specimen strength remained well above the typical construction limits.

Figure 7.7 presents the influence of changes in plaster thickness on the relative strength of plastered straw bale wall assemblies. The results indicate a linear relationship between plaster thickness and wall strength. Figure 7.7 also indicates that for the specific specimen studied, if the plaster thickness is reduced below approximately 10 mm, the specimen strength will fall below the lower typical residential limit.

7.0 Design Recommendations for Straw Bale Construction

Finally, Figure 7.8 presents the influence of changes in plaster strength on the relative strength of plastered straw bale wall assemblies. The results indicate a linear relationship between plaster strength and the strength of a plastered straw bale wall assembly. It can also be seen from Figure 7.8 that for the specific specimen studied, if the plaster strength is reduced below approximately 0.4 MPa, the specimen strength will fall below the lower typical residential limit.

7.4 Design Recommendations

7.4.1 Introduction

The current study has yielded data and analysis regarding the compressive behaviour of plastered straw bale walls, and the plasters used for their construction. Figures 7.1 and 7.2 indicate the potential for the use of plastered straw bale walls in residential construction. The results presented in this study support the experimental and the anecdotal evidence presented in the literature, which indicate that the strength of plastered straw bale walls is sufficient for residential construction. As noted previously, the only specimens for which the strengths fell below the lower limits expected for typical residential construction were fabricated with non-typical construction techniques. All specimens representative of the most common construction practices exhibited strengths greater than the lower limit expected for typical residential construction. A number of recommendations for the design and construction of plastered straw bale walls and lime-cement plaster follow from this study.

7.0 Design Recommendations for Straw Bale Construction

7.4.2 Design and Construction Recommendations for Plastered Straw Bale Walls

The following are a number of key design recommendations for the use of plastered straw bale walls in residential construction:

- The theoretical strength of plastered straw bale walls can be determined by considering the strength of the plaster applied to the wall. For concentrically loaded plastered straw bale walls the strength can be calculated using Equation 4.1. For this equation the contribution from the straw may be conservatively ignored. For eccentrically loaded plastered straw bale walls, Equations 3.10 and 5.1 provide an envelope for the stress-strain response of lime-cement plaster, which may be utilized to determine the ultimate strength of eccentrically loaded plastered straw bale walls.

$$F_{Ult} = 2f'_{cube} Lt_p + E_{Straw} \epsilon_{straw} A_{Straw} \quad 4.1$$

$$f_c = f'_c \left(\frac{764.8\epsilon}{0.935 + \left(\frac{\epsilon}{0.00253} \right)^{1.935}} \right) \quad 3.10$$

$$f_c = f'_c \left(\frac{331.4\epsilon}{0.405 + \left(\frac{\epsilon}{0.00424} \right)^{1.405}} \right) \quad 5.1$$

7.0 Design Recommendations for Straw Bale Construction

- Figures 3.10 and 5.1 may be utilized to determine the load-deflection response of concentrically and eccentrically loaded plastered straw bale walls. Furthermore, the Modulus of Elasticity of lime-cement plaster may be used to determine the deflection of a concentrically loaded plastered straw bale wall under service loading. The Modulus of elasticity may be taken as 818 times the plaster strength for low-strength lime-cement plaster.
- Plastered straw bale walls fabricated utilizing typical construction techniques and with plaster less than 10 MPa achieved average ratio of experimental to theoretical strengths of 0.310, while for plaster strengths greater than 10 MPa, the average ratio was 0.063. Thus the following recommendations are made:
 - Plastered straw bale walls should be designed with plaster strength not greater than 10 MPa, as increasing plaster strength beyond 10 MPa yields diminishing returns on the strength of a plastered straw bale wall assembly.
 - Assuming plaster strengths less than 10 MPa, a reduction factor of no greater than 0.30 should be utilized for the theoretical wall strength obtained using the analytical models presented in this thesis.
- Plastered straw bale walls fabricated with bales on edge were found (in the literature and in this thesis) to have strengths less than equivalent

7.0 Design Recommendations for Straw Bale Construction

walls fabricated with bales laid flat. As such it is recommended that for optimum performance, plastered straw bale walls should be designed with the bales laid flat. Plastered straw bale walls constructed with the bales on edge may still have sufficient capacity for residential construction; however additional testing and analysis may be required to quantify the strength of these walls.

- Design considerations for plastered straw bale walls should focus on the ultimate strength of the walls. However, a number of other design considerations should be made:
 - Because plastered straw bale walls have relatively low stiffness relative to known materials such as concrete and steel, deflection considerations may influence the design of plastered straw bale walls, especially around openings in the walls.
 - The post-failure response of plastered straw bale walls is important for considering the service loading of the walls. However, this is outside the scope of this thesis.
- The durability of plastered straw bale walls is also a key concern. While this is outside of the scope of this thesis, it can be noted that it is important for designers to ensure the integrity of the bond between the plaster and the straw as it is this bond which prevents buckling of the plaster skins.

7.0 Design Recommendations for Straw Bale Construction

The following are a number of key construction recommendations for the use of plastered straw bale walls in residential construction:

- It can be seen in Figure 7.4 that typical construction practices will not yield plastered straw bale walls which achieve strengths as predicted by the models. This is because additional factors such as wall out-of-straightness and imperfect plastering techniques may lead to less than predicted strength. As a result, the following construction recommendations are suggested:
 - Builders should utilize methods to fabricate walls which are plumb. Such methods include trimming the straw bales and filling in the spaces between the bales.
 - Because the plaster contributes significantly to the behaviour of plastered straw bale walls it is important that walls are fabricated with plaster skins of consistent thickness and strength.
 - Care should be taken to ensure that an adequate bond between the straw and the plaster is achieved in order to mitigate the potential for local buckling of the plaster skins.
 - Care should be taken in plastering the top and bottom portions of the plaster skins in order to mitigate bearing failure in these regions, as was noted in Chapter 4.

7.0 Design Recommendations for Straw Bale Construction

7.4.3 Lime-Cement Plaster Design Considerations

There is currently a lack of standards for plasters used for straw bale construction. As a result, there are a great number of mix designs utilized by straw bale builders. The various equations and relationships presented in Chapter 3 can be utilized to aid designers in estimating the strength of various low-strength lime-cement plasters, and in understanding the influence of the various mix components on the behaviour of the plaster.

Furthermore, the expected variability in the plaster strength was discussed. While it was noted that inherent variability in plaster properties makes it impossible to determine the exact strength of a plaster applied to a plastered straw bale wall, the appropriate use and understanding of the estimation methods presented in Chapter 3 will present the greatest opportunity for ensuring appropriate plaster design. When estimating the compressive strength of a plaster applied to a straw bale wall the following steps should be taken to ensure the greatest degree of accuracy:

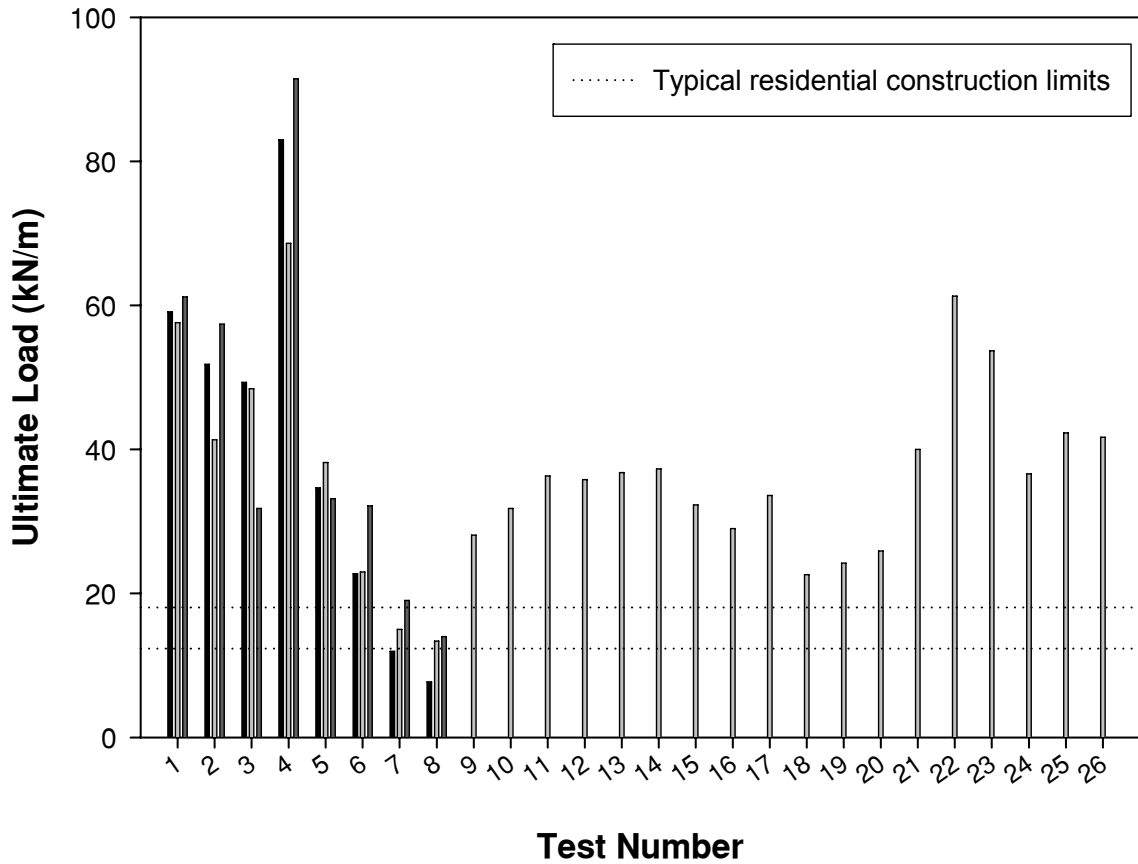
1. The proportions of dry materials should first be determined. Equation 3.2 may aid in determining dry proportions for desired plaster strength.
2. The quantity of water required to create a plaster of desired workability should then be determined through trial and error. The slump of the finalized mix should be recorded
3. Cube compression experiments should then be performed prior to construction to confirm that the proportions produce plaster of adequate

7.0 Design Recommendations for Straw Bale Construction

strength. If increased strength is needed the quantity of cement can be increased or the quantity of sand or water can be decreased.

4. When the plaster is used for construction, great care should be taken in ensuring accurate proportioning of the dry mix materials. In addition, a slump test should be performed on each batch to ensure the appropriate quantity of water is used in the mix.
5. Cube samples may be taken from the batches during construction in order for them to be tested at a later date to provide additional confirmation of the in-situ plaster strength.
6. All compressive testing experiments should be conducted using cubes tested after 28 days curing. If cubes are tested prior to the 28 day curing time, Equation 3.11 may provide an estimation of the ratio of tested strength to 28 day strength.

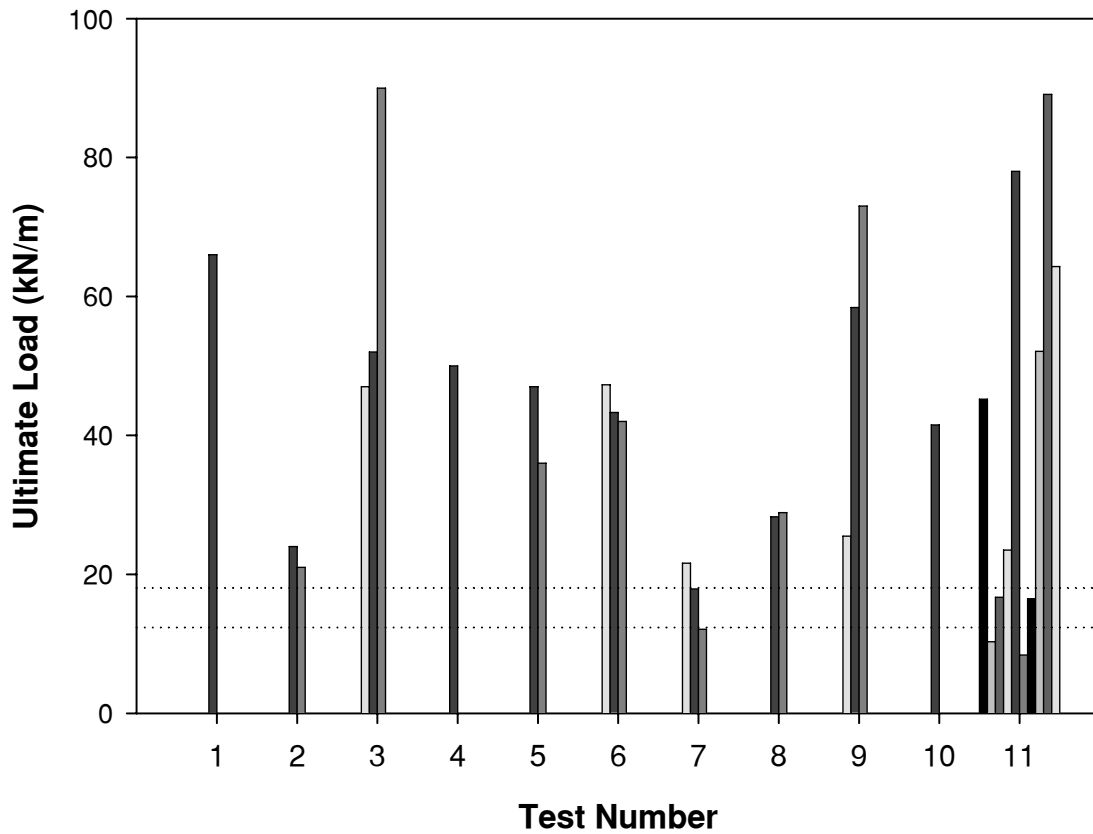
7.0 Design Recommendations for Straw Bale Construction



- | | |
|----------------------|-----------------------------------|
| 1 – Ch. 4 # 1,2,3 | 8 – On-Edge 0.80 MPa |
| 2 – Ch. 4 # 7,8,9 | 9,10,11 – Ch. 5 0.99m |
| 3 – Ch. 4 # 13,14,15 | 12,13,14 – Ch. 5 2.31m |
| 4 – Ch. 4 # 28,29,30 | 15,16,17 – Ch. 6 0.33m Eccentric |
| 5 – Ch. 4 # 25,26,27 | 18,19,20 – Ch. 6 1.05m Eccentric |
| 6 – On-Edge 1.43 MPa | 21,22,23 – Ch. 6 0.33m Concentric |
| 7 – On-Edge 1.12 MPa | 24,25,26 – Ch. 6 1.05m Concentric |

**Figure 7.1: Summary of Experimental Ultimate Strengths
(Multiple Bars Indicate Test Repetition)**

7.0 Design Considerations for Straw Bale Construction



1 - Fibrehouse Ltd and Scanada
Consultants Ltd., 1996

2 - Carrick and Glassford, 1998

3 - Grandsaert, 1999 (average of 3)

4 - Zhang, 2002 (approx values)

5 - Faine and Zhang, 2002

6 - Field et al., 2005

7 - Mar, 2003 (average of 3)

8 - Dreger, 2002 (premature failure noted)

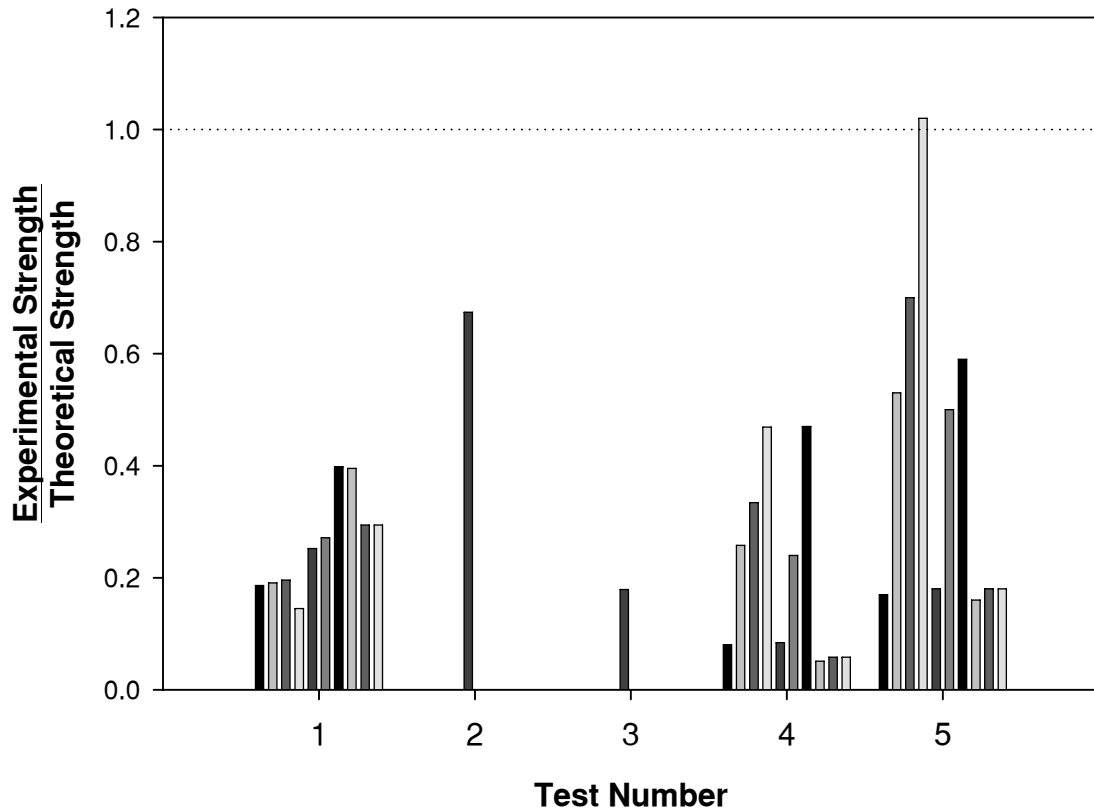
9 - Wheeler et al., 2004 (approx values)

10 - Walker, 2005

11 - MacDougall et al., 2008

**Figure 7.2: Summary of Experimental Results from the Literature
(Multiple Bars Indicate Test Repetition)**

7.0 Design Considerations for Straw Bale Construction



1 – Grandsaert, 1999

2 – Faine and Zhang, 2002

3 – Walker, 2005

4 – MacDougall et al., 2008 (design plaster strength)

5 – MacDougall et al., 2008 (minimum plaster strength)

Figure 7.3: Summary of Experimental to Theoretical Strength Ratios for Results from the Literature (Multiple Bars Indicate Test Repetition)

7.0 Design Considerations for Straw Bale Construction

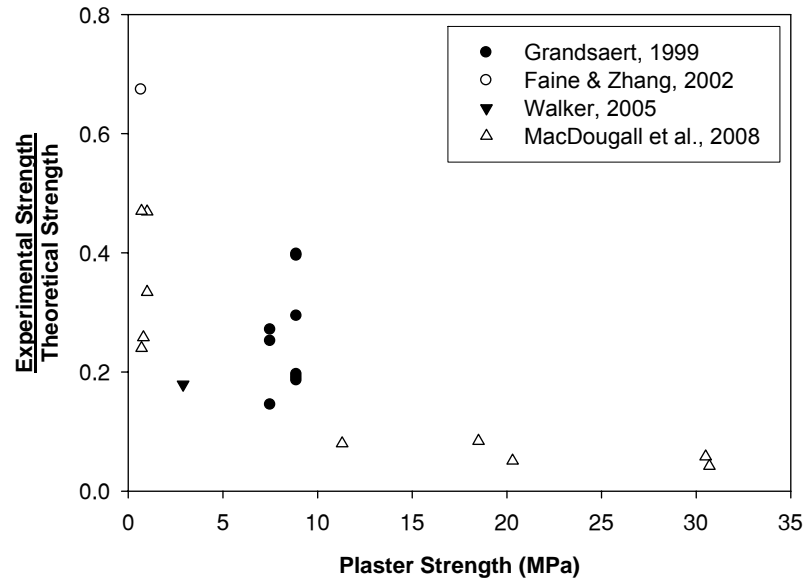


Figure 7.4: Relationship Between Plaster Strength and Experimental to Theoretical Strength Ratio

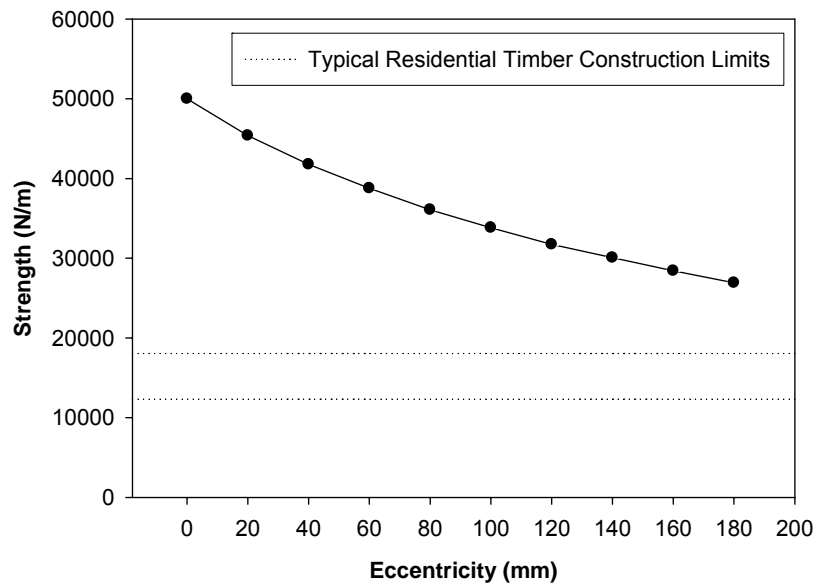


Figure 7.5: Effect of Eccentricity on Plastered Straw Bale Assembly Strength

7.0 Design Considerations for Straw Bale Construction

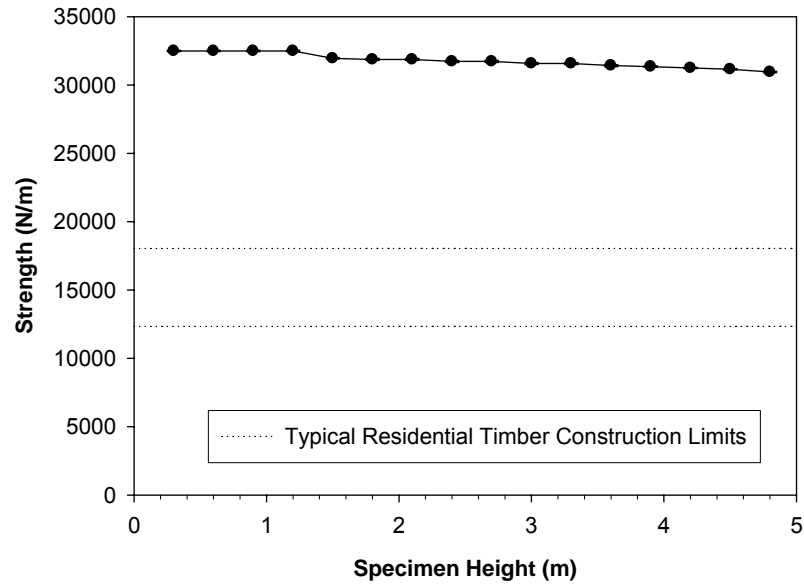


Figure 7.6: Effect of Specimen Height on Plastered Straw Bale Assembly Strength

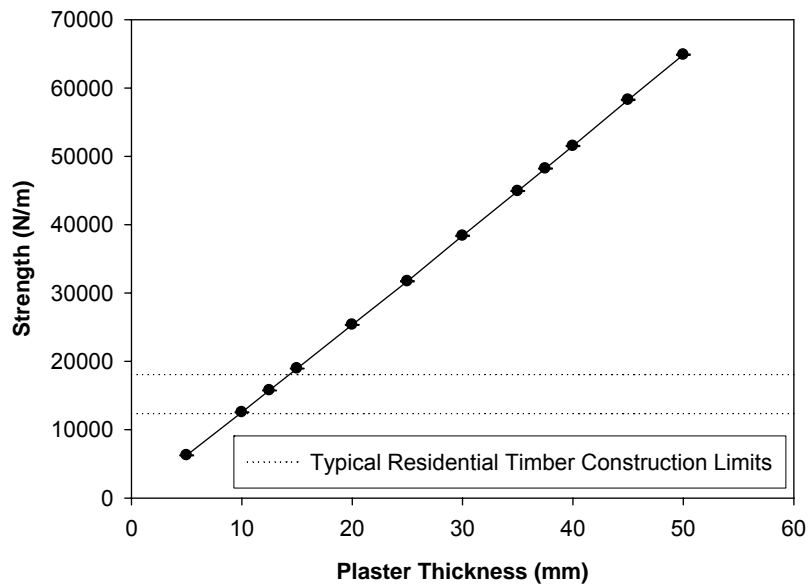


Figure 7.7: Effect of Plaster Thickness on Plastered Straw Bale Assembly Strength

7.0 Design Considerations for Straw Bale Construction

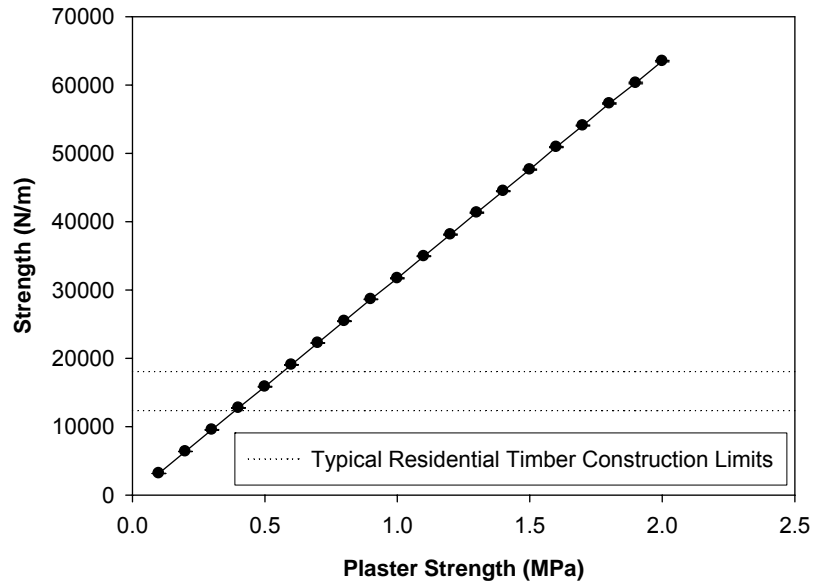


Figure 7.8: Effect of Plaster Strength on Plastered Straw Bale Assembly Strength

Chapter 8: Conclusions

8.1 Summary

The main objective of this research program was to provide a greater understanding of the compressive behaviour of plastered straw bale walls. Experiments of plastered straw bale wall assemblies subjected to concentric and eccentric compression provided support for the use of plastered straw bale walls as a viable method of residential construction. Material testing provided a detailed understanding of the stress-strain response of lime-cement plaster and the parameters which can influence that response. The stress-strain response of lime-cement plaster provided a basis for analytical models developed to predict the structural performance of plastered straw bale walls subjected to concentric and eccentric compressive loads. Finally, the experimental and theoretical results provided specific design and construction recommendations for straw bale builders, designers and engineers.

8.2 Key Findings

8.2.1 Major Conclusions

The main conclusions are:

- Plastered straw bale walls which are fabricated using typical best-practice construction techniques have compressive strength greater than 20 kN/m. This exceeds the strength typically required for single-storey residential construction.
- Analytical models proposed in this thesis provide an accurate representation of the load-deflection response and ultimate strength of plastered straw bale walls in compression. The average ratio of experimental to theoretical strength for specimens fabricated using the innovative steel jigs was 1.06. The models assume failure of plastered straw bale walls from crushing of the plaster and are based on the stress-strain response, the relationship between strength and Modulus of Elasticity, and the assumed strain at ultimate failure of lime-cement plaster.

8.2.2 Conclusions from Experiments on Lime-Cement Plaster and Un-Plastered Straw Bales

Based on results of compression experiments conducted on lime-cement plaster and un-plastered straw bales in Chapter 3, the following conclusions can be drawn.

8.0 Conclusions

- The modified Collins and Mitchell (1997) stress-strain model presented in Equation 3.10 is an appropriate fit for the stress-strain response of low-strength lime-cement plaster:

$$f_c = f'_c \left(\frac{764.8\varepsilon}{0.935 + \left(\frac{\varepsilon}{0.00253} \right)^{1.935}} \right) \quad 3.10$$

- The Modulus of Elasticity of low-strength lime-cement the plaster is 818 times the strength of the plaster.
- Equation 3.12 provides an estimate of the compressive strength of lime-cement plaster based on the proportions of lime, cement and sand in the plaster mix, while Figure 3.13 presents the influence of the w/cm ratio on the strength of the plaster:

$$f'_{cube28} = -1.119 + 35.075 \left(\frac{V_{cm}}{V_s} \right) \left(\frac{V_c}{V_l} \right) \quad 3.12$$

- The average bale modulus for flat un-plastered straw bales is 0.364 MPa at low stress.

8.2.3 Conclusions from Experiments on Concentrically Compressed Plastered Straw Bale Assemblies

Based on results of concentric compression experiments conducted on plastered straw bale wall assemblies in Chapter 5, the following conclusions can be drawn.

8.0 Conclusions

- Well-fabricated plastered bale assemblies with design plaster thickness of 25 mm and strength of 0.783 MPa have average experimental ultimate strength of 34.4 MPa.
- At the 95% confidence level there is not a statistically significant difference between the strength of 0.99 m assemblies and 2.31 m assemblies, supporting the assumption that the plastered straw bale assemblies fail as a result of compression failure of the plaster.
- The average experimental to theoretical strength ratio of 0.994 for concentrically loaded specimens indicates the applicability of the ultimate strength model based on the crushing strength of lime-cement plaster.
- A model based on the stress-strain response of lime-cement plaster provides an estimate (within 10%) of the load-deflection response of plastered straw bale assemblies so long as the plaster strength variability and the potential for larger strains at failure are considered.

In addition, in Chapter 6 it was shown that pin-ended concentrically loaded plastered straw bale assemblies with design plaster thickness of 25 mm and design plaster strength of 0.783 MPa have average experimental ultimate strength of 45.9 MPa. The higher strength for these specimens was attributed to alternative failure mechanisms as a result of the pinned end conditions.

8.2.4 Conclusions from Experiments on Eccentrically Compressed Plastered Straw Bale Assemblies

Based on results of eccentric compression experiments conducted on plastered straw bale wall assemblies in Chapter 6, the following conclusions can be drawn.

- Well-fabricated plastered bale assemblies, loaded with 120 mm eccentricity, with design plaster thickness of 25 mm and strength of 0.783 MPa have average experimental ultimate strength of 27.92 MPa.
- For plastered straw bale wall assemblies which are constructed 330 mm to 1050 mm high, with pinned ends, bales stacked flat, and 25 mm thick low-strength plaster skins, the results and observations support the assumption that the assemblies fail as a result of compression failure of the plaster.
- The average experimental to theoretical strength ratio of 1.07 for eccentrically loaded specimens indicates the applicability of an ultimate strength model based on the modified Collins and Mitchell (1997) stress-strain model for lime-cement plaster.
- An analytical model based on the modified Collins and Mitchell (1997) model for the stress-strain behaviour of lime-cement plaster provides not only an excellent estimate of the ultimate strength of eccentrically loaded plastered straw bale assemblies, but also provides an estimate of the pre-failure lateral and vertical load-deflection behaviour of these specimens.

8.3 Design Recommendations for Straw Bale Construction

Based on discussions presented in Chapters 4 and 7, the following key design recommendations for straw bale construction can be made.

- For concentrically loaded plastered straw bale walls the strength can be calculated using Equation 4.1.
- For eccentrically loaded plastered straw bale walls, Equations 3.10 and 5.1 provide an envelope for the stress-strain response of lime-cement plaster, which may be utilized to determine the ultimate strength of eccentrically loaded plastered straw bale walls.
- Equations 3.10 and 5.1 may be utilized to determine the pre-ultimate load-deflection response of plastered straw bale walls.
- Plaster shall be designed to have strength no greater than 10 MPa as increasing strength beyond 10 MPa yields diminishing returns on the strength of plastered straw bale assemblies.
- When the models presented in this thesis are utilized in the design of plastered straw bale walls, a reduction factor of no greater than 0.3 is suggested for plaster strength less than 10 MPa.
- To avoid bearing failure of the plaster skins of plastered straw bale walls it is important that care be taken to ensure that at the top and bottom of the plaster skins, the plaster is effectively worked into the straw, that the

8.0 Conclusions

plaster is applied to the appropriate thickness, and that there are no gaps between the finished plaster skins and the box beam or base plate.

- To maximize the strength of a plastered straw bale wall, builders should utilize methods to fabricate walls which are plumb, and which have plaster skins of consistent thickness.
- The potential for local buckling indicates that care should be taken to ensure that plaster is bonded well to the straw when plastered straw bale walls are fabricated.
- When designing lime-cement plaster, Equation 3.2 may aid in determining dry proportions for desired plaster strength, however cube tests should be performed in advance of construction to verify the plaster strength.
- Slump tests should be conducted when plastering in the field to ensure that the appropriate quantity of water is being included in the plaster mix. This will ensure that the plaster is as close to the design strength as possible.

8.4 Recommendations for Future Research

While the presented research program represents an important advance in understanding the structural behaviour of plastered straw bale walls, further studies are required to continue to verify the theoretical behaviour of plastered straw bale walls and to broaden the current knowledge of the parameters that influence the

8.0 Conclusions

strength and deflection characteristics of these assemblies. The following are recommendations for further research

- Additional compressive experiments on lime-cement plaster appear warranted as there are still many deficiencies in the knowledge regarding the design and quality control of lime-cement plaster.
- The post-failure load carrying capacity of plastered straw bale walls may provide design guidance for the appropriate service load of plastered straw bale walls. It was noted that eccentrically loaded plastered straw bale walls with pinned ends exhibited very little load-carrying capacity following ultimate failure. However, the pinned end conditions of these specimens may not be representative of conditions within a structure and as such, the analysis of the post-failure load-carrying capacity of concentrically and eccentrically loaded specimens with end-conditions representative of common construction practice requires further study.
- Analysis of the effect of changing wall designs on the compressive response of plastered straw bale walls is warranted in order to determine the applicability of the proposed models for plastered straw bale assemblies incorporating reinforcing mesh, and different box beam and base plate designs.
- Experimental data utilizing similar testing and fabrication techniques as outlined in this research program, but with plaster greater than 10 MPa is

8.0 Conclusions

required in order to verify the existence of alternative failure modes, such as local buckling.

- Further analysis of the bond between the plaster and the straw, and the variations in the bond strength with varying construction techniques is warranted in order to study the potential for local buckling of the plaster skins.
- Testing and analysis of specimens fabricated on-edge is warranted in order to determine the applicability of the proposed models for plastered straw bale walls constructed with the bales on edge. New fabrication and testing techniques will be required to mitigate the issues associated with the rebound of the straw for the on-edge specimens described herein.
- The creep response of plastered straw bale walls subjected to sustained loading is an important property which requires further study.
- Further analysis of the design of foundations for plastered straw bale walls and the response of plastered straw bale walls to ground movements is important for understanding the impact of the various foundation designs used in straw bale construction practice.
- The behaviour of straw bale walls plastered with earthen plaster should be studied as there is a desire among builders to utilize more environmentally friendly earth plasters for straw bale construction. The material properties of earthen plasters will first need to be studied in order to understand the influence of the properties of earthen plasters on the

8.0 Conclusions

behaviour of plastered straw bale walls. A similar research program as that presented herein may be utilized to analyze the compressive behaviour of earthen plastered straw bale walls.

- Predictive models of the behaviour of plastered straw bale walls under non-compressive loading conditions would be useful for the understanding of the structural behaviour of these assemblies. Specifically, experimental and theoretical analysis of plastered straw bale walls subjected to lateral in-plane and out-of-plane loading is recommended.
- While the analytical model for concentrically loaded plastered straw bale walls may be appropriate for use by designers, the complexity of the eccentric model may limit its practical use. The determination and validation of a simpler closed-form solution for eccentrically loaded plastered straw bale walls is recommended.
- It has been noted that well-constructed laboratory specimens are not representative of conventionally constructed plastered straw bale walls. This has led to the need for reduction factors when using theoretical models for the strength of plastered straw bale walls. As such, there is a need to develop construction techniques to fully utilize the strength of straw bale walls. Development of methods of pre-fabricating plastered straw bale walls under controlled conditions may yield walls with strengths closer to the theory. Testing which focuses on in-the-field construction techniques and practices, and which may yield specific best-practice

8.0 Conclusions

recommendations is warranted, as are experiments aimed at developing methods of pre-fabricating plastered straw bale walls.

- Plastered straw bale wall assemblies with pinned ends subjected to compressive loads have been observed to achieve higher than expected strengths. As such, further testing and analysis of plastered straw bale assemblies with various plaster strengths and thickness utilizing pinned and non-pinned concentric compressive test configurations is recommended to further understand the behaviour of these specimens.

References

Allen, G., Allen, J., Elton, N., Farey, M., Holmes, S., Livesey, P., Radonjic, M. (2003). *Hydraulic Lime Mortar: for Stone, Brick and Block Masonry*, Donhead Publishing, Dorset, England, 104 pp.

Arbour, E. (2000). "Design Dead Load of a Straw Bale Wall," *Thesis Project*, Department of Civil Engineering, University of Manitoba, Winnipeg, Manitoba.

Arkin, D., and Donahue, K. (2001). "Preliminary Report on the Out-of-Plane Testing of an 8 foot by 8 foot Straw Bale/PISE Wall Panel," in *First International Conference on Ecological Building Structure*, San Rafael, California. 5 pp. Retrieved January 9, 2009 from <http://www.cc-w.co.uk/Documents/DonahueArkin.pdf>

Ash, C., and Aschheim, M. (2003). "In-Plane Cyclic Tests of Plastered Straw Bale Wall Assemblies." *Research Report*, Ecological Building Network, Sausalito, California. 31 pp. Retrieved January 10, 2009 from http://www.ecobuildnetwork.org/pdfs/InPlane_Wall_Tests_Large.pdf

Ashour, T. (2003). "The Use of Renewable Agricultural By-Products as Building Materials," *Doctoral Thesis*, Zagazig University, Benha, Egypt.

ASTM (2007a) Standard Practice for Making and Curing Concrete Test Specimens in the Laboratory, ASTM Standard C192, American Society for Testing of Materials, West Conshohocken, Pennsylvania.

ASTM (2007b) Standard Specification for Portland Cement, ASTM Standard C150, American Society for Testing of Materials, West Conshohocken, Pennsylvania.

ASTM (2006) Standard Specification for Hydrated Lime for Masonry Purposes, ASTM Standard C207, American Society for Testing of Materials, West Conshohocken, Pennsylvania.

ASTM (2004a) Standard Test Method for Compressive Strength of Cylindrical Concrete Specimens, ASTM Standard C39, American Society for Testing of Materials, West Conshohocken, Pennsylvania.

References

ASTM (2004b) Standard Specification for Aggregate for Masonry Mortar, ASTM Standard C144, American Society for Testing of Materials, West Conshohocken, Pennsylvania.

ASTM (2003) Standard Practice for Capping Cylindrical Concrete Specimens, ASTM Standard C 617 – 98, American Society for Testing of Materials, West Conshohocken, Pennsylvania.

ASTM (2002a) Standard Test Method for Static Modulus of Elasticity and Poisson's Ratio of Concrete in Compression, ASTM Standard C469, American Society for Testing of Materials, West Conshohocken, Pennsylvania.

ASTM (2002b) Standard Test Methods of Conducting Strength Tests of Panels for Building Construction, ASTM Standard E72, American Society for Testing of Materials, West Conshohocken, Pennsylvania.

ASTM (1998) Standard Test Method for Compressive Strength of Hydraulic Cement Mortars (Using 2-in. or [50-mm] Cube Specimens), ASTM Standard C109, American Society for Testing of Materials, West Conshohocken, Pennsylvania.

ASTM (1997) Standard Test Method for Slump of Hydraulic Cement Concrete, ASTM Standard C143, American Society for Testing of Materials, West Conshohocken, Pennsylvania.

ASTM (1994) Standard Practice for Mechanical Mixing of Hydraulic Cement Pastes and Mortars of Plastic Consistency, ASTM Standard C305, American Society for Testing of Materials, West Conshohocken, Pennsylvania.

ASTM (1993) Standard Practice for Use of Unbonded Caps in Determination of Compressive Strength of Hardened Concrete Cylinders, ASTM Standard C1231, American Society for Testing of Materials, West Conshohocken, Pennsylvania.

Black, G., and Mannik, H. (1997). "Spar and Membrane Structure," *The Last Straw Journal*, (17), pp. 10-11.

References

- Bilello, J., Carter, R., (1999). "Missile Perforation Threshold Speeds for Straw Bale Wall Construction with a Stucco Finish," *Project Report*, The Wind Engineering Research Centre, Texas Tech University. 9 pp. Retrieved May 23, 2009 from http://www.osbbc.ca/wordpress/wp-content/uploads/2009/02/missile_perforation_threshold_speeds.pdf
- Blum, B. (2002). "Load Carrying Behavior of On Edge Straw Bale Walls," University of Manitoba, Winnipeg, Manitoba.
- Bolles, R. (1998). "Straw Bale Exterior Pinning Report", *Research Report*, Sustainability International, Poway, California.
- Bou-Ali, G. (1993). "Straw Bales and Straw Bale Wall Systems," *M.Sc. Thesis*, Department of Civil Engineering and Engineering Mechanics, University of Arizona, Tucson, Arizona.
- Boynton, J. (1999). "Straw-Bale Bending and Cement Plaster/Straw Bale Bond Testing," *Undergraduate Research Project*, Architectural Engineering Department, California Polytechnic State University, San Luis Obispo, California.
- Boynton, R.S. and Gutschick, K.A. (1964). "Strength Considerations in Mortar and Masonry." *Technical Note*, National Lime Association, Arlington, Virginia, 10 pp. Retrieved January 10, 2009 from <http://www.nationallimeassociation.org/PublicationArchives/StrengthConsiderationMortarMasonry1989.pdf>
- Canadian Standards Association (CSA) (2004) "Design of Concrete Structures," *CSA Standard A23.3-04*, Toronto, Ontario
- Carrick, J., and Glassford, J. (1998). "Compressive, Transverse and Racking Tests of Load-Bearing Walls," *Research Report*, Building Research Centre, University of New South Wales, Australia.
- Collins, M.P., and Mitchell, D. (1997). *Prestressed Concrete Structures*, Response Publications, Canada.
- Desayi, P. and Krishnan, S. (1964) "Equation for the Stress-Strain Curve of Concrete," *ACI Journal, Proceedings*, **61**(3), pp. 345-350.

References

Dick, K.J., and Britton, M.G. (2002). "Design Approach for Load-Bearing Strawbale Walls," *CSAE Annual Conference*, Saskatoon, Saskatchewan, July 2002.

Donahue, K. (2003). "Testing of Straw Bale Walls with Out of Plane Loads" *Research Report*, Ecological Building Network, Sausalito, California. 11 pp. Retrieved January 10, 2009 from http://www.ecobuildnetwork.org/pdfs/Out-of-plane_wall_tests.pdf

Dreger, D. (2002). "Compression Resistance of a Stuccoed Straw Bale Wall," *Undergraduate Thesis*, University of Manitoba, Winnipeg, Manitoba.

Faine, M., and Zhang, J.Q. (2002). "A Pilot Study Examining and Comparing the Load Bearing Capacity and Behaviour of an Earth Rendered Straw Bale Wall to Cement Rendered Straw Bale Wall," *International Straw Bale Building Conference*, Wagga Wagga, Australia, 19 pp. Retrieved January 10, 2009 from <http://www.strawbalebuilding.ca/pdf/Mike%20Faine%20and%20Dr%20John%20Zhang's%20Earthen%20Render%20Tests.pdf>

Faine, M., and Zhang, J. (2000). "A Pilot Study Examining the Strength, Compressibility, and Serviceability of Rendered Straw Bale Walls for Two Storey Load Bearing Construction," *First International Conference on Ecological Building Structure*, San Rafael, California, 14 p. Retrieved January 10, 2009 from <http://www.strawbalebuilding.ca/pdf/Two-Storey%20LB.pdf>

Fibrehouse Ltd and Scanada Consultants Ltd. (1996). "Developing and Proof-Testing the 'Prestressed Nebraska' Method for Improved Production of Baled Fibre Housing," *Research Report*, Canada Mortgage and Housing Corporation (CMHC), Ottawa, Ontario.

Field, K., Woods, J., Fedrigo, C. (2005). "Structural Testing of Straw Bales in Axial Compression," *Undergraduate Presentation*, University of Colorado at Boulder, Colorado.

Grandsaert, M. (1999). "A Compression Test of Plastered Straw-Bale Walls," *M.Sc. Thesis*, University of Colorado at Boulder, Boulder, Colorado.

Hansen, H., Kielland, A., Nielsen, K.E.C., Thaulow, S. (1962). "Compressive Strength of Concrete – Cube or Cylinder," *Bulletin RILEM*, (17), pp. 23-30.

References

Intertek (2007a) "1-Hr Fire Resistance Test of a Non-Loadbearing Straw Bale Wall," Project No. 3098054B, Intertek Testing Services, Elmendorf, Texas, *Research Report*, Prepared for the Ecological Building Network, Sausalito, California. Retrieved January 9, 2009 from

http://www.ecobuildnetwork.org/pdfs/Non-Bearing_Clay_Wall.pdf

Intertek (2007b) "2-Hr Fire Resistance Test of a Non-Loadbearing Wheat Straw Bale Wall," Project No. 3098054A, Intertek Testing Services, Elmendorf, Texas, *Research Report*, Prepared for the Ecological Building Network, Sausalito, California. Retrieved January 9, 2009 from

http://www.ecobuildnetwork.org/pdfs/Cement_Stucco_Wall.pdf

Kaushik, H.B., Rai, D.C., Jain, S.K. (2007). "Stress-Strain Characteristics of Clay Brick Masonry under Uniaxial Compression," *Journal of Materials in Civil Engineering*, **19**(9), pp. 728-739.

King, B. (2006). *Design of Straw Bale Buildings*, Green Building Press, San Rafael, California. 260 pp.

King, B. (1996). *Buildings of Earth and Straw*. Green Building Press, San Rafael, California. 169 pp.

Kosmatka, S.H., Kerkhoff, B., Panarese, W.C., MacLeod, N.F., McGrath, R.J. (2002). *Design and Control of Concrete Mixtures, 7th Ed.*, Cement Association of Canada, Ottawa, Ontario, 372 pp.

Lerner, K., and Donahue, K. (2003). "Structural Testing of Plasters for Straw Bale Construction," *Research Report*, Ecological Building Network, Sausalito, California, 23 pp. Retrieved January 10, 2009 from

<http://www.strawbalebuilding.ca/pdf/Structural%20Testing%20of%20Plasters%20for%20Straw%20Bale%20Construction.pdf>

Lerner, K., Theis, B., and Smith, D. (2000). "Straw-Bale," *Alternative Construction: Contemporary Natural Building Materials*, L. Elizabeth, and C. Adams, eds., John Wiley & Sons, Inc., New York, N.Y., pp. 209-234.

Lyse, I., and Johansen, R. (1962). "An Investigation on the Relationship Between the Cube and Cylinder Strengths of Concrete," *Bulletin RILEM*, (14), pp. 125-133.

References

- MacDougall, C., Vardy, S., Magwood, C. (2008). Effect of Mesh and Bale Orientation on the Strength of Straw Bale Walls. Research Report, External Research Program, Canada Housing and Mortgage Corporation, 60 pp.
- Magwood, C., Mack, P., Therrien, T. (2005). *More Straw Bale Building: How to Plan, Design and Build with Straw*. New Society Publishers, Gabriola Island, B.C., 288 pp.
- Magwood, C., and Walker, C. (2001). *Straw Bale Details*. New Society Publishers, Gabriola Island, B.C., 68 pp.
- Magwood, C., and Mack, P. (2000). *Straw Bale Building: How to Plan, Design and Build with Straw*, New Society Publishers, Gabriola Island, B.C., 256 pp.
- Mar, D. (2003). "Bearing Test of Plastered Straw Bales." *Research Report*, Ecological Building Network, Sausalito, California.
- Mar, D. (1998). "Full Scale Straw Bale Vault Test," *Research Report*, Skillful Means Architecture and Construction, Berkeley, California.
- National Lime Association (NLA) (2002). "Fact Sheet: Hydrated Lime for Masonry Purposes." National Lime Association, Arlington, Virginia, 7 pp. Retrieved January 10, 2009 from <http://www.lime.org/Masonry.pdf>
- Nichols, J., Raap, S. (2000). "Straw Bale Shear Wall Lateral Load Test," *First International Conference on Ecological Building Structure*. San Rafael, California, 24 pp. Retrieved January 9, 2009 from <http://www.cc-w.co.uk/Documents/nichols.pdf>
- Ontario Straw Bale Building Coalition (OSBBC) (2004). Retrieved January 9, 2009 from <http://www.strawbalebuilding.ca/gallery.shtml>
- Pritchett, I. (2003). "The Future is Green – Lime Green," *Concrete Engineering International*, Winter, 2003, pp. 49-50.
- Richardson, D.N. (1990). "Effects of Testing Variables on the Comparison of Neoprene Pad and Sulfur Mortar-Capped Concrete Test Cylinders," *ACI Materials Journal*, **87**(5), pp. 489-495.

References

- Riley, D., and Palleroni, S. (2001). "Community-Built Housing Solution: A Model Strawbale Home Design." *Proceedings of Sustainable Buildings III*, Fall BETEC Symposium, Santa Fe, New Mexico, CD-ROM.
- Riley, D., MacRae, G., Ramirez, J.C. (1998). "Strength Testing of Stucco and Plaster Veneered Straw-Bale Walls," *The Last Straw Journal*, (24), pp. 8-9.
- Sangster, W. (2006). "Benchmark Study on Green Buildings: Current Policies and Practices in Leading Green Building Nations," Retrieved January 15, 2008 from http://www.raic.org/raic/green_architecture/gb-benchmarkstudy.pdf
- Smith, C., and MacDougall, C. (2008) "An Investigation of Bond Strength in Straw Bale Construction," *2008 International Conference on Flax and Other Bast Plants*, Saskatoon, Saskatchewan, 10 pp. Retrieved January 10, 2009 from http://www.saskflax.com/documents/fb_papers/32_MacDougall.pdf
- Smith, D. (2003). "Creep in Bale Walls," *Research Report*, Ecological Building Network, Sausalito, California. 9 pp. Retrieved January 10, 2009 from http://www.ecobuildnetwork.org/pdfs/Creep_report.pdf
- Stephens, D. (2000). "'Strawblocks' – A Bit Beyond Your Average 'Field-Bale'," Spokane, Washington. Retrieved May 23, 2009 from <http://greenershelter.org/index.php?pg=4>
- Stepnuk, L. (2002). "Resistance to Shear in Stuccoed Straw Bale Walls," *Undergraduate Thesis*, University of Manitoba, Winnipeg, Manitoba.
- Stone, N., (2003). "Thermal Performance of Straw Bale Wall Systems," *Research Report*, Ecological Building Network, Sausalito, California, Retrieved January 9, 2009 from http://www.ecobuildnetwork.org/pdfs/Thermal_properties.pdf
- Straube, B. (2006). "Moisture," *Design of Straw Bale Buildings*, Green Building Press, San Rafael, California. Pp. 133-172.
- Taylor, B., Vardy, S., and MacDougall, C. (2006). "Compressive Strength Testing of Earthen Plasters for Straw Bale Wall Application." *International Conference on Advances in Engineering Structures, Mechanics and Construction*, Waterloo, Ontario. 12 pp. Retrieved January 10, 2009 from

References

<http://www.strawbalebuilding.ca/pdf/Earth%20Plaster%20Report%20Oct%2010.pdf>

Thomson, M. (2005). "Properties of Lime Mortar: Understanding the Nature of Lime-Sand Mortars," *Structure Magazine*, May, 2005, pp. 26-29.

Trejo, D., Folliard, K., and Du, L. (2003). "Alternative Cap Materials for Evaluating the Compressive Strength of Controlled Low-Strength Materials," *Journal of Materials in Civil Engineering*, **15**(5).

US Department of Energy (U.S. DOE) (1995). "House of Straw – Straw Bale Construction Comes of Age," Retrieved January 9, 2009 from <http://www.grisb.org/publications/pub23.pdf>

Vardy, S., and MacDougall, C. 2007. "Compressive Response of Plastered Straw Bale Wall Panels." *International Conference on Sustainable Construction Materials and Technologies, Coventry, UK, June 2007*, pp.789-800.

Vardy, S., and MacDougall, C. 2006. "Compressive Testing and Analysis of Plastered Straw Bales." *Journal of Green Building* 1(1): pp. 65-79

Vardy, S., Tipping, T., and MacDougall, C. 2005. "Compressive Testing and Analysis of a Typical Straw Wall Plaster." *Proc. of Engineering Sustainability 2005 Conference, Pittsburgh, U.S.A., April 2005*.

Wackernagel, M., and Rees, W. (1996). *Our Ecological Footprint: Reducing Human Impact on the Earth*, New Society Publishers, Gabriola Island, B.C., 160 pp.

Walker, P. (2004). "Compression Load Testing Straw Bale Walls," Department of Architecture and Civil Engineering, University of Bath, Bath, U.K. 10 pp. Retrieved January 10, 2009 from <http://www.strawbalebuilding.ca/pdf/Compression%20Load%20Testing%20Straw%20Bale%20Walls.pdf>

Watts, K., Wilkie, K., Thompson, K., and Corson, J. (1995). "Thermal and Mechanical Properties of Straw Bales As They Relate To a Straw House," *Rep. No. 95-209*, Canadian Society for Agricultural Engineering, Ottawa, Ontario.

References

Wheeler, A., Riley, D., Boothby, T. (2004). "The Effects of Plastered Skin Confinement on the Performance of Straw Bale Wall Systems." *Research Report*, Pennsylvania State University, Pennsylvania, 12 pp. Retrieved January 10, 2009 from

<http://www.strawbalebuilding.ca/pdf/The%20Effects%20of%20Plaster%20Skin%20Confinement%20on%20the%20Performance%20of%20Straw%20Bale%20Wall%20Systems.pdf>

White, D.J., Take, W.A., and Boulton, M.D. (2003). "Soil deformation measurement using Particle Image Velocimetry (PIV) and photogrammetry," *Geotechnique*, **53**(7) pp. 619-631.

White, N., and Iwanicha, C. (1997). "Lateral Testing of a Stucco-Covered Straw-Bale Wall," Architectural Engineering Department, California Polytechnic State University, San Luis Obispo, California

Wilson, A. (1993). "Cement and Concrete: Environmental Considerations," *Environmental Building News*, **2**(2). Retrieved January 9, 2009 from <http://www.buildinggreen.com/auth/article.cfm?fileName=020201b.xml>

World Wildlife Fund (2004). "Living Planet Report 2004," Retrieved January 9, 2009 from <http://assets.panda.org/downloads/lpr2004.pdf>

Zhang, J. (2000). "Load-Carrying Characteristics of a Single Straw Bale Under Compression," *International Straw Bale Building Conference*, Wagga Wagga, Australia, 16 pp.

Appendix A: Experimental Procedures and Instrumentation

A.1 Introduction

This Appendix provides detailed information pertaining to the instrumentation and apparatus used for the experiments described in this thesis. The manufacturers of the various apparatus used for specimen load application and data acquisition are provided.

A.2 Experimental Procedures and Instrumentation

A.2.1 Plaster Mixing Apparatus

Aside from the specimens discussed in Chapter 6, the plaster for all cube, cylinder, and wall specimens was mixed using a Lancaster Counter Current Batch Mixer; Type: LVD, Year: 1980, Number 277. For the specimens discussed in Chapter 6 the plaster was mixed using a single drum, tilting drum mixer.

Appendix A: Experimental Procedures and Instrumentation

A.2.2 Plaster Capping Techniques

Due to difficulties capping the soft plaster cylinders using traditional sulphur material, a number of alternative capping techniques and materials were utilized.

First, an attempt was made to cap the cylinders using a gypsum compound. This technique was found to be difficult to apply and it was challenging to achieve a smooth surface.

The second method was the use of elastomeric caps for the cylinders as described in ASTM C1231 (1993). Richardson (1990) studied the relationship between specimens capped with elastomeric caps and those capped traditionally with sulphur. The author concluded that for strengths between 23.4 and 236.2 MPa the cylinders tested using elastomeric caps “correlated well with those tested using sulphur mortar caps”. However, the author also noted that below 30.0 MPa, elastomeric caps gave lower results for the strengths. Trejo et al. (2003) tested the effect that different capping methods had on materials with low compressive strengths. It was reported that the elastomeric end caps typically provided strengths no less than 80% of strengths that would be found using a sulphur capping compound.

The third method was the use of a soft fiber board material as a cap as can be seen in Figure 3.1. This technique has not been explored thoroughly in the literature but was suggested based on previous success in its use by laboratory technicians. It was believed that the non-expansive properties of the fiber board will eliminate some the issues associated with the use of elastomeric caps. It was found

Appendix A: Experimental Procedures and Instrumentation

that using elastomeric caps and fiber board produced similar results, and thus both techniques were used, depending on availability of materials.

A.2.3 Load and Deflection Application and Measurement

A wide variety of apparatus were used for application and measurement of the loads and for measurement of the deflections. These apparatus are described in Table A.1. Note that for many of the devices the precision was governed by the setup of the amplifier and power supply rather than the device itself. Not described in Table A.1 is the technique of deflection measurement using Particle Image Velocimetry (PIV). This technique is described in Appendix B.

A.2.4 Data Acquisition

All data was recorded using Measure Foundry ® by Data Translation Inc., a program used to acquire and record experimental data. The program used a 32-channel DT3003 board, manufactured by Data Translation Inc.

Appendix A: Experimental Procedures and Instrumentation

Table A.1: Load and Deflection Application and Measurement Apparatus

Experiments	Device	Company	Capacity	Approx. Precision
Un-Plastered Bales	Load Cell	Sensotec	111 kN	0.1 kN
Un-Plastered Bales	LP – TRS 100	Novotechnik	100 mm	0.01 mm
Un-Plastered Bales	LP – TRS 25	Novotechnik	25 mm	0.0025 mm
Plaster Tests	Unitomatic MG-37074	Unitomatic	50 kN	0.05 kN
Plaster Tests	Instron M1350	Instron	Set at 50 kN	0.05 kN
Plaster Tests	Riehle Concrete Testing Machine	Riehle	13352 kN	0.1 kN
Plaster Tests	Riehle Universal Testing Machine	Riehle	Set at 100 kN	0.001 kN
Plaster Tests	Compressometer LP – TR 10	Novotechnik	10 mm	0.001 mm
Plaster Tests	Extensometer 632.24F-50	MTS	25 mm	0.0025 mm
Chapter 4 Bales	Load Cell	Sensotec	111 kN	0.1 kN
Chapter 4 Bales	LP – TRS 100	Novotechnik	100 mm	0.01 mm
Chapter 4 Bales	LP – TRS 25	Novotechnik	25 mm	0.0025 mm
Chapter 5 0.99 m	Riehle Universal Testing Machine	Riehle	Set at 100 kN	0.001 kN
Chapter 5 2.31 m	Load Cell	Sensotec	111 kN	0.1 kN
Chapter 5 All Tests	LP – TRS 100	Novotechnik	100 mm	0.01 mm
Chapter 5 All Tests	LP – TRS 25	Novotechnik	25 mm	0.0025 mm
Chapter 6 Tests	Riehle Universal Testing Machine	Riehle	Set at 100 kN	0.001 kN
Chapter 6 Tests	LP – TRS 100	Novotechnik	100 mm	0.01 mm

Appendix B: Particle Image Velocimetry Details

B.1 Introduction

This Appendix provides detailed information pertaining to the use of Particle Image Velocimetry (PIV) for measurement of displacement in structural testing. While the theory behind PIV and the use of PIV to track soil displacements is documented by White et al. (2003), there is a need to justify its use for the specific structural testing configurations described in this thesis. The justification for the use of PIV is presented along with the procedures used to obtain the displacement data and the expected precision and accuracy of the results.

B.2 Reason for Use

In a PIV analysis, a camera is utilized to take photographs of the test specimens at given time intervals. The photographs are then compared with one-another, and based on the comparison, the displacement of any portion of the

Appendix B: Particle Image Velocimetry Details

specimen can be determined. There are a number of benefits associated with the use of PIV.

One key benefit is that it is not necessary to determine in advance of testing the exact location where the displacement is to be tracked. As long as there is sufficient colour texturing on the specimen, the displacement tracking location can be determined during post-testing analysis.

A second key benefit is the ability to determine the lateral displacements of the plastered straw bale wall assembly specimens. It was noted during testing that the surface of the plaster skins was not completely smooth. As a result, the LPs which were intended to measure the lateral deflections were also measuring the surface contours of the plaster skins as the walls were compressed, leading to erroneous results. The use of PIV ensures that the lack of smoothness of the plaster skins will not influence the measurements.

The final key benefit is the ability to track displacement of materials for which the use of traditional displacement measuring techniques may not be suitable due to the properties of the materials. For the plaster cylinder experiments, there were noted issues with the use of both the compressometer and the extensometer with some specimens due to the weakness of the plaster. Similarly, it was found impossible to attach gauges directly to the plaster skins for the wall assembly specimens due to the weakness of the plaster. It was also found to not be possible to determine the deformations of the straw bales in the plastered wall assembly specimens using traditional techniques. For all of these situations, it was found that

Appendix B: Particle Image Velocimetry Details

PIV provided a means of obtaining results which were un-obtainable using traditional techniques

An additional benefit of the use of PIV is that it allowed for an alternative measurement to LPs. This is important as it was noted in this thesis that the LPs captured deformations of the testing jigs and re-compression of the straw bales, leading to erroneous results. Figure B.1 provides a comparison of vertical load-deflection data obtained from PIV and LP's. As can be seen, the LP's measured large deflections at the beginning of the experiment as a result of the recompression of the straw. It is important to note in Figure B.1, the lack of precision of the PIV data can be seen with the larger scatter in the PIV data. Note that Figure B.1 only presents the pre-failure load-deflection data as the PIV does not produce reliable data following initial ultimate failure.

B.3 Materials and Procedure

In order to track the displacements of the plastered straw bale wall assemblies using PIV the following procedure was followed:

1. The specimen was painted with randomized splatters or blotches of paint in order to provide colour texture to the surface being photographed. This can be seen in Figure B.2 and in Figures 3.1 and 5.8.
2. A camera was positioned on a tripod in order to photograph the surface being tracked. The camera was then connected to the photograph acquisition computer. This setup can be seen in Figure B.3, where two cameras can be seen set-up to take photographs of the face and edge of the specimen.

Appendix B: Particle Image Velocimetry Details

3. Throughout the duration of the experiment the camera took photographs at specified time intervals (5 seconds for Chapter 3, 20 seconds for Chapter 5, and 30 seconds for Chapter 6). The photographs were recorded using the photograph acquisition computer. This step of the procedure produced a series of photographs for each experiment.
4. The photographs were then compared with one-another to determine the displacements as the test progressed. This made possible a correlation between displacement and time at the 30 second intervals. This step was conducted using Matlab programs “geoPIV76.m” and “consolidate7.m”
5. The displacement-time relationship was used with the load-time relationship determined from the data acquisition system to determine the relationship between load and displacement.

This procedure enabled the displacement vector for any point on the specimen to be determined for the entire duration of the experiment. The displacement vector yielded both the horizontal and vertical displacements. The ability to determine the displacement vector for any point provided the ability to perform a great number of analyses; such as finding the overall vertical load-deflection response for the assembly, or determining the horizontally deflected shape at ultimate failure.

A number of different cameras were used throughout the experiments. The minimum resolution camera was 8 megapixels, used for the Chapter 5 experiments. For most experiments the resolution was 10 megapixels.

B.4 Expected Precision

White et al. (2003) present methods for determining the performance of systems using PIV. They suggest the precision may be determined using Equation B.1:

$$\rho_{pixel} = \frac{0.6}{S_p} + \frac{150000}{S_p^8} \quad \text{B.1}$$

where ρ_{pixel} is a conservative estimate of precision error expected using PIV (in pixels) and S_p is the size of the patch used to define the point being tracked (width of patch in pixels). For the experiments conducted in this thesis, a patch size of 64 pixels was chosen yielding an expected precision error of 0.0094 pixels. Considering an average scale factor of 0.4 mm/pixel, this corresponds to an expected error of 0.004 mm.

B.5 Validation

As shown above, White et al. (2003) suggest the use of Equation B.1 to estimate the expected error when using PIV. However, the authors also caution that the precision can be significantly affected by a number of parameters specific to the test setup and the environmental conditions. As a result, a number of control experiments were conducted to study the true setup-specific precision of the PIV.

For the first control experiment, the test was set up and the cameras were run for approximately 20 minutes while no load or displacement was applied. This time corresponds to the time a typical experiment would require to reach ultimate failure of the specimens. Because no load was applied to the specimen, it is expected that

Appendix B: Particle Image Velocimetry Details

the displacement would remain at zero for the duration of the analysis. The resulting displacement-time plot is provided in Figure B.4. According to Figure B.4 there is more variation in the data than expected, with values ranging from approximately -0.06 mm to +0.08 mm. There are a number of potential reasons for the discrepancy between these values and the value obtained using Equation B.1. Potential sources of error include building vibrations, changes in lighting throughout the duration of the experiment, and slippage of the camera or tripod. Thus, use of Figure B.4 to determine the error is more appropriate than Equation B.1 because Figure B.4 will account for these potential sources of error. Based on Figure B.4, the PIV precision can be estimated to be +/- 0.1 mm.

A second control experiment served to validate the calibration used to provide displacement data from the PIV results. In analyzing the data from PIV the displacements are first presented in units of pixels. However, it is desirable to determine the displacements in millimetres. As a result, a calibration is performed to determine the conversion from pixel distances to millimetre distances. This is done by determining the distance in pixels between two points on a photograph which are a known distance (in mm) apart. To ensure that this technique was accurate a validation experiment was conducted.

The calibration validation experiment involved moving two objects away from one-another at a given rate in the field of view of the PIV camera. Using the known rate of movement a “known” displacement-time plot could be created. A PIV analysis was conducted for the experiment, and using the PIV results a “PIV” displacement-time plot was created. Ideally these plots will be identical. Both plots

Appendix B: Particle Image Velocimetry Details

are presented in Figure B.5. A linear regression analysis was performed comparing the PIV data with the known plot. As expected, a strong correlation was found between the results from the PIV analysis and the known displacement values. An R^2 value of 0.995 was found for the comparison. This provided validation of the methods used to calibrate the PIV results.

It should be noted that the precision may deviate from the assumed value of +/- 0.1 mm if the calibration between pixel displacements and millimetre displacements varies significantly from the value used for the first control experiment. However, the calibration is approximately equal for all experiments in this thesis, thus justifying the assumption of PIV precision of +/- 0.1 mm for all experiments.

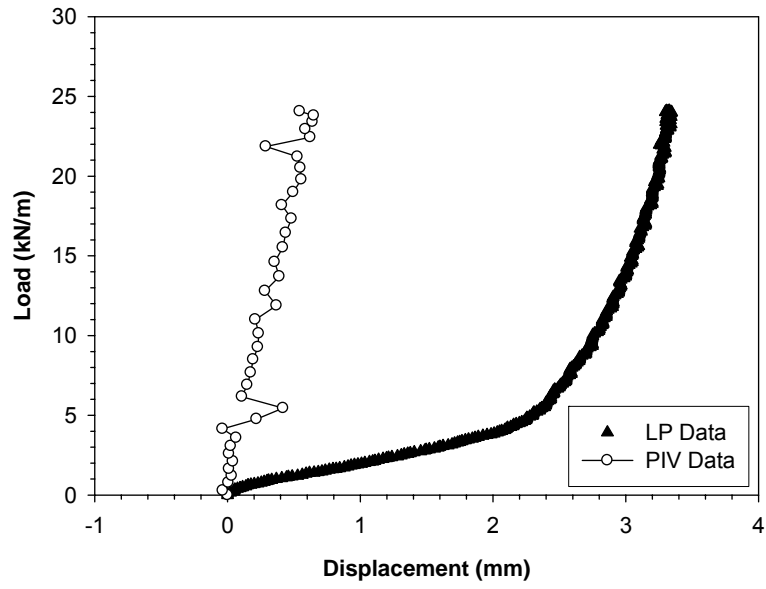


Figure B.1: Comparison of PIV and LP Data

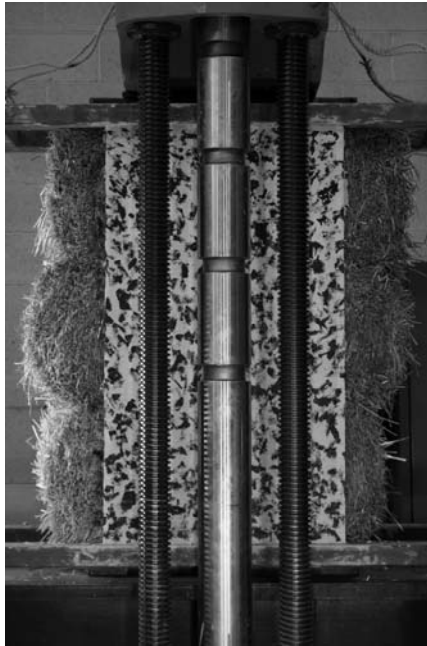


Figure B.2: Colour Texturing of Plastered Straw Bale Wall Assembly for PIV

Appendix B: Particle Image Velocimetry Details

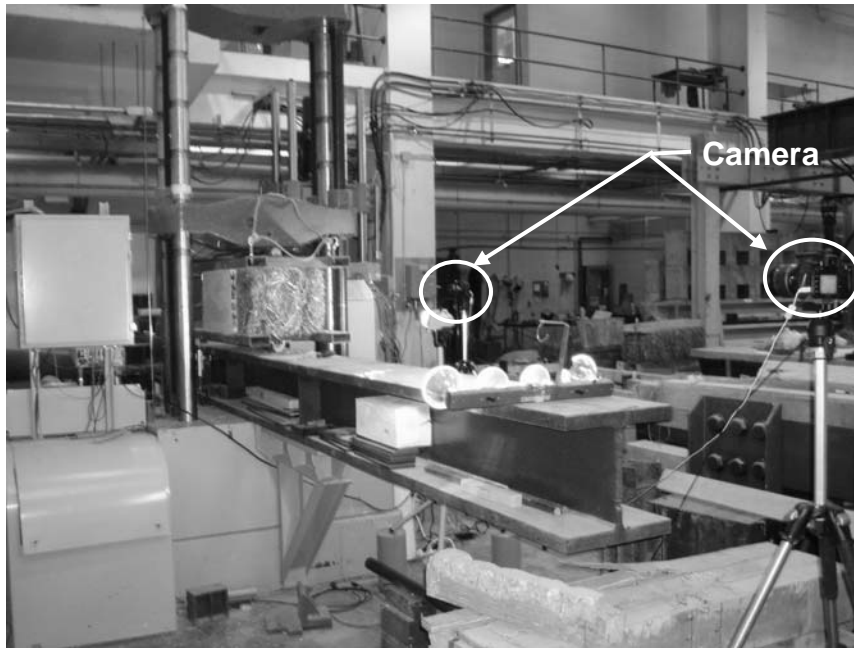


Figure B.3: Camera Set-Up for PIV

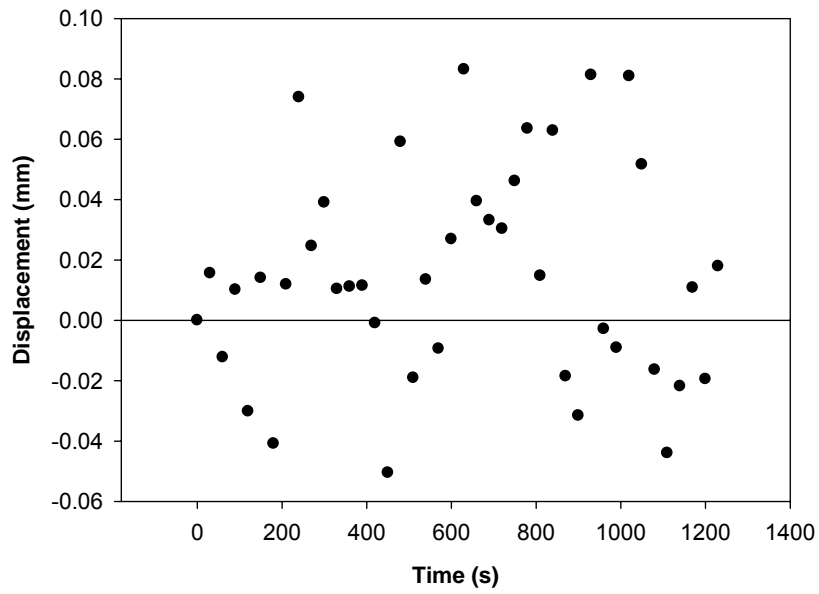


Figure B.4: Control Test #1 – Zero Load

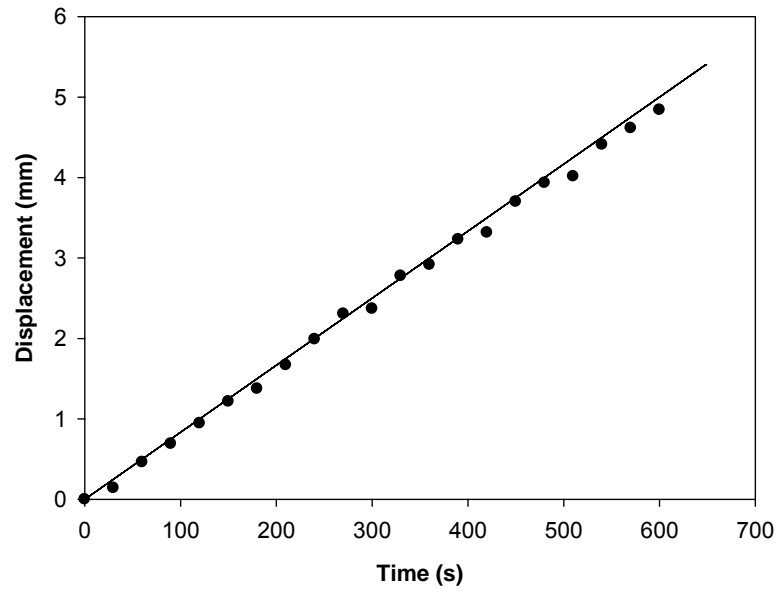


Figure B.5: Control Test #2 – Known Displacement

Appendix C: Experimental Results

C.1 Introduction

This Appendix provides tables summarizing the experimental results. Table C.1 presents the results of plaster compression test experiments, while Table C.2 presents the results of experiments conducted on plastered straw bale wall assembly specimens.

For the plaster thickness values in Table C.2, the notation D refers to a design thickness, where no measurements of the in-situ thickness were taken, the notation E refers to an estimated thickness, where an estimate of the in-situ thickness was based on results from other experiments, and the notation M refers to a measured thickness, where the thickness was measured for the specific specimen. Similarly, for the plaster strength values in Table C.2, the notation D refers to a design strength, where no measurements of the in-situ strength were taken, the notation E refers to an estimated strength, where the strength was estimated based

Appendix C: Experimental Results

on one batch for the specimen (where multiple batches were used to fabricate the specimen), and the notation M refers to a measured strength, where the strength was measured for the single batch used to fabricate the specimen.

Appendix C: Experimental Results

Table C.1: Plaster Compression Test Results

<i>Cement</i>	Proportions (By Volume)			Slump	Curing Time (d)	Strength (MPa)		Modulus (MPa)
	<i>Lime</i>	<i>Sand</i>	<i>W/CM (by mass)</i>			<i>Cube</i>	<i>Cyl</i>	
0.25	1.25	4.5	1.08	45	28	1.64 1.72 1.80		
0.25	1.25	4.5	1.13	51	28	0.96 0.76 1.00		
0.25	1.25	4.5	1.18	58	7	0.72 0.76 0.76		
0.25	1.25	4.5	1.18	58	14	0.96 0.96 0.84		
0.25	1.25	4.5	1.18	58	28	1.20 1.20 1.20		
0.25	1.25	4.5	1.23	84	28	0.80 0.72 0.72		
0.25	1.25	4.5	1.28	98	28	0.64 0.76 0.68		
0.92	4.58	0.5	0.59	80	28	5.948 5.057 6.202	4.942 4.626 4.777	3408 2180 2033
0.67	3.33	2.0	0.66	55	28	5.371 4.641 5.006	3.918 4.477 4.167	2181 3805
0.17	0.83	5.0	2.05	38	28	0.458 0.484 0.501	0.300 0.332 0.313	333 370 650
0.08	0.42	5.5	4.75	45	28	0.136 0.127 0.085	0.105 0.081 0.113	
0.28	0.75	4.97	1.73	33	28	1.154 1.239 1.290	0.897 0.984 0.919	865 790 1209
0.30	0.25	5.45	3.09	32	28	0.670 0.602 0.662	0.538 0.676 0.586	1110 751 1213
0.20	2.25	3.55	0.84	49	28	1.162 1.230 1.128	0.994 0.951 0.946	1029 810 855
0.14	3.25	2.61	0.67	45	28	1.239 1.239 1.417	1.005 0.781 0.835	1456 1415 1511

Appendix C: Experimental Results

Table C.1 (Continued): Plaster Compression Test Results

<i>Cement</i>	Proportions (By Volume)			Slump	Curing Time (d)	Strength (MPa)		Modulus (MPa)
	<i>Lime</i>	<i>Sand</i>	<i>W/CM (by mass)</i>			<i>Cube</i>	<i>Cyl</i>	
0.05	1.29	4.66	1.61	37	28	0.322	0.219	3157
						0.322	0.227	1091
						0.365	0.243	588
0.15	1.27	4.58	1.35	35	28	0.501	0.376	545
						0.679	0.367	333
						0.619	0.359	580
1.25	1.03	3.72	0.57	30	28	25.13	22.96	19567
						26.08	23.63	16255
						25.66	23.86	20333
2.25	0.82	2.93	0.40	43	28	45.95		
						47.13		
						45.95		
0.25	1.25	4.5	1.13	31	28	1.383	1.008	1124
						1.442	1.038	1002
						1.307	0.830	1716
0.264	1.000	4.736	1.350	40	28	1.078	0.859	1035
						1.273	0.951	1061
						1.264	0.911	1013
0.224	1.750	4.026	0.924	44	28	1.332	0.697	1010
						1.442	0.803	970
						1.341	0.835	930
0.289	0.500	5.211	2.169	62	28	1.001	0.897	1626
						0.933	0.824	1327
						0.959	0.792	1273
0.417	2.083	3.500	0.732	50	28	4.005	4.456	6464
						4.089	4.140	4278
						5.413	5.058	14647
0.50	1.20	4.30	0.88	40	28	4.972	5.558	4910
						4.972	4.945	4928
						3.572	2.735	2637
0.43	3.57	2.00	0.60		28	4.531	2.545	1755
						3.250	3.129	2835
						13.575	13.485	8485
0.99	3.01	2.00	0.48		28	12.871	11.744	11365
						14.992	14.082	10723
						2.214	1.089	1211
0.268	2.23	3.50	0.81	45	28	2.002	1.405	925
						2.002	1.075	1297
						7.661	5.922	5712
0.62	1.88	3.50	0.69	70	28	7.568	6.083	5500
						6.910	5.810	8379
						1.162	0.686	710
0.25	1.25	4.5	1.33	25	28	1.035	0.651	672
						1.247	0.597	721
						0.916	0.540	1118
0.25	1.25	4.5	1.31	48	28	1.069	0.592	1269
						1.027	0.462	1668

Appendix C: Experimental Results

Table C.1 (Continued): Plaster Compression Test Results

<i>Cement</i>	Proportions (By Volume)			Slump	Curing Time (d)	Strength (MPa)		Modulus (MPa)
	<i>Lime</i>	<i>Sand</i>	<i>W/CM (by mass)</i>			<i>Cube</i>	<i>Cyl</i>	
0.375	1.125	4.500	1.121	28	28	2.248	2.032	2455
						2.656	2.143	4445
						3.139	1.600	4655
0.00	1.50	4.50	1.54	31	28	0.348	0.322	4660
						0.280	0.297	863
						0.348		
0.25	1.25	4.50	1.08		28	1.010	0.769	393
						1.181	0.707	389
						1.160	0.781	414
						1.178		
0.25	1.25	4.50	1.18		28	1.025	0.804	765
						1.088	0.700	715
						1.121	0.743	964
						0.945		
0.25	1.25	4.50	1.28		28	0.922	0.562	310
						0.914	0.519	412
						0.869	0.506	381
0.25	1.25	4.50	1.08		11	1.055	0.796	306
						0.545	0.790	528
						1.043	0.840	530
0.25	1.25	4.50	1.08		32	1.272	0.908	407
						1.236	0.896	380
							0.982	742
0.25	1.25	4.50	1.08		32	1.046	0.765	342
						1.062	0.716	397
						1.063	0.765	283
0.25	1.25	4.50	1.08		32	1.112	0.699	197
						1.017	0.787	295
0.25	1.25	4.50	1.08		14	0.934		
						0.893		
						0.581		
0.25	1.25	4.50	1.08		13	0.982		
						1.091		
						1.018		
0.25	1.25	4.50	1.08		8	0.800		
						0.946		
						0.982		
0.25	1.25	4.50	1.08		8	0.836		
						0.836		
						0.836		
0.25	1.25	4.50	1.08		11	0.909		
						0.836		
						0.800		
0.25	1.25	4.50	1.08		7	0.873		
						0.873		
						0.909		

Appendix C: Experimental Results

Table C.1 (Continued): Plaster Compression Test Results

<i>Cement</i>	Proportions (By Volume)			Slump	Curing Time (d)	Strength (MPa)		Modulus (MPa)
	<i>Lime</i>	<i>Sand</i>	<i>W/CM (by mass)</i>			<i>Cube</i>	<i>Cyl</i>	
0.25	1.25	4.50	1.08		8	0.873	0.836	0.764
0.25	1.25	4.50	1.08		7	0.836	0.873	0.836
0.25	1.25	4.50	1.08		7	0.691	0.727	0.655
0.25	1.25	4.50	1.08		13	0.546	0.582	0.691
0.25	1.25	4.50	1.08		7	0.800	0.836	0.836
0.25	1.25	4.50	1.08		7	0.764	0.800	0.764
0.25	1.25	4.50	1.08		7	0.686	0.672	0.622
0.25	1.25	4.50	1.08		7	0.806	0.817	0.796
0.25	1.25	4.50	1.08		7	0.953	0.859	0.963
0.25	1.25	4.50	1.08		7	0.712	0.870	0.744
0.25	1.25	4.50	1.08		7	0.767	0.773	0.751
0.25	1.25	4.50	1.08		7	0.690	0.667	0.606

Appendix C: Experimental Results

Table C.2: Assembly Testing Results

Jig Type	Eccentricity (mm)	Plaster Thickness (mm)	Plaster Strength (MPa)	Wall Height (mm)	Wall Strength (kN/m)
Wood	0	25 D	1.43 D	330	59.1
					57.6
					61.2
Wood	0	25 D	1.12 D	330	51.8
					31.8
					57.4
Wood	0	25 D	0.80 D	330	49.3
					48.4
					31.6
Wood	0	13 D	1.43 D	330	34.7
					38.2
					33.2
Wood	0	38 D	1.43 D	330	82.7
					68.6
					91.5
Steel Flat	0	23 E	0.660 E	990	28.1
			0.806 E		31.8
			0.925 E		36.3
Steel Flat	0	23 E	0.775 E	2310	35.8
			0.764 E		36.8
			0.645 E		37.3
Steel Pinned	120	28 M	0.824 M	330	32.9
		27 M	0.848 M		30.5
		34 M	0.691 M		34.8
Steel Pinned	120	26 M	0.606 M	1050	23.7
		26 M	0.824 M		26.2
		27 M	0.776 M		27.0
Steel Pinned	0	23 M	0.803 M	330	41.4
		23 M	1.030 M		62.1
		24 M	0.909 M		55.7
Steel Pinned	0	18 M	0.836 M	1050	37.7
		21 M	0.848 M		43.5
		22 M	0.885 M		41.7

Appendix D: On-Edge Assembly Results

D.1 Introduction

Experiments were conducted on on-edge plastered straw bale wall assemblies. The specimens were fabricated and tested in the same manner as the specimens presented in Chapter 4. However, because of fabrication issues with the on-edge specimens the results were not included in the analysis in that Chapter. This Appendix presents the results from the on-edge plastered straw bale wall assemblies. Because of the fabrication issues, no theoretical analysis was performed for the results presented in this Appendix.

D.2 Fabrication

Chapter 4 can be referred to for the majority of the materials and procedure information; however, portions of the fabrication procedure are presented below where the procedure differed from that presented in Chapter 4. The fabrication processes for the on-edge bales is illustrated in Figure D.1. The process was the

Appendix D: On-Edge Assembly Results

same as that for the flat bales except that following trimming of the straw (Step 2a), the bales were removed from the jigs, rotated 90 degrees and placed in taller, narrower jigs as shown in step 2b of Figure D.1. Thus the height of the on-edge specimens was controlled by first trimming the straw, then by compressing the bales on-edge in the second jigs. However, the width was only controlled by the pre-compression provided in step 1. This lack of control of the straw width was the root of the noted fabrication issues.

The resulting specimens had plaster skins with designed length of 600 +/- 1 mm, height of 405 +/- 1 mm and a thickness of 25 +/- 1 mm. However, following fabrication and prior to plastering it was found that the bales rebounded, resulting in bales with thickness greater than desired and specimens with plaster thickness less than desired. The edging which was designed to ensure appropriate plaster thickness acted to restrain the straw and prevent rebound. However, away from the edging (towards the centre of the plaster skin) the straw was observed to rebound into the region in which the plaster was intended to be applied. This resulted in plaster skins which were thinner where the straw had rebounded. It was difficult to ascertain how much this rebounding reduced the plaster skin thickness. As a result, there were inconsistencies observed in the results for the on-edge plastered bales.

D.3 Results and Discussion

On-edge specimens were fabricated with design plaster thickness of 25 mm and design plaster strengths of 1.43 MPa, 1.12 MPa, and 0.80 MPa. The results are discussed below.

Appendix D: On-Edge Assembly Results

Figure D.2 gives the axial load versus axial deflection response for a typical bale plastered on edge. The plaster was designed to be 25 mm thick, but as a result of bulging of the bale the actual plaster thickness was significantly less than that. The specimen presented in Figure D.2 had a design strength = 1.43 MPa. Because the top and bottom of the on-edge bales were cut flat there is no initial non-linearity evident in Figure D.2 as a result of bale rebound, as there was with the flat plastered bales. The load-displacement relationship shown in Figure D.2 is linear until the ultimate load was reached at 13 kN.

The load-displacement responses for the bales plastered on edge followed similar trends to those of the bales plastered flat. For the specimen presented in Figure D.2 there was a linear portion to the relationship prior to failure at 13 kN, at which point failure occurred with a sudden crack as shown in Figure D.3. This caused the load to drop to about 3 kN. Following failure, the plastered bale behaved in a ductile manner, as it continued to take load immediately after the initial cracking.

The failure mode of the plastered bales tested on edge appears to have been different than for the flat plastered bales presented in Chapter 4. The flat plastered bales failed as a result of crushing of the plaster at the contact point between the plaster and the loading apparatus, while the on-edge bales failed at mid-height of the specimen as can be seen in Figure D.3. This is most likely a result of the noted premature failures of the flat specimens and the noted thinness of the plaster skins towards the middle of the specimen for the on-edge specimens.

Appendix D: On-Edge Assembly Results

The results for the on-edge experiments are presented in Table D.1. If it is assumed that all specimens had equal plaster thickness following the rebounding of the straw, an analysis of the results can be used to determine the influence of the plaster strength on the strength of the specimens. Figure D.4 presents the relationship between plaster strength and the strength of the specimens.

From Figure D.4 and Table D.1, it can be seen that the plaster cube strength had an influence on the strength of the specimens. As the plaster cube strength was increased 40% from 0.80 MPa to 1.12 MPa, it is expected based on the theoretical discussion in Chapter 4 that the average plastered bale strength would also have increased 40%. However, the average plastered bale strength increased only 31% from 11.71 kN/m to 15.33 kN/m. Similarly, as the plaster cube strength was increased 79% from 0.80 MPa to 1.43 MPa, it is expected that the average plastered bale strength would also have increased 79%. However, the average plastered bale strength increased 122% from 11.71 kN/m to 25.96 MPa. For the first comparison the increase in plaster strength had less of an effect on the assembly strength than expected, while for the second comparison the increase in plaster strength had a greater effect on the assembly strength than expected. On average, the increase in plaster strength did lead to an approximate equal percentage increase in assembly strength, however further testing is required to confirm this.

Appendix D: On-Edge Assembly Results

Table D.1: Results for On-Edge Plastered Straw Bale Assemblies

Bale Orientation	Design Plaster Strength (MPa)	Plastered Bale Strength (kN/m)				
		<i>First Test</i>	<i>Second Test</i>	<i>Third Test</i>	<i>Avg.</i>	<i>St. Dev.</i>
On Edge	0.80	7.73	13.39	14.01	11.71	3.46
On Edge	1.12	11.95	15.00	19.04	15.33	3.56
On Edge	1.43	22.73	23.00	32.16	25.96	5.37

Appendix D: On-Edge Assembly Results

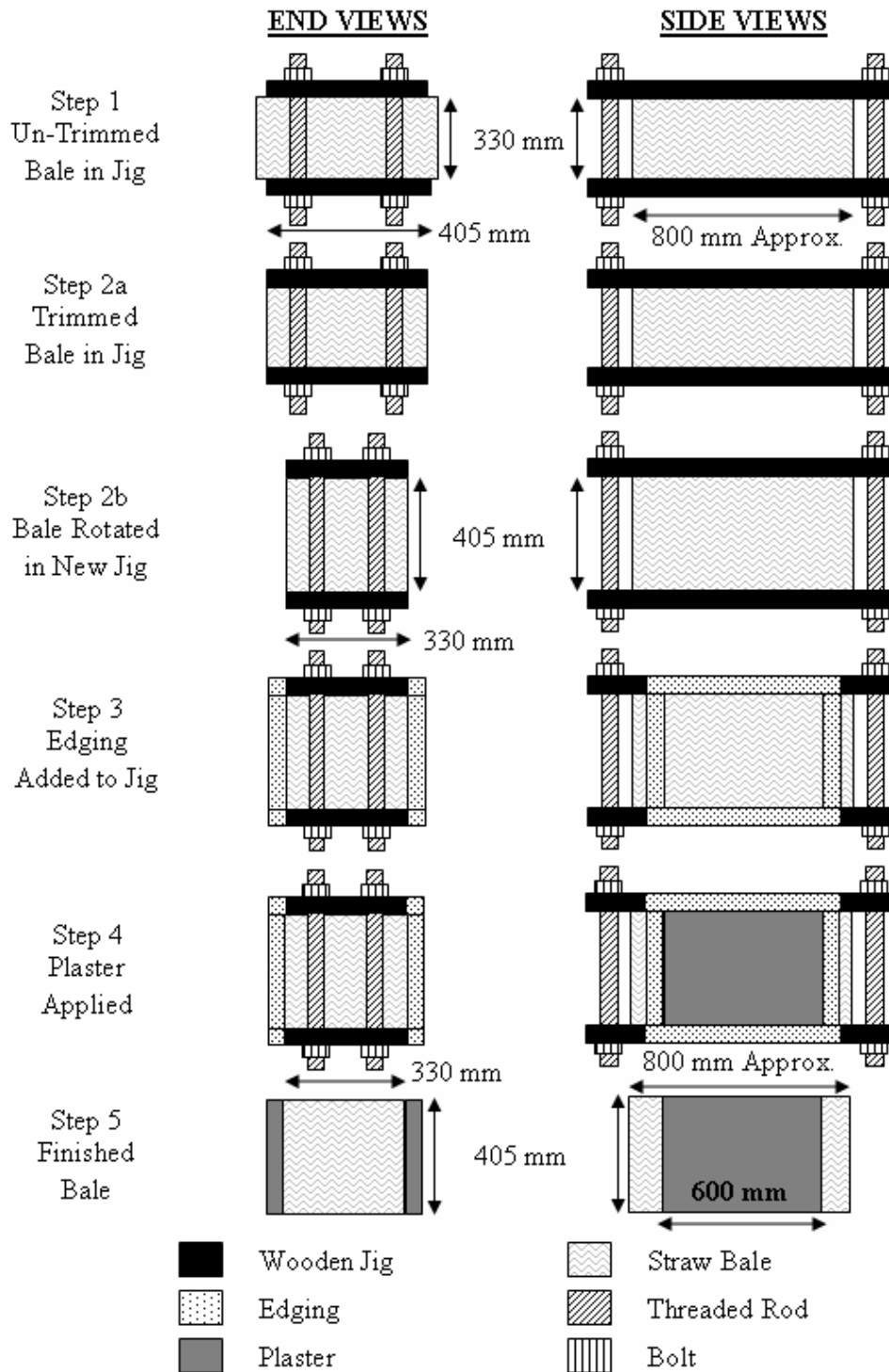


Figure D.1: Procedure for Preparing On-Edge Plastered Straw Bale Assemblies

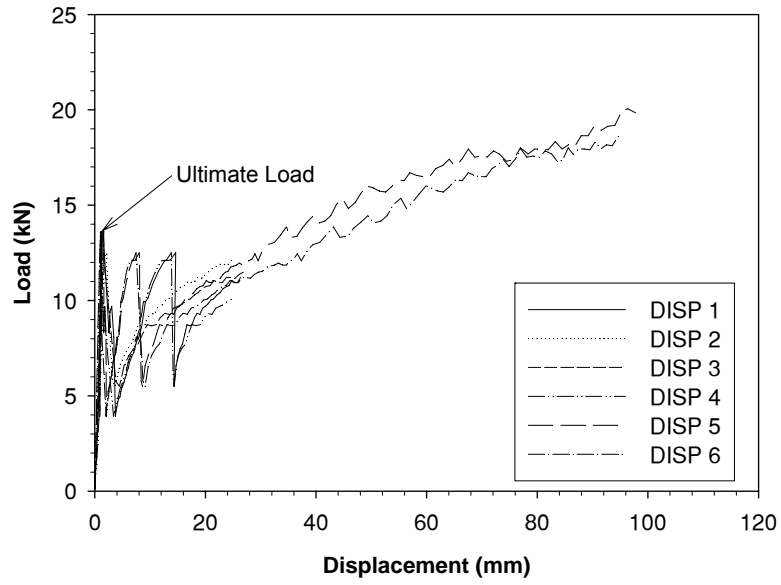


Figure D.2: Typical Load-Displacement Response for On-Edge Plastered Straw Bale



Figure D.3: Typical Failure of an On-Edge Plastered Straw Bale

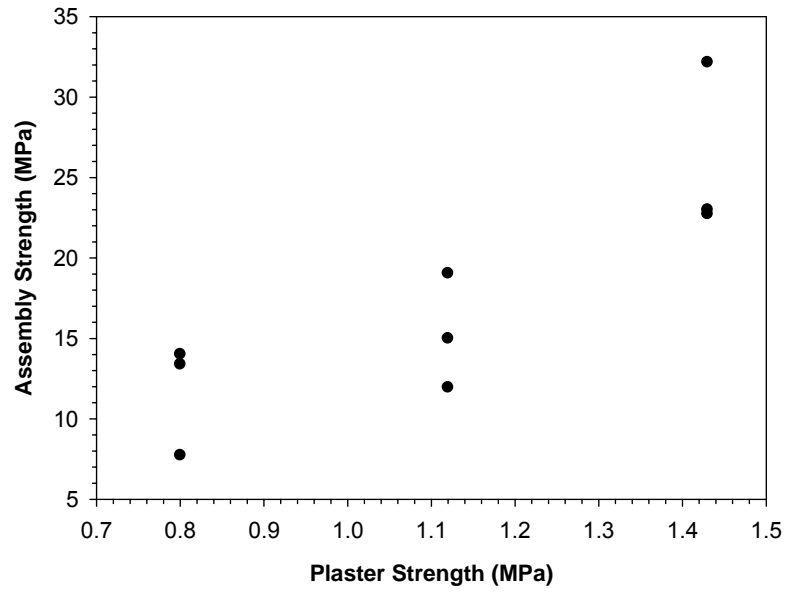


Figure D.4: Relationship Between Plaster Strength and Assembly Strength for On-Edge Assemblies

Appendix E: Validation of Behaviour Assumptions

E.1 Introduction

The formulation of a theoretical model for the compressive behaviour of plastered straw bale wall assemblies involved a number of significant assumptions regarding the behaviour of the assemblies. One significant assumption was that the concentric compression specimens were assumed not to fail as a result of buckling. Additionally, the formulation of the eccentric model involved the assumption that the assemblies were not subject to shear distortion of the straw bales, and that there was no slippage at the straw-plaster interface as a result of shear stress at the interface. This appendix provides support for the appropriateness of these assumptions.

E.2 Failure Mode Assumption

E.2.1 Introduction

The analysis in this Thesis regarding the failure of the plastered straw bale wall assemblies assumes that the assemblies fail as a result of compressive failure of the plaster. This assumption was supported by experimental results showing that the specimens achieved strengths as predicted by the theoretical models, and did not fail prematurely as a result of buckling. However, previous authors have suggested the potential for failure as a result of local or global buckling of the plaster skins as described in Chapter 2. This section will present additional support for the assumption that buckling failure is not a governing failure mode for the specimens discussed in this thesis.

E.2.2 Local Buckling

If it is assumed that the plaster skins work as columns in resisting load applied to the wall, it is important to consider the lateral support that the straw provides to these columns. If the lateral support of the straw is ignored, the thin plaster skins may buckle with an unsupported length equal to the entire wall height. However, considering that there exists a mechanical bond (even without mesh) between the plaster and the straw, it stands to reason that the straw must be providing some lateral support to the plaster skins. To consider the possibility of local buckling one may consider each plaster skin to act individually as a column which is laterally braced by the straw. For this situation, the critical buckling load for the column can be calculated from Equation E.1:

Appendix E: Validation of Behaviour Assumptions

$$P_{cr} = \frac{\pi^2 EI}{(kh)^2} \quad \text{E.1}$$

where P_{cr} is the load at which the column will buckle, E is the Modulus of Elasticity of the column material, I is the Moment of Inertia of the column, and kh is the unsupported length of the column. The value of k can be found for a particular column based on the end conditions of the column. For this analysis it will be conservative to assume the column is pin ended, for which $k = 1$. For a particular plastered straw bale, the value of E may be determined for the plaster based on Equation 3.1, and I can be calculated based on the plaster dimensions where $I = Lt_p^3/12$. Thus a relationship between P_{cr} and kh for a particular plastered straw bale assembly may be determined.

Furthermore, as discussed in Chapter 2, in order to prevent buckling of the plaster skins, the bond between the plaster and straw must be sufficient to provide lateral support equal to 5% of the applied load. Thus, the area of the bond region multiplied by the bond strength (in MPa) must equal 5% of the applied load. Re-arranged, the height of plaster required to provide the necessary lateral load may be described as:

$$h' = \frac{0.05P}{S_B L} \quad \text{E.2}$$

where P is the applied load, S_B is the bond strength, L is the length of the plaster skin, and h' is the height of straw required to provide the necessary lateral support.

Appendix E: Validation of Behaviour Assumptions

If it is assumed that the load on the plaster skin column is increased until buckling occurs, then P will equal P_{cr} . In addition, in order for buckling to occur, the column height (h) must be less than the height required to provide necessary lateral load (h') (thus indicating insufficient lateral support). Therefore, if P is set equal to P_{cr} and h' is set equal h , it is possible to determine the point at which buckling will first be initiated. As a result, Equations E.1 and E.2 can be simplified giving Equation E.3:

$$P_{cr}^3 = 33.3\pi^2 Et_p^3 \left(\frac{S_B}{k} \right)^2 L^3 \quad \text{E.3}$$

It is important to check the values of P_{cr} found using both Equation E.1 and Equation E.3. If the value from Equation E.1 is found to be greater than the value from Equation E.3 it indicates that h' is greater than the true specimen height h . As such, Equation E.3 becomes invalid in this situation and the value calculated from Equation E.1 shall be taken as the critical buckling load. If the value from Equation E.3 is found to be greater than the value from Equation E.1 it indicates that h' is less than the true specimen height h . As such, Equation E.3 remains valid and the value calculated from Equation E.3 shall be taken as the critical buckling load. Simply put, the critical buckling load shall be taken as the greater of the two values calculated from Equations E.1 and E.3.

In order to use Equation E.3 the bond strength for the plastered straw bales must be determined. Based on the values found in the literature, the bond strength for on-edge bales can be assumed to range from 5 kPa to 19 kPa, while the bond

Appendix E: Validation of Behaviour Assumptions

strength for flat bales can be assumed to range from 15 kPa to 58 kPa (Smith and MacDougall, 2008). If the worst case scenario is assumed, and it is assumed that the bond strength for on-edge bales is 5 kPa while the bond strength for flat bales is 15 kPa, then the critical buckling load can be calculated for each set of tests as described above, and this value can be taken as the theoretical ultimate strength. It is important to note that the value calculated for P_{cr} corresponds to the load on one of the plaster skins (one individual column), and thus the value must be doubled to determine the load on an entire plastered straw bale.

E.2.3 Global Buckling

The potential of global buckling of a plastered straw bale wall has been identified in the literature as discussed in Chapter 2. In this situation, while the straw may adequately support the plaster skins eliminating the potential for local buckling, the entire wall assembly can be considered as a column which may buckle as a whole with zero lateral support. Thus, Equation E.1 may be used for this analysis where P_{cr} is the load at which the column will buckle, E is the Modulus of Elasticity of the column material, I is the Moment of Inertia of the column, and kh is the unsupported length of the column. The value of k can be found for a particular column based on the end conditions of the column. For this situation it will be conservative to assume the column is fixed at one end (the base) and free at the other (the top), such that $k = 2$. For a particular plastered straw bale, the value of E may be determined for the plaster based on Equation 3.4, and I can be calculated

Appendix E: Validation of Behaviour Assumptions

based on the assembly dimensions (accounting only for the plaster) using Equation

E.4:

$$I = \frac{L((2t_p + W_s)^3 - W_s^3)}{12} \quad \mathbf{E.4}$$

where t_p is the thickness of the plaster (in mm), L is the length of the plaster skin (in mm), and W_s is the width of the straw bale (in mm).

E.2.4 Analysis

Based on Equations E.1, E.3, and E.4 the load required to buckle a plastered straw bale wall assembly with given properties can be determined. These values are presented in Table E.1, which provides the buckling loads calculated for each of the concentric compression specimens tested in this Thesis. Note that the theoretical strengths do not consider the compressive resistance of the straw. Also note that for the theoretical buckling strengths, the value in bold is the governing buckling strength. The greater of the two local buckling values will govern local buckling, while the smaller value between global and local buckling will govern the overall buckling behaviour. It was found for all configurations presented in this thesis, that the buckling load was higher than the failure load calculated based on the compressive failure of the plaster, and thus buckling will not theoretically govern the failure of the concentrically loaded specimens.

E.3 Analysis of Straw/Plaster Interface and Shear Distortion

It was assumed that the bond between the straw and the plaster was adequate to ensure that there was no slippage between the straw and the plaster at the straw/plaster interface and that the straw did not undergo shear distortion. These issues are illustrated in Figures 2.9 and 2.10. Furthermore, because of the configuration of the loading it is expected that plane sections will remain plane for the duration of the experiment. Essentially, it is expected that because shear stress was not applied to the specimens, they will not undergo shear distortion or slippage at the straw/plaster interface. This was discussed in Chapter 2, and is further discussed below.

For one of the 1.05 m eccentrically loaded specimens, PIV was used to determine the vertical displacements of points on either side of the straw/plaster interface (in the straw and in the plaster) in order to validate the assumption that slippage does not occur at the straw/plaster interface. This was done for a number of points from the base of the specimen to the top, for the two plaster skins of the specimen. The difference between the plaster vertical deflection and the straw vertical deflection for a number of points for the two plaster skins over the entire height of the specimen, are plotted in Figure E.1. Ideally, the difference between the plaster vertical deflection and the straw vertical deflection would be zero for all points. It can be seen from Figure E.1 that this is not the case.

The differences in the plaster and straw vertical deflections range from -1.0 mm to +0.6 mm. The data is scattered about 0.0 mm. While there appears to be some slippage, the magnitude of the slippage is small for all points. It is important to

Appendix E: Validation of Behaviour Assumptions

note that the measured deflections and the scatter in the data are likely a result of two separate issues. Firstly, the precision of the PIV is ± 0.1 mm, and thus it is expected that there would be some scatter about the expected 0.0 mm slippage. Secondly, there is not expected to be great accuracy in the straw deflection measurements. This is because the straw is quite loose and likely to shift significantly during the testing, even if slippage is not occurring, and because the straw extended beyond the plaster skins, and thus the points which were used for the PIV analysis were not directly connected to the plaster, but rather are an estimate of the behaviour of the straw which was connected to the plaster. Despite the potential inaccuracies and the lack of precision, it does appear from Figure E.1 that there was no significant slippage at the straw/plaster interface.

Further validation that slippage of the straw/plaster interface did not occur is provided by the correlation between the experimental and theoretical vertical load-deflection plots presented for the eccentric specimens in Chapter 6. These plots present the deflection of the plaster skins, and validation is provided because the experimental results correlated with the theoretical results which assumed there was no slippage. Essentially, the correlation between the experimental results indicates that the specimens deformed as shown in Figure 2.8, rather than slipping as shown in Figure 2.9.

A similar argument can be made to validate the assumption that the straw did not deform with shear distortion. Because Chapter 6 showed that the specimens behaved as theoretically expected (Figure 2.8), then it can be stated that the straw did not deform with shear distortion as shown in Figure 2.10.

Appendix E: Validation of Behaviour Assumptions

Table E.1: Theoretical Strength Analyses

Plaster Thickness (mm)	Plaster Strength (MPa)	Wall Height (mm)	Exp. Strength (kN/m)	Theoretical Strengths (kN/m)			
				Comp. Failure	Buckling Failure		
					Local (Eq. E.1)	Local (Eq. E.3)	Global
25	1.43	330	59.1	71.5	276.1	106.3	61224.9
			57.6				
			61.2				
25	1.12	330	51.8	56.0	216.2	98.0	48030.7
			31.8				
			57.4				
25	0.80	330	49.3	40.0	154.4	87.6	3407.7
			48.4				
			31.6				
13	1.43	330	34.7	37.2	38.8	55.3	30109.7
			38.2				
			33.2				
38	1.43	330	82.7	108.7	969.5	161.6	99066.3
			68.6				
			91.5				
23	0.660	990	28.1	30.4	11.0	75.6	2866.0
	0.806		31.8	37.1	13.5	80.8	3499.9
	0.925		36.3	42.6	15.5	84.6	4016.7
23	0.775	2310	35.8	35.7	2.4	79.7	618.1
	0.764		36.8	35.1	2.3	79.4	609.3
	0.645		37.3	29.7	2.0	75.0	514.4
23.2	0.803	330	41.4	37.3	123.9	81.4	31685.2
22.8	1.030		62.1	47.0	150.8	86.9	39865.7
24.2	0.909		55.7	44.0	159.2	88.5	37591.9
17.8	0.836	1050	37.7	29.8	5.8	63.3	2436.3
20.6	0.848		43.5	34.9	9.0	73.6	2898.6
22.2	0.885		41.7	39.3	11.8	80.4	3285.0

Appendix E: Validation of Behaviour Assumptions

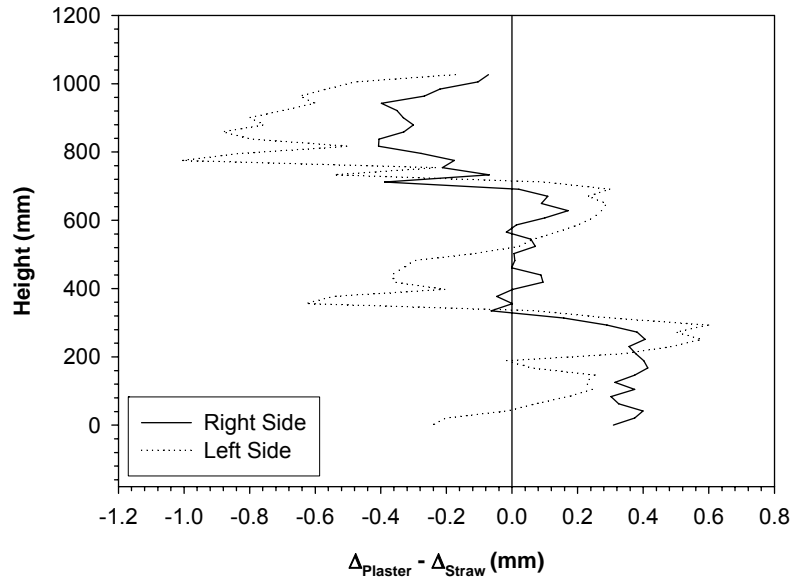


Figure E.1: Slippage at Straw/Plaster Interface

Appendix F: Analysis of Assembly Plaster Thickness

F.1 Introduction

It was recognized that, for a variety of reasons, the in-situ plaster thickness of the plastered straw bale wall assembly specimens varied from the designed thickness. In order to understand the variability in the in-situ plaster thickness, thickness measurements were made following testing of the specimens presented in Chapter 6. This Appendix describes the procedure and results for the measurement of the in-situ plaster thickness of plastered straw bale wall assembly specimens.

F.2 Procedure

Following testing of the plastered straw bale wall assemblies presented in Chapter 6, the following steps were followed to determine the thickness of the plaster skins:

Appendix F: Analysis of Assembly Plaster Thickness

1. A number of holes were drilled through the plaster skins. 15 holes were drilled for each plaster skin of the 330 mm specimens while 45 holes were drilled for each plaster skin of the 1050 mm specimens.
2. A bolt was pushed into the hole with the wide end pushed through first.
3. The bolt was then slowly pulled back out of the hole until the head of the bolt caught on the inside of the plaster skin. This can be seen in Figure F.1.
4. The point on the bolt which was in-line with the outside of the plaster skin was marked, and the bolt was removed from the hole.
5. The distance between the marked point on the bolt, and the base of the head of the bolt was then measured, and this was taken as the thickness of the plaster at the location of the hole.

This procedure was performed for each hole drilled into the specimens. Due to the un-evenness of the inside face of the plaster skins and the imprecision and inaccuracy associated with the measurement technique it is expected that this measurement technique provided thickness measurements accurate to +/- 3 mm.

F.3 Results

The measurement procedure resulted in five measurements at three different heights (15 total) for each side of the 330 mm specimens and five measurements at nine different heights (45 total) for each side of the 1050 mm specimens. For each side of every specimen the average plane thickness was determined at each height

Appendix F: Analysis of Assembly Plaster Thickness

by averaging the five measurements at the particular height. Thus, for each specimen, the average failure-plane thickness was determined as the minimum average plane thickness for the specimen.

Because the failures were observed to occur along a horizontal plane, it is the average thickness of plaster along this plane which will govern the failure of the specimen. However, the true average thickness of this failure region is not possible to determine due to crushing of the plaster. Thus, the above method for determining the average failure-plane thickness will provide a best estimate of the true average failure-plane thickness

Table F.1 presents the average thickness of each specimen. In addition, Table F.1 presents the average failure-plane thickness of each specimen, as noted above. Finally, Table F.1 presents the failure-side average failure-plane thickness of each eccentrically loaded specimen. This value is the minimum plane thickness for the plaster skin which was subjected to the greatest compressive stress due to the eccentricity. Note that for the 330 mm specimens the average thickness was 30 mm and the average of the average failure-plane thicknesses was 27 mm, while for the 1050 mm specimens the average thickness was 30 mm and the average of the average failure-plane thicknesses was 23 mm.

To show the variation in the plaster thickness for the specimens Figures F.2 to F.13 provide contour plots showing the thicknesses of the specimens. Figures F.2a to F.13a present the failure sides of the specimens, while Figures F.2b to F.13b present the non-failure sides of the specimens.

Appendix F: Analysis of Assembly Plaster Thickness

Table F.1: Summary of Plaster Thicknesses

Test Name	Average Thickness (mm)	Average Failure-Plane Thickness (mm)	Average Failure Side Failure-Plane Thickness (mm)
E11	31	28	28
E12	29	24	27
E13	33	29	34
E31	31	23	26
E32	30	26	26
E33	32	26	27
C11	27	23	23
C12	29	23	23
C13	30	24	24
C31	28	18	18
C32	27	21	21
C33	31	22	22

Appendix F: Analysis of Assembly Plaster Thickness

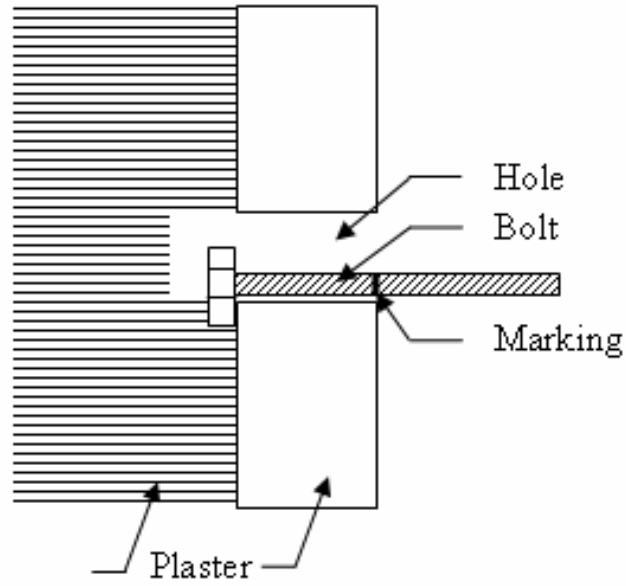


Figure F.1: Measurement of Plaster Thickness

Appendix F: Analysis of Assembly Plaster Thickness

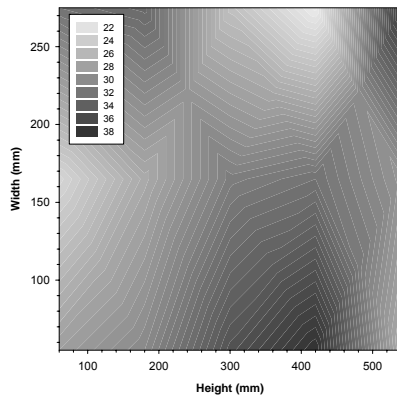


Figure F.2a: E11 Failure Side

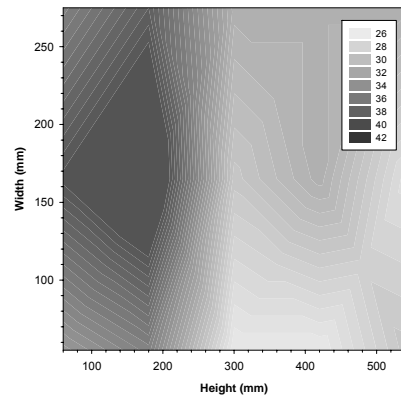


Figure F.2b: E11 Non-Failure Side

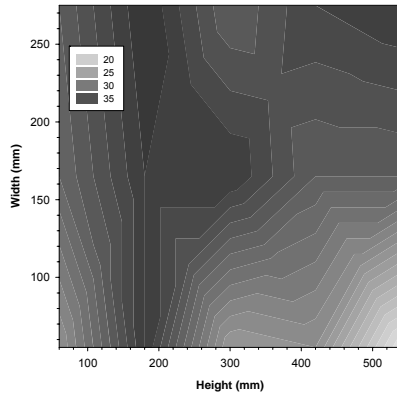


Figure F.3a: E12 Failure Side

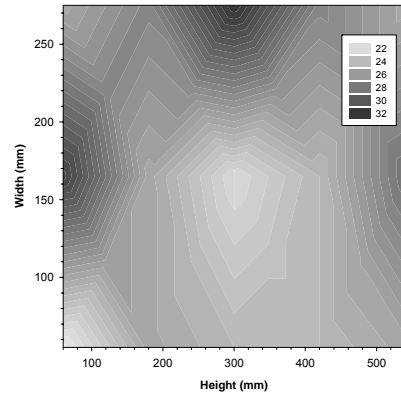


Figure F.3b: E12 Non-Failure Side

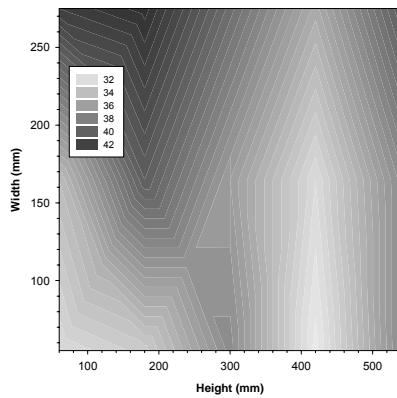


Figure F.4a: E13 Failure Side

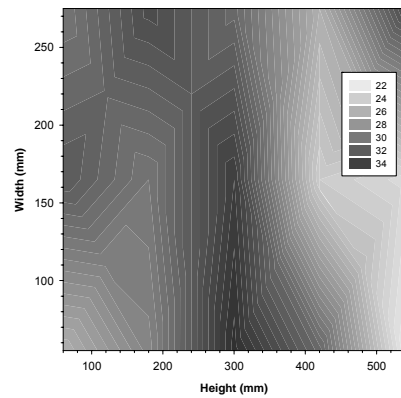


Figure F.4b: E13 Non-Failure Side

Appendix F: Analysis of Assembly Plaster Thickness

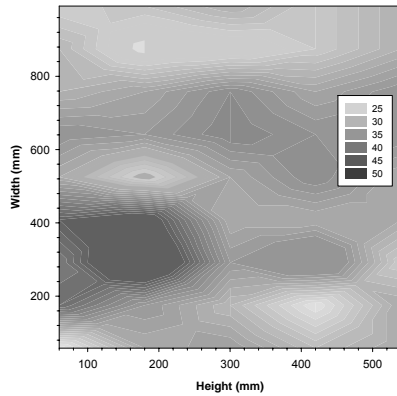


Figure F.5a: E31 Failure Side

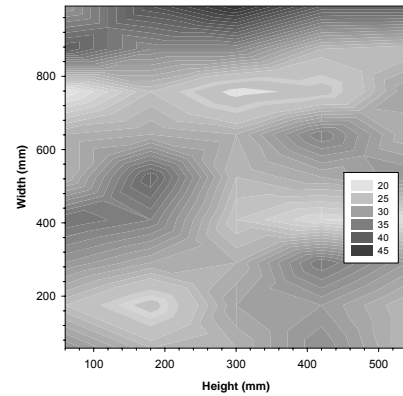


Figure F.5b: E31 Non-Failure Side

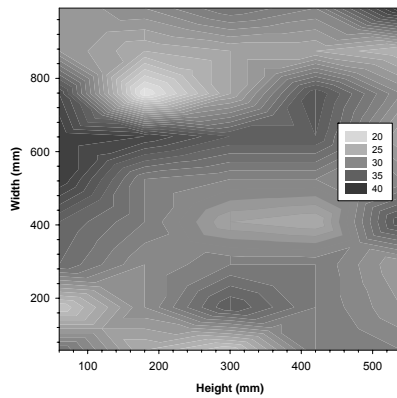


Figure F.6a: E32 Failure Side

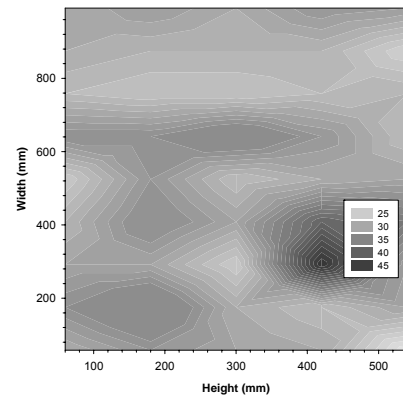


Figure F.6b: E32 Non-Failure Side

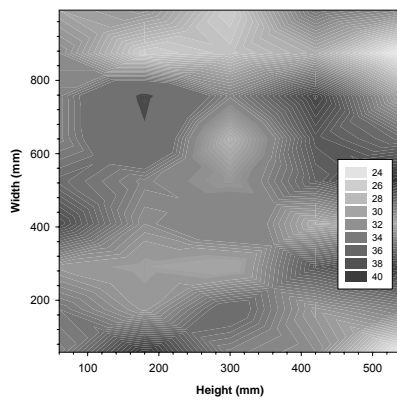


Figure F.7a: E33 Failure Side

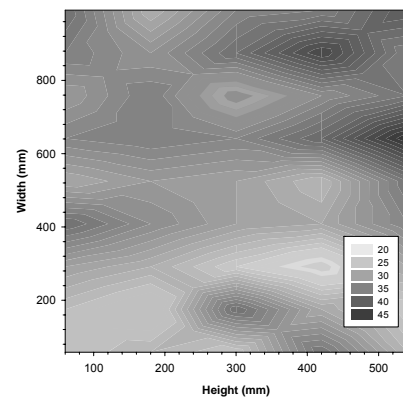


Figure F.7b: E33 Non-Failure Side

Appendix F: Analysis of Assembly Plaster Thickness

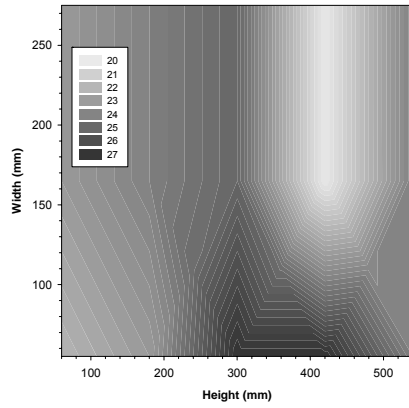


Figure F.8a: C11 Failure Side

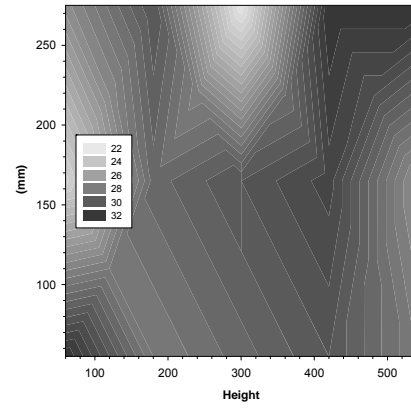


Figure F.8b: C11 Non-Failure Side

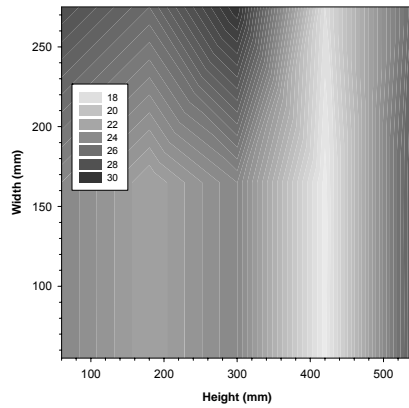


Figure F.9a: C12 Failure Side

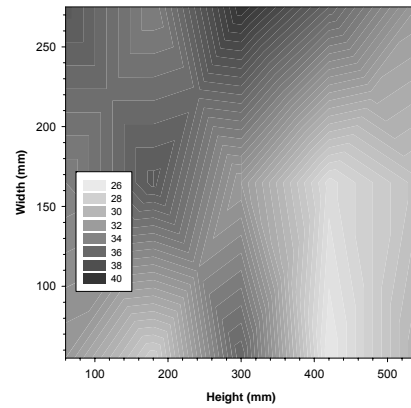


Figure F.9b: C12 Non-Failure Side

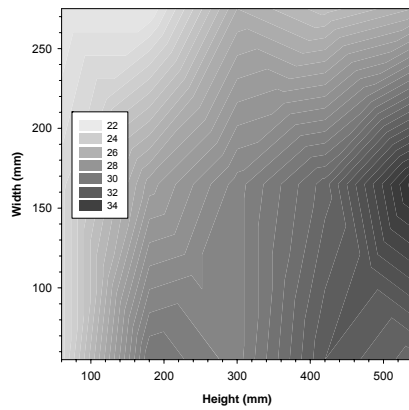


Figure F.10a: C13 Failure Side

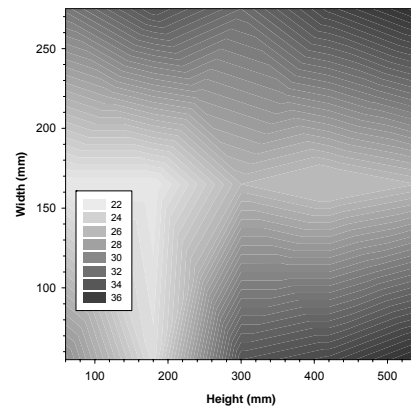


Figure F.10b: C13 Non-Failure Side

Appendix F: Analysis of Assembly Plaster Thickness

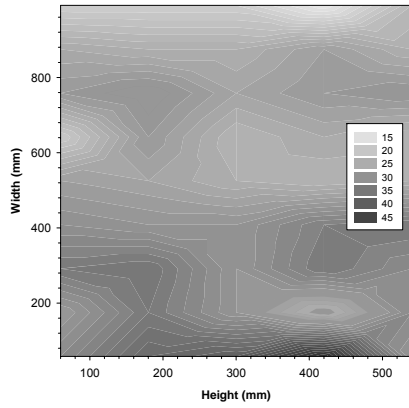


Figure F.11a: C31 Failure Side

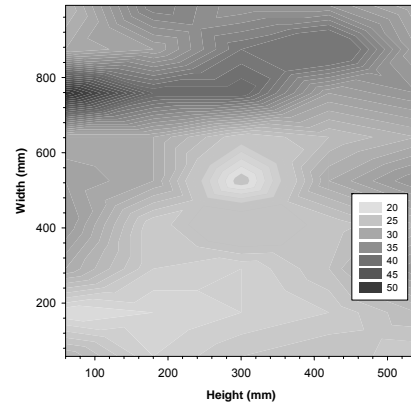


Figure F.11b: C31 Non-Failure Side

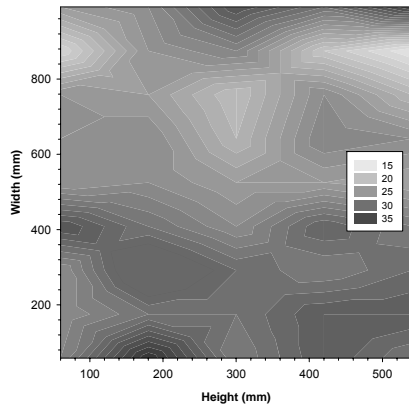


Figure F.12a: C32 Failure Side

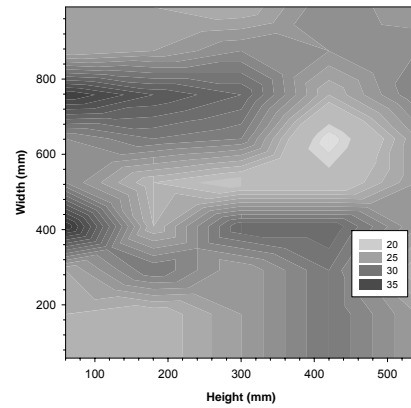


Figure F.12b: C32 Non-Failure Side

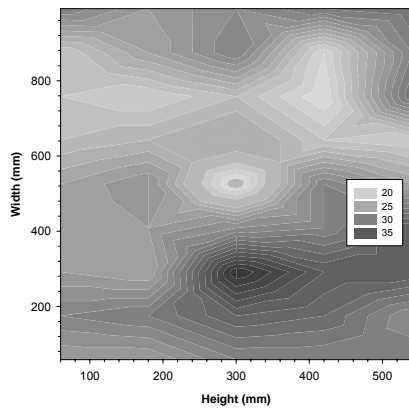


Figure F.13a: C33 Failure Side

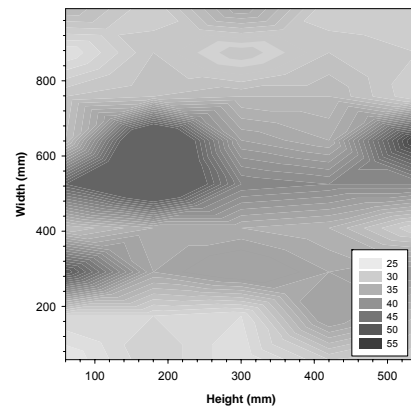


Figure F.13b: C33 Non-Failure Side

Appendix G: LP Measurement Correction

G.1 Introduction

It was noted in Chapter 5 that during testing, the HSS sections running along the top and bottom of the plaster skins deformed under load. The LPs capturing the vertical deflections were situated such that they measured the displacement of the top of the steel sections, at the top of the specimens. Because of this configuration the LPs captured the deflections in the HSS sections in addition to the vertical deformation of the wall. This is shown in Figure G.1. Note that Figure G.1 is a simplification as it shows only the plaster and the portion of the steel jig bearing on the plaster.

In order to account for this phenomenon, a correction was found for the LP measurements to account for the deflection of the steel jig. The methods of determination and utilization of the correction are presented in this Appendix.

G.2 Procedure for Correction Determination

A control experiment was conducted to determine the correction for the LP data. For the control experiment, aluminum plates were placed in the testing jig where the plaster skins would typically be located. This setup is shown in Figure G.2. The aluminum was then compressed in the jig utilizing the same procedure as was used for the plastered straw bale assembly specimens. The LPs recorded the deflections in the same manner as was used for the plastered straw bale assembly specimens. Once the test was completed, the deflection as a result of deformation of the steel jig was determined by subtracting the LP data from the theoretical deflection.

Because the properties of the aluminum were known in advance, it was possible to determine the exact theoretical load-deflection response for the aluminum in the jig based on Equation G1:

$$\Delta_A = \frac{P_A L_A}{A_A E_A} \quad \text{G.1}$$

where Δ_A is the theoretical aluminum deflection, P_A is the applied load, L_A is the height of the aluminum plates (75 mm), A_A is area of the aluminum upon which the load was applied (2x25 mm x 600 mm), and E_A is the Modulus of Elasticity of the aluminum (70 GPa).

For the range of applied loads, the theoretical deflections were subtracted from the LP deflection readings in order to determine the difference between the measured LP deflections and the true specimen deflection. This difference is the

Appendix G: LP Measurement Correction

correction factor which must be applied to the LP data to determine the true deflection results. The correction value with respect to the applied load is plotted in Figure G.3. A regression was performed to fit a cubic polynomial to the data resulting in the following relationship, with R^2 value of 0.998:

$$Corr = 7.95 \times 10^{-3} P + 3.68 \times 10^{-4} P^2 - 2.79 \times 10^{-6} P^3 \quad \mathbf{G.2}$$

where $Corr$ is the correction amount and P is the applied load. Equation G.2 gives the amount which must be subtracted from the LP deflection readings in order to obtain the true specimen deflection values. Essentially, Equation G.2 provides the unintended deflection of the jig for a given load.

The correction equation (G.2) was used to modify the LP results to remove the additional deflection recorded as a result of deformation of the jig. This procedure was used for all LP results presented using the steel jigs.

For the eccentric specimens, separate correction factors were determined. For this case, there were separate correction factors for each side of the specimen. These related the correction required for each side to the load applied to the specimen. These correction factors are (with R^2 values of 0.996 and 0.992 respectively):

$$Corr_{EccFail} = 5.72 \times 10^{-2} P - 1.80 \times 10^{-4} P^2 + 5.50 \times 10^{-8} P^3 \quad \mathbf{G.3}$$

$$Corr_{EccNonFail} = 6.70 \times 10^{-2} P - 1.01 \times 10^{-3} P^2 + 7.30 \times 10^{-6} P^3 \quad \mathbf{G.4}$$

Appendix G: LP Measurement Correction

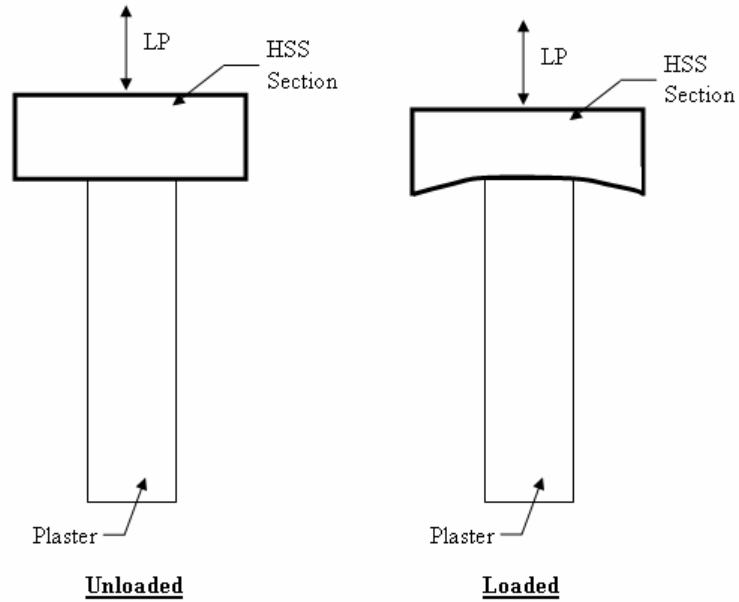


Figure G.1: Diagram of Deformation in HSS Section

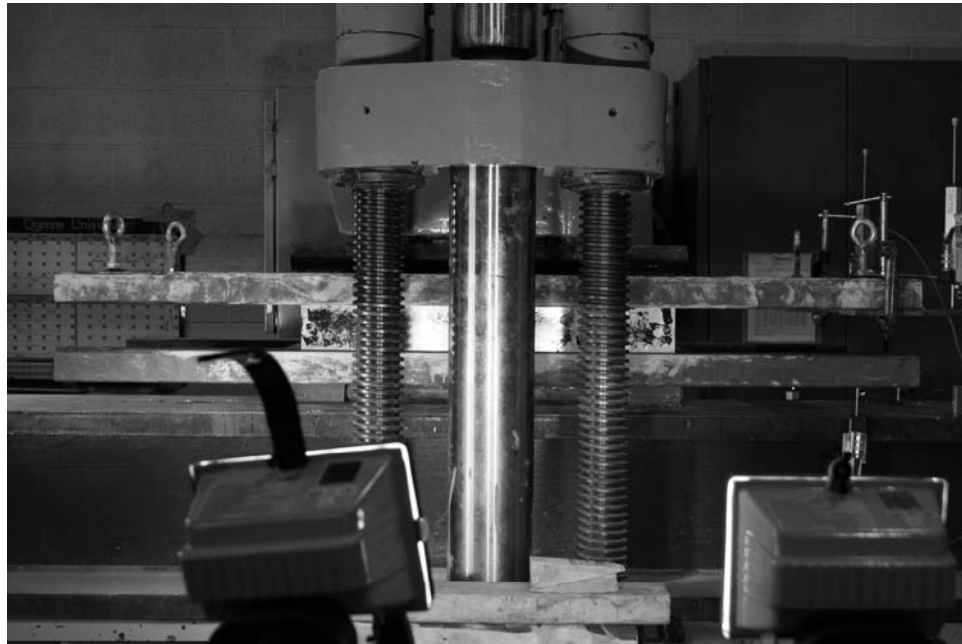


Figure G.2: Aluminum Plates in Testing Jig

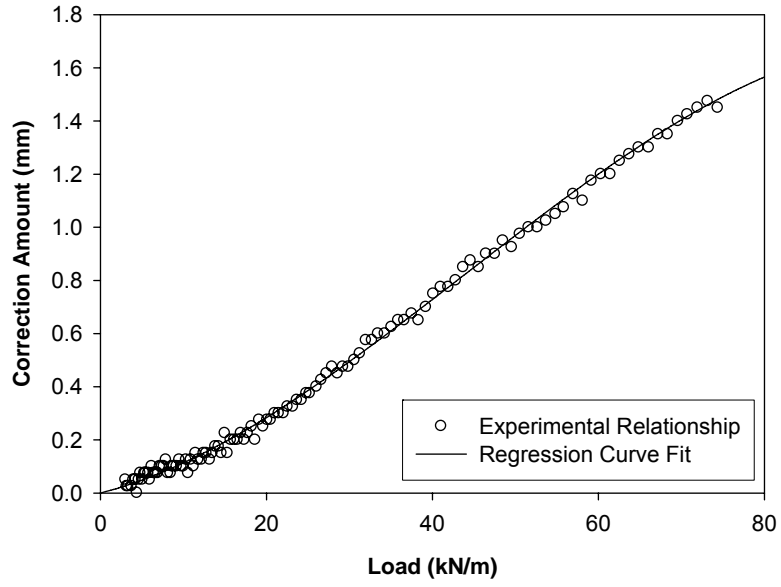


Figure G.3: Correction Amount

Appendix H: Eccentric Model Coding

H.1 Introduction

Chapter 6 presented a theoretical model for the behaviour of plastered straw bale wall assemblies subjected to eccentric compressive load. In order to perform the analysis of plastered straw bale wall assemblies of varying configurations, the model presented in Chapter 6 was coded in Matlab. The Matlab coding is presented in this Appendix, with notation provided to explain the code. The main program was entitled “compmodel2.m”. Two sub-programs entitled “stress.m” and “stressx.m” were also created. These sub programs represent the stress-strain relationships utilized to calculate the load and moment as described in the main program. The coding for both sub-programs is also provided.

H.2 Main Program

```

C:\Matlab7\work\Final Model\compmodel2.m
March 4, 2009
Page 1
4:41:09 PM

function compmodel2 % Model for prediction behaviour of eccentric compression

clear

%Initial settings
done = 0; %becomes 1 when completed
format('short') %Determines format for number display
output = 1; %Turns output on or off. 1 = on, 0 = off.

%INPUT PARAMETERS
%-----
filetemplate = 'Template.xls'; %Template file for excel output
filesave = 'Trial.xls'; %Name for file to save data

%Input Wall Dimensions and Plaster Properties
global h
h = 2310; %Wall Height (mm)
global l
l = 600; %Wall Length (mm)
global pt
pt = 23; %Plaster Thickness (mm)
global st
st = 455-2*pt; %Straw Thickness (mm) - assume overall thickness of 455 and subtract plaster thickness
global ps
ps = 0.783; %Plaster Strength (MPa)
global pm
pm = ps*818; %Plaster Moduli (MPa) - function of plaster strength
ei = 4.0; %Initial eccentricity (mm) - must be > C
global Plim
Plim = 40000; %Max Limit of Load (N) - Typically set this very high and the model will continue to run
until the wall "fails", as long as failure is less than max value
Pinc = 100; %Size of Load Increments (N). Model will increment load by this value up to max or until
all "failure" occurs. Higher number is more accurate but slower analysis
increments = 2500; %Number of increments for analysis of strain profile. Strains are incremented until
strain value matching given load and moment is found. Higher number is more accurate but slower analysis
tol = 1; %Load tolerance. Program increments strains until load equals actual value. 'tol' tells it
how close to the actual value is close enough. Smaller value is more accurate but slower analysis
vertinc = 20; % Vertical Increments (must be even number). From base to top of wall, there will be
vertinc number of points of evaluation. Higher value will yield more accurate results but take longer
for analysis
%-----
%END OF INPUT PARAMETERS

%SET UP ANALYSIS
%-----
copyfile(filetemplate,filesave); %Create file to save to based off of template file

%Set initial eccentricity for all evaluation points. This will equal the defined initial eccentricity
.
%Also define 'deltaec' which tracks horiz deflection for each load increment and adds it to the eccentricity 'ec' after each load increment.
for i = 1 : vertinc
    ec(i) = ei; %Initial Eccentricity (mm)
    deltec(i) = 0; %Eccentricity increment (mm) will add 'e' from defelections (deltaec) to initial
    (ei) as model progresses to account for more eccentricity from deflection.
end

global P
P = 0; %Will hold the current load value, increases by Pinc as model progresses

global e1
e2=e1
%The will define the strain profile as it is incremented for each P
e1 refers to the strain at the extreme fibre of the non-failure side while e2 refers to the
strain at the extreme fibre of the failure side

```

Appendix H: Eccentric Model Coding

```
C:\Matlab7\work\Final Model\compmodel2.m                                     Page 3
March 4, 2009                                                                4:41:09 PM

%Track time - Used for the display and output - keeps track of model run-time
starttime = fix(clock);
currenttime = fix(clock);
global timeelapsed
timeelapsed(1) = starttime(4)-currenttime(4);
timeelapsed(2) = starttime(5)-currenttime(5);
timeelapsed(3) = starttime(6)-currenttime(6);

% Variables for counting and tracking progress
global count1disp
count1disp = 0;
global count2disp
count2disp = 0;
global count3disp
count3disp = 0;

%Based on the parameters given, the plaster will have a defined stress-strain curve with maximum stress
equal to 'ps'. We will now find the strain at this stress.
global maxstrain
ystress = @(xstrain)xstrain.*ps.*331.4./(0.405+(xstrain./0.00424).^1.405); %Plaster Stress-strain relationship
xystress = @(xstrain)ps.*331.4./(0.405+(xstrain./0.00424).^1.405); %Plaster stress-strain relationship
negystress = @(xstrain)-(xstrain.*ps.*331.4./(0.405+(xstrain./0.00424).^1.405)); %Negative stress-strain relationship
%We need to find the maximum of the previous equation, but matlab only has functions to find minimum, so we invert it).
maxstrain = fminbnd((negystress),0,1) %Find strain at minimum value (max stress)

format('bank')%change the number display format

strain1 = 0; %Will hold the strain values from the previous load step, thus, starts at 0

for P = Pinc:Pinc:Plim %Repeats for every load increment
P %Display load, so we can see where we are at
result = 0; %Will store the final values for P, e (eccentricity) and M
ec = ec + deltec; %Eccentricity at all evaluation points. For all evaluation points we add horizontal

C:\Matlab7\work\Final Model\compmodel2.m                                     Page 4
March 4, 2009                                                                4:41:09 PM

displacement from previous step to eccentricity
strain2 = 0; %Will hold the strain values as we try to determine which one is appropriate for given load and eccentricity
%-----
%END OF SET UP ANALYSIS

%First step is to find various combinations of e1 and e2 which give appropriate P, then find which combination gives appropriate M

%BEGINNING OF ANALYSIS STEP 1 - FIND VARIOUS STRAIN PROFILES FOR GIVEN P
%-----
%This step will determine e1 and e2 for a particular load. e1 and e2 define the strain profile, where e1 is the smallest strain and e2 is the largest strain on the section
count = 0; %Indicie for storing the different strain combinations which will give P (data points)
dispcount = 0;
countdown1 = increments;%Counter
for emin = maxstrain/increments:maxstrain/increments:maxstrain %Vary min strain (basically e1) from near zero to max strain.
    %For each value of min strain, we find the max strain (e2) value which will give our desired load
    if count <= 0 %No data points found yet
        emax = maxstrain;
    else
        emax = emaxmax; %If we have found a data point, and now we have increased e1, then e2 cannot be larger than emaxmax from previous iteration. This is because if we just incremented e1 up, then for the same load, e2 must increment down
    end
    %if e1 = minstrain and e2 = maxstrain, this will give greatest possible load based on the set value of minstrain
    %if e1 and e2 both = minstrain, this will give the smallest possible load based on the set value of minstrain
    e1=emin; e2=emax; Pmax = 1*(quad('stress',0,pt) + quad('stress',pt+st,2*pt+st)); %These steps integrate the stress profile based on given strains to find the load
    e1=emin; e2=emin; Pmin = 1*(quad('stress',0,pt) + quad('stress',pt+st,2*pt+st));
    if Pmax >= P & Pmin <= P % If actual load is within min and max, there will be a strain combination
```

Appendix H: Eccentric Model Coding

```

C:\Matlab7\work\Final Model\compmodel2.m                                     Page 5
March 4, 2009                                                                4:41:09 PM
on with e1 = emin and e2 = something between emin and emax
    % We will hold the min strain constant now and find what max strain will give us the appropriate P
te P
    count = count + 1; %We will have a strain combination which gives us the desired P, thus we increment
    the indice to store the values
    strain2(count,1) = emin; %Store the min strain value (e1) and now find max strain value
    %e2 is somewhere between emin and emax
    emaxmin = emin; %minimum value of max strain
    emaxmax = emax; %maximum value of max strain
    while Pmax - Pmin > tol % Until we are close to P - search for correct value of max strain
        emax = mean([ emaxmin,emaxmax] );
        %find the load when the max e is between the min and max possible values
        e1=emin; e2=emax; Pmid = l*(quad('stress',0,pt) + quad('stress',pt+st,2*pt+st)); % Find load
        ad between max and min
        if Pmid >= P % So we decide if the calculated load is above or below the desired value, then
        we can redefine the min and max possible values narrowing the bracket with each step
            Pmax = Pmid;
            Pmin = Pmid;
            emaxmax = emax;
            emaxmin = emaxmin;
        else
            Pmax = Pmax;
            Pmin = Pmid;
            emaxmax = emaxmax;
            emaxmin = emax;
        end
        end
        strain2(count,2) = mean([ emaxmin,emaxmax] ); % When P is close, define e2 as the average of the
        max and min emax
        end
        countdown1 = countdown1 - 1; % And now we bump e1 up a little higher and search for a new combination
        ion
        dispcount = dispcount + 1;
        countldisp = (increments - countdown1)/increments*100;

C:\Matlab7\work\Final Model\compmodel2.m                                     Page 6
March 4, 2009                                                                4:41:09 PM
    %Display time etc.
    if dispcount > increments / 100 -1
        dispcount = 0;
        currenttime = fix(clock);
        timeelapsed(1) = currenttime(4)-starttime(4);
        timeelapsed(2) = currenttime(5)-starttime(5);
        timeelapsed(3) = currenttime(6)-starttime(6);
    end
end
if count <= 0 %No combination found that gave us 'P' - Note it is possible that our load increment was
too small, so we must always have many more strain increments than load incements.
    done = 1;
end
%-----
%END OF ANALYSIS STEP 1

% Now we find which strain profile for 'P' also correspond to 'M' for each evaluation point

%BEGINNING OF ANALYSIS STEP 2 - FIND WHICH STRAIN PROFILE GIVES DESIRED M
%-----
countdown2 = length(ec);
M = P.*(ec+(pt + st./2)); %Desired Moment at each evaluation point (with P and ec)
%Note that desired moment is different for each evaluation point because eccentricity different for each
evaluation point as a result of horizontal deflections
for i = 1 : length(ec) %Must complete this step for each evaluation point
    e1 = strain2(1,1); %Check first strain combo, corresponding to max moment (first strain combo)
    e2 = strain2(1,2);
    if l*(quad('stressx',0,pt) + quad('stressx',pt+st,2*pt+st)) < M(i) %This equation calculates the moment
    from the strain combo
        %If strain combo does not give large enough moment, the moment is unobtainable, thus model is
done
        done = 1;
        break
    end
end

```

Appendix H: Eccentric Model Coding

C:\Matlab7\work\Final Model\compmodel2.m
March 4, 2009

Page 7
4:41:09 PM

```
else
    %Find which strain combo gives the appropriate moment
    sizestrain2 = size(strain2);
    for j = 1 : sizestrain2(1);%Calculate moment from each strain profile
        e1 = strain2(j,1);
        e2 = strain2(j,2);
        if l*(quad('stressx',0,pt) + quad('stressx',pt+st,2*pt+st)) < M(i)
            %The strain profiles are organized such that each stored profile will give decreasing
            moment, thus when one profile gives moment greater than desired and next profile gives moment less than
            desired we have found the right profile
            break %save e1, e2
        end
    end
    E2(i,1) = e1; %Store these as our answers! :) E2 store the correct e1 and e2 for each load step
    E2(i,2) = e2;
    countdown2 = countdown2-1; %move on to next evaluation point as they all have different eccentricity,
    thus different moment
    count2disp = (length(ec) - countdown2)/length(ec)*100;
    currenttime = fix(clock); %Clock stuff
    timeelapsed(1) = currenttime(4)-starttime(4);
    timeelapsed(2) = currenttime(5)-starttime(5);
    timeelapsed(3) = currenttime(6)-starttime(6);
end
if done >= 1
    break
end
%-----
%END OF ANALYSIS STEP 2
```

% Because we only want to deal with incremental strain (strain change between load steps) we need to find strain profiles with given eccentricity and previous load

%BEGINNING OF ANALYSIS STEP 3 - FIND STRAINS FOR PREVIOUS LOAD AND CURRENT ECCENTRICITY

C:\Matlab7\work\Final Model\compmodel2.m
March 4, 2009

Page 8
4:41:09 PM

```
%-----
if strain1 <= 0 %Basicly, we ask if this is our first load step
    E1(i,1) = 0;%If it is, our answers from the previous load step are zero
    E1(i,2) = 0;%E1 stores previous strains
else
    %We need to subtract the strains from 0 load to P-Pinc. because we only want to find the strains from
    P-Pinc to P (ie, for the current load step). At the end we add strains from each load step
    %Same procedure as previous step in analysis
    countdown3 = length(ec);
    M = (P-Pinc).*(ec+(pt + st./2)); %Moment
    for i = 1 : length(ec) %For each evaluation point
        e1 = strain1(1,1); %Check first strain combo, corresponding to max moment
        e2 = strain1(1,2);
        if l*(quad('stressx',0,pt) + quad('stressx',pt+st,2*pt+st)) < M(i) %Strain combo does not give large
        enough moment, thus moment unobtainable
            error('Moment Is Too High');
        else
            sizestrain1 = size(strain1);
            for j = 1 : sizestrain1(1);
                e1 = strain1(j,1); %Calculate moment from each strain profile
                e2 = strain1(j,2);
                if l*(quad('stressx',0,pt) + quad('stressx',pt+st,2*pt+st)) < M(i) %Reached the point where
                e calculated moment goes from greater than to less than actual, found answer
                    break %save e1,e2
                end
            end
            E1(i,1) = e1; %Store these as previous strains
            E1(i,2) = e2;
            countdown3 = countdown3-1; %Move on to our next evaluation point as they all have different eccentricity
            count3disp = (length(ec) - countdown3)/length(ec)*100;
            currenttime = fix(clock);
        end
    end
end
```

Appendix H: Eccentric Model Coding

```

C:\Matlab7\work\Final Model\compmodel2.m
March 4, 2009
Page 9
4:41:09 PM

timeelapsed(1) = currenttime(4)-starttime(4);
timeelapsed(2) = currenttime(5)-starttime(5);
timeelapsed(3) = currenttime(6)-starttime(6);
end
end
%-----
%END OF ANALYSIS STEP 2

%Because we only want to deal with incremental strain (strain change between load steps) we need to find strain profiles with given eccentricity and previous load

%BEGINNING OF RESURTS STEP - PRESENT RESULTS
%-----
%We now have strain profile for each load step and corresponding moment (Stored in E2)
%At each load step we also have a corresponding strain profile for the previous load step with the current eccentricity (Stored in E1)
deltE = E2-E1;%Finds strain increment for each load step, this is what we want.

%Calculate vertical deflections for given P
%Note values are inverted
leftvert(1,1) = 0; %First location (bottom) is zero
leftvert(1,P/Pinc+1) = 0; %First deflection (bottom) is zero
rightvert(1,1) = 0; %First location (bottom) is zero
rightvert(1,P/Pinc+1) = 0; %First deflection (bottom) is zero
for i = 1 : length(ec)
    leftvert(i+1,1) = i*h/vertinc; %Heights in first column
    leftvert(i+1,P/Pinc+1) = leftvert(i,P/Pinc+1) + (deltE(i,1)+(pt/(2*pt+st))*(deltE(i,2)-deltE(i,1)))*h/vertinc; %Other columns contain deflections for each load increment
    %Deflection is calculated by using strain profile to determine strain in plaster skin. Multiply strain by height of vertical increment to find deflection in that vertical increment for the given load increment.
    %Add deflection for one vertical increment to deflection of lower vertical increment.
    %Same procedure for right side
    rightvert(i+1,1) = i*h/vertinc; %Heights in first column

C:\Matlab7\work\Final Model\compmodel2.m
March 4, 2009
Page 10
4:41:09 PM
    rightvert(i+1,P/Pinc+1) = rightvert(i,P/Pinc+1) + (deltE(i,2)-(pt/(2*pt+st))*(deltE(i,2)-deltE(i,1)))*h/vertinc; %Other columns contain deflections for each load increment
end

%Calculate Horizontal deflections
angle = (deltE(:,2)-deltE(:,1))/(2*pt+st); %strain profile slope
horizmax = 0; % Calculate max (mid-height) deflection
for i = 1 : length(ec)/2
    horizmax = horizmax + (h/vertinc)^2*(angle(i)*(2*i-1)/2);
end
%calculate deflections at various heights (calculated for only the heights between (not including) 0 and mid-height, will be mirror image for the rest)
%horizontal deflections are calculated based on the slope of the strain profile
%horizontal deflections are calculated at every evaluation point and for each load increment
for i = 1 : length(ec)/2-1
    horizval(i) = 0;
    for j = i+1 : length(ec)/2
        horizval(i) = horizval(i) + (h/vertinc)^2*(angle(j)*(2*(j-i)-1)/2);
    end;
    horizval(i) = horizmax - horizval(i);
end

horiz(1,1) = 0; %Top location is zero
horiz(1,P/Pinc+1) = 0; %Top deflection is zero
for i = 1 : length(ec)
    horiz(i+1,1) = i*h/vertinc; %Heights in first column
end
horiz(length(ec) + 1, P/Pinc+1) = 0; %Bottom deflection is zero
horiz(length(ec)/2 + 1, P/Pinc+1) = -horizmax; %Middle deflection is max
for i = 1 : length(horizval)
    horiz(i+1,P/Pinc+1) = -horizval(i); %Horizontal displacements for top half
    horiz(length(ec) + 1 - i,P/Pinc+1) = -horizval(i); %Same horizontal displacements for bottom half
end
%-----

```

Appendix H: Eccentric Model Coding

```
C:\Matlab7\work\Final Model\compmodel2.m Page 11
March 4, 2009 4:41:10 PM
%END OF RESULTS STEP

%Results are calculated for each load step, now increment load and repeat

%BEGINNING OF PREPARATION FOR NEXT LOAD STEP
%-----
%Note that results are calculated for each load step, then load is incremented and procedure repeats.
strain1 = strain2; %Define old strain as current strain and find new strain for new load step in a bgn
nd new cycle
for i = 1:length(ec)
    deltec(i) = -(horiz(i,P/Pinc+1) + horiz(i+1,P/Pinc+1))/2; %deltaec is equal to avarage displacement
t from points above and below each evaluation point
end
%This step (above) adds the horizontal deflection from previous load step to the eccentricity

%update time elapsed
currenttime = fix(clock);
timeelapsed(1) = currenttime(4)-starttime(4);
timeelapsed(2) = currenttime(5)-starttime(5);
timeelapsed(3) = currenttime(6)-starttime(6);

end
%-----
%END OF PREPARATION FOR NEXT LOAD STEP

%Analysis is complete. Horizontal and vertical deflections have been found for each load step, at egn
h vertical increment (evaluation point)

%BEGINNING OF OUTPUT
%-----
% Add up deflections for every step and place the sum in the last column - total deflection
for i = 1:length(ec)+1
    leftvert(i,P/Pinc +2) = sum(leftvert(i,:)) - leftvert(i,1);
    rightvert(i,P/Pinc +2) = sum(rightvert(i,:)) - rightvert(i,1);

C:\Matlab7\work\Final Model\compmodel2.m Page 12
March 4, 2009 4:41:10 PM
    horiz(i,P/Pinc +2) = sum(horiz(i,:)) - horiz(i,1);
end

%Prepare to output elapsed time
if timeelapsed(3) < 0
    timeelapsed(3) = timeelapsed(3) + 60;
    timeelapsed(2) = timeelapsed(2) - 1;
end
if timeelapsed(2) < 0
    timeelapsed(2) = timeelapsed(2) + 60;
    timeelapsed(1) = timeelapsed(1) - 1;
end

%Save files
if output >= 1
stringtime = strcat(num2str(timeelapsed(1)), 'h_', num2str(timeelapsed(2)), 'min_', num2str(timeelapsed(2)
), 's');
siminfo = { 'Wall Height:', h, 'mm'; 'Wall Length:', l, 'mm'; 'Straw Thickness:', st, 'mm'; 'Plaster Thickness',
pt, 'mm'; 'Plaster Strength:', ps, 'MPa'; 'Plaster Modulus:', pm, 'MPa'; 'Initial Eccentricity:', ei, 'mm'; 'Lga
d Increments:', Pinc, 'N'; 'Strain Steps:', increments, ' '; 'Max Load:', P, 'N'; 'Simulation Time:', stringtime
, ' ' };
xlswrite(filesave, siminfo, 'Simulation Info');
loads = Pinc:Pinc:P;
headings = { 'Displacements (mm)', 'Loads (kN)', 'Height', 0 };
xlswrite(filesave, headings, 'Left Vertical Disp');
xlswrite(filesave, loads, 'Left Vertical Disp', 'B2');
xlswrite(filesave, leftvert, 'Left Vertical Disp', 'A3');
xlswrite(filesave, headings, 'Right Vertical Disp');
xlswrite(filesave, loads, 'Right Vertical Disp', 'B2');
xlswrite(filesave, rightvert, 'Right Vertical Disp', 'A3');
xlswrite(filesave, headings, 'Horizontal Disp');
xlswrite(filesave, loads, 'Horizontal Disp', 'B2');
xlswrite(filesave, horiz, 'Horizontal Disp', 'A3');
end
```

H.3 Sub-Programs

```

C:\Matlab7\work\Final Model\stress.m
March 4, 2009
Page 1
5:55:01 PM
% Stress-Strain Equation where 'x' is distance through wall in mm. Similar triangles to convert stress-strain to stress-distance
function y = stress(x)

global e1
global e2
global pt
global st
global pm
global ps

y = ps.*331.4.*(e1 + x.*(e2-e1)./(2.*pt+st))./(0.405+((e1 + x.*(e2-e1)./(2.*pt+st))./0.00424).^1.505);

```

```

C:\Matlab7\work\Final Model\stressx.m
March 4, 2009
Page 1
5:55:20 PM
% 'x' * Stress-Strain Equation where 'x' is distance through wall in mm. Similar triangles to convert stress-strain to stress-distance
%For finding moment
function y = stressx(x)

global e1
global e2
global pt
global st
global pm
global ps

y = x.*(ps.*331.4.*(e1 + x.*(e2-e1)./(2.*pt+st))./(0.405+((e1 + x.*(e2-e1)./(2.*pt+st))./0.00424).^1.505));

```

Appendix I: Supplemental Lateral Deflection Plots

I.1 Introduction

Chapter 6 presented the lateral deflection plots for eccentrically loaded 1.05 m specimens. The lateral deflection plots were not provided in that Chapter for the concentrically loaded specimens or the 0.33 m eccentrically loaded specimens. This was because those specimens did not exhibit significant bending, and thus did not deflect laterally to an extent which could be captured accurately by the measurement techniques. The lateral deflection plots for those specimens are presented in this appendix.

I.2 Results

Figures I.1 – I.3 present the lateral deflection plots for the eccentrically loaded 0.33 m specimens, Figures I.4 – I.6 present the lateral deflection plots for the concentrically loaded 0.33 m specimens, and Figures I.7 – I.8 present the lateral deflection plots for the concentrically loaded 1.05 m specimens. Note that Figures

Appendix I: Supplemental Lateral Deflection Plots

I.1a – I.8a present the mid-height lateral load-deflection plots, while Figures I.1b – I.8b present the full-height deflected shape at ultimate load.

Figures I.1 – I.3 also present the theoretical lateral load deflection plots obtained by utilizing the theoretical model for the behaviour of eccentrically loaded specimens presented in Chapter 6. Note that similar to the plots presented in Chapter 6, the eccentric lateral load plots presented in this Appendix provide a theoretical envelope between the “Theoretical” curve and the “Upper Strain Boundary” curve. No theoretical behaviour is presented for the concentric specimens as they will theoretically have zero lateral deflection.

I.3 Discussion

I.3.1 Eccentric 0.33 m Specimens

The theoretical curves for the eccentrically loaded 0.33 m specimens indicate that the specimens are expected to undergo a maximum of approximately 0.1 mm deflection at mid-height at ultimate load, as a result of bending of the specimens. Considering that the precision of the PIV used to measure displacements is +/- 0.1 mm, it is expected that the specimens will exhibit little or no measured displacement.

Figures I.1 – I.3 indicate that there was some displacement measured for the eccentrically loaded 0.33 m specimens. However, it appears as if these lateral displacements were a result of the entire plaster skins shifting, rather than being a result of bending of the specimen. Figure I.1 indicates that both plaster skins shifted approximately 0.5 mm entirely to the left. Both plaster skins exhibited lateral deflections which may be attributed to bending of less than 0.5 mm. Similarly,

Appendix I: Supplemental Lateral Deflection Plots

Figure I.2 indicates that the top of this specimen shifted to the left, with indication that the plaster deflected only about 0.2 mm as a result of bending. Finally, Figure I.3 indicates that the left plaster skin for this specimen shifted approximately 0.2 mm to the left, but that the deflection which may be attributed to bending was less than about 0.3 mm for either plaster skin.

I.3.2 Concentric Specimens

All concentric specimens were expected to have zero lateral deflection. However, lateral deflections were recorded for these specimens. Similar to the eccentrically loaded 0.33 m specimens, these deflections are largely attributed to the shifting of the plaster skins during testing. For all specimens, either the entire specimen or the top of the specimen was observed to shift laterally during testing. Lateral deflections were approximately equal for both plaster skins, indicating an entire shift of the specimen. The deflected shape at ultimate failure of the specimens indicates that bending is not occurring, and that the measured deflections are a result of the specimens shifting in the loading apparatus.

Unusual results are evident for specimen C12, shown in Figure I.5b. The very top and bottom of the specimen appear to have deflected significantly relative to the rest of the specimen. This is most likely a result of the plaster crumbling at the top and bottom of the specimen as ultimate load is just being reached. This crumbling results in erroneous PIV data where the crumbling is occurring.

I.4 Conclusions

While it was expected that the lateral deflections for the eccentric 0.33 m specimens and the concentric specimens would essentially be zero, the inhomogeneous nature of the plastered straw bale wall assembly specimens lead to very small measurements of lateral deflection during experimentation. The small lateral deflections were primarily attributed to the shifting of the specimens during testing. As expected, the specimens exhibited zero or very little lateral deflection as a result of bending or buckling. Given the small magnitude of the measured deflections it is not expected that the measured shifting of the specimens influenced the results or the behaviour of the specimens.

Appendix I: Supplemental Lateral Deflection Plots

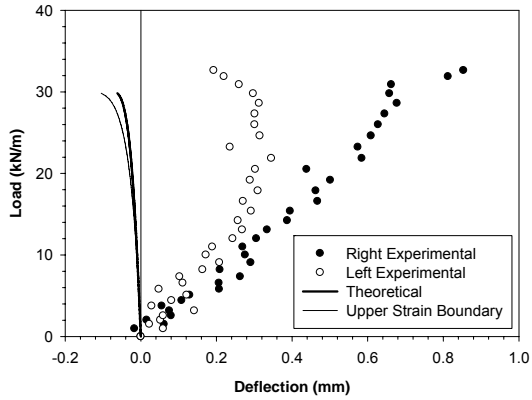


Figure I.1a: Mid-Height Lateral Load-Deflection Plot for Specimen E11

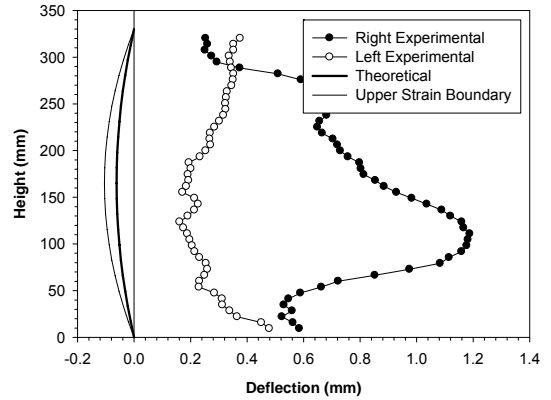


Figure I.1b: Full-Height Lateral Deflection at Ultimate Load for Specimen E11

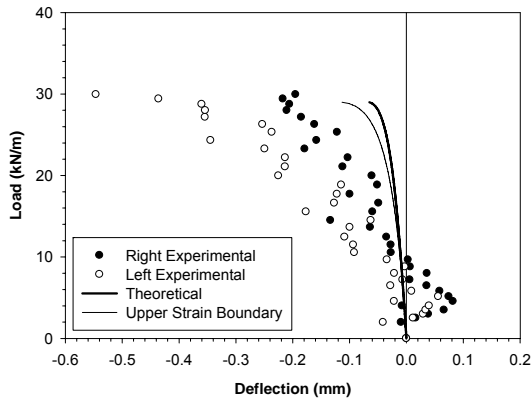


Figure I.2a: Mid-Height Lateral Load-Deflection Plot for Specimen E12

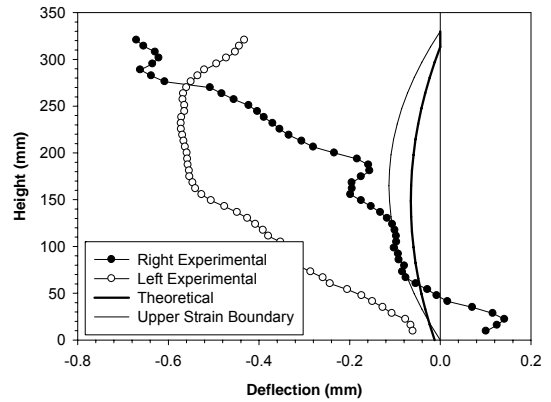


Figure I.2b: Full-Height Lateral Deflection at Ultimate Load for Specimen E12

Appendix I: Supplemental Lateral Deflection Plots

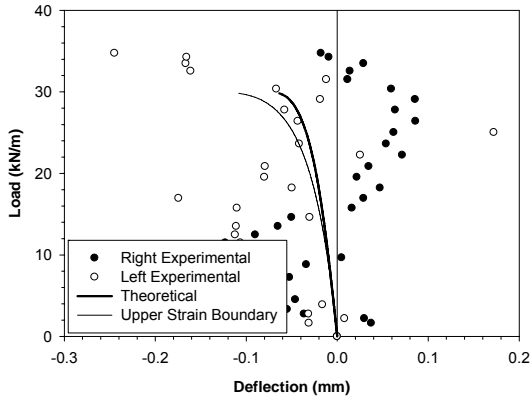


Figure I.3a: Mid-Height Lateral Load-Deflection Plot for Specimen E13

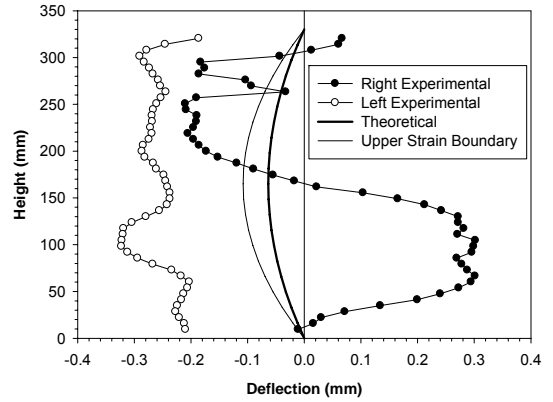


Figure I.3b: Full-Height Lateral Deflection at Ultimate Load for Specimen E13

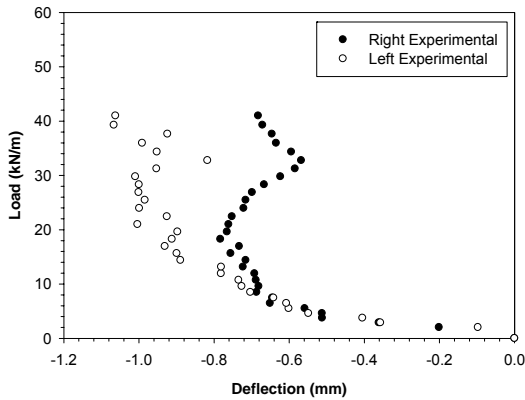


Figure I.4a: Mid-Height Lateral Load-Deflection Plot for Specimen C11

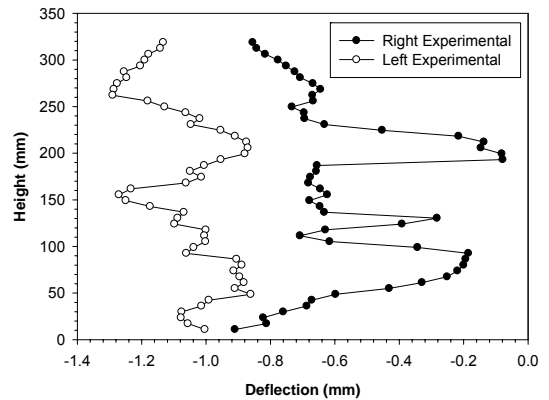


Figure I.4b: Full-Height Lateral Deflection at Ultimate Load for Specimen C11

Appendix I: Supplemental Lateral Deflection Plots

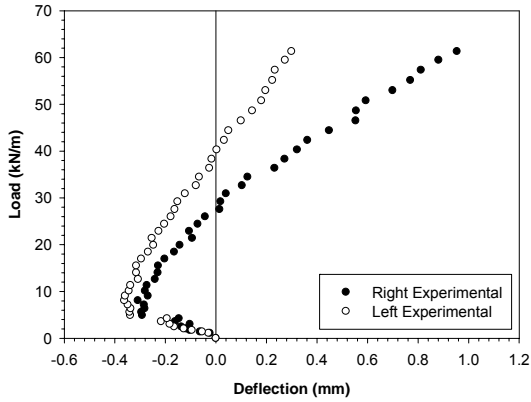


Figure I.5a: Mid-Height Lateral Load-Deflection Plot for Specimen C12

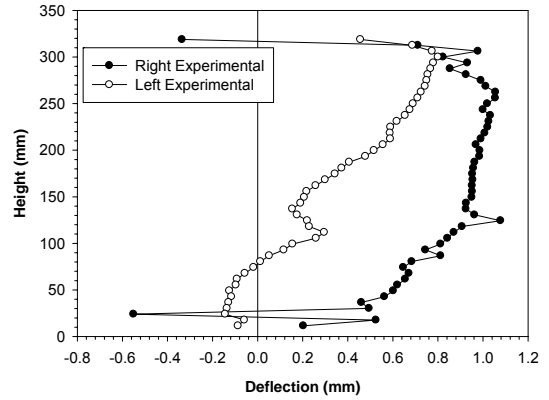


Figure I.5b: Full-Height Lateral Deflection at Ultimate Load for Specimen C12

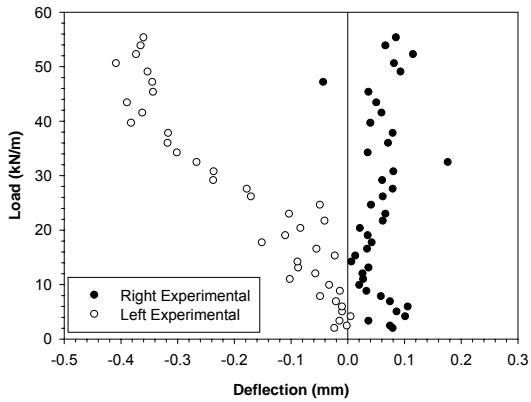


Figure I.6a: Mid-Height Lateral Load-Deflection Plot for Specimen C13

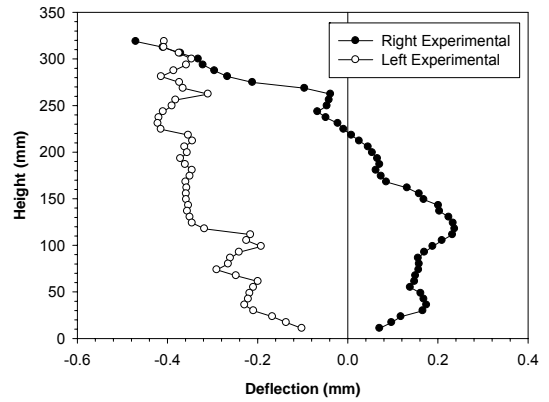


Figure I.6b: Full-Height Lateral Deflection at Ultimate Load for Specimen C13

Appendix I: Supplemental Lateral Deflection Plots

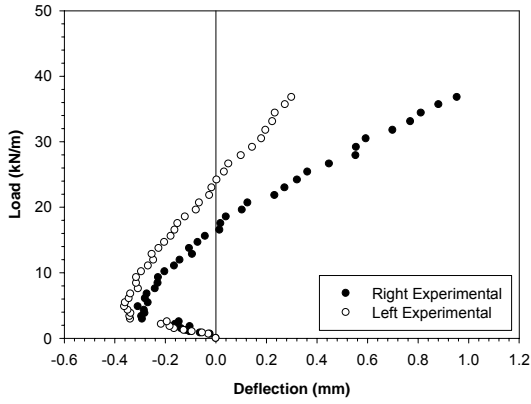


Figure I.7a: Mid-Height Lateral Load-Deflection Plot for Specimen C31

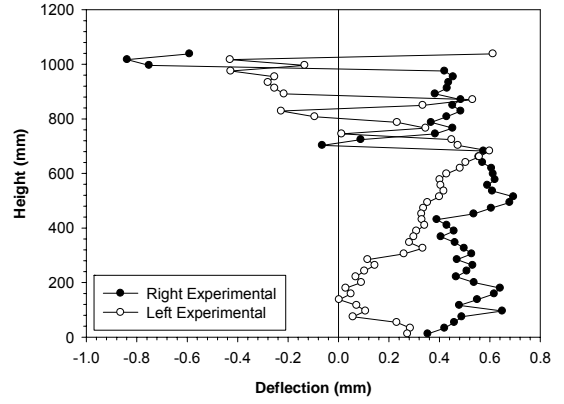


Figure I.7b: Full-Height Lateral Deflection at Ultimate Load for Specimen C31

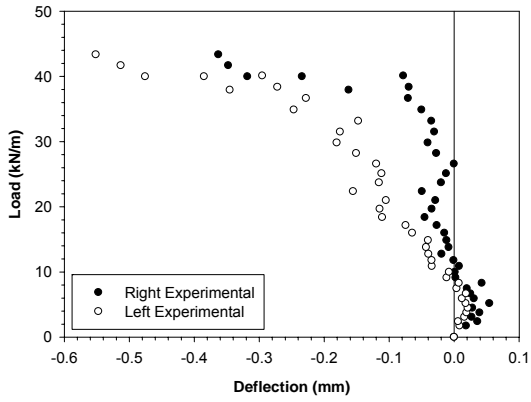


Figure I.8a: Mid-Height Lateral Load-Deflection Plot for Specimen C32

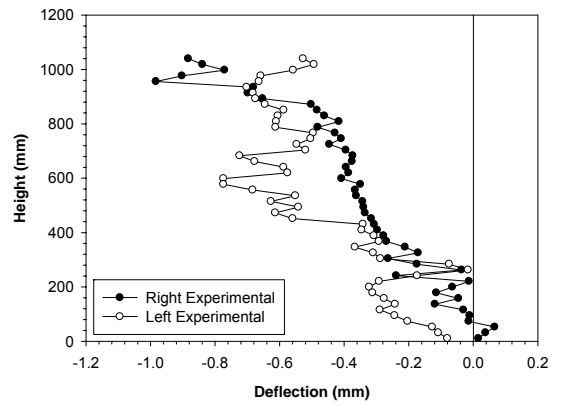


Figure I.8b: Full-Height Lateral Deflection at Ultimate Load for Specimen C32